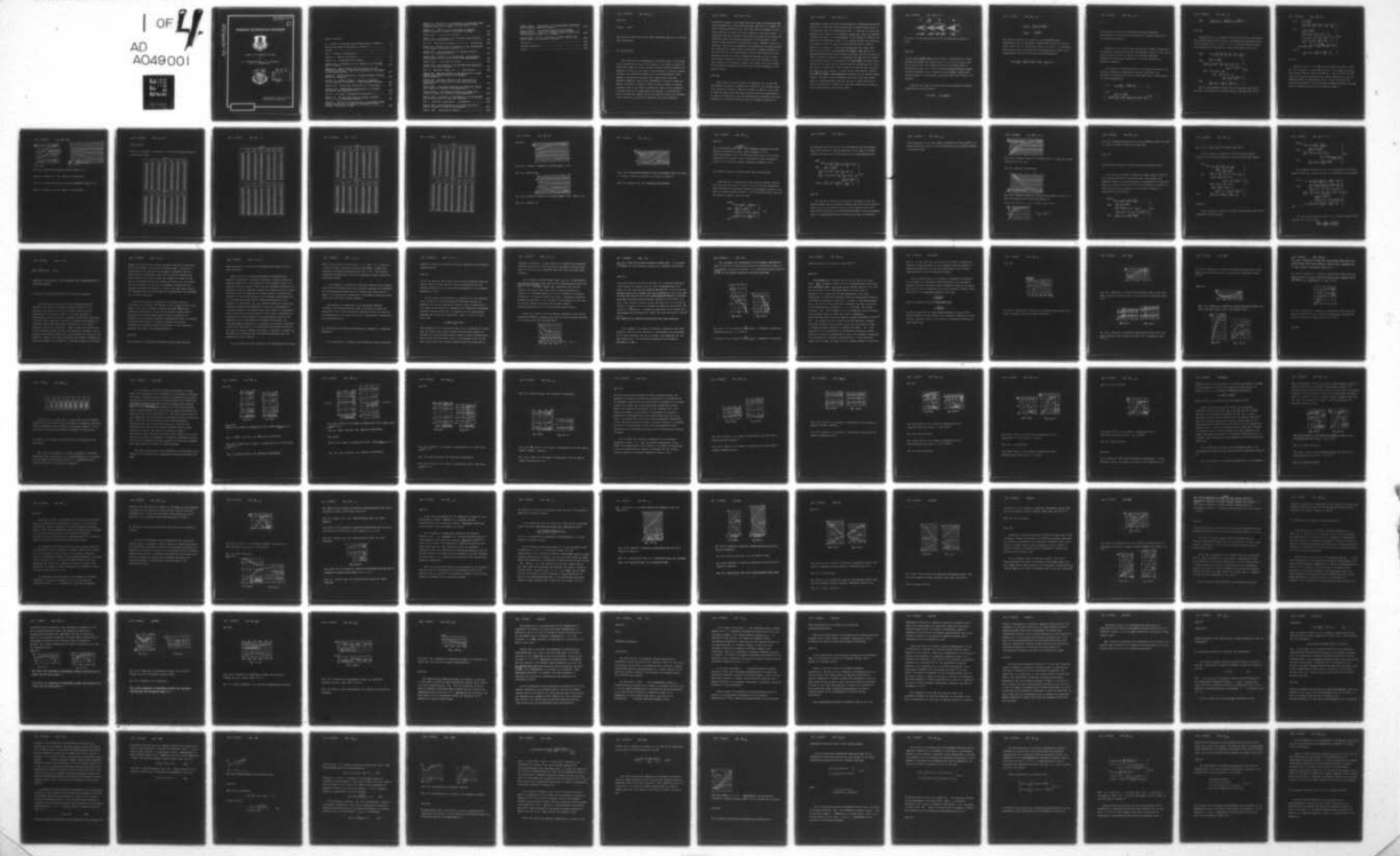
AD-A049 001 FOREIGN TECHNOLOGY DIV WRIGHT-PATTERSON AFB OHIO F/G 1/3
A WING IN AN UNSTEADY GAS FLOW. PART 3,(U)
SEP 77 S M BELOTSERKOVSKIY, B K SKRIPACH
UNCLASSIFIED FTD-ID(RS)T-1543-77-PT-3 NL

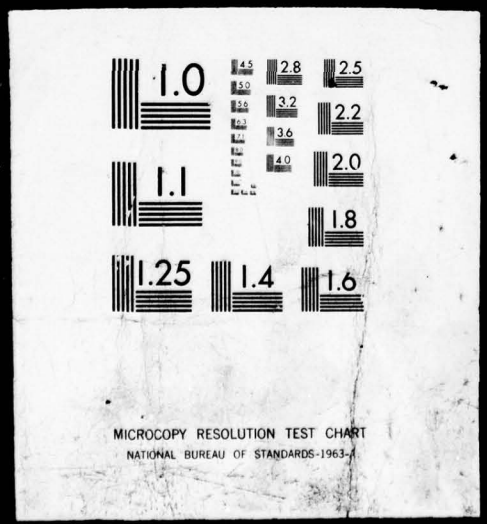
1 OF 4
AD
A049001



SIFIED

1 OF 4

AD
A049001



AD-A049001

FTD-ID(RS)T-1543-77
Part 3 of 3

(1)

FOREIGN TECHNOLOGY DIVISION

A WING IN AN UNSTEADY GAS FLOW

by

S. M. Belotserkovskiy, B. K. Skripach,
and V. G. Tabachnikov

DDC
RECEIVED
JAN 30 1978
F

Approved for public release;
distribution unlimited.

Table of Contents

U. S. Board on Geographic Names Transliteration System.... iv

Russian and English Trigonometric Functions..... v

Preface..... 1

Part I. General Considerations..... 8

Chapter I. General Information..... 14

Chapter II. Aerodynamic Coefficients..... 29

Chapter III. Formulation of the Problem of the Unsteady Motion of Wing..... 118

Chapter IV. Basic Formula for the Potential of the Disturbed Velocities. Some Exact Solutions for the Wings of Arbitrary Platform..... 167

Chapter V. Common Properties of Linear Unsteady Problems. Similarity Parameters..... 198

Chapter VI. Duhamel Integral. Theorem of Momentum. Rational Method of Solution of Linear Unsteady Problems... 229

Chapter VII. Reciprocity Theorem and Its Corollaries..... 289

Chapter VIII. Experimental Determination of Unsteady Aerodynamic Wing Characteristics..... 337

Part II. Low Speeds (Incompressible Medium M = 0)..... 410

Chapter IX. The Velocity Field of Oblique Horseshoe Vortex in an Incompressible Medium..... 415

Chapter X. Method of the Calculation of Aerodynamic Wing Characteristics with the Harmonic Dependences of the Kinematic Parameters on Time..... 438

Chapter XI. Method of the Calculation of Aerodynamic Wing Characteristics with the Arbitrary Dependences of the Kinematic Parameters on Time..... 467

Chapter XII. Method of the Calculation of Apparent Additional Masses of Wings of Arbitrary Planform..... 510

Chapter XIII. Some Point Solutions..... 555

Chapter XIV. Calculation of the Unsteady Wing Characteristics of Arbitrary Planform..... 604

Part III. High Subsonic Speeds ($0 < M < 1$). Introduction 689

Chapter XV. Method of the Calculation of the Coefficients of Aerodynamic Derivatives with $p^* \to 0$..... 695

Chapter XVI. The Velocity Field of Unsteady Discrete Vortex in a Compresses Medium..... 734

Chapter XVII. Method of the Calculation of Aerodynamic Wing Characteristics with Arbitrary Time Dependences..... 759

Chapter XVIII. Some Known Solutions..... 796

Chapter XIX. Calculation of the Unsteady Wing Characteristics of Arbitrary Planform..... 814

Part IV. Supersonic Speeds ($M > 1$). Introduction..... 855

Chapter XX. Numerical Method of the Calculation of Aerodynamic Wing Characteristics with Harmonic Time Dependences..... 861

Chapter XXI. Numerical Method of the Calculation of Aerodynamic Wing Characteristics with Arbitrary Time Dependences..... 917

Chapter XXII. Some Exact Solutions for Wings with Supersonic Edges with Harmonic Time Dependences..... 950

Chapter XXIII. Some Precise Solutions for Wings with Supersonic Edges with Arbitrary Time Dependences..... 1001

Chapter XXIV. Procedure of Calculation of the Aerodynamic Wing Characteristics of Arbitrary Planform..... 1023

Part V. Practical Applications. Introduction..... 1071

Chapter XXV. Special Features of the Practical Use of Duhamel Integral in Tasks of Aerodynamics..... 1077

Chapter XXVI. Approximation Method..... 1104

Chapter XXVII. Coefficients of the Aerodynamic Derivative and of Apparent Additional Masses..... 1145

Chapter XXVIII. Some Common Properties of Unsteady Characteristics. Effect of Planform, Numbers M and p* on the Aerodynamic Derivatives of Wings..... 1240

Chapter XXIX. Effect of Planform, the Mach Numbers and Laws of Motion for Transient Functions..... 1300

Literature..... 1333

Principal Notations..... 1352

Index..... 1362

Page 545.

Chapter XXIII

Some precise solutions for wings WITH supersonic edges with arbitrary time dependences.

§1. Generalities.

With arbitrary time dependences of boundary conditions on wing, it is possible in the case of the absence of the wing-tip effect to obtain from equation (4.10) a precise value of velocity potential as functions of time for any point of wing surface. If wing has complex planform, then obtaining solution will be hinder/hampered, since ranges of integration also will have complex form. This fact, generally speaking, leads to the advisability of using a numerical method, presented in chapter of XXI, and for the wings of complex planform, even if tip effect is absent and edge of wing supersonic. For some wings of the simple form, for example, of infinite-span wing, with all Mach numbers and at any value of time of the boundary of the region of integration in question they are determined

sufficiently simply. Also simple form have ranges of integration for direct/straight and reverse/inverse wedge wings with the numbers M, which satisfy condition $k\lambda \geqslant 4$. This fact makes it possible for the wings indicated to obtain the exact solution of the task through elementary functions [1.65], [1.78]. Below for them will be given the solutions, when the kinematic parameters of motion change in the course of time according to stepped law or wing gradually enters in step gust. Solutions for arbitrary time dependences are obtained from the solutions for stepped laws by applying an integral Duhamel. We will note that for an infinite-span wing the exact solutions can be obtained also with the aid of supersonic analogy, as this is made, for example, in works [1.19], [1.26], [2.26]. The obtained in this case results, it is logical, ccincide with those, that are obtained on the basis of expression (4.10) for the velocity potential of the driving source.

Page 546.

Before how to give the results of solutions, let us note that the transient process is divided into a series of the characteristic time intervals, in each of which the action of sources on the point in question differs not only quantitatively (for the size/dimension of range of integration), but also qualitatively. Therefore the final formulas for a velocity potential and the transient functions of

aerodynamic loading and force coefficients and torque/moments will be different for different interval/gaps for an infinite-span wing. For the reference point of dimensionless time $\tau = tU_0/b$ let us accept the beginning of a change in the kinematic parameters, and at the gradual entrance into gust - the torque/moment of the meeting of leading wing edge with the boundary of gust. Let us examine as they will change in the course of time of range of integration for point P, which is located at a distance $\xi = x/b$ from leading wing edge (Fig. 23.1). When to see that into time interval $0 \leqslant \tau < \frac{M}{M+1}\xi$ (Fig. 23.1a) the disturbance/perturbation from leading wing edge will not have time to reach the point in question, and therefore this edge will not affect the disturbed state of the medium in it. With $\tau = \frac{M}{M+1}\xi$ to point P will arrive for the first time by leading edge the interference wave from one point of leading edge (Fig. 23.1b), and from this point on, will be begun the time interval, in which leading edge affects. Further, with $\frac{M}{M+1}\xi \leqslant \tau < \frac{M}{M-1}\xi$ disturbance/perturbations will be created partly leading edge (Fig. 23.1c), whereupon from part, which lies within range σ_1, disturbance/perturbations will be it comes into point P only by leading edge of wave, but from part, which lies at range σ_2, and by front/leading and trailing edges.

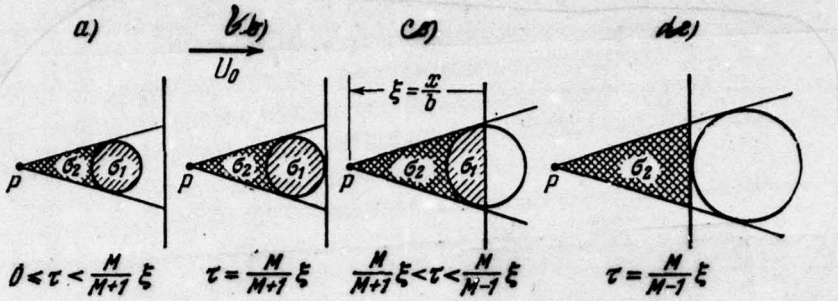


Fig. 23.1. To the determination of the characteristic moments of time.

Page 547.

Finally, with $\tau \geqslant \frac{M}{M-1}\xi$ (Fig. 23.1d) range of integration will remain constant/invariable and consist only of σ_2, i.e., all sources will act on point P both front/leading and by the trailing edges of interference waves, and a phase difference between them will remain constant/invariable. Thus, transient process during $\tau = \frac{M}{M-1}\xi$ and a stepped variation in the boundary conditions will be for point P (ξ) finished.

Thus, for the points of wing surface let us have the following characteristic time intervals:

the first $0 \leqslant \tau \leqslant \frac{M}{M+1}\xi$,

second $\frac{M}{M+1}\xi \leqslant \tau \leqslant \frac{M}{M-1}\xi,$

third. $\tau \geqslant \frac{M}{M-1}\xi.$

The transient process of a change in the aerodynamic wing coefficients will be, obviously, finished when it will end for the point, which lies on trailing wing edge, i.e., with $\xi = 1$. Therefore characteristic time intervals for the transient force function and torque/moments of entire wing they will be respectively

$$0 \leqslant \tau \leqslant \frac{M}{M+1}, \quad \frac{M}{M+1} \leqslant \tau \leqslant \frac{M}{M-1} \quad \text{and} \quad \frac{M}{M-1} \leqslant \tau < \infty.$$

§2. Transient functions of aerodynamic loading, forces and torque/moments of infinite-span wing during a stepped variation in the kinematic parameters.

Solution for an infinite-span wing during a stepped variation in the kinematic parameters of motion was obtained in works [1.26], [1.65] [1.78], [2.26]. Let us give here in the adopted previously designations the results, obtained in the works indicated for transient functions.

In α-problem (a stepped variation in the angle of attack α) the transient function of aerodynamic loading at point with the coordinate ξ, measured from leading edge along flow, is determined by the relationship/ratios:

$$\text{with} \quad 0 \leqslant \tau \leqslant \frac{M}{M+1}\xi \quad \left[\frac{\Delta\bar{p}(\tau)}{\alpha^{\circ}}\right] = \frac{4}{M};$$

$$\text{with} \quad \frac{M}{M+1}\xi \leqslant \tau \leqslant \frac{M}{M-1}\xi \quad \left[\frac{\Delta\bar{p}(\tau)}{\alpha^{\circ}}\right] = \frac{4}{\pi k}\left\{\arccos M\left(1-\frac{k^2}{M^2}\frac{\tau}{\xi}\right)+\frac{k}{M}\arccos M\left(1-\frac{\xi}{\tau}\right)\right\}; \tag{23.1}$$

with $\frac{M}{M-1}\xi \leqslant \tau \leqslant \infty \quad \left[\frac{\Delta\bar{p}(\tau)}{\alpha^\circ}\right] = \frac{4}{k};\ k = \sqrt{M^2-1}.$

Page 458.

Expressions for the transient functions of the lift coefficients and pitching moment we will obtain, by integrating expressions (23.1) by wing section from $\xi = 0$ to $\xi = 1$. As a result in standard system of coordinates with beginning on leading wing edge, let us have:

with $0 \leqslant \tau \leqslant \frac{M}{M+1} \quad \left[\frac{c_y}{\alpha^\circ}\right] = \frac{4}{M},\ \left[\frac{m_z}{\alpha^\circ}\right] = -\frac{2}{M}\left(1 - \frac{\tau^2}{2M^2}\right);$

with $\frac{M}{M+1} \leqslant \tau \leqslant \frac{M}{M-1}$

$$\left[\frac{c_y}{\alpha^\circ}\right] = \frac{4}{\pi k}\arccos M\left(1 - \frac{k^2}{M^2}\tau\right) + \frac{4}{\pi M}\arccos M\left(1 - \frac{1}{\tau}\right) + \frac{4}{\pi M}\sqrt{2\tau - \frac{k^2}{M^2}\tau^2 - 1},$$

$$\left[\frac{m_z}{\alpha^\circ}\right] = -\frac{2}{\pi k}\arccos M\left(1 - \frac{k^2}{M^2}\tau\right) - \frac{2}{\pi M}\left(1 - \frac{\tau^2}{2M^2}\right)\arccos M\left(1 - \frac{1}{\tau}\right) - \frac{1}{\pi M}(1+\tau)\sqrt{2\tau - \frac{k^2}{M^2}\tau^2 - 1}; \qquad (23.2)$$

with $\frac{M}{M-1} \leqslant \tau \leqslant \infty \quad \left[\frac{c_y}{\alpha^\circ}\right] = \frac{4}{k},\ \left[\frac{m_z}{\alpha^\circ}\right] = -\frac{2}{k}.$

For ω_z the problem of formula for the transient functions of the force coefficients and pitching moment, they take form [1.19]

with $0 \leqslant \tau \leqslant \frac{M}{M+1}$

$$\left[\frac{c_y}{\dot{\omega}_z}\right] = \frac{2}{M}\left(1 + \frac{\tau^2}{2M^2}\right), \quad \left[\frac{m_z}{\dot{\omega}_z}\right] = -\frac{4}{3M}\left(\tau + \frac{\tau^3}{2M^2}\right);$$

with $\frac{M}{M+1} \leqslant \tau \leqslant \frac{M}{M-1}$

$$\left[\frac{c_y}{\dot{\omega}_z}\right] = \frac{2}{\pi}\left\{\frac{1}{M}\left(1 + \frac{\tau^2}{2M^2}\right)\arccos M\left(1 - \frac{1}{\tau}\right) + \right.$$

$$\left. + \frac{1}{k}\arccos M\left(1 - \frac{k^2}{M^2}\tau\right) + \frac{(3-\tau)}{2M}\sqrt{\frac{\tau^2}{M^2} - (1-\tau)^2}\right\},$$

$$\left[\frac{m_z}{\dot{\omega}_z}\right] = -\frac{4}{3\pi}\left\{\frac{1}{M}\left(1 + \frac{\tau^3}{2M^2}\right)\arccos M\left(1 - \frac{1}{\tau}\right) + \right.$$

$$\left. + \frac{1}{k}\arccos M\left(1 - \frac{k^2}{M^2}\tau\right) + \frac{\left(8 - \tau - \tau^2 - \frac{2\tau^2}{M^2}\right)}{6M}\sqrt{\frac{\tau^2}{M^2} - (1-\tau)^2}\right\}; \qquad (23.3)$$

with

$$\frac{M}{M-1} \leqslant \tau \leqslant \infty \quad \left[\frac{c_y}{\dot{\omega}_z}\right] = \frac{2}{k}, \quad \left[\frac{m_z}{\dot{\omega}_z}\right] = -\frac{4}{3k}.$$

Page 549.

Numerical values of the transient functions are given in table 23.1 for the range of numbers $M = 1.1\text{-}5.0$. As an example for three Mach numbers: $M = 1.4$ $M = 2.0$ and $M = 3.0$ - Fig. by 23.2-23.5 solid lines gives precise dependences of transient functions of lift and pitching moment of dimensionless time τ. Figure 23.6 shows the displacement/movement of mean aerodynamic center of wing $[\bar{x}_a]$ in time during a stepped variation in the angle of attack α.

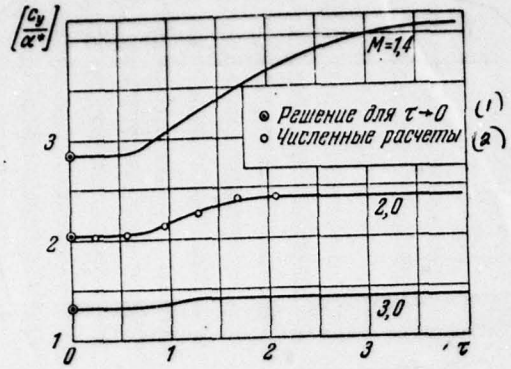


FIG. 23.2.

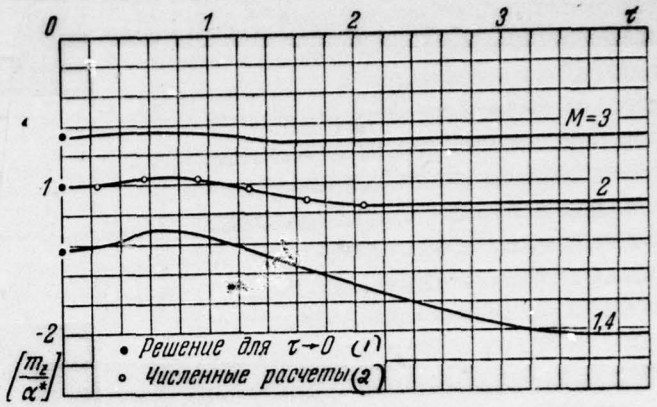


FIG. 23.3.

Fig. 23.2. Transient function of lift $[c_y/\alpha^*]$ wing $\lambda = \infty$.

Key: (1). Solution for. (2). Numerical calculations.

Fig. 23.3. Transient function of pitching moment $[m_z/\alpha^*]$ wing $\lambda = \infty$, $\bar{x}_T = 0$.

Key: (1). Solution for. (2). Numerical calculations.

Pages 550-553.

Table 23.1. Transient functions of lift and the pitching moment of infinite-span wing.

M = 1,1

τ	$\left[\frac{c_y}{\alpha^*}\right]$	$\left[\frac{m_z}{\alpha^*}\right]$	$\left[\frac{c_y}{\dot{\omega}_z^*}\right]$	$\left[\frac{m_z}{\dot{\omega}_z^*}\right]$	$\left[\frac{c_y}{\dot{\omega}_{y\Delta}^*}\right]$	$\left[\frac{m_z}{\dot{\omega}_{y\Delta}^*}\right]$
0,000	3,636	−1,818	1,818	−1,212	0,000	0,000
0,550	3,645	−1,600	2,045	−1,295	1,991	−0,541
1,100	4,169	−1,688	2,481	−1,554	3,188	−1,074
1,650	4,720	−1,833	2,837	−1,780	4,000	−1,406
2,200	5,212	−2,088	3,124	−1,970	4,648	−1,703
2,750	5,650	−2,220	3,359	−2,131	5,194	−1,971
3,300	6,011	−2,487	3,554	−2,269	5,668	−2,218
3,850	6,395	−2,678	3,717	−2,387	6,036	−2,449
4,400	6,715	−2,862	3,853	−2,489	6,459	−2,667
4,950	7,006	−3,039	3,966	−2,576	6,794	−2,875
5,500	7,270	−3,210	4,060	−2,650	7,007	−3,071
6,050	7,511	−3,374	4,137	−2,712	7,320	−3,238
6,600	7,729	−3,530	4,199	−2,764	7,616	−3,475
7,150	7,927	−3,678	4,249	−2,806	7,837	−3,601
7,700	8,104	−3,816	4,288	−2,840	8,036	−3,757
8,250	8,261	−3,945	4,317	−2,865	9,212	−3,900
8,800	8,100	−4,063	4,338	−2,884	8.366	−4,030
9,350	8,518	−4,167	4,352	−2,897	8,407	−4,147
9,900	8,616	−4,236	4,360	−2,905	8,605	−4,245
10,450	8,640	−4,325	4,363	−2,909	8,685	−4,322
11,000	8,729	−4,365	4,364	−2,909	8,729	−4,365
∞	8,729	−4,365	4,364	−2,909	8,729	−4,365

M = 1,15

τ	$\left[\frac{c_y}{\alpha^*}\right]$	$\left[\frac{m_z}{\alpha^*}\right]$	$\left[\frac{c_y}{\dot{\omega}_z^*}\right]$	$\left[\frac{m_z}{\dot{\omega}_z^*}\right]$	$\left[\frac{c_y}{\dot{\omega}_{y\Delta}^*}\right]$	$\left[\frac{m_z}{\dot{\omega}_{y\Delta}^*}\right]$
0,000	3,478	−1,739	1,739	−1,159	0,000	0,000
0,383	3,478	−1,643	1,836	−1,184	1,333	−0,256
0,767	3,639	−1,642	2,097	−1,325	2,450	−0,769
1,150	4,004	−1,650	2,354	−1,486	3,145	−1,079
1,533	4,356	−1,788	2,568	−1,626	3,688	−1,331
1,917	4,679	−1,933	2,746	−1,748	4,141	−1,555
2,300	4,973	−2,078	2,895	−1,853	4,533	−1,760
2,683	5,241	−2,221	3,020	−1,943	4,878	−1,951
3,067	5,485	−2,360	3,125	−2,021	5,185	−2,132
3,450	5,708	−2,496	3,212	−2,089	5,460	−2,302
3,833	5,912	−2,627	3,285	−2,146	5,708	−2,464
4,217	6,097	−2,753	3,345	−2,194	5,932	−2,617
4,600	6,266	−2,873	3,393	−2,234	6,134	−2,762
4,983	6,420	−2,988	3,431	−2,267	6,315	−2,898
5,367	6,557	−3,095	3,462	−2,293	6,478	−3,025
5,750	6,680	−3,195	3,485	−2,313	6,621	−3,143
6,133	6,788	−3,287	3,501	−2,328	6,747	−3,249
6,517	6,880	−3,368	3,512	−2,338	6,854	−3,344
6,900	6,956	−3,438	3,518	−2,344	6,942	−3,425
7,283	7,013	−3,492	3,521	−2,347	7,008	−3,487
7,667	7,044	−3,522	3,522	−2,348	7,044	−3,522
∞	7,044	−3,522	3,522	−2,348	7,044	−3,522

M = 1,2

τ	$\left[\frac{c_y}{\alpha^\circ}\right]$	$\left[\frac{m_z}{\alpha^\circ}\right]$	$\left[\frac{c_y}{\dot{\omega}_z}\right]$	$\left[\frac{m_z}{\dot{\omega}_z}\right]$	$\left[\frac{c_y}{\dot{w}_{y\Delta}}\right]$	$\left[\frac{m_z}{\dot{w}_{y\Delta}}\right]$
0,000	3,333	−1,667	1,667	−1,111	0,000	0,000
0,300	3,333	−1,615	1,719	−1,121	1,000	−0,150
0,600	3,353	−1,479	1,874	−1,194	1,974	−0,574
0,900	3,556	−1,519	2,067	−1,312	2,617	−0,872
1,200	3,851	−1,614	2,236	−1,422	3,102	−1,101
1,500	4,103	−1,723	2,380	−1,519	3,502	−1,301
1,800	4,336	−1,836	2,500	−1,603	3,846	−1,481
2,100	4,552	−1,949	2,602	−1,677	4,147	−1,649
2,400	4,749	−2,061	2,688	−1,741	4,415	−1,807
2,700	4,931	−2,171	2,760	−1,796	4,655	−1,956
3,000	5,097	−2,278	2,820	−1,844	4,871	−2,097
3,300	5 249	−2,381	2,869	−1,883	5,066	−2,230
3,600	5,388	−2,479	2,909	−1,916	5,241	−2,356
3,900	5,514	−2,573	2 941	−1,943	5,399	−2,474
4,200	5,628	−2,662	2,966	−1,964	5,540	−2,584
4,500	5,729	−2,745	2,984	−1,982	5,664	−2,686
4,800	5,818	−2,820	2,998	−1,994	5,773	−2,779
5,100	5,895	−2,888	3,007	−2,002	5,866	−2,861
5,400	5,937	−2,945	3,012	−2,007	5,943	−2,931
5,700	6,005	−2,990	3,015	−2,009	6,000	−2,985
6,000	6,030	−3,015	3,015	−2,010	6,030	−3,015
∞	6,030	−3,015	3,015	−2,010	6,030	−3,015

M = 1,4

τ	$\left[\frac{c_y}{\alpha^\circ}\right]$	$\left[\frac{m_z}{\alpha^\circ}\right]$	$\left[\frac{c_y}{\dot{\omega}_z}\right]$	$\left[\frac{m_z}{\dot{\omega}_z}\right]$	$\left[\frac{c_y}{\dot{w}_{y\Delta}}\right]$	$\left[\frac{m_z}{\dot{w}_{y\Delta}}\right]$
0,000	2,857	−1,429	1,428	−0,952	0,000	0,000
0,175	2,857	−1,417	1,440	−0.954	0,500	−0,044
0,350	2,857	−1,384	1,473	−0,963	1,000	−0,175
0,525	2,857	−1,328	1,529	−0,987	1,500	−0,394
0,700	2,901	−1,297	1,604	−1,032	1,933	−0,628
0,875	3,005	−1,328	1,677	−1,080	2.246	−0,791
1,050	3,118	−1,375	1,743	−1,126	2,506	−0,932
1,225	3,230	−1,430	1,800	−1,166	2,729	−1,058
1,400	3,337	−1,488	1,849	−1,203	2,925	−1,174
1,575	3,438	−1,548	1,890	−1,234	3,100	−1,283
1,750	3,532	−1,607	1,925	−1,262	3,255	−1,385
1,925	3,620	−1,666	1,954	−1,285	3,395	−1,482
2,100	3,701	−1,723	1,978	−1,305	3,521	−1,572
2,275	3,774	−1,778	2,000	−1,321	3,634	−1,657
2,450	3,842	−1,830	2,011	−1,334	3,734	−1,735
2,625	3,902	−1,879	2,023	−1,344	3,823	−1,808
2,800	3,955	−1,924	2,031	−1,351	3,900	−1,874
2,975	4,001	−1,964	2,036	−1,356	3,966	−1,932
3,150	4,038	−1,999	2,039	−1,359	4,020	−1,982
3,325	4,067	−2,026	2,041	−1,360	4,061	−2,020
3,500	4,082	−2,041	2,041	−1,361	4,082	−2,041
∞	4,082	−2,041	2,041	−1,361	4,082	−2,041

M = 1,6

τ	$\left[\frac{c_y}{a^*}\right]$	$\left[\frac{m_z}{a^*}\right]$	$\left[\frac{c_y}{\omega_z^*}\right]$	$\left[\frac{m_z}{\omega_z^*}\right]$	$\left[\frac{c_y}{\omega_{y\Delta}^*}\right]$	$\left[\frac{m_z}{\omega_{y\Delta}^*}\right]$
0,000	2,500	−1,250	1,250	−0,833	0,000	−0,000
0,133	2,500	−1,246	1,254	−0,834	0,333	−0,022
0,267	2,500	−1,233	1,267	−0,836	0,667	−0,089
0,400	2,500	−1,210	1,289	−0,844	1,000	−0,200
0,533	2,500	−1,181	1,319	−0,858	1,333	−0,356
0,667	2,511	−1,152	1,358	−0,881	1,649	−0,537
0,800	2,564	−1,164	1,398	−0,908	1,883	−0,670
0,933	2,627	−1,192	1,435	−0,934	2,077	−0,781
1,067	2,693	−1,226	1,468	−0,958	2,244	−0,882
1,200	2,739	−1,264	1,496	−0,979	2,390	−1.974
1,333	2,821	−1,301	1,520	−0,998	2,521	−0,060
1,467	2,880	−1,340	1,540	−1,014	2,637	−1,140
1,600	2,935	−1,379	1,556	−1,028	2,741	−1,215
1.733	2,986	−1.416	1,570	−1,039	2,834	−1,286
1,867	3,033	−1,462	1,580	−1,048	2,917	−1,351
2.000	3,075	−1,487	1,588	−1,056	3,000	−1,410
2,133	3,112	−1,518	1,594	−1,060	3,054	−1,464
2,267	3,144	−1,547	1,598	−1,064	3,108	−1,512
2,400	3,171	−1,571	1,600	−1,066	3,152	−1,553
2,533	3,192	−1,591	1,601	−1,067	3,185	−1,584
2,667	3,203	−1,601	1,601	−1,067	3,203	−1,601
∞	3,203	−1,601	1,601	−1,067	3,203	−1,601

M = 2,0

τ	$\left[\frac{c_y}{a^*}\right]$	$\left[\frac{m_z}{a^*}\right]$	$\left[\frac{c_y}{\omega_z^*}\right]$	$\left[\frac{m_z}{\omega_z^*}\right]$	$\left[\frac{c_y}{\omega_{y\Delta}^*}\right]$	$\left[\frac{m_z}{\omega_{y\Delta}^*}\right]$
0,000	2,000	−1,000	1,000	−0,666	0,000	−0,000
0,100	2,000	−0,999	1,001	−0,667	0,200	−0,010
0,200	2,000	−0,995	1,005	−0,667	0,400	−0.040
0,300	2,000	−0,989	1,011	−0,669	0,600	−0,090
0,400	2,000	−0,980	1,020	−0,672	0,800	−0,160
0,500	2,000	−0,968	1,031	−0,677	1,000	−0,250
0,600	2,000	−0,955	1,045	−0,685	1,200	−0,360
0,700	2,004	−0,943	1,061	−0,695	1,392	−0,482
0,800	2,027	−0,949	1,078	−0,707	1,540	−0,575
0,900	2,057	−0,963	1,093	−0,718	1,663	−0,654
1,000	2,088	−0,982	1,106	−0,729	1,770	−0,726
1,100	2,120	−1,002	1,118	−0,738	1,864	−0,791
1,200	2,150	−1,023	1,128	−0.746	1,947	−0,851
1,300	2,180	−1,044	1,136	−0,753	2,021	−0,907
1,400	2,207	−1,065	1,142	−0,758	2,086	−0,959
1,500	2,232	−1,085	1,147	−0,762	2,144	−1,095
1,600	2 254	−1,194	1,150	−0,765	2,193	−1,048
1,700	2,274	−1,121	1,152	−0,768	2,236	−1,085
1,800	2,280	−1,136	1,153	−0,769	2,270	−1,117
1,900	2,303	−1,148	1,154	−0,770	2,296	−1,141
2,000	2,309	−1,155	1,154	−0,770	2,309	−1,155
∞	2,309	−1,155	1,154	−0,770	2,309	−1,155

M = 3,0

τ	$\left[\frac{c_y}{\alpha^*}\right]$	$\left[\frac{m_z}{\alpha^*}\right]$	$\left[\frac{c_y}{\dot{\omega}_z^*}\right]$	$\left[\frac{m_z}{\dot{\omega}_z^*}\right]$	$\left[\frac{c_y}{\dot{\omega}_{y\Delta}^*}\right]$	$\left[\frac{m_z}{\dot{\omega}_{y\Delta}^*}\right]$
0,000	1,333	−0,667	0,667	−0,444	0,000	−0,000
0,075	1,333	−0,666	0,667	−0,444	0,100	−0,004
0,150	1,333	−0,666	0,667	−0,444	0,200	−0,015
0,225	1,333	−0,665	0,668	−0,445	0,300	−0,034
0,300	1,333	−0,663	0,670	−0,445	0,400	−0,060
0,375	1,333	−0,661	0,672	−0,445	0,500	−0,094
0,450	1,333	−0,669	0,674	−0,447	0,600	−0,135
0,525	1,333	−0,656	0,677	−0,448	0,700	−0,184
0,600	1,333	−0,653	0,680	−0,450	0,800	−0,240
0,675	1,333	−0,650	0,683	−0,452	0,900	−0,304
0,750	1,333	−0,646	0,687	−0,455	1,000	−0,375
0,825	1,339	−0,647	0,692	−0,458	1,081	−0,434
0,900	1,348	−0,653	0,695	−0,461	1,147	−0,483
0,975	1,359	−0,660	0,699	−0,464	1,204	−0,526
1,050	1,369	−0,668	0,701	−0,466	1,253	−0,565
1,125	1,379	−0,676	0,703	−0,468	1,295	−0,600
1,200	1,389	−0,684	0,705	−0,469	1,331	−0,631
1,275	1,398	−0,692	0,706	−0,470	1,362	−0,658
1,360	1,405	−0,698	0,707	−0,471	1,386	−0,680
1,425	1,411	−0,704	0,707	−0,471	1,405	−0,698
1,500	1,414	−0,707	0,707	−0,471	1,414	−0,707
∞	1,414	−0,707	0,707	−0,471	1,414	−0,707

M = 5,0

τ	$\left[\frac{c_y}{\alpha^*}\right]$	$\left[\frac{m_z}{\alpha^*}\right]$	$\left[\frac{c_y}{\dot{\omega}_z^*}\right]$	$\left[\frac{m_z}{\dot{\omega}_z^*}\right]$	$\left[\frac{c_y}{\dot{\omega}_{y\Delta}^*}\right]$	$\left[\frac{m_z}{\dot{\omega}_{y\Delta}^*}\right]$
0,000	0,800	−0,400	0,400	−0,267	0,000	0,000
0,062	0,800	−0,400	0,400	−0,267	0,050	−0,002
0,125	0,800	−0,400	0,400	−0,267	0,100	−0,006
0,188	0,800	−0,400	0,400	−0,267	0,150	−0,014
0,250	0,800	−0,400	0,400	−0,267	0,200	−0,025
0,312	0,800	−0,399	0,401	−0,267	0,250	−0,039
0,375	0,800	−0,399	0,401	−0,267	0,300	−0,056
0,438	0,800	−0,398	0,401	−0,267	0,350	−0,076
0,500	0,800	−0,398	0,402	−0,267	0,400	−0,100
0,563	0,800	−0,397	0,402	−0,268	0,450	−0,127
0,623	0,800	−0,397	0,403	−0,268	0,500	−0,156
0,688	0 800	−0,396	0,404	−0,268	0,550	−0,182
0,750	0,800	−0,396	0,404	−0,269	0,600	−0,225
0,813	0,800	−0,395	0,405	−0,269	0,650	−0,264
0,873	0,801	−0,395	0,406	−0,270	0,695	−0,301
0,938	0,804	−0,397	0,407	−0,271	0,725	−0,328
1,000	0,807	−0,392	0,407	−0,271	0,756	−0,352
1,063	0,810	−0,405	0,408	−0,272	0,777	−0,373
1,125	0,813	−0,405	0,408	−0,272	0,796	−0,389
1,137	0,815	−0,407	0,408	−0,272	0,810	−0,401
1,250	0,816	−0,408	0,408	−0,272	0,816	−0,405
∞	0,816	−0,408	0,408	−0,272	0,816	−0,405

Page 554.

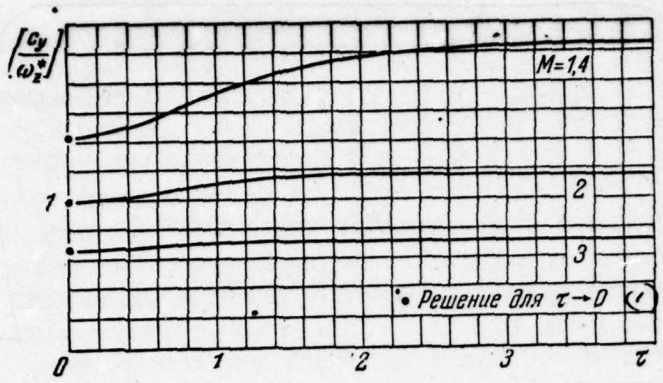


Fig. 23.4. Transient function of lift $[c_y/\omega_z^*]$ wing $\lambda=\infty, \bar{x}_T=0.$

Key: (1). Solution for.

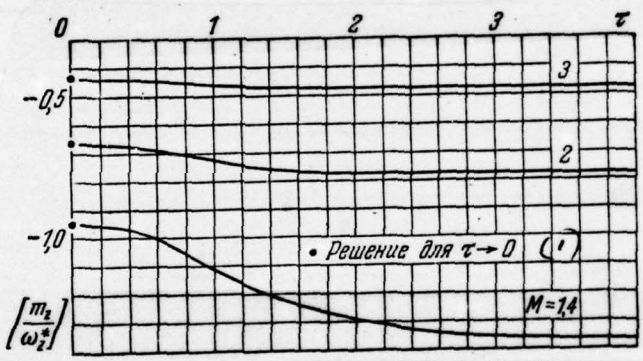


Fig. 23.5. Transient function of pitching moment $[m_z/\omega_z^*]$ wing $\lambda=\infty, \bar{x}_T=0.$

Key: (1). Solution for.

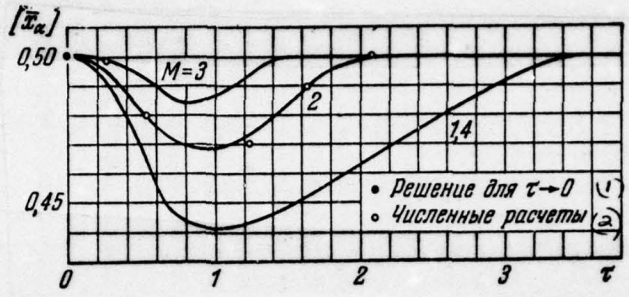


Fig. 23.6. Displacement/movement of mean aerodynamic center of wing $\lambda = \infty$ during a stepped variation in the angle of attack α.

Key: (1). Solution for. (2). Numerical calculations.

It is evident that with $\tau \geqslant M/M-1$ the transient functions and focus take the steady-state values, which correspond to the establish/installed flow. For $M = 2.0$ in Fig. 23.2, 23.3 and 23.6 points gave the results of the calculations of the corresponding values by the numerical method, presented in chapter of XXI.

§3. Gradual entrance of infinite-span wing into step gust.

Solutions for an infinite-span wing upon the gradual entrance into step gust are given in works [1.19], [1.78]. The expressions, which determine the transient function of aerodynamic loading at the points of wing, distant to value $\xi = x/b$ from leading edge, they will for different ranges τ take the form:

$$\left.\begin{aligned}
&\text{when } 0 \leqslant \tau \leqslant \frac{M}{M+1}\xi \quad \left[\frac{\Delta\bar{p}(\tau)}{\overset{\circ}{w}_{y\Delta}}\right] = 0;\\
&\text{when } \frac{M}{M+1}\xi \leqslant \tau \leqslant \frac{M}{M-1}\xi\\
&\left[\frac{\Delta\bar{p}(\tau)}{\overset{\circ}{w}_{y\Delta}}\right] = \frac{4}{\pi k}\arccos M\left(1 - \frac{k^2}{M^2}\frac{\tau}{\xi}\right);\\
&\text{with } \frac{M}{M-1}\xi \leqslant \tau \leqslant \infty \quad \left[\frac{\Delta\bar{p}(\tau)}{\overset{\circ}{w}_{y\Delta}}\right] = \frac{4}{k}.
\end{aligned}\right\} \qquad (23.4)$$

The transient functions of the lift coefficients and longitudinal moment with respect to leading edge/nose $(\bar{x}_T = 0)$ upon the gradual entrance into gust will be determined by the relationship/ratios:

$$
\left.
\begin{aligned}
&\text{with} \quad 0 \leqslant \tau \leqslant \frac{M}{M+1} \quad \left[\frac{c_y}{\dot{w}_{y\Delta}}\right] = \frac{4}{M}\tau, \quad \left[\frac{m_z}{\dot{w}_{y\Delta}}\right] = -\frac{2}{M}\tau^2;\\
&\text{with} \quad \frac{M}{M+1} \leqslant \tau \leqslant \frac{M}{M-1}\\
&\left[\frac{c_y}{\dot{w}_{y\Delta}}\right] = \frac{4}{\pi k}\arccos M\left(1 - \frac{k^2}{M^2}\tau\right) + \frac{4\tau}{\pi M}\arccos\left(1 - \frac{1}{\tau}\right),\\
&\left[\frac{m_z}{\dot{w}_{y\Delta}}\right] = -\frac{2}{\pi k}\arccos M\left(1 - \frac{k^2}{M^2}\tau\right) - \frac{2\tau^2}{\pi M}\arccos M\left(1 - \frac{1}{\tau}\right) +\\
&\qquad + \frac{2\tau}{\pi M}\sqrt{2\tau - \frac{k^2}{M^2}\tau^2 - 1};\\
&\text{when} \quad \frac{M}{M-1} \leqslant \tau \leqslant \infty \quad \left[\frac{c_y}{\dot{w}_{y\Delta}}\right] = \frac{4}{k}, \quad \left[\frac{m_z}{\dot{w}_{y\Delta}}\right] = -\frac{2}{k}.
\end{aligned}
\right\} \quad (23.5)
$$

Page 556.

The numerical values of the transient functions of lift and pitching moment upon the gradual entrance into gust are also given in table 23.1, but for $M = 1.4$, 2.0 and 3.0 are given in Fig. 23.7, 23.8. Figure 23.9 shows the displacement/movement of mean aerodynamic center of wing $\left[\bar{x}_{\dot{w}_{y\Delta}}\right]$ upon gradual entrance into gust at velocities,

which correspond to the Mach numbers indicated. For the case M = 2.0 points showed the results of the calculations by the numerical method of chapter of XXI.

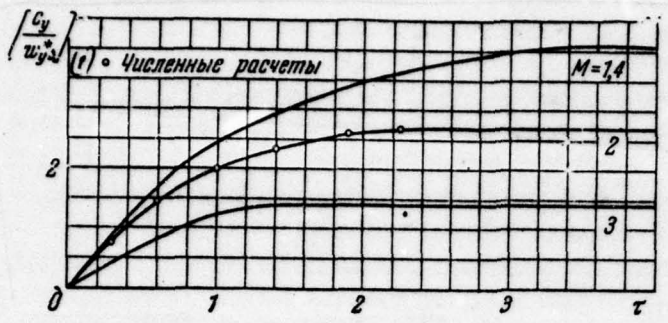


Fig. 23.7. Transient function of airfoil lift $\lambda = \infty$ upon the gradual entrance into step gust.

Key: (1). Numerical calculations.

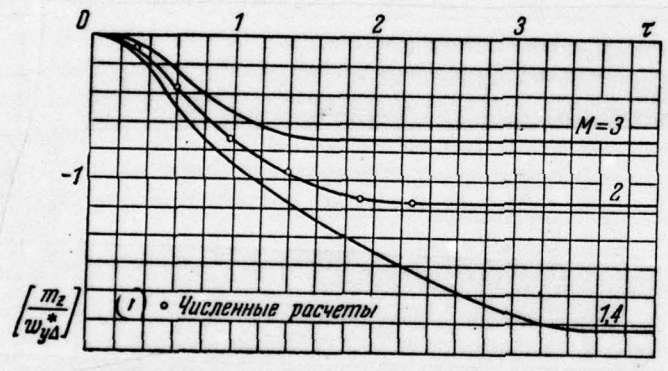


Fig. 23.8. Transient function of the pitching moment of wing $\lambda = \infty$ upon the gradual entrance into step gust, $x_T=0$.

Key: (1). Numerical calculations.

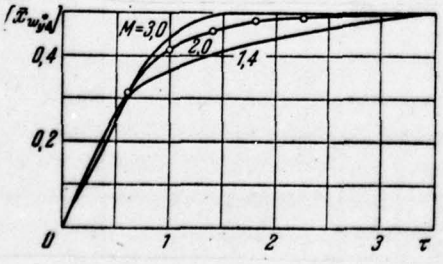


Fig. 23.9.

Fig. 23.9. Displacement/movement of mean aerodynamic center of wing $\lambda = \infty$ upon the gradual entrance into step gust.

§4. Transient functions of delta wings with supersonic edges.

Let us give the results, obtained in works [1.26], [1.78] for the transient functions of direct/straight delta wings, with supersonic edges, i.e., corresponding to condition $k\lambda \geqslant 4$. For such wings the transient function of the lift coefficient of section $\xi = \text{const}$ during a stepped variation in the angle of attack α is determined by the formulas:

$$\left.\begin{aligned}
&\text{with} \quad 0 \leqslant \tau \leqslant \frac{M}{M+1}\xi \quad \left[\frac{c'_{y\xi}}{\alpha^\circ}\right] = \frac{8\xi \operatorname{ctg}\chi_0}{M};\\
&\text{with} \quad \frac{M}{M+1}\xi \leqslant \tau \leqslant \frac{M}{M-1}\xi\\
&\left[\frac{c'_{y\xi}}{\alpha^\circ}\right] = \frac{8\xi \operatorname{ctg}\chi_0}{\pi k}\left[\arccos M\left(1 - \frac{k^2}{M^2}\frac{\tau}{\xi}\right) + \right.\\
&\left. + \frac{k}{M}\arccos M\left(1 - \frac{\xi}{\tau}\right) + \frac{k}{M}\sqrt{2\frac{\tau}{\xi} - \frac{k^2}{M^2}\frac{\tau^2}{\xi^2} - 1}\right];\\
&\text{with} \quad \frac{M}{M-1}\xi \leqslant \tau \leqslant \infty \quad \left[\frac{c'_{y\xi}}{\alpha^\circ}\right] = \frac{8\xi \operatorname{ctg}\chi_0}{\pi k}.
\end{aligned}\right\} \quad (23.6)$$

Here χ_0 is a sweep angle of leading wing edge.

For the transient functions of lift and pitching moment (relative to the leading edge/nose of root chord) we will obtain:

$$
\left.
\begin{aligned}
&\text{with} \quad 0 \leqslant \tau \leqslant \frac{M}{M+1} \quad \left[\frac{c_y}{\alpha^\circ}\right] = \frac{4}{M}\left(1 + \frac{\tau^2}{2M^2}\right), \\
&\qquad \left[\frac{m_z}{\alpha^\circ}\right] = -\frac{8}{3M}\left(1 + \frac{\tau^3}{2M^2}\right); \\
&\text{with} \quad \frac{M}{M+1} \leqslant \tau \leqslant \frac{M}{M-1} \quad \left[\frac{c_y}{\alpha^\circ}\right] = \frac{4}{\pi k}\arccos M\left(1 - \frac{k^2}{M^2}\tau\right) + \\
&+ \frac{4}{\pi M}\left(1 + \frac{\tau^2}{2M^2}\right)\arccos M\left(1 - \frac{1}{\tau}\right) + \\
&\qquad + \frac{2}{\pi M}(3 - \tau)\sqrt{2\tau - \frac{k^2}{M^2}\tau^2 - 1}, \\
&\left[\frac{m_z}{\alpha^\circ}\right] = -\frac{8}{3\pi k}\arccos M\left(1 - \frac{k^2}{M^2}\tau\right) - \\
&- \frac{8}{3\pi M}\left(1 + \frac{\tau^3}{2M^2}\right)\arccos M\left(1 - \frac{1}{\tau}\right) - \\
&\qquad - \frac{4}{9\pi M}\left(8 - \tau - \tau^2 - 2\frac{\tau^2}{M}\right)\sqrt{2\tau - \frac{k^2}{M^2}\tau^2 - 1}; \\
&\text{with} \quad \frac{M}{M-1} \leqslant \tau \leqslant \infty \quad \left[\frac{c_y}{\alpha^\circ}\right] = \frac{4}{k}, \quad \left[\frac{m_z}{\alpha^\circ}\right] = -\frac{8}{3k}.
\end{aligned}
\right\} \qquad (23.7)
$$

Page 558.

Upon the gradual entrance of tapered wing into step gust for an aerodynamic loading namely:

$$
\left.\begin{aligned}
&\text{with} \quad 0 \leqslant \tau \leqslant \frac{M}{M+1}\xi \quad \left[\frac{c'_{y\xi}}{\dot{w}_{y\Delta}}\right] = 0;\\
&\text{with} \quad \frac{M}{M+1}\xi \leqslant \tau \leqslant \frac{M}{M-1}\xi\\
&\left[\frac{c'_{y\xi}}{\dot{w}_{y\Delta}}\right] = \frac{8\xi \operatorname{ctg}\chi_0}{\pi k}\left\{\arccos M\left(1 - \frac{k^2}{M^2}\frac{\tau}{\xi}\right) + \right.\\
&\qquad \left. + \left(\frac{\tau}{\xi} - 1\right) k \operatorname{arch}\left(\frac{\tau}{\xi M\left|\frac{\tau}{\xi} - 1\right|}\right)\right\};\\
&\text{with} \quad \frac{M}{M-1}\xi \leqslant \tau \leqslant \infty \quad \left[\frac{c'_{y\xi}}{\dot{w}_{y\Delta}}\right] = \frac{8\xi \operatorname{ctg}\chi_0}{k}.
\end{aligned}\right\} \tag{23.8}
$$

The transient functions of the lift coefficients and pitching moment $(\bar{x}_T = 0)$ upon gradual entrance are determined by the formulas:

$$
\left.\begin{aligned}
&\text{with} \quad 0 \leqslant \tau \leqslant \frac{M}{M+1} \quad \left[\frac{c_y}{\dot{w}_{y\Delta}}\right] = \frac{4}{M}\tau^2, \quad \left[\frac{m_z}{\dot{w}_{y\Delta}}\right] = -\frac{8}{3M}\tau^3;\\
&\text{with} \quad \frac{M}{M+1} \leqslant \tau \leqslant \frac{M}{M-1} \quad \left[\frac{c_y}{\dot{w}_{y\Delta}}\right] = \frac{4}{\pi k}\arccos M\left(1 - \frac{k^2}{M^2}\tau\right) + \\
&\qquad + \frac{4\tau^2}{\pi M}\arccos M\left(1 - \frac{1}{\tau}\right) - \frac{4(\tau-1)^2}{\pi}\operatorname{arch}\left(\frac{\tau}{M|\tau-1|}\right),\\
&\left[\frac{m_z}{\dot{w}_{y\Delta}}\right] = -\frac{8}{3\pi k}\arccos M\left(1 - \frac{k^2}{M^2}\tau\right) - \frac{8\tau^3}{3\pi M}\arccos M\left(1 - \frac{1}{\tau}\right) + \\
&\qquad + \frac{4\tau^2}{3\pi M}\sqrt{2\tau - \frac{k^2}{M^2}\tau^2 - 1} + \\
&\qquad + \frac{4}{3\pi}\left[3(\tau-1)^2 + (\tau-1)^3\right]\operatorname{arch}\left(\frac{\tau}{M|\tau-1|}\right);\\
&\text{with} \quad \frac{M}{M-1} \leqslant \tau \leqslant \infty \quad \left[\frac{c_y}{\dot{w}_{y\Delta}}\right] = \frac{4}{k}, \quad \left[\frac{m_z}{\dot{w}_{y\Delta}}\right] = -\frac{8}{3k}.
\end{aligned}\right\} \tag{23.9}
$$

The lift coefficient of section ξ is as follows connected with section lift and the load:

$$
\left[\frac{c'_{y\xi}}{\dot{q}_i}\right] = \frac{2dY_\xi}{\rho_\infty U_0^2 b^2 d\xi} = 2\int_0^{\zeta_0}\left[\frac{\Delta\bar{p}}{\dot{q}_i}\right]d\zeta.
$$

[Page 559] Chapter XXIV.

PROCEDURE OF CALCULATION OF THE AERODYNAMIC WING CHARACTERISTICS OF ARBITRARY PLANFORM.

§1. Special feature/peculiarities of calculation procedure.

The basic idea of the method of the numerical flow-field analysis of the wings of arbitrary planform consists in the following. The wing and the range of effect outside wing are divide/marked off into unit cells by the lines, parallel to characteristic axes. For this the semirange of wing they divide into N of equal parts, whereupon real wing is replaced approximately by close wing with broken sonic edges. The values of the velocity potential ϕ and of its derivative $\partial\varphi/\partial y$ in each cell outside wing at each calculated moment of time are accepted as constants. Also as constants are accepted they, also, on wing during the solution of the problem of effect on the wing of harmonic gust. Below as examples in aperiodic problems in the ranges of integration, which do not emerge

beyond the limits of wing, values consider accurately in each cell, but in the problem of the effect of harmonic gust - the use of a theorem about "the average". The accuracy of numerical data to a great extent is determined by how close to real the broken wing, which consists of the whole cells. The greater the number N, into which is divide/marked off the semirange of wing, i.e., the thicker the grid, that more precise such replacement. Furthermore, with increase N increases the number of terms of the sums, which replace the integrals, with the aid of which is record/written the expression for a velocity potential.

During the solution of problem must be made a series of conditions, in particular the equality of zero load on trailing wing edges in the case of subsonic trailing wing edges (Chaplygina - Joukowski's hypothesis). In the case of subsonic leading edges at them appear the special feature/peculiarities (velocities and pressures go to infinity). Systematic investigations make it possible to control, does provide the selected diagram of numerical calculation at supersonic speeds the execution of the conditions indicated and special feature/peculiarities.

Page 560.

The adjustment of numerical calculation usually begins from the

application/use of a method for obtaining known, first of all of exact solutions.

One of the basic reception/procedures, establishing the practical convergence of numerical solutions, is their analysis at different values of N. The selection of the necessary number N is determined by this value, at which with the necessary accuracy it is possible to consider solution achieved its asymptotic value. In this case along with the selection of network density is conducted the selection of the intervals between the calculated torque/moments $\Delta\tau$, are reveal/detected some special feature/peculiarities of the procedure of calculation, etc. The important method of checking the accuracy of numerical calculations is the use of consequences of reciprocity theorem (see Chapter VII), valid within the framework of linear theory with any Mach numbers. In this case is conducted the calculation of direct/straight and reverse/inverse wings and the comparison of the corresponding aerodynamic coefficients. By utilizing Duhamel integral, it is possible from transient functions to find the coefficients of the aerodynamic derivatives of wing in all range of Strouhal numbers. This makes it possible to produce the verification of numerical data indicated by comparison with the coefficients, found directly.

For the checking of the accuracy of the calculations can be also

used two data points, obtained with $\tau \to 0$ and $\tau \to \infty$. With $\tau \to 0$ there are exact solutions, valid for any numbers M and wing planforms. Aerodynamic characteristics with $\tau \to \infty$ are obtained independently numerically or from the appropriate exact solutions of stationary problem.

It is possible to indicate one additional method of the integral verification of obtained data. For transient functions are determined the momentum/impulse/pulses (see §11 chapters VI), which must be equal to the appropriate coefficients of aerodynamic derivatives with points with very small Strouhal numbers.

And finally, the comparison of the accurately obtained theoretical and experimental data makes it possible to judge the correctness of the taken theoretical procedure for and the limits of its applicability, and also to carry out a cross check of calculation and experimental data.

§2. Distributed aerodynamic characteristics. Chaplygina - Joukowski's hypothesis.

It is interesting to explain, does provide the taken theoretical

diagram of numerical calculation reliable obtaining the distributed characteristics.

Page 561.

Let us note that for delta wings and the plate of infinite span are precise values of loads both for harmonic oscillations and any Strouhal numbers and for the arbitrary dependences of the kinematic parameters on time τ.

Let us examine the character of a change in the load chordwise in an example of the delta wing ($\chi_0 = 60°$), at whose leading edge subsonic, and rear are supersonic. For the value of number $M = \sqrt{2}$ from numerical calculation is determined the coefficient aerodynamic derivative dimensionless load p^a depending on the dimensionless coordinate $\bar{x}$ in three wing sections $\bar{z} = 2z/l = 0; 0.1; 0.3$ (Fig. 24.1). Here

$$p^a = \frac{4}{k}\frac{\partial\bar{\varphi}}{\partial\bar{x}},\ \bar{\varphi} = \frac{\varphi}{U_0 b},\ \bar{x} = \frac{x - x_0}{b'};$$

l is wingspan, b' is the current chord, x_0 is a coordinate of leading edge. Are given also curves, obtained from the exact solution of problem. For a central wing section, which is special (apex/vertex of wing is point of inflection), value p^a is constant on $\bar{x}$. For any other wing section with subsonic leading edges the coefficient of

aerodynamic derivative p^{α} with approach to leading edge approaches infinity. Since wing in this section has supersonic trailing edge, value p^{α} is here final. Numerical data will agree well with exact solution.

Let us examine sweptback wing ($\lambda \operatorname{tg} \chi_0 = 8,\ k\lambda = 6,\ \eta = 1$) with leading and trailing subsonic edges, and also the reverse/inverse delta wing ($\lambda \operatorname{tg} \chi_0 = 0,\ k\lambda = 2{,}4,\ \eta = \infty$), at whose leading edge supersonic, and rear are subsonic with $M = \sqrt{2}$. For these wings of exact solutions no; therefore the numerical calculation of the derivative of pressure coefficient p^{α} conducted shows, how taken a calculation procedure provides satisfaction of the condition of the equality of zero load on trailing subsonic wing edge and do appear special feature/peculiarities of the front/leading stern of wing.

Figure 24.2 lepicts load distribution chordwise in the form of dependences $p^{\alpha}(\bar{x})$ for a sweptback wing and its three sections according to the spread/scope: $\bar{z}$ = 0; 0.21; 0.71.

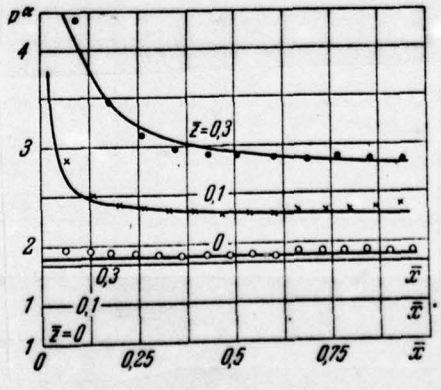


Fig. 24.1.

Fig. 24.1. Load distribution chordwise of delta wing ($\chi_0 = 60°$) during $M = \sqrt{2}$. Curves are exact solution, points are a numerical calculation.

Page 562.

A somewhat different picture is observed for a wing with supersonic front/leading and subsonic rear by edges (reverse/inverse delta wing). For this wing and all examined sections ($\bar{z}$ = 0; 0.2; 0.6) the constant value load coincides with exact solution ($p^{\alpha} = 4/k$) to the half of wing chord ($0 \leqslant \bar{x} < 0.5$). With approach/approximation to trailing wing edge, the load factor decreases, turning in zero with $\bar{x}$ = 1.0 (Fig. 24.3). Curves, depicted in Fig. 24.2 and 24.3, are carried out through the points, which are obtained in numerical calculations. The execution of Chaplygina - Joukowski's hypothesis can be judged from the tendency of the behavior of curves near rear the lumps of wing ($\bar{x}$ = 1).

§3. Comparison of numerical calculations with exact solutions.

Let us compare the results of numerical calculation with exact solutions. This will make possible to rate/estimate the reliability of the taken procedure for. Let us conduct this comparison for the most complex case - the arbitrary dependence of the kinematic parameters on time τ.

Let us examine the coefficients of the transient functions of load, of lift and pitching moment during an instantaneous change in the kinematic parameters of motion q_i in time along stepped law ($q_i = \alpha, \omega_z, \omega_x$) and at the gradual entrance of wing into step gust.

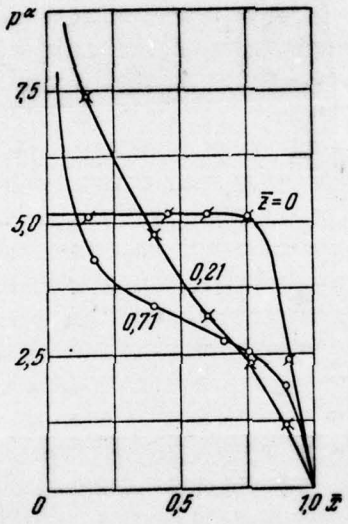


Fig. 24.2.

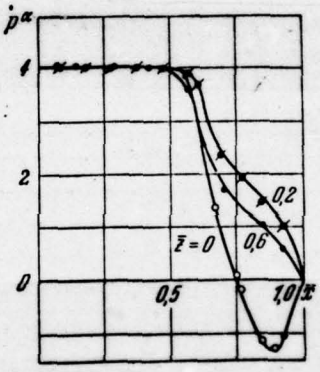


Fig. 24.3.

Fig. 24.2. To the execution of Chaplygina - Joukowski's hypothesis. Sweptback wing ($k\lambda = 6$, $\lambda \operatorname{tg} \chi_0 = 8$, $\eta = 1$).

Fig. 24.3. To the execution of Chaplygina - Joukowski's hypothesis.

Reverse/inverse delta wing ($k\lambda = 2.4$, $\lambda \operatorname{tg} \chi_0 = 0$, $\eta = \infty$).

Page 563.

The dependence of relation $[\Delta\bar{p}\ (\tau)\ /\alpha^*] / [\Delta\bar{p}\ (\infty)\ /\alpha^*]$ on value $\frac{M-1}{M}\tau$ is shown in Fig. 24.4 for a direct/straight delta wing with supersonic edges ($\operatorname{tg}\chi_0/k = 0{,}83$) and an infinite plate ($\lambda = \infty$). Load at the end/lead of the root chord (point A in Fig. 24.4) is determined for a number $M = 1{,}93$. The dependences of the total coefficients of transient functions during an instantaneous change in the kinematic parameters of motion α, ω_z and ω_{x1} from dimensionless time τ are given in Fig. 24.5-24.11, whereupon Fig. 24.5 is related to rectangular wings (including $\lambda = \infty$) - for number $M = \sqrt{2}$, Fig. 24.6-24.8 - for $M = 2$. Figures 24.9, 24.10 show the gradual entrance of rectangular wing into gust. Fig. 24.11 is related to direct/straight delta wing with subsonic leading edge ($\operatorname{tg}\chi_0/k = 1{,}43$, $M = 1{,}8$). In all figures are given precise or known solutions, borrowed from works [1.63], [1.78], [2.26], [2.36]. In this case the points $\tau = 0$ answer the exact solution of problem, and value $\tau \to \infty$ they correspond to the coefficients of aerodynamic derivatives without points. If during an instantaneous change in the kinematic parameters the coefficients of transient functions with $\tau = 0$ are final and depend only on number M that upon the gradual entrance of wing into

gust ($\tau = 0$) they they turn into zero. In all cases in question is observed the good agreement of exact solution with the results of numerical calculation, and also the output/yield of the studied characteristics to their steady-state values.

For the illustration of the accuracy of numerical calculation let us examine the aerodynamic characteristics of the triangular deformed wing with supersonic leading edge ($\chi_0 = 60°$, $M = 4{,}12$), for which were carried out the comparisons with exact solutions [1.54], [1.84]. The strain of this wing was assigned in the form

$$\eta = \sum_{\mu=1}^{5} \sum_{\nu=0}^{3} \xi^{\mu} \zeta^{2\nu}.$$

Then lift coefficient can be represented thus:

$$c_y = \sum_{\mu=1}^{5} \sum_{\nu=0}^{3} c_{y\mu\nu}.$$

In table on page 566 are given precise values of relation $c_{y\mu\nu}/c_{y10}$ (second columns) and the results of the numerical calculation (first columns), made for number N, into which is divided the semirange of wing, equal to 30.

Page 564.

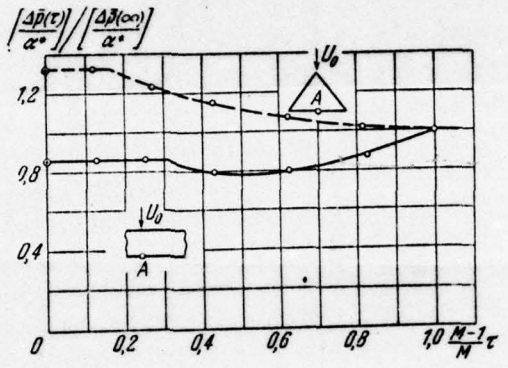


Fig. 24.4. Comparison of numerical calculations (white point) with exact solutions (curved and black points) $(M=\sqrt{2})$.



Fig. 24.5. Comparison of numerical calculations (white point) with exact solutions (unbroken curve and black point). Rectangular wings $(M=\sqrt{2})$.

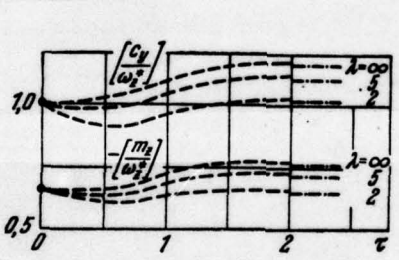


Fig. 24.6.

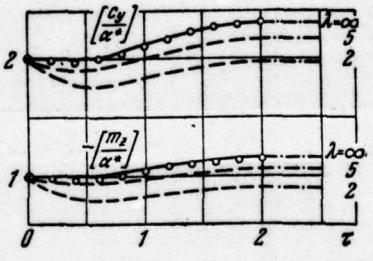


Fig. 24.7.

Fig. 24.6. Comparison of numerical calculations (dotted line) with exact solutions (black points, dot-dash line). Rectangular wings $(M=2,\ \bar{x}_T=0)$.

Fig. 24.7. Comparison of numerical calculations (dotted line) with exact solutions (black points, dot-dash line). Rectangular wings ($M=2$, $\bar{x}_T=0$).

Page 565.

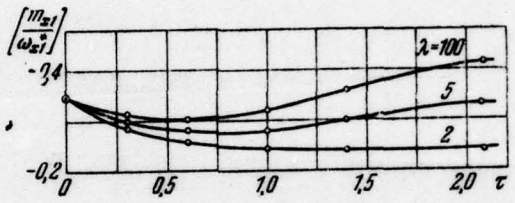


Fig. 24.8. Comparison of numerical calculations white points) with exact solutions (black point). Rectangular wings ($M=2$).

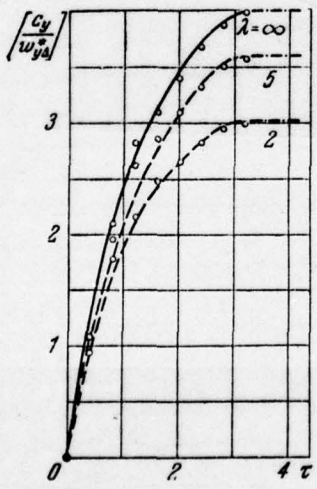


Fig. 24.9.

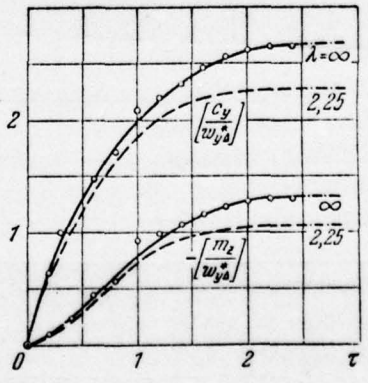


Fig. 24.10.

Fig. 24.9. Comparison of numerical calculations (white point and dotted curves) with exact solutions (black point, continuous and dot-dash curves). Rectangular wings ($M=\sqrt{2}$).

Fig. 24.10. Comparison of numerical calculations (white point and dotted curves) with exact solutions (black point, unbroken curves dot-dash lines. Rectangular wings ($M=1,8$). $\bar{x}_T=0$.

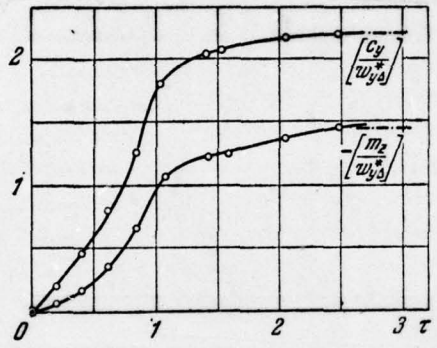


Fig. 24.11. Comparison of numerical calculations (white point and unbroken curves) with exact solutions (black point, strix-dotted line). Direct/straight delta wing ($\operatorname{tg}\chi_0/k=1,43$, $M=1,8$). $\bar{x}_T=0$.

μ	ν=0		ν=1		ν=2		ν=3	
1	1.00	1,00	0,054	0,055	0,0070	0,0073	0,0012	0,0013
2	1,35	1,33	0,086	0,088	0,011	0,012	0,0022	0,0023
3	1,53	1,50	0,107	0,110	0,016	0,016	0,0029	0,0036
4	1,65	1,60	0,121	0,126	0,018	0,019	0,0034	0,0037
5	1,73	1,67	0,131	0,138	0,020	0,022	0,0039	0,0043

From the given in table data it follows that for the examined deformed wing is obtained a good coincidence of numerical calculation with the appropriate exact solution. Furthermore, number N = 30 is sufficient for obtaining acceptable aerodynamic characteristics.

§4. Effect of the number of separations into the accuracy of the calculation.

Much study on developing the rational procedure of numerical calculations were carried out by N. A. Kudryavtsevoy, N. G. Lavrenko for an harmonic time dependence and by S. A. Popytalov during a stepped variation in the kinematic parameters.

Let us examine at first the harmonic oscillations of rigid wings. For the purpose of the explanation of the question concerning the effect of network density, by which is replaced the wing being investigated, were carried out the calculations of the coefficients aerodynamic derivative following wings: triangular with subsonic ($\operatorname{tg}\chi_0/k = 1{,}67$, $k\lambda = 2{,}4$, $M = \sqrt{2}$) and supersonic ($\operatorname{tg}\chi_0/k = 0{,}5$, $k\lambda = 8$, $M = 2{,}24$) by leading edges; complex planform with that which was mixed front/leading and supersonic rear by edges ($\chi_0^{(2)} = 30°$, $M = 1{,}5$ and $M = 2{,}5$). The results of the calculations for delta wings are represented in Fig. 24.12-24.17, on which are plotted/applied precise values appropriate characteristics. Figure 24.18-24.23 gives the results of the calculations for the wings of complex planform. From the given materials it follows that during an increase in number N (curve/graphs bear conditional character, since number N can be only whole) of the value of aerodynamic derivatives sufficiently rapidly they emerge at asymptotic values, whereupon for delta wings somewhat more rapid than for the wings of complex planform.

For delta wings there are exact solutions. At sufficiently large values of N the results of the calculations virtually coincide with them.

Page 567.

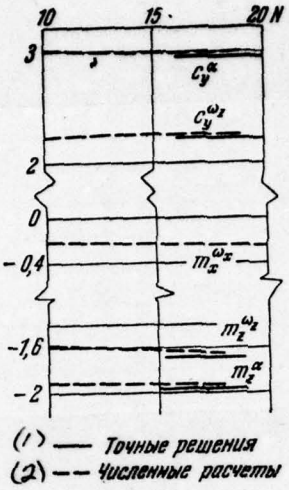


Fig. 24.12.

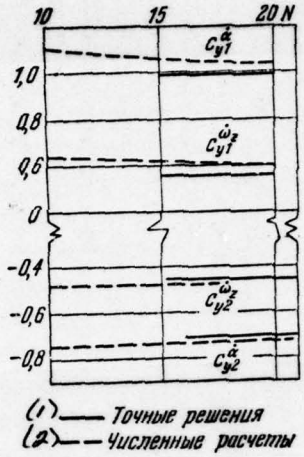


Fig. 24.13.

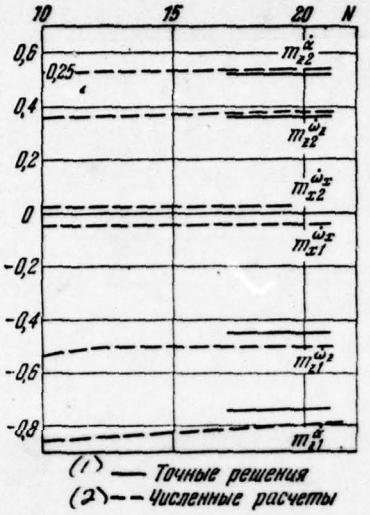
Fig. 24.12.
Effect of the number of separations N for a delta wing $\frac{\text{tg}\,\chi_0/k = 1{,}67,\ k\lambda = 2{,}4}{(M = \sqrt{2})}$.

Key: (1). Exact solutions. (2). Numerical calculations.

Fig. 24.13. Effect of the number of separations N for a delta wing $\frac{\text{tg}\,\chi_0/k = 1{,}67,\ k\lambda = 2{,}4}{(M = \sqrt{2})}$.

Key: (1). Exact solution. (2). Numerical calculations.

Fig. 24.14.



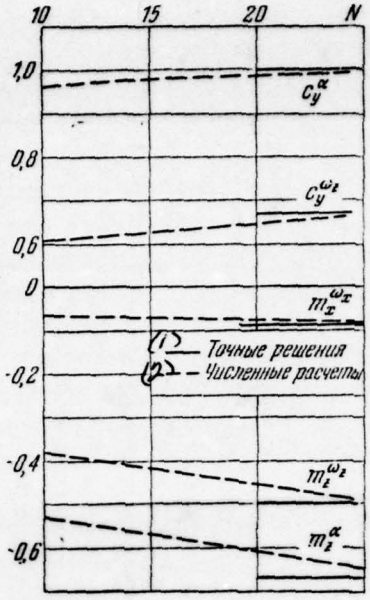


Fig. 24.15.

Fig. 24.14. Effect of the number of separations N for a delta wing ($M = \sqrt{2}$, $\operatorname{tg}\chi_0/k = 1{,}67$, $k\lambda = 2{,}4$).

Key: (1). Exact solutions. (2). Numerical calculations.

Fig. 24.15.

Effect of the number of separations N for a delta wing ($M = 2{,}24$, $\operatorname{tg}\chi_0/k = 0{,}5$, $k\lambda = 8$).

Key: (1). Exact solutions. (2). Numerical calculations.

Page 568.

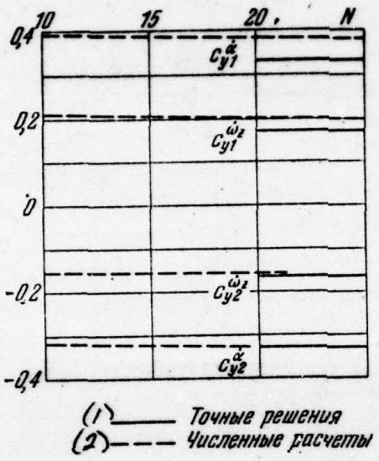


Fig. 24.16.



Fig. 24.17.

Fig. 24.16. Effect of the number of separations N for a delta wing $(M = 2,24).^{\operatorname{tg}\chi_0/k = 0,5,\quad k\lambda = 8}$

Key: (1). Exact solutions. (2). Numerical calculations.

Fig. 24.17. Effect of the number of separations N for a delta wing $(M = 2,24).^{\operatorname{tg}\chi_0/k = 0,5,\quad k\lambda = 8}$

Key: (1). Exact solutions. (2). Numerical calculations.

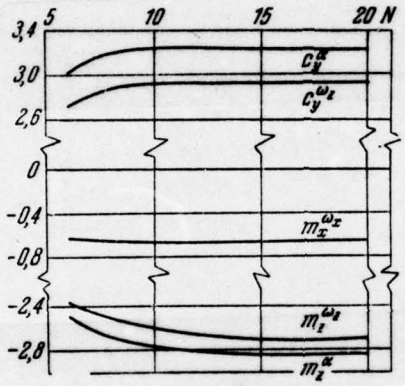


Fig. 24.18.

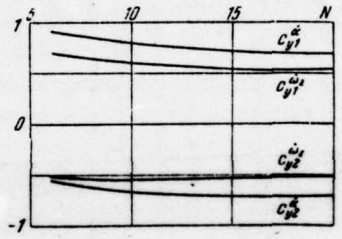


Fig. 24.19.

Fig. 24.18. The effect of the number of separations N for the wing of complex planform $\chi_0^{(2)} = 30°$ (M = 1,5).

Fig. 24.19. Effect of the number of separations N for the wing of complex planform $\chi_0^{(2)} = 30°$ (M = 1,5).

Page 569.

As can be seen from the presented in Fig. 24.12-24.23 data, for providing an identical accuracy the calculation of the coefficients of aerodynamic derivatives with points must be performed at the large values of N, rather than the corresponding coefficients without points. This completely is regular, if one considers that in the second case during the calculation of derivatives the velocity potentials are summarized only for trailing wing edge, but in the first - for entire wing. Let us note that the greatest disagreement of the numerical and precise values of velocity potential is obtained in cell at the apex/vertex of wing. With removal/distance from apex/vertex, this inaccuracy decreases and on trailing edge virtually is absent.

Let us examine the arbitrary dependences of the kinematic parameters on time τ. So as for harmonic oscillations, let us conduct the investigation of the effect of the number of separations N into the coefficients of transient functions with one constant interval between the calculated moments of time $\Delta\tau = 0.2$.

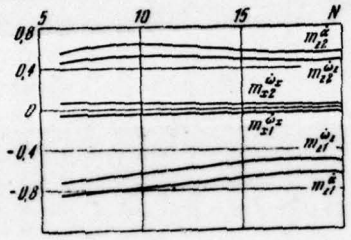


Fig. 24.20.

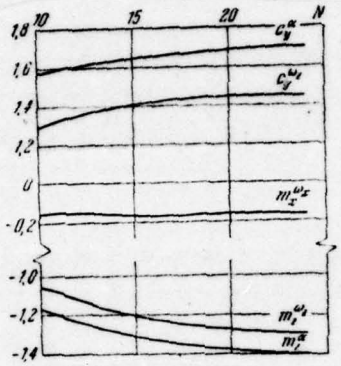


Fig. 24.21

Fig. 24.20. Effect of the number of separations N for the wing of complex planform $\chi_0^{(2)} = 30°$ (M = 1,5).

Fig. 24.21. Effect of the number of separations N for the wing of complex planform $\chi_0^{(2)} = 30°$ (M = 2,5).

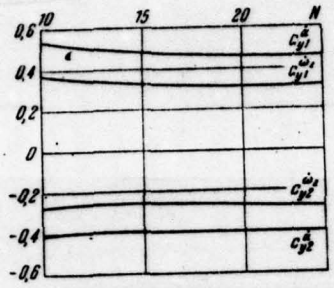


Fig. 24.22.

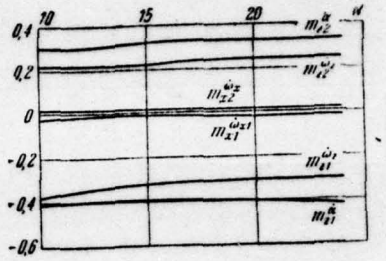


Fig. 24.23.

Fig. 24.22. Effect of the number of separations N for the wing of complex planform $\chi_0^{(2)} = 30°$ (M = 2,5).

Fig. 24.23. Effect of the number of separations N for the wing of complex planform $\chi_0^{(2)} = 30°$ (M = 2,5).

Page 570.

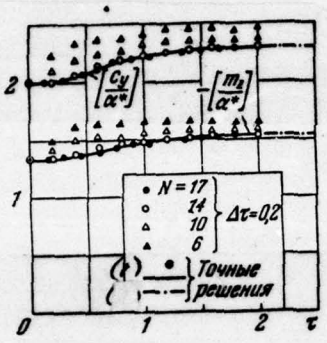


Fig. 24.24.

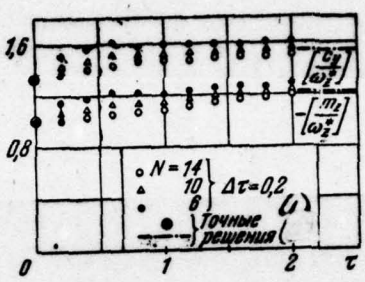


Fig. 24.25.

Fig. 24.24. Effect of the number of separations N for a direct/straight delta wing $\lambda = 3.0$; $\bar{x}_T = 0$ (M = 2,0).

Key: (1). Exact solutions.

Fig. 24.25. Effect of the number of separations N for a direct/straight delta wing $\lambda = 3.0$, $\bar{x}_T = 0$ (M = 2,0).

Key: (1). Exact solutions.

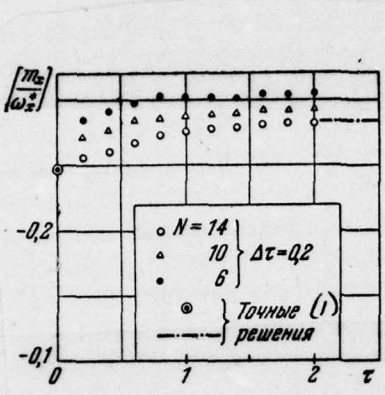


Fig. 24.26.

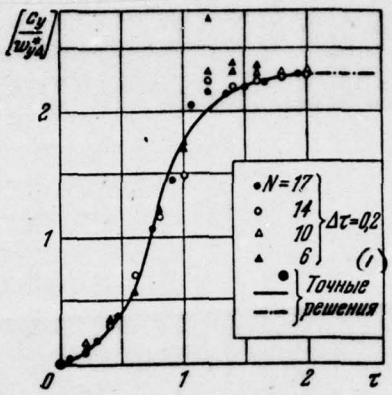


Fig. 24.27.

Fig. 24.26. Effect of the number of separations N for a direct/straight delta wing $\lambda = 3.0$ (M=2,0).

Key: (1). Exact solutions.

Fig. 24.27. Effect of the number of separations N for a direct/straight delta wing $\lambda = 3.0$ (M=2,0).

Key: (1). Exact solutions.

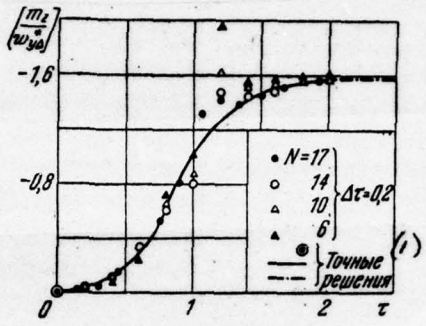


Fig. 24.28. Effect of the number of separations N for a direct/straight delta wing $\lambda = 3.0$, $x_T=0$ (M = 2,0).

Key: (1). Exact solutions.

Page 571.

Let us examine at first the delta wing of lengthening $\lambda = 3$ with supersonic edges. The number of sections of the separation of the

semirange of wing N was assigned to 17, while the number of sections of the separation of chord N' was obtained in this case to 13. Between N and N' - is following communication/connection:

$$N' = N\frac{2b}{lk}, \quad k = \sqrt{M^2 - 1}.$$

Here b and l are a chord and the spread/scope of wing.

Figure 24.24-24.26 gives the results of the numerical calculation of this wing with $M = 2{,}0$ for the case of a stepped variation in the kinematic parameters in time (α-, ω_z- and ω_x- problems). The same data are acquired for the gradual entrance of wing into step gust (Figs. 24.27, 24.28). Precise values of the corresponding characteristics at zero time ($\tau = 0$) are designed by formulas (4.41) - (4.57), the beginning of dot-dash line indicates the end/lead of the transient process, and lines themselves they answer the steady-state values of aerodynamic characteristics. The available exact solutions are plotted/applied on the curve/graphs by solid line.

Let us note that the given in this paragraph values of the rolling-moment coefficients are calculated with significant dimension l.

From the analysis of the given characteristics it is possible to

draw the conclusion that for the wing of simple planform already N = 15-20 is sufficient for providing the necessary accuracy. The greatest errors are obtained with small τ. In the case of the gradual entrance of wing into gust the effect of network density manifests itself in essence at values τ, close to unity; however, even, here the number of separations of order N = 20-25 sufficiently for obtaining reliable results.

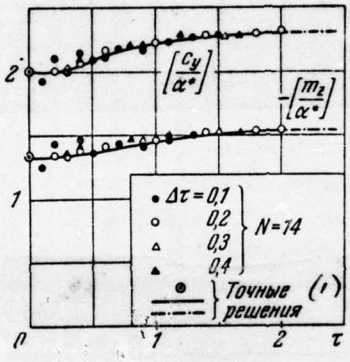


Fig. 24.29.

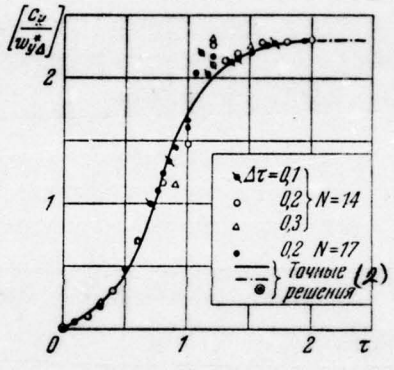


Fig. 24.30.

Fig. 24.29. Effect of the calculated moments of time $\Delta\tau$ for a direct/straight delta wing λ = 3.0, $\bar{x}_T$=0 (M = 2,0).

Key: (1). Exact solutions.

Fig. 24.30. Effect of the calculated moments of time $\Delta\tau$ for a direct/straight delta wing λ = 3.0 (M = 2,0).

Key: (1). Exact solutions.

Page 572.

Examining the effect of estimated time $\Delta\tau$, we see that the best results are obtained for the interval of order $\Delta\tau = 0.1\text{-}0.2$ (Fig. 24.29-24.31). During a decrease in the time interval the accuracy descends, when interval approaches value $1/N'$, while with an increase in the interval deterioration in the accuracy is caused by exaggerated spaces during numerical differentiation. This picture is observed for wings with supersonic and subsonic edges.

The conducted investigations show that the greatest scatter of the calculation points is obtained, obviously, when during a change in the time occurs an abrupt change in the boundary conditions. During an instantaneous change in the kinematic parameters in stepped law this occurs near $\tau = 0$. Upon the gradual entrance into gust, especially for the wing of triangular or close to it form, this occurs near the values τ, which correspond to the complete entrance of wing into step gust ($\tau = 1.0$).

For conducting the calculations it is possible to recommend following. Are selected parameters N or N' on the basis of possibilities EVM [computer]. In this case one should

consider that excessively an increase in the number of cells produces an increase in the duration of count. To take N and N* than less recommended (N = 20-25) does not follow. Time interval $\Delta\tau$ can be selected on the approximate empirical dependence $\Delta\tau \approx 2/N^*$.

§5. Checking of numerical calculations with the aid of reciprocity theorem.

The use of consequences, which escape/ensue from reciprocity theorem, makes it possible to conduct testing the numerical values of the coefficients aerodynamic derivative and transient functions. The consequences indicated are valid for the arbitrary values of Strouhal numbers, Makh and any τ; therefore the checking of the obtained from numerical calculation coefficients aerodynamic derivative and transient function is carried out for entire range p * and dimensionless time τ.

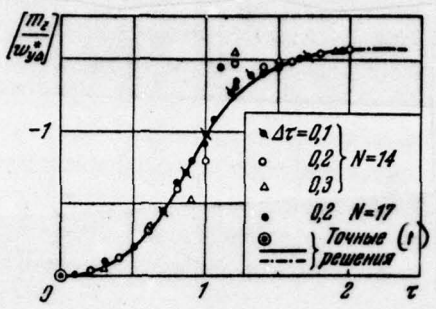


Fig. 24.31. Effect of the calculated moments of time $\Delta\tau$ for a direct/straight delta wing $\lambda = 3.0$, $\bar{x}_T = 0$ (M = 2,0).

Key: (1). Exact solutions.

Page 573.

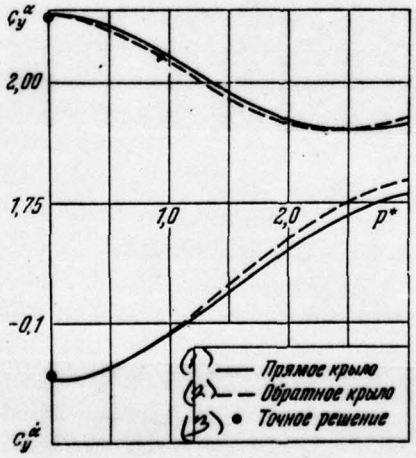


Fig. 24.32.

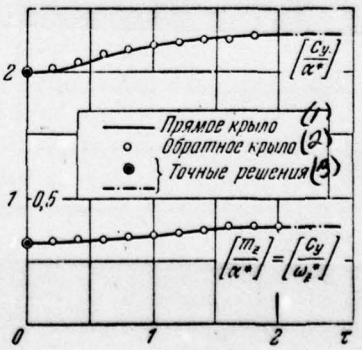


Fig. 24.33.

Fig. 24.32. To the checking of numerical calculations with the aid of reciprocity theorem. Delta wings $\operatorname{tg}\chi_0/k = 1{,}25$ $(M = 2{,}0)$.

Key: (1). Straight wing. (2). Reverse/inverse wing. (3). Exact solution.

Fig. 24.33. To the checking of numerical calculations with the aid of the theorem of invertibility. Delta wings $\operatorname{tg}\chi_0/k = 1{,}25$, $\bar{x}_T = 0{,}5$ $(M = 2{,}0)$.

Key: (1). Straight wing. (2). Reverse/inverse wing. (3). Exact solutions.

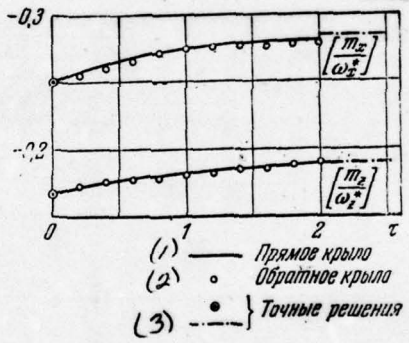


Fig. 24.34.

Fig. 24.34. To the checking of numerical calculations with the aid of reciprocity theorem. Delta wings $\operatorname{tg}\chi_0/k = 1{,}25$, $\bar{x}_T = 0{,}5$ $(M = 2{,}0)$.

Key: (1). Straight wing. (2). Reverse/inverse wing. (3). Exact solutions.

Page 574.

In Fig. 24.32 is carried out the comparison of numerical these derivatives c_y^{α} and $c_y^{\dot{\alpha}}$, obtained for a straight line and reverse/inverse delta wings with subsonic edges ($\operatorname{tg}\chi_0/k = 1{,}25$, $M = 2{,}0$) at the values of Strouhal number $0 \leqslant p^* \leqslant 3$.

Let us examine an instantaneous change in the kinematic parameters (α-, ω_z-, ω_x problems) for the same direct/straight and reverse/inverse delta wings with subsonic edges ($\operatorname{tg}\chi_0/k = 1{,}25$, $M = 2{,}0$) (Figs. 24.33, 24.34). The comparison of numerical calculations for these wings shows that with selected N and $\Delta\tau$ are fulfilled sufficiently well the consequences of reciprocity theorem, also, for aperiodic motion. The points, which correspond to the exact solution of problem with $\tau = 0$, completely satisfactorily they coincide with numerical calculations.

Thus, the reciprocity theorem is a good method of the control of numerical data for aerodynamic wing characteristics both at the arbitrary law of a change in the kinematic parameters in time and at harmonic dependences also at supersonic speeds.

§6. Checking of numerical calculations with the aid of the theorem of momentum and Duhamel integral.

As the important means of testing the results of the calculation serves theorem of momentum (see Chapter VI), according to which

$$I\left(\frac{c}{q_i^*}\right)=\int_0^\infty \left\{\left[\frac{c(\tau)}{q_i^*}\right]-\left[\frac{c(\infty)}{q_i^*}\right]\right\} d\tau = c^{\phi_i}|_{p^*\to 0}.$$

Here c is a coefficient of aerodynamic characteristics, q_i is the kinematic parameter $(\alpha, \omega_z, \omega_x)$.

Let us examine infinite-span wings ($\lambda = \infty$) and rectangular with lengthening $\lambda = 2$ and $\lambda = 5$, and also straight line and reverse/inverse delta wings with subsonic leading edges $\operatorname{tg}\chi_0/k = 1{,}25$, $\operatorname{tg}\chi_0/k = 1{,}43$ (Fig. 24.35-24.37). Transient functions for these wings are given above. The coefficients of aerodynamic derivatives with points c_y^{α}, m_z^{α}, $c_y^{\omega_z}$, $m_z^{\omega_z}$ with $p^* \to 0$ are obtained for two Mach numbers: $M=\sqrt{2}$ and $M=2$, but the aerodynamic coefficients with points, caused by harmonic gust, $c_y^{\dot{\Delta}}$ and $m_z^{\dot{\Delta}}$ ($p^* \to 0$) - with number $M = 1{,}8$. Along the axis of abscissas on these diagrams is deposit/postponed the value of the momentum/impulse/pulse of the corresponding transient function $I(c/q_i^*)$. Straight line, carried out at an angle of 45° to

axes, corresponds to the ideal execution of theorem of momentum.

Page 575.

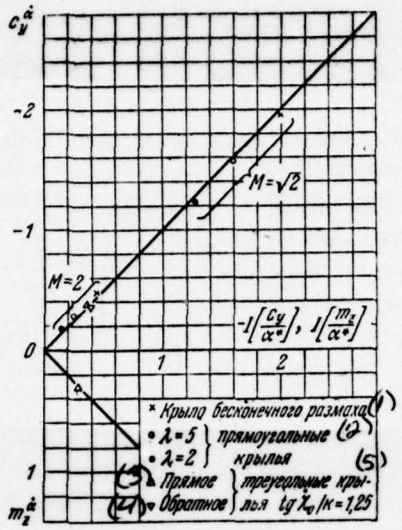


Fig. 24.35.

Fig. 24.35. Checking of numerical calculations with the aid of theorem of momentum.

Key: (1). Infinite-span wing. (2). rectangular wings. (3). Straight line. (4). Reverse/inverse. (5). triangular wings.

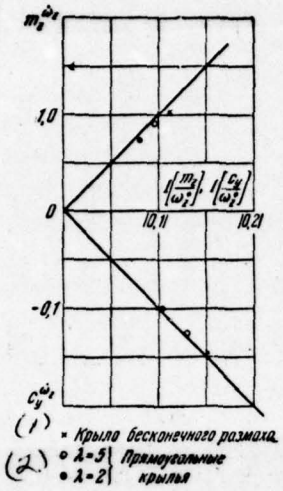


Fig. 24.36.

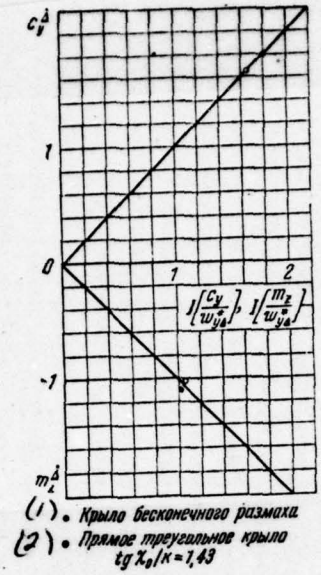


Fig. 24.37.

Fig. 24.36. Checking of numerical calculations with the aid of theorem of momentum.

Key: (1). Infinite-span wing. (2). Rectangular wings.

Fig. 24.37. Checking of numerical calculations with the aid of theorem of momentum.

Key: (1). Infinite-span wing. (2). Direct/straight delta wing.

Page 576.

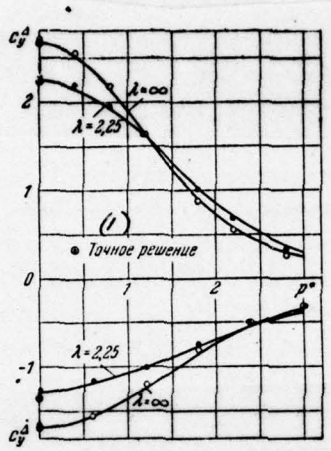


Fig. 24.38.

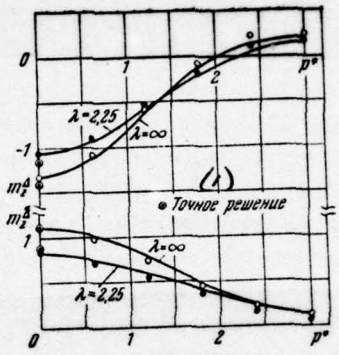


Fig. 24.39.

Fig. 24.38. To the checking of numerical calculations (point) with the aid of Duhamel integral (curves). Rectangular wing (M = 1,8).

Key: (1). Exact solution.

Fig. 24.39. To the checking of numerical calculations (point) with the aid of Duhamel integral (curves). Rectangular wing ($\bar{x}_T$ = 0, M = 1,8).

Key: (1). Exact solution.

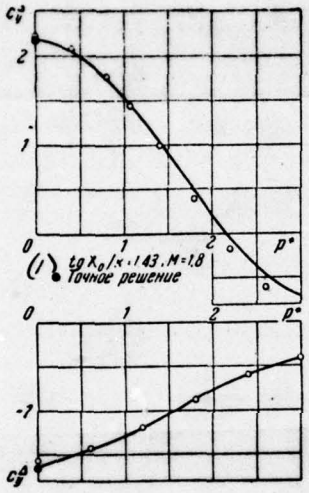


Fig. 24.40.

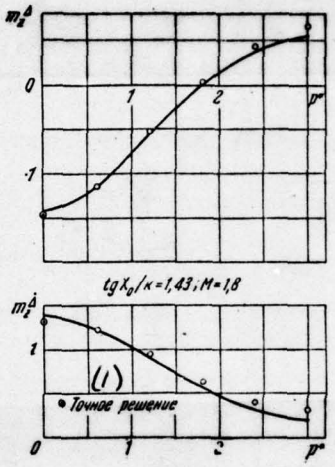


Fig. 24.41.

Fig. 24.40. To the checking of numerical calculations (point) with the aid of Duhamel integral (curves). Delta wing ($tg\,\chi_0/\kappa = 1{,}43$, $M = 1{,}8$)

Key: (1). Exact solution.

Fig. 24.41. To the checking of numerical calculations (point) with the aid of Duhamel integral (curves). Delta wing ($\operatorname{tg}\chi_0/k = 1{,}43$, $M = 1{,}8$, $\bar{x}_T = 0$).

Key: (1). Exact solution.

Page 577.

Checking of numerical data can be carried out also with the aid of Duhamel integral (see Chapter VI). Utilizing transient functions, we compute the coefficients of aerodynamic derivatives over a wide range of Strouhal numbers. Their comparison with the results of directly numerical calculation makes it possible to produce the verification of obtained data.

For an infinite plate, a rectangular wing $\lambda = 2.25$ and a direct/straight delta wing with subsonic leading edge ($\operatorname{tg}\chi_0/k = 1{,}43$) with number $M = 1{,}8$ were determined the aerodynamic derivatives c_y^{Δ}, $c_y^{\dot{\Delta}}$, m_z^{Δ}, $m_z^{\dot{\Delta}}$, caused by the effect of harmonic gust on the wings indicated.

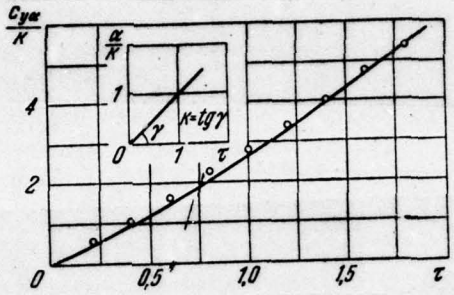


Fig. 24.42.

Fig. 24.42. The comparison of exact solution (is curve) with the calculation according to Duhamel integral (point) for a wing λ = ∞ (M = 1,4).

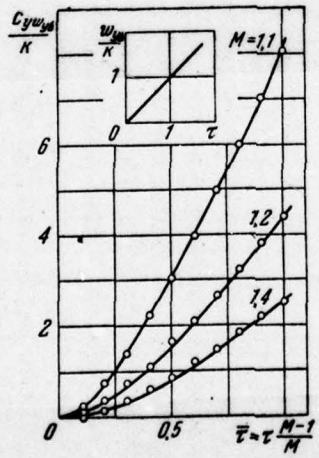


Fig. 24.43

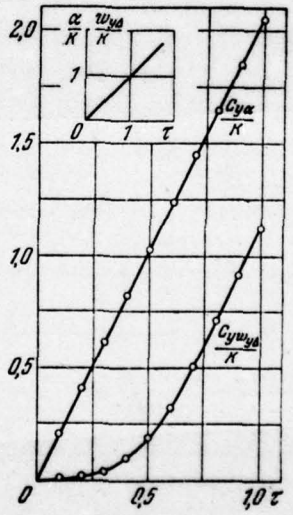


Fig. 24.44.

Fig. 24.43. Comparison of exact solution (curves) with the calculation according to Duhamel integral (point) for a wing $\lambda = \infty$ (M = 1,4).

Fig. 24.44. Comparison of exact solution (curves) with the calculation according to Duhamel integral (point) for a delta wing $\lambda = 2.5$ (M = 3).

Page 578.

On curve/graphs (Fig. 24.38-24.41) are given exact solutions for the derivatives in question with very small Strouhal number ($p^* \longrightarrow 0$).

The use of a Duhamel integral makes it possible also to determine aerodynamic characteristics for any law of a change in the kinematic parameters in time, knowing transient functions during their stepped change.

Let us make a comparison of the obtained thus lift coefficient with its value, determined by direct method - numerically or from exact solution for the linearly growing gust. For an infinite plate $\lambda = \infty$ (M = 1,4) are given the lift coefficients with an instantaneous change in the angle of attack $c_{y\alpha}$ (Fig. 24.42) and the upon gradual entrance into gust $c_{yw_{y\Delta}}$ (Fig. 24.43). For a delta wing $\lambda = 2.5$ (M = 3) the same data are represented in Fig. 24.44.

All the given materials show that the obtained from indirect

calculation aerodynamic characteristics for linearly the growing gust coincide sufficiently well with the appropriate characteristics, obtained by the direct solution of problem.

§7. Comparison of experimental and calculated data.

Experimental data in different time were obtained by V. S. Bykov, Yu. A. Prudnikov, V. S. Khomenko et al., and also Skretonom and Vudgetom [2.41]. Is given below the comparison of experimental data with numerical calculations, whereupon the primary attention is devoted to unsteady aerodynamic characteristics. In certain cases the comparison of experimental and theoretical data to conveniently carry out in the similarity parameters.

Figures 24.45, 24.46 depict to the dependence $kc_y^{\omega_z}$, $km_z^{\omega_z}$ on the given lengthening for delta wings with different sweep angles on the leading edge: $\chi_0 = 45°, 60°, 75°$. Derivatives $c_y^{\omega_z}$ and $m_z^{\omega_z}$ are determined from experiment by the method of the bent models (see Chapter VIII). Everywhere on curve/graphs together with experimental points are plotted/applied the calculated curves, obtained from linear theory. These experiments are carried out by V. S. Bykov and Yu. A. Prudnikov. From curve/graphs it follows that for entire range of the

parameters being investigated, which determine the geometry of wing and the mode/conditions of flow, the calculation sufficiently satisfactorily converges with experiment. The use of coordinates, which are the similarity parameters in linear theory (coefficients of aerodynamic derivatives without points), makes it possible to construct more compact dependences not only for theoretical, but also for experimental data.

Page 574.

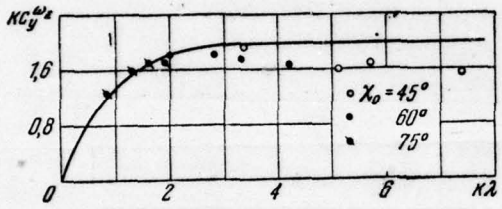


Fig. 24.45.

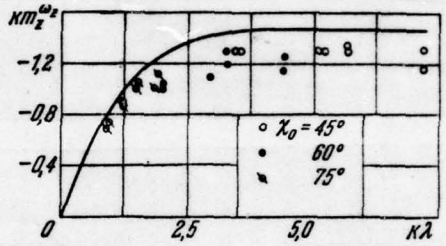


Fig. 24.46.

Fig. 24.45. The comparison of experimental (point) and calculated (is curve) data for delta wings $(\bar{x}_T - 0)$.

Fig. 24.46. The comparison of experimental (point) and calculated (is curve) data for delta wings $(\bar{x}_T - 0)$.

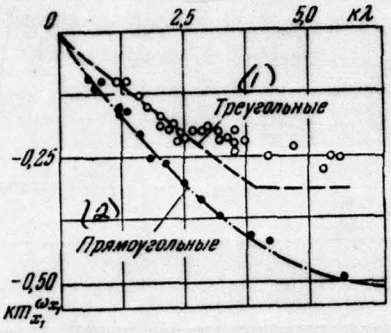


Fig. 24.47.

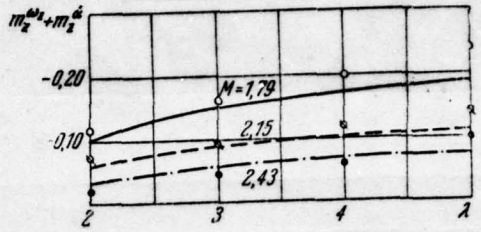


Fig. 24.48.

Fig. 24.47. Comparison of experimental (point) and calculated (curves) data for rectangular and delta wings.

Key: (1). Triangular. (2). Rectangular.

Fig. 24.48. Comparison of experimental (point) and calculated (curves) data for rectangular wings ($\bar{x}_T = 0.5$).

Page 580.

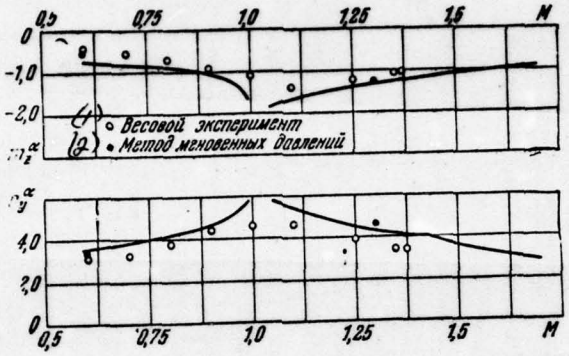


Fig. 24.49.

Fig. 24.49. Comparison of experimental (point) and calculated (curves) data for a delta wing $\chi_0 = 45°$ ($\bar{x}_T = 0{,}37$).

Key: (1). Weight experiment. (2). Method of instantaneous pressures.

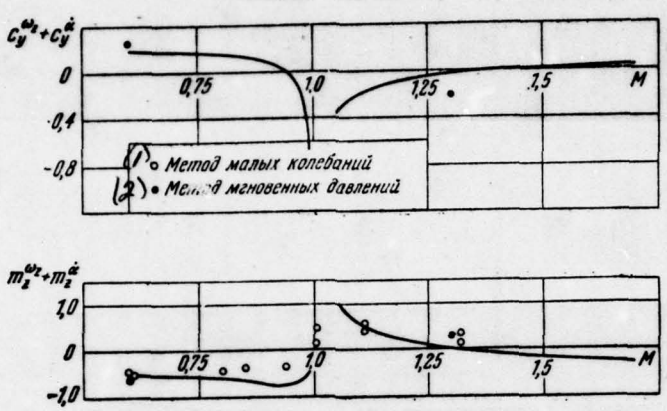


Fig. 24.50.

Fig. 24.50. Comparison of experimental (point) and calculated (curves) data for a delta wing $\chi_0 = 45°$ ($x_T = 0{,}37$).

Key: (1). Method of small oscillations. (2). Method of instantaneous pressures.

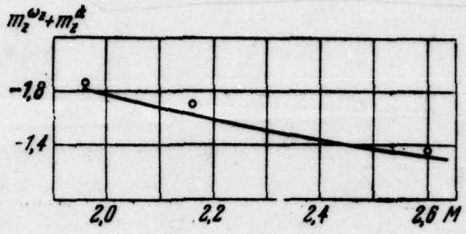


Fig. 24.51.

Fig. 24.51. The comparison of experimental (point) and calculated (is curve) data for the wing of complex planform $(\chi_0^{(2)}=30°)$.

Page 581.

The coefficient $m_{x1}^{\omega_{x1}}$, which determines roll damping, is obtained in wind tunnel by method of small oscillations (chapter VIII). Figure 24.47 gives dependences $km_{x1}^{\omega_{x1}}=f(k\lambda)$ for the rectangular and delta wings of different lengthening. It is evident that are obtained two common/general/total with any $M>1$ dependences for rectangular and delta wings, if we as coordinates utilize the parameters of the similarity of linear airfoil theory.

The combination of the coefficients $m_z^{\omega_z} + m_z^{\dot{\alpha}}$, determining the longitudinal attenuation of wing during rotary oscillations, is obtained in work [2.41] with the method of forced oscillations for the rectangular wings of different lengthening (λ = 2-5) with centering $\bar{x}_T = 0{,}5$. The comparison of experiment on the calculation is shown in Fig. 24.48.

Figures 24.49, 24.50 give the comparison of calculation and experimental data for a delta wing with sweep angle $\chi_0 = 45°$ with centering $\bar{x}_T = 0{,}37$. Comparison is made for stationary (c_y^{α} and m_z^{α}) and unsteady ($c_y^{\omega_z} + c_y^{\dot{\alpha}}$, $m_z^{\omega_z} + m_z^{\dot{\alpha}}$) aerodynamic characteristics. Experimental data are obtained by two methods: small oscillations (in this case are measured the total characteristics) and instantaneous pressures ($c_y^{\omega_z} + c_y^{\dot{\alpha}}$ and $m_z^{\omega_z} + m_z^{\dot{\alpha}}$ obtained by the integration of pressures). These experiments are made V. S. Khomenko. The given comparison it indicates the satisfactory coincidence of the calculated and experimental results.

for the coefficient of the longitudinal attenuation $m_z^{\omega_z} + m_z^{\dot{\alpha}}$ are compared experimental and calculated data of the wing of complex planform (wing of aircraft F-111). This wing has mixed front/leading and supersonic rear edges ($\chi_0^{(2)} = 30°$, $M = 1{,}5$ and $M = 2{,}5$). From curve/graph (Fig. 24.51) it is evident that and for such wings the unsteady linear theory will agree sufficiently well with experiment.

Part V

PRACTICAL APPLICATIONS

Introduction

The fifth part of the monograph contains materials and information, which have first of all practical value. Are here given the formulas and the data of procedural nature, relating to special feature/peculiarities application/uses of a Duhamel integral in the different unsteady problems of aerodynamics. Are examined motions with different Mach numbers.

The first case ($M = 0$ - the incompressible medium) is characteristic by inversion into infinity of transient functions with $\tau = 0$. The isolation/liberation of this special feature/peculiarity of the type of delta function is conducted by means of the examination of noncirculatory flow about a wing and by the introduction of the apparent additional masses of wing.

In the second case ($0 < M < 1$ - the compressed medium, subsonic speeds) with $\tau = 0$ transient functions are final and with all $\tau \geq 0$ continuous. However, they undergo powerful changes near $\tau = 0$, whereupon thereby sharper, the lesser the number M, which superimposes impression to choose from of the rational procedure of the application/use of a Duhamel integral. In each the cases transient process bears asymptotic character (transit time infinitely). Since it is necessary to calculate integrals from zero to infinity, is examined the question concerning the selection of the functions, which interpolate the course of transient process from the last/latter calculation point to $\tau = \infty$.

In the third case ($M > 1$ - supersonic speeds) transient process is final, since disturbance/perturbations are spread only downstream. Transient functions continuously change in time. All this simplifies the use of a Duhamel integral during transition from a stepped variation in the kinematic parameters to arbitrary, including harmonics, to time dependences.

Another group of the questions, examine/considered below, is related to the approximate determination of the unsteady characteristic of wing. Along with precise methods, the approximate,

rough estimates play the sizable role in practical application/appendices.

First, not always and not in all stages of the investigation are necessary data of high degree of accuracy, especially as this is reached by the value of sufficiently complex calculations.

Page 583.

In the second place, such estimates can serve as the determined means of the analysis of the role of separate factors, help to monitor the obtained results.

Thirdly, they can be used in the method successive approximation, especially in the problems of aeroelasticity [1.19], [1.20], [1.32]. Here always arises the question concerning the rational combination of elastic problem with aerodynamic, since the loads depend on the strains of wing, and strain they are determined by loads. In the first approximation, of strain it is possible to find through the loads, calculated approximately, and then to transfer/convert to the determination of loads by precise calculations.

Among approximation methods are examined, first of all, the

hypotheses of harmony and stability, which can be applied both at small and at high speeds. For supersonic speeds wide acceptance received piston theory. And finally, by supersonic speeds of estimation and stationary and unsteady characteristics they can be conducted according to the method of tangential wedges. These approaches are also illuminated in work.

Large value have the distinct physical representations of the peculiarities of unsteady wing characteristics. Since the total analysis of this question, based on the examination of the setting of problem or any formulas, is impossible, remains one path. It is connected with research on the results of the numerical calculations, accompanied by considerations and the explanations of general character, which sometimes rest on the data of experiment or the approximation formulas. Thus is studied the effect of the Mach number, the geometric parameters of wing, Strouhal number, laws of the motion of wing or change in the gust in time for the fundamental wing characteristics. In many instances this is made in an example of the wings of three planforms: rectangular, triangular and swept one elongation ($\lambda = 2.5$).

Each researcher in his work must rest not only on the calculation methods, but also for ready data. It is logical, them must be sufficiently in order that it would be possible to study the

motions, corresponding to different numbers M, with different wing planform, etc. But their must not be too much, otherwise initial material becomes bulky and and cumbersome. The authors paid considerable attention to the rational selection of this material and weighed out to it noticeable place in the last/latter part of the work. In the preceding/previous sections already were given some known and sufficiently numerous precise values of the coefficients aerodynamic derivative and transient functions mainly for two-dimensional problems. They also can be used by the reader.

Page 584.

Are given below systematic materials for finite-span wings with constant sweepback on leading and trailing edges. the planform for this wing is determined by three dimensionless parameters: the elongation λ, by contraction η and by sweep angle on leading wing edge χ_0. The coefficients aerodynamic derivative these wings, furthermore, they will depend on numbers M and p *. The there is basic interest for above target/purposes indicated in case of $p^* \to 0$. Then the number of arguments can be abbreviated/reduced to one by introduction of the similarity parameters. As them are undertaked $k\lambda$, $\lambda \operatorname{tg} \chi_0$, η. Are given the corresponding data at subsonic and supersonic speeds, including the cases, when wings have subsonic leading and trailing edges.

Furthermore, mainly for rectangular and delta wings are represented in the form of curve/graphs transient functions for the different problems $(\alpha, \omega_z, \omega_x, \Delta)$, which characterize the motion of wings without strain.

As it shows the multiflight work experience of the authors, this material most frequently it is required with the solution of the most diverse tasks with the use of unsteady aerodynamics.

Page 585.

Chapter XXV.

SPECIAL FEATURES OF THE PRACTICAL USE OF DUHAMEL INTEGRAL IN TASKS OF AERODYNAMICS.

§1. Calculation formulas for arbitrary time dependences.

Let the wing complete arbitrary aperiodic motion and enters in the gust, dimensionless kinematic parameters of which are assigned in the form

$$q_i(\tau) = q_i^* f(\tau). \qquad (25.1)$$

Here $q_i^* = \alpha^*, \omega_z^*, \omega_x^*, w_{y\Delta}^*$ — the maximum value of the module/modulus of the dimensionless kinematic parameter, $\tau = tU_0/b$ - dimensionless time, f (τ) are an arbitrary function of dimensionless time. To the beginning of unsteady process it corresponds $\tau = 0$, whereupon $q_i \equiv 0$ in $\tau < 0$.

Let us introduce for the aerodynamic coefficients of the

designation

$$c_{q_i}(\tau)=\left(\frac{c(\tau)}{q_i^*}\right), \quad c=c_y,\ m_x,\ m_z. \tag{25.2}$$

then, as shown in chapter VI, the aerodynamic characteristics with the motion and the gust, assigned in the form (25.1), are determined from the dependences

$$c_{q_i}(\tau)=f(0)\,A_{q_i}(\tau)+2\mu k_{q_i}\frac{df(\tau)}{d\tau}+\int_0^\tau \frac{df}{d\tau_1}A_{q_i}(\tau-\tau_1)\,d\tau_1. \tag{25.3}$$

Here $A_{q_i}(\tau)=[c(\tau)/q_i^*]$ is a transient function of the corresponding characteristics during stepped variation in the kinematic parameter q_i; k_{q_i} - the coefficients of apparent additional masses for the total characteristics. If are examined distributed loads, then instead of k_{q_i} are taken circulations $\Gamma^{(i)}$ [see part of I, the formulas (6.79) - (6.82)], which are determined during noncirculatory flow about a wing of the incompressible medium. Factor μ is equal to one with $M=0$ and zero with $M\neq 0$ and with any M in the case of the gradual entrance into gust.

Page 586.

Transient functions can have special feature/peculiarities. Thus, for instance, in the case of the incompressible fluid ($M=0$) with $\tau = 0$ value of transient functions goes to infinity. The isolation/liberation of this special feature/peculiarity is conducted

by means of the examination of noncirculating flow and by the introduction of the apparent additional masses of wing (see Chapter VI). In formula (25.3) this special feature/peculiarity is isolated and are accepted the value only of regular part of the transient function. In this case, and also in the case of the compressed medium ($0<M<1$ - subsonic speeds) transient process bears asymptotic character (transit time infinitely), as this is shown by dotted line in Fig. 25.1. At supersonic perturbation rates they are spread only downstream and transient process is final in time (Fig. 25.1). This simplifies the use of a Duhamel integral at supersonic speeds. The special feature/peculiarities of the behavior of transient functions indicated must be taken into account in obtaining the calculation formulas.

In practice transient functions are obtained by the calculations according to above numerical methods presented. Therefore the values of transient function will be known for a series of the discrete values of dimensionless time τ_j up to certain finite quantity τ_k. Are known also of the calculations of the coefficients of aerodynamic derivatives with $p^* \to 0$ limiting values of transient functions with $\tau = \infty$:

$$A_{q_i}(\infty) = c^{q_i}(0). \qquad (25.4)$$

Therefore during the derivation of the formulas of this paragraph let

us consider that the values of transient function are assigned for a series of the equidistant from each other discrete values τ_j in the form of table $A_{q_i}^{(j)} = A_{q_i}(\tau_j)$ to the finite value τ_k. Furthermore, are known limiting values $A_{q_i}(\infty)$, whereupon with $M > 1$ τ_k it is undertaked in such a way that the transient process ended. Thus, with $M > 1$

$$A_{q_i}(\tau \geqslant \tau_k) = A_{q_i}(\tau_k) = A_{q_i}(\infty). \qquad (25.5)$$

With $M < 1$ and sufficiently large $\tau \geqslant \tau_{k-1}$ let us assume that the transient function can be approximately represented in the form

$$A_{q_i}(\tau) = A_{q_i}(\infty) - Be^{-\sigma\tau}, \qquad (25.6)$$

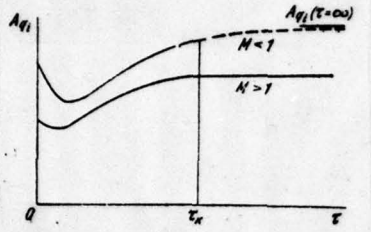


Fig. 25.1. Typical form of transient functions.

Page 587.

Then from the conditions

$$A_{q_i}(\tau_k) = A_{q_i}^{(k)}, \quad A_{q_i}(\tau_{k-1}) = A_{q_i}^{(k-1)}, \quad \tau_k > \tau_{k-1}$$

we find σ and B:

$$\left.\begin{aligned} \sigma &= \frac{1}{\tau_k - \tau_{k-1}} \ln \frac{A_{q_i}(\infty) - A_{q_i}^{(k-1)}}{A_{q_i}(\infty) - A_{q_i}^{(k)}}, \\ B &= \left[A_{q_i}(\infty) - A_{q_i}^{(k)}\right] e^{\sigma \tau_k}. \end{aligned}\right\} \qquad (25.7)$$

Thus, for any $\tau > \tau_k$ value of transient function with $M < 1$ they are determined from the relationship/ratio

$$A_{q_i}(\tau) = A_{q_i}(\infty) - \left[A_{q_i}(\infty) - A_{q_i}^{(k)}\right] e^{-\sigma(\tau - \tau_k)}. \qquad (25.8)$$

Further cut $0 \leqslant \tau \leqslant \tau_k$ a change in the transient function is divisible to interval/gaps $\Delta\tau$ (Fig. 25.2) in such a way that values τ_j would coincide with the data of the table of the calculation of transient function. For each of by section $\tau_{j-1} \leqslant \tau \leqslant \tau_j$ transient function we approximate by the line segment:

$$A_{q_i}(\tau) = A_{q_i}^{(j-1)} + \frac{A_{q_i}^{(j)} - A_{q_i}^{(j-1)}}{\tau_j - \tau_{j-1}} (\tau - \tau_{j-1}). \qquad (25.9)$$

It is analogous, function f (τ), that characterizes a change in the kinematic parameter in time, also we approximate by piecewise linear function (Fig. 25.3) in the same interval/gaps, as transient function, i.e., in interval/gap $\tau_{j-1} \leqslant \tau \leqslant \tau_j$ we set/assume

$$f(\tau) = f_{j-1} + \frac{f_j - f_{j-1}}{\tau_j - \tau_{j-1}} (\tau - \tau_{j-1}). \qquad (25.10)$$

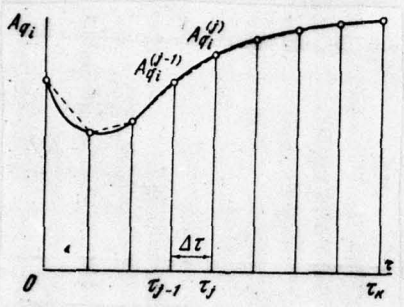


Fig. 25. 2.

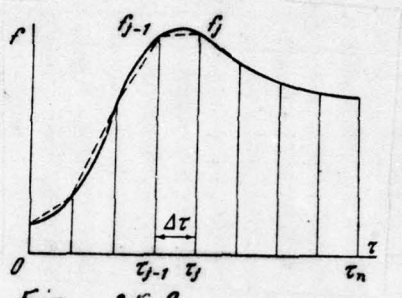


Fig. 25. 3.

Fig. 25.2. Approximation of transient function.

Fig. 25.3. Approximation of a change in the kinematic parameter.

Page 588.

By substituting (25.9) and (25.10) in (25.3), by performing the integration for sections, we will obtain the calculation formula for determining reaction at torque/moment τ_n:

$$c_{q_i}(\tau_n) = f(0)\, A_{q_i}^{(n)} + 2\mu k_{q_i} \frac{f_n - f_{n-1}}{\tau_n - \tau_{n-1}} + \sum_{l=1}^{n} \frac{A_{q_i}^{(n-l+1)} + A_{q_i}^{(n-l)}}{2} (f_l - f_{l-1}). \tag{25.11}$$

Here $\mu = 0$ with $M > 0$ and $\mu = 1$ with $M = 0$, but during the determination of loads on the wing, entering gradually the alternating/variable from coordinate gust, $\mu = 0$ with all numbers M. For the total characteristics k_{q_i} they are the appropriate values of the coefficients of apparent additional masses k_{22}, k_{26}, k_{44}, k_{66}, while for those which were distributed they are equal to $\Gamma^{(2)}$, $\Gamma^{(4)}$ or $\Gamma^{(6)}$. These values can be undertaked from chapter of XXVII or determined by the method, presented in chapter XII.

In the form of examples in Fig. 14.67, 14.68 and 24.42 were given the comparisons of the results of the calculation according to formula (25.11) of the lift of different wings at the linearly growing in time angle of attack α with the results of direct/straight calculations with $M = 0$ and $M = 1{,}4$. Direct/straight calculations with $M = 0$ were performed by the numerical method, presented in chapter XI, with $M = 1{,}4$ were utilized the formulas [1.78].

Figure 25.4 gives the analogous comparisons of a change in the

airfoil lift of infinite elongation ($\lambda = \infty$) with $M = 1,4$ and change in the angle of attack according to the law

$$\alpha(\tau) = \begin{cases} \alpha_0\left(1 - \frac{\tau}{T}\right) & \text{when } 0 \leqslant \tau \leqslant T, \\ 0 & \text{when } \tau > T. \end{cases} \qquad (25.12)$$

Fig. 24.43 contains the comparison of analogous calculations upon the gradual entrance of this wing into the linearly growing in coordinate gust. Figure 24.44 gives for $M = 3$ data on the lift of delta wing $\lambda = 2.5$ upon the gradual entrance into the linearly growing gust and a with change in the angle of attack α in linear law.

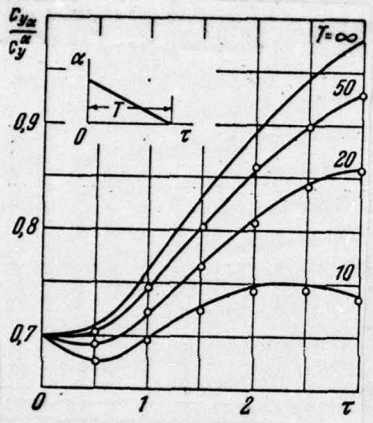


Fig. 25.4. Wing $\lambda = \infty$, M=1.4. Comparison of the calculations according to Duhamel integral (point) with by precise data (curves).

Page 589.

§2. Calculation formulas for determining the coefficients of

aerodynamic derivatives with finite Strouhal numbers.

For the coefficients aerodynamic derivative loads of the harmonically oscillating wing we have (see Chapter VI) following communication/connection with the transient functions:

$$\left.\begin{aligned} c^{q_i}(p^*) &= p^* \int_0^\infty A_{q_i}(\tau) \sin p^*\tau \, d\tau, \\ c^{q_i}(p^*) &= \int_0^\infty A_{q_i}(\tau) \cos p^*\tau \, d\tau + 2\mu k_{q_i}, \end{aligned}\right\} \qquad (25.13)$$

where

$$c = c_y,\ m_x,\ m_z;\ q_i = \alpha,\ \omega_x,\ \omega_z,$$
$$\mu = 1 \text{ with } M = 0 \text{ и } \mu = 0 \text{ with } M \neq 0.$$

As in the preceding/previous paragraph, we count that the values of transient function $A_{q_i}(\tau)$ are assigned for discrete values τ_i up to the finite number τ_k. Furthermore, is known value A_{q_i} with $\tau = \infty$. We take also, that the value τ_k in $M > 1$ corresponds to the end/lead of the transient process.

As we see, the integrands are the oscillatory functions and the numerical determination of integrals it can lead to a considerable reduction in the accuracy. Therefore for the calculations is utilized the procedure, when the integrals are determined analytically in the separate interval/gaps of integration and then are summarized. For this let us present expressions (24.13) in the form

$$\left.\begin{aligned} c^{q_l}(p^*) &= p^* \int_0^{\tau_k} A_{q_l}(\tau)\sin p^*\tau\, d\tau + p^* \int_{\tau_k}^{\infty} A_{q_l}(\tau)\sin p^*\tau\, d\tau, \\ c^{q_l}(p^*) &= \int_0^{\tau_k} A_{q_l}(\tau)\cos p^*\tau\, d\tau + \int_{\tau_k}^{\infty} A_{q_l}(\tau)\cos p^*\tau\, d\tau + 2\mu k_{q_l}. \end{aligned}\right\} \quad (25.14)$$

We consider that for all $\tau_k < \tau < \infty$ with $M < 1$ the transient function can be represented in the form (25.8), where σ is determined according to the results of numerical calculations $A_{q_l}(\tau)$ according to (25.7). With $M > 1$ and $\tau_k < \tau < \infty$ the values of transient functions are constant and are determined by relationship/ratio (25.5).

Page 590.

For the calculation of integrals we approximate transient function by the functions, which allow/assume the analytical determination of the integrals entering expressions (25.14). For example as in the preceding/previous paragraph, transient function for each of the cuts $\tau_{j-1} \leqslant \tau \leqslant \tau_j$ we approximate by the cut of straight line, determined on (25.9), but with $\tau > \tau_k$ let us present it in the form (25.8).

During integration let us accept [1.94]

$$\left.\begin{aligned} \int_{\tau_k}^{\infty} \sin p^*\tau\, d\tau &= \lim_{\sigma \to 0} \int_{\tau_k}^{\infty} \sigma^{-\sigma\tau} \sin p^*\tau\, d\tau = \frac{\cos p^*\tau_k}{p^*}, \\ \int_{\tau_k}^{\infty} \cos p^*\tau\, d\tau &= \lim_{\sigma \to 0} \int_{\tau_k}^{\infty} e^{-\sigma\tau} \cos p^*\tau\, d\tau = -\frac{\sin p^*\tau_k}{p^*}. \end{aligned}\right\} \quad (25.15)$$

As a result we will obtain the following relationship/ratios for the calculation of the coefficients of the aerodynamic derivatives:

$$\left.\begin{aligned}
c^{q_i}(p^*) &= A_{q_i}(\tau_0) + \frac{1}{p^*}\sum_{l=1}^{k}\frac{A_{q_i}(\tau_l) - A_{q_i}(\tau_{l-1})}{\tau_l - \tau_{l-1}} \times \\
&\times (\sin p^*\tau_l - \sin p^*\tau_{l-1}) + \left[A_{q_i}(\tau_\infty) - A_{q_i}(\tau_k)\right]\cos p^*\tau_k - \\
&- \nu\left[A_{q_i}(\tau_\infty) - A_{q_i}(\tau_k)\right] p^* \frac{\sigma \sin p^*\tau_k + p^* \cos p^*\tau_k}{\sigma^2 + p^{*2}}, \\
c^{\dot{q}_i}(p^*) &= \frac{1}{p^*}\left\{\frac{1}{p^*}\sum_{l=1}^{k}\frac{A_{q_i}(\tau_l) - A_{q_i}(\tau_{l-1})}{\tau_l - \tau_{l-1}} \times\right. \\
&\times (\cos p^*\tau_l - \cos p^*\tau_{l-1}) - \left[A_{q_i}(\tau_\infty) - A_{q_i}(\tau_k)\right]\sin p^*\tau_k + \\
&\left. + \nu\left[A_{q_i}(\tau_\infty) - A_{q_i}(\tau_k)\right] p^* \frac{p^* \sin p^*\tau_k - \sigma \cos p^*\tau_k}{\sigma^2 + p^{*2}}\right\} + 2\mu k_{q_i}.
\end{aligned}\right\} \quad (25.16)$$

Here $\nu = 0$ with $M > 1$, $\mu = 0$ with $M > 0$ and $\mu = 1$ with $M = 0$, but values k_{q_i} with $M = 0$ are equal chorrespond to bound masses, as this was shown in chapter VI.

Formulas (25.16) can be used also for the calculation of the coefficients of aerodynamic derivatives with harmonic gust. In this case $\mu = 0$ with all Mach numbers. Recall that in this case the coefficients of aerodynamic derivatives will correspond to the

position of the beginning of the connected with wing axes on the spout of root chord (if reading τ is conducted from the torque/moment of the beginning of the entrance of the spout of root chord into step gust), and as characteristic linear dimension is accepted root chord.

Page 591.

The coefficients of aerodynamic derivatives in the case of harmonic gust in the other position of the axes are obtained by the recalculation of data according to the formulas

$$\left.\begin{aligned}
c_{y1}^{\Delta} &= c_y^{\Delta}\cos p^*\xi_0 + p^* c_y^{\dot{\Delta}}\sin p^*\xi_0,\\
c_{y1}^{\dot{\Delta}} &= -\frac{1}{p^*}c_y^{\Delta}\sin p^*\xi_0 + c_y^{\dot{\Delta}}\cos p^*\xi_0,\\
m_{z1}^{\Delta} &= (m_z^{\Delta} - \xi_0 c_y^{\Delta})\cos p^*\xi_0 + p^*(m_z^{\dot{\Delta}} - \xi_0 c_y^{\dot{\Delta}})\sin p^*\xi_0,\\
m_{z1}^{\dot{\Delta}} &= -\frac{1}{p^*}(m_z^{\Delta} - \xi_0 c_y^{\Delta})\sin p^*\xi_0 + (m_z^{\dot{\Delta}} - \xi_0 c_y^{\dot{\Delta}})\cos p^*\xi_0.
\end{aligned}\right\} \quad (25.17)$$

Here through c are designated the coefficients in the position of the beginning of axes in the spout of root chord, and through c_1 - in new position, $\xi_0 = x_0/b$ - displacement into the portions of the root chord of new beginning relative old.

The recalculation of the coefficients of aerodynamic derivatives for other characteristic size/dimensions is conducted by formulas (27.8), given below.

Higher in Figs. 13.2-13.5, 19.24-19.31, 22.3, 22.4, 22.8 and 22.9 were carried out the comparisons of the coefficients of the aerodynamic derivatives of wing λ = ∞ with the different Mach numbers and Strouhal, obtained by the calculations according to Duhamel integral, with the results of the precise or direct/straight numerical calculations. Figure 25.5 in the form of an example gives a change in the square modulus of the transfer function of lift $|H_{c_y}(p^*)|^2$ delta wing with $M = 1{,}4$, obtained from Duhamel integral and from exact solution. As we see, and these results are located in good agreement.

§3. calculation procedure with the aid of Duhamel integral.

During the final adjustment of the procedure of the application/use of formulas (25.16) for the calculation of the coefficients of aerodynamic derivatives the primary attention was given to the effect of the number of separations of the range of a change in the transient functions $0 \leqslant \tau \leqslant \tau_k$ to the accuracy of the calculation.

AD-A049 001 FOREIGN TECHNOLOGY DIV WRIGHT-PATTERSON AFB OHIO F/G 1/3
A WING IN AN UNSTEADY GAS FLOW. PART 3,(U)
SEP 77 S M BELOTSERKOVSKIY, B K SKRIPACH
UNCLASSIFIED FTD-ID(RS)T-1543-77-PT-3 NL

2 OF 4
AD
A049001

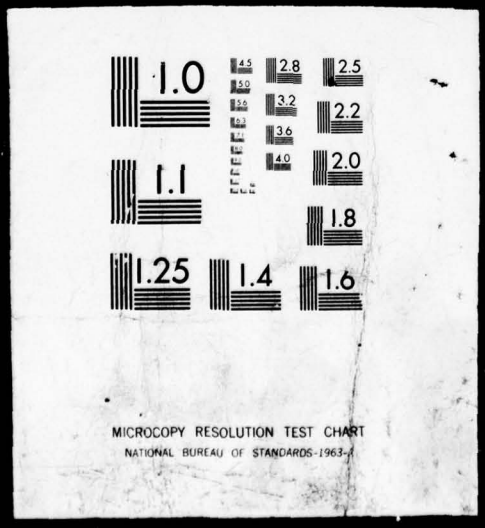


IFIED

2 OF 4

AD

A049001



Tables 25.1 and 25.2 in the form of an example shows the effect of the number of separations n into value c_y^α for a wing $\lambda = \infty$ at numbers $M = 0$ and $M = 1{,}4$.

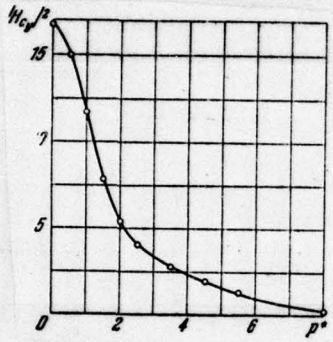


Fig. 25.5. Square modulus of the transfer function of airfoil lift $\lambda = \infty$ with $M = 1{,}4$. Curve is exact solution, points are the calculation according to Duhamel integral.

Page 592.

In the calculation were utilized precise values of transient functions $\left[\frac{c_y(\tau)}{\alpha^\circ}\right]$, given respectively in chapters XIII and XXIII. Value $\tau_k = 5$ at $M = 0$ and $\tau_k = 3{,}5$ at $M = 1{,}4$. Section $0 \leqslant \tau \leqslant \tau_k$ was

divided consecutively into n = 5, 10 and 20 interval/gaps. The results of the calculations according to the method, presented in §2 the present chapter, were compared with the results of exact solutions for the series of the numbers of Strouhal p * and the dimensionless parameter $\omega = p' \frac{M^2}{k^2}$ (see Tables 25.1 and 25.2).

Table 25.1. c_y^α for a wing $\lambda = \infty$, $M = 0$.

p^*	(1) Точное решение	(2) Расчет с помощью интеграла Дюамеля		
		$n = 5$, $\Delta\tau = 1$	$n = 10$, $\Delta\tau = 0,5$	$n = 20$, $\Delta\tau = 0,25$
0,12	5,593	5,689	5,677	5,637
0,4	4,572	4,505	4,514	4,520
0,8	3,927	3,954	3,951	3,951
1,2	3,637	3,633	3,632	3,632
1,6	3,482	3,465	3,478	3,480
2	3,389	3,378	3,395	3,393
3	3,274	3,231	3,273	3,271
4	3,223	3,181	3,218	3,225
5	3,196	3,177	3,190	3,199
10	3,157	3,148	3,153	3,144

Key: (1). Exact solution. (2). Calculation with the aid of Duhamel integral.

Table 25.2. c_y^α for a wing $\lambda = \infty$, $M = 1.4$.

p^*	(1) Точное решение	(2) Расчет с помощью интеграла Дюамеля		
		$n = 5$, $\Delta\tau = 0,7$	$n = 10$, $\Delta\tau = 0,35$	$n = 20$, $\Delta\tau = 0,175$
0,2	4,062	4,061	4,064	4,032
0,6	3,903	3,901	3,917	3,910
1,0	3,618	3,614	3,647	3,633
1,5	3,178	3,169	3,206	3,191
2,0	2,763	2,750	2,757	2,758
2,5	2,477	2,459	2,419	2,447
3,5	2,382	2 350	2,328	2,361
5,0	2,632	2,585	2,770	2,696

Key: (1). Exact solution. (2). Calculation with the aid of Duhamel integral.

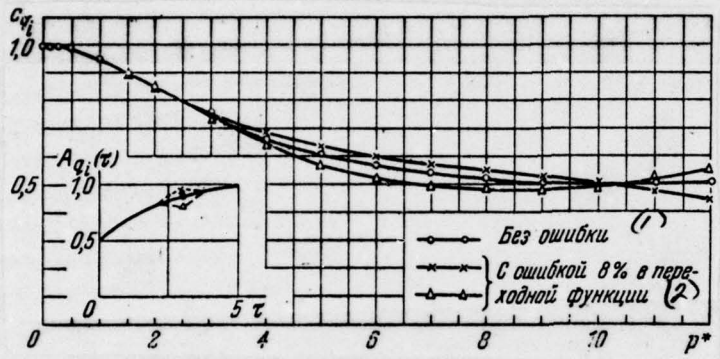


Fig. 25.6. Effect of the error in transient function on the coefficients of aerodynamic derivatives.

Key: (1). Without error. (2). With error 8o/o in transient function.

Page 593.

As is evident, already with n = 10 results of numerical calculations with the aid of Duhamel integral differ from precise values $c_y^{\alpha}(p^*)$

only in the third sign. Thus, the proposed procedure gives sufficient practical accuracy.

When conducting the calculations in practice largely are utilized the transient functions, obtained by the calculations according to numerical methods. In this case there can be the small local distortions of the form of transient function (Fig. 25.6). This local distortion of transient function leads to the oscillatory error in the coefficients of aerodynamic derivatives as is shown in Fig. 25.6. In this case, if the distortion of transient function occurs at large values τ, frequency increases, and if with small τ - decreases.

§4. Examples of the calculations.

The order of numerical determination with the use of a Duhamel integral of aerodynamic characteristics under the arbitrary laws of motion, and also the coefficients of aerodynamic derivatives with finite Strouhal numbers let us show for a Mach number $M=0$. This case is common/general/total, since for $M=0$ transient functions with $\tau \rightarrow$ - the aim is asymptotic for limiting values and it is necessary to consider the apparent additional masses of wing.

Arbitrary law of motion. In the form of an example let us find, as will be changed depending on dimensionless time τ the airfoil lift of infinite elongation ($\lambda = \infty$), when angle of attack is changed as follows (dotted line in Fig. 25.7):

$$\left.\begin{aligned}
&\alpha(\tau)=\alpha^{\circ}\tau && \text{when } 0\leqslant\tau\leqslant 1,\\
&\alpha(\tau)=\alpha^{\circ} && \text{when } 1\leqslant\tau\leqslant 2,\\
&\alpha(\tau)=\alpha^{\circ}-\alpha^{\circ}(\tau-2) && \text{when } 2\leqslant\tau\leqslant 3,\\
&\alpha(\tau)=0 && \text{when } \tau>3.
\end{aligned}\right\} \qquad (25.18)$$

For an infinite-span wing according to (13.36) $k_{22} = \pi/4$.

Calculations, carried out by formula (25.11), are given in table 25.3. For the purpose of an abridgement of table the interval/gap of dimensionless time $\Delta\tau$ between the calculated torque/moments is undertaked large, namely $\Delta\tau = 0.5$. In the table it is taken into account, that with $\tau_j = 1$, $\tau_j = 2$ and $\tau_j = 3$ the derivative $\partial\alpha(\tau)/\partial\tau$ is changed by jump. For these values τ the derivative and final results have two values. The numerical values of transient function $[c_y(\tau)/\alpha^{\circ}]$

are undertaked from Table 13.3. The results of the calculation of a change in the lift coefficient $(c_y(\tau)/\alpha^*)$ for the law of change α in question are shown in Fig. 25.7 to unbroken curve.

Page 594.

Table 25.3. Calculation of aerodynamic loading under the arbitrary law of motion.

1	i, j	0	1	2	3	4	5	6	7	8	9	10
2	$\tau_j = j\,\Delta\tau,\ \tau_i = i\,\Delta\tau$	0	0,5	1,0	1,5	2,0	2,5	3,0	3,5	4,0	4,5	5,0
3	f_j	0	0,5	1,0	1,0	1,0	0,5	0	0	0	0	0
4	$f_j - f_{j-1}$	0	0,5	0,5	0	0	−0,5	−0,5	0	0	0	0
5	$\frac{\partial f_j}{\partial \tau} = \frac{f_j - f_{j-1}}{\Delta\tau}$	0 1	1	1 0	0	0 −1	−1	−1 0	0	0	0	0
6	$2k_{22}\frac{\partial f_j}{\partial \tau}$	0 1,57	1,57	1,57 0	0	0 −1,57	−1,57	−1,57 0	0	0	0	0
7	$\left[\frac{c_y(\tau_i)}{\alpha^*}\right]$	3,14	3,77	4,21	4,52	4,76	4,95	5,11	5,23	5,34	5,42	5,50
8	$\frac{1}{2}\left\{\left[\frac{c_y(\tau_i)}{\alpha^*}\right] + \left[\frac{c_y(\tau_{i-1})}{\alpha^*}\right]\right\}$	—	3,46	3,99	4,37	4,64	4,86	5,03	5,17	5,29	5,38	5,46
9	$(f_1 - f_0)\cdot(8)$	—	1,73	2,00	2,19	2.32	2,43	2,52	2,59	2,65	2,69	2,73
10	$(f_2 - f_1)\cdot(8)$	—	—	1,73	2,00	2,19	2,32	2,43	2,52	2,59	2,65	2,69
11	$(f_3 - f_2)\cdot(8)$	—	—	—	0	0	0	0	0	0	0	0
12	$(f_4 - f_3)\cdot(8)$	—	—	—	—	0	0	0	0	0	0	0
13	$(f_5 - f_4)\cdot(8)$	—	—	—	—	—	−1,73	−2,00	−2,19	−2,32	−2,43	−2,52
14	$(f_6 - f_5)\cdot(8)$	—	—	—	—	—	—	−1,73	−2,00	−2,19	−2,32	−2,43
15	$\left[\frac{c_y(\tau_j)}{\alpha^*}\right] = (6) + \sum_{(9)}^{(14)}$	0 1,57	3,30	5,30 3,73	4,19	4,51 2,94	1,45	−0,37 1,22	0,92	0,73	0,59	0,47

Page 595.

Table 25.4. Calculation of the coefficients of the aerodynamic derivatives

$$\lambda = \infty,\ M = 0,\ p^* = 3,\ \Delta\tau = 0{,}5,$$

$$\left[\frac{c_y}{\alpha^*}\right]_{\tau=0} = \pi,\ \left[\frac{c_y}{\alpha^*}\right]_{\tau=\infty} = 2\pi,\quad k_{22} = \frac{\pi}{4},\quad \sigma = 0{,}19$$

1	i	1	2	3	4	5	$k=6$	
2	$\tau_i = i\,\Delta\tau$	0,5	1,0	1,5	2,0	2,5	$\tau_k = 3{,}0$	
3	$\tau_{i-1} = (i-1)\,\Delta\tau$	0	0,5	1,0	1,5	2,0	2,5	
4	$\left[\frac{c_y(\tau_i)}{\alpha^*}\right]$	3,774	4,205	4,521	4,762	4,952	5,105	
5	$\left[\frac{c_y(\tau_{i-1})}{\alpha^*}\right]$	3,142	3,774	4,205	4,521	4,762	4,952	
6	$\frac{(4)-(5)}{(2)-(3)}$	1,264	0,863	0,631	0,484	0,381	0,305	
7	$p^*\tau_i$	1,5	3,0	4,5	6,0	7,5	9,0	
8	$p^*\tau_{i-1}$	0	1,5	3,0	4,5	6,0	7,5	
9	$\sin p^*\tau_i$	0,9975	0,1411	—0,9775	—0,2794	0,9380	0,4122	
10	$\cos p^*\tau_i$	0,0707	—0,9900	—0,2108	0,9602	0,3466	—0,9111	
11	$\sin p^*\tau_{i-1}$	0	0,9975	0,1411	—0,9775	—0,2794	0,9380	
12	$\cos p^*\tau_{i-1}$	1,00	0,0707	—0,9900	—0,2108	0,9602	0,3466	
13	(9) — (11)	0,9975	—0,8564	—1,1186	0,6981	1,2174	—0,5258	
14	(10) — (12)	1,2610	—0,7392	—0,9296	0,3376	0,4635	—0,1606	
15	(6) · (13)	—0,9293	—1,0607	0,7792	1,1710	—0,6135	—1,2577	$A = \sum_{i=1}^{i=k} = 0{,}2328$
16	(6) · (14)	—1,1748	—0,9156	0,6475	0,5663	—0,2337	—0,3841	$B = \sum_{i=1}^{i=k} = -1{,}4944$

Page 596.

Harmonic laws of motion. The coefficients of the aerodynamic derivatives of the airfoil lift of infinite elongation ($\lambda = \infty$) with $M = 0$, $p^* = 3$ and a change in the angle of attack in harmonic law, designed in formulas (25.16), are brought to tables 25.4 and 25.5. The interval/gap of integration from $\tau = 0$ to $\tau = 3$ is broken into cuts $\Delta\tau = 0.5$.

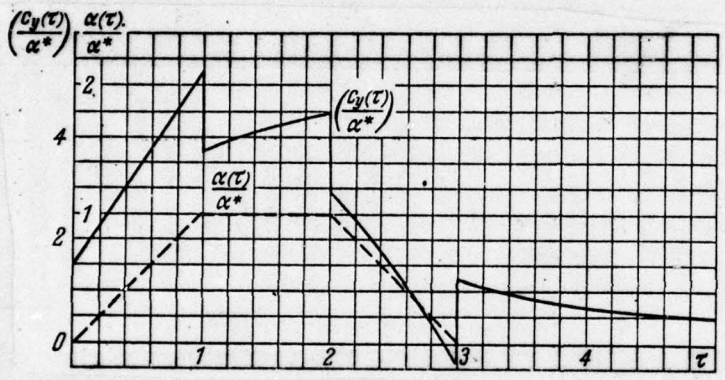


Fig. 25.7. Change of the airfoil lift $\lambda = \infty$ in the incompressible medium for the assigned law $\alpha(\tau)$.

Table 25.5.

1	$\left[\frac{c_y}{\alpha^\circ}\right]_{\tau=\infty} - \left[\frac{c_y(\tau_k)}{\alpha^\circ}\right]$	1,1781	10	$\frac{(9)}{\sigma^2 + p^{\circ 2}}$	−0,8815
			11	(1) · (10)	−1,0385
2	$\left\{\left[\frac{c_y}{\alpha^\circ}\right]_{\tau=\infty} - \left[\frac{c_y(\tau_k)}{\alpha^\circ}\right]\right\} \times \cos p^\circ \tau_k$	−1,0734	12	$c_y^\alpha = (5) - (11)$ (6)	3,1843
			13	$B/p^{\circ 2}$ (B из таблицы 25.4)	−0,1660
			14	$\frac{(1)}{p^\circ} \sin p^\circ \tau_k$	0,1619
3	$\frac{A}{p^\circ}$ (A из таблицы 25.4) (1)	0,0776	15	(13) − (14)	−0,3279
			16	$p^\circ \sin p^\circ \tau_k$	1,2366
4	$\left[\frac{c_y}{\alpha^\circ}\right]_{\tau=0}$ + (3)	3,2192	17	$\sigma \cos p^\circ \tau_k$	−0,1731
			18	(16) − (17)	1,4097
5	(2) + (4)	2,1458	19	$\frac{(18)}{p^{\circ 2} + \sigma^2}$	0,1560
6	$\sigma \sin p^\circ \tau_k$	0,0783			
7	$p^\circ \cos p^\circ \tau_k$	−2,7333	20	(1) · (19)	0,1838
8	(6) + (7)	−2 6550	21	(15) + (20)	−0,1441
9	p° (8)	−7,9650	22	$c_y^\alpha = (21) + 2k_{22}$	1,4267

Key: (1). from table.

Page 597.

The numerical values of transient function $[c_y(\tau)/\alpha^*]$ are undertaked from table 13.3. Value of the coefficient of apparent additional mass $k_{22} = \pi/4$. The values σ it was determined from (25.7), for which were taken the value $[c_y(\tau)/\alpha^*]$ with $\tau = \tau_k = 3$ and $\tau = \tau_{k+j} = 6$. Substituting the appropriate values in formula (25.7), we have $\sigma = 0.19$. With p * = 3 were obtained the following values of the coefficients of the aerodynamic derivatives:

$$c_y^a|_{p^*=3} = 3{,}184, \quad c_y^{\dot{a}}|_{p^*=3} = 1{,}427.$$

Precise values of these coefficients with this Strouhal number (see table 13.1) are equal to $c_y^a = 3{,}274$, $c_y^{\dot{a}} = 1{,}417$. Consequently, even during the taken rough separation of the interval of integration error does not exceed 3o/o.

Chapter XXVI.

APPROXIMATION METHOD.

§1. Hypothesis of harmony and its substantiation. Stability hypothesis.

The use of the integrals of Fourier or Duhamel in principle solves the problem concerning the determination of aerodynamic loadings on lifting surface during its unsteady motion along any laws. However, the practical application/use of these methods frequently turns out to be difficult. For example, for using a Fourier integral it is required to preliminarily study of the aerodynamic loads on body during his harmonic oscillations in the range of frequencies (or Strouhal numbers) from zero to infinity. During the use of a Duhamel integral it is necessary to preliminarily calculate transient functions in all range of dimensionless time $0 \leqslant \tau \leqslant \tau_h < \infty$. Therefore one of the important tasks is the indication let less strict, but sufficiently simple method of determining the unsteady total and distributed aerodynamic characteristics. In this paragraph are given the presentation and the substantiation of the approximate procedure, named the "hypothesis of harmony".

Lift coefficients c_y, as was shown earlier [see (2.24)], it can

be represented in the form

$$c_y = c_y^{\alpha}\alpha + c_y^{\dot{\alpha}}\dot{\alpha} + c_y^{\omega_z}\omega_z + c_y^{\dot{\omega}_z}\dot{\omega}_z + c_y^{\delta}\delta + c_y^{\dot{\delta}}\dot{\delta} + c_y^{\Delta}\Delta + c_y^{\dot{\Delta}}\dot{\Delta}. \quad (26.1)$$

Analogously can be written another total and distributed aerodynamic characteristics. The coefficients of aerodynamic derivatives c^{q_l}, $c^{\dot{q}_l}$ do not depend on time and for this lifting surface are the functions of the mean incidence α_0, of the amplitude values of the kinematic parameters, Mach numbers, Strouhal and Reynolds. In the linear theory, which examines the ideal medium, they will not depend on the amplitude values of the parameters and on Reynolds number.

Page 599.

Representations of type (26.1) are convenient by the facts that are isolated the relationship/ratios, which in a whole series of the cases turn out to be basic, and the main parameters, which affect aerodynamic characteristics, are given in an explicit form. The coefficients of aerodynamic derivatives possess therefore series convenient for their use properties. Specifically, the calculations according to linear theory and the analysis, conducted in the following chapter, testify to the weak dependence of these coefficients on Strouhal number for low-aspect-ratio wings with all Mach numbers and for the wings of any planform at large values M.

When the dependence of the coefficients aerodynamic derivative total and distributed aerodynamic characteristics on Strouhal number is obtained weakly, it is possible to expect that these coefficients will bear a comparatively universal character. In their this case it is possible to utilize in the approximate computations for any laws of a change in the kinematic parameters and parameters of strain in time. The assumption indicated, introduced into the practice of the aerodynamic investigations by S. M. Belotserkovskiy into 1959, let us call the hypothesis of harmony. According to this hypothesis determining the total and distributed aerodynamic characteristics one should produce on the basis of representations of type (26.1). The coefficients of aerodynamic derivatives in similar relationship/ratios are taken from the calculations or experiments at harmonic dependences, and the value of the kinematic parameters $q_i, \dot{q}_i$ they are determined on the basis of their time dependences.

Let us give the substantiation of this hypothesis for periodic processes. Since for linear tasks is valid the principle of superposition, particular motions and strains it is possible to study independent of each other, but the general case to represent in the form of the linear combination of quotients. Therefore let us examine a change in any kinematic paramete, e.g., α (t). Reasonings let us give only for a lift coefficient c_y, since for all other aerodynamic characteristics result is obtained analogous.

Let the period of a change in the angle of attack in time will be 2T. Is decomposed α (t) and $\dot{\alpha}$ (t) in Fourier series:

$$\left.\begin{aligned}\alpha(t)&=\sum_{n=1}^{\infty}\alpha_n,\quad \alpha_n=a_n\cos n\pi\frac{t}{T}+b_n\sin n\pi\frac{t}{T}.\\ \dot{\alpha}(t)&=\sum_{n=1}^{\infty}\dot{\alpha}_n,\quad \dot{\alpha}_n=c_n\cos n\pi\frac{t}{T}+d_n\sin n\pi\frac{t}{T}.\end{aligned}\right\}\qquad(26.2)$$

For each α_n and $\dot{\alpha}_n$ the appropriate value of lift coefficient let us designate

$$c_{yn}=c_{yn}^{\alpha}(p_n,\ \mathrm{M})\alpha_n+c_{yn}^{\dot{\alpha}}(p_n,\ \mathrm{M})\dot{\alpha}_n,\quad p_n=\frac{n\pi b}{U_0T}.\qquad(26.3)$$

Page 600.

Assuming that the coefficients of aerodynamic values α_n and $\dot{\alpha}_n$, according to the principle of superposition the total lift coefficient c_y let us present in the form

$$c_y=\sum_{n=1}^{\infty}c_{yn},\qquad(26.4)$$

whereupon we consider that all series in question converge. If the dependence of coefficients c_{yn}^{α} and $c_{yn}^{\dot{\alpha}}$ on p_n is small and it can be

disregarded, then, by omitting index n, we will obtain

$$c_y = c_y^{\alpha} \sum_{n=1}^{\infty} \alpha_n + c_y^{\dot{\alpha}} \sum_{n=1}^{\infty} \dot{\alpha}_n.$$

Taking into account of relationship/ratio (26.2), we come to the formula

$$c_y = c_y^{\alpha}\alpha + c_y^{\dot{\alpha}}\dot{\alpha}, \tag{26.5}$$

which and it expresses the hypothesis of harmony.

In the case of the aperiodic processes of reasoning they are conducted in perfect analogy, only instead of series are examined Fourier integrals. Let us introduce dimensionless time, after assuming

$$\tau = \frac{tU_0}{b}. \tag{26.6}$$

Functions $\alpha(\tau)$ and $\dot{\alpha}(\tau)$ let us present in the form of Fourier integrals:

$$\left.\begin{aligned} \alpha(\tau) &= \int_0^{\infty} \alpha_p(p^*, \tau)\, dp^*, \quad \alpha_p(p^*, \tau) = a(p^*)\cos p^*\tau + b(p^*)\sin p^*\tau, \\ \dot{\alpha}(\tau) &= \int_0^{\infty} \dot{\alpha}_p(p^*, \tau)\, dp^*, \quad \dot{\alpha}_p(p^*, \tau) = c(p^*)\cos p^*\tau + d(p^*)\sin p^*\tau. \end{aligned}\right\} \tag{26.7}$$

For each α_p and $\dot{\alpha}_p$ let us find the appropriate values of coefficients c_{yp}:

$$c_{yp} = c^{\alpha}_{yp}(p^*, M)\,\alpha_p + c^{\dot{\alpha}}_{yp}(p^*, M)\,\dot{\alpha}_p. \qquad (26.8)$$

Utilizing principle of superposition, we find

$$c_y(\tau, M) = \int_0^{\infty} c_{yp}\,dp^*,$$

whereupon we consider that all integrals, examined above, make sense.

Page 601.

If the dependence of coefficients c^{α}_{yp}, $c^{\dot{\alpha}}_{yp}$ on p * can be disregarded, then, after designating the constant values of these coefficients by c^{α}_{y} and $c^{\dot{\alpha}}_{y}$, let us have

$$c_y(\tau, M) = c_y^{\alpha} \int_0^{\infty} \alpha_p \, dp^* + c_y^{\dot{\alpha}} \int_0^{\infty} \dot{\alpha}_p \, dp^*,$$

or

$$c_y(\tau, M) = c_y^{\alpha} \alpha(\tau) + c_y^{\dot{\alpha}} \dot{\alpha}(\tau).$$

Thus, the hypothesis of harmony gives, for example, the following approximate dependences for the total characteristics during any motions of wing as solid body

$$\left.\begin{aligned} c_y(\tau, M) &= c_y^{\alpha} \alpha(\tau) + c_y^{\dot{\alpha}} \dot{\alpha}(\tau) + c_y^{\omega_z} \omega_z(\tau) + c_y^{\dot{\omega}_z} \dot{\omega}_z(\tau), \\ m_z(\tau, M) &= m_z^{\alpha} \alpha(\tau) + m_z^{\dot{\alpha}} \dot{\alpha}(\tau) + m_z^{\omega_z} \omega_z(\tau) + m_z^{\dot{\omega}_z} \dot{\omega}_z(\tau), \\ m_x(\tau, M) &= m_x^{\omega_x} \omega_x(\tau) + m_x^{\dot{\omega}_x} \dot{\omega}_x(\tau). \end{aligned}\right\} \quad (26.9)$$

From the given reasonings it follows that the hypothesis of harmony will give thereby more accurate results, the lesser the dependence of the coefficients of aerodynamic derivatives of Strouhal number. Furthermore, the accuracy of results will depend also on the law of change in time of the kinematic parameters. The lesser number of harmonics it is possible to present these laws, those will be more precise, other conditions being equal, the results of the hypothesis of harmony.

During determining the aerodynamic characteristics of the bodies, which accomplish unsteady motion, comparatively wide acceptance has the so-called "stability hypothesis". According to this hypothesis it is considered that all aerodynamic loadings the same as during flow of stationary flow at an angle of attack, equal in magnitude to instantaneous true angle of attack. Thus, upon consideration only of linear terms in stability hypothesis instead of the dependences of type (26.9) using the dependence of the form

$$c_y(t) = c_y^{\alpha}\alpha(t), \qquad (26.10)$$

where α (t) - the instantaneous value of true angle of attack, c_y^{α} - the coefficient during steady motion.

In the case of rotary motion around transverse axis sometimes is applied the "expanded stability hypothesis", in which, for example, the dependences for c_y are accepted in the form

$$c_y(t) = c_y^{\alpha}\alpha(t) + c_y^{\omega_z}\omega_z(t). \qquad (26.11)$$

Page 602.

§2. Hypotheses of harmony and stability upon the gradual entrance of wing into gust.

The hypotheses of harmony or stability in the form (26.9) and respectively (26.10) can be used for determining aerodynamic loadings on wing from the effect of linear gust only when gust simultaneously (instantly) encompasses whole wing.

If body at any speed gradually enters in gust, then the hypothesis of harmony is formulated as follows: that part of the body, which is enveloped by gust, it is subject to the influence from its side; on remaining part it is accepted that there are no aerodynamic loadings. Loads are calculated under the usual assumptions of the hypothesis of harmony, after which aerodynamic loading, for example $\Delta\bar{p}$, it is represented in the form

$$\Delta\bar{p} = p^{\alpha}\alpha + p^{\dot{\alpha}}\dot{\alpha}.$$

The coefficients p^{α} and $p^{\dot{\alpha}}$ are determined for a planform for that part of the body, which is enveloped by gust, during its harmonic oscillations (usually with $p^* \longrightarrow 0$). Thus, p^{α} and $p^{\dot{\alpha}}$ depends on time, thus far the process of the entrance of body into the gust not is stopped. Further it is accepted that the gust can change in the course of time, but on coordinates it does not depend.

Let us examine the order of the determination of coefficients

c_y, m_z, $\bar{x}_a$ for the wing, entering the gust along root chord (Fig. 26.1). Index t let us note all values, which are related to part of the wing, included by gust (in Fig. 26.1 it is shaded). For a lift we have

$$Y_t = c_{yt} q S_t, \quad c_{yt} = c_{yt}^{\alpha} \alpha + c_{yt}^{\dot{\alpha}} \dot{\alpha}, \qquad (26.12)$$

whereupon aerodynamic derivatives c_{yt}^{α} and $c_{yt}^{\dot{\alpha}}$ they are determined for a wing with geometric parameters λ_t, η_t, χ_{0t}. By relating, as usual, the lift coefficients of wing to the area of entire wing S, we will obtain

$$c_y = \frac{\left(c_{yt}^{\alpha} \alpha + c_{yt}^{\dot{\alpha}} \dot{\alpha}\right) S_t}{S}. \qquad (26.13)$$

Let us find torque/moment M_z, by counting that the force Y_t and torque/moment M_{zt} are known.

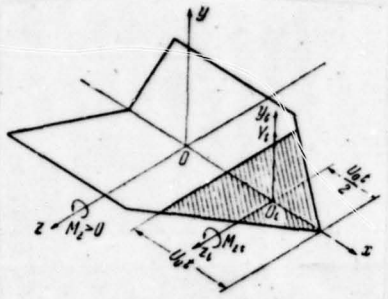


Fig. 26.1. On the calculation of wing characteristics according to the hypothesis of harmony upon the gradual entrance into gust.

Page 603.

Utilizing standard coordinate system with beginning on the middle of root chord, we have $M_z = M_{zt} + Y_t \cdot \overline{OO_t}$, but

$$\overline{OO_t} = \frac{b}{2} - \frac{U_0 t}{2} = \frac{b}{2}\left(1 - \frac{U_0 t}{b}\right) = \frac{b}{2}(1 - \tau),$$

therefore

$$M_z = M_{zt} + Y_t b \frac{1-\tau}{2}. \qquad (26.14)$$

In accordance with the hypothesis of the harmony

$$\left.\begin{aligned} M_{zt} &= m_{zt} q S_t b_t, \quad b_t = U_0 t, \\ m_{zt} &= m_{zt}^{\alpha}\alpha + m_{zt}^{\dot{\alpha}}\dot{\alpha}, \end{aligned}\right\} \qquad (26.15)$$

Y_t is determined by formula (26.12). Relating torque/moment to root chord and the areas of entire wing, from (26.12), (26.15), taking into account that

$$\frac{b_t}{b} = \frac{tU_0}{b} = \tau,$$

we will obtain

$$m_z = (m_{zt}^{\alpha}\alpha + m_{zt}^{\dot{\alpha}}\dot{\alpha})\tau\frac{S_t}{S} + (c_{yt}^{\alpha}\alpha + c_{yt}^{\dot{\alpha}}\dot{\alpha})\frac{1-\tau}{2}\frac{S_t}{S}. \qquad (26.16)$$

After are determined the coefficients m_z and c_y, it is not difficult to find the coordinate of the center of pressure or focus $\bar{x}_{\alpha}$:

$$\bar{x}_{\text{ц. д}} = \frac{m_z}{c_y}, \qquad \bar{x}_{\text{ц. д}} = \frac{x_{\text{ц. д}}}{b},$$

$$\bar{x}_{\alpha} = \frac{m_z^{\alpha}}{c_y^{\alpha}}, \qquad \bar{x}_{\alpha} = \frac{x_{\alpha}}{b}.$$

If we in all formulas of this paragraph disregard value $\dot{\alpha}$, then we will obtain the calculation of the gradual entrance of wing into gust according to stability hypothesis.

§3. Examples of the application/use of hypotheses of harmony and stability.

In the form of an example let us examine the application/use of a hypothesis of harmony to the case of the gradual entrance into the gust of rectangular and delta wings (Fig. 26.2).

For the rectangular wing

$$S_t = lU_0 t, \quad \frac{S_t}{S} = \frac{lU_0 t}{lb} = \frac{U_0 t}{b} = \tau, \quad \lambda_t = \frac{l}{U_0 t} = \frac{b}{U_0 t}\frac{l}{b} = \frac{\lambda}{\tau}$$

and according to (26.13), (26.16)

$$\left.\begin{aligned} c_y &= \left(c_{yt}^{\alpha}\alpha + c_{yt}^{\dot\alpha}\dot\alpha\right)\tau, \\ m_z &= \left(m_{zt}^{\alpha}\alpha + m_{zt}^{\dot\alpha}\dot\alpha\right)\tau^2 + \left(c_{yt}^{\alpha}\alpha + c_{yt}^{\dot\alpha}\dot\alpha\right)\frac{\tau(1-\tau)}{2}. \end{aligned}\right\} \qquad (26.17)$$

Page 604.

The coefficients c_{yt}^{α}, $c_{yt}^{\dot\alpha}$, m_{zt}^{α}, $m_{zt}^{\dot\alpha}$ are determined for a rectangular wing with $\lambda_t = \lambda/\tau$.

For a delta wing (see Fig. 26.2)

$$\lambda_t = \lambda, \quad \frac{S_t}{S} = \frac{l_t U_0 t}{lb} = \frac{l_t}{l}\tau = \tau^2$$

and according to (26.13), (26.16)

$$\left.\begin{aligned} c_y &= (c_y^{\alpha}\alpha + c_y^{\dot\alpha}\dot\alpha)\tau^2, \\ m_z &= (m_z^{\alpha}\alpha + m_z^{\dot\alpha}\dot\alpha)\tau^3 + (c_y^{\alpha}\alpha + c_y^{\dot\alpha}\dot\alpha)\frac{1-\tau}{2}\tau^2. \end{aligned}\right\} \qquad (26.18)$$

Here c_y^{α}, $c_y^{\dot\alpha}$, m_z^{α}, $m_z^{\dot\alpha}$ they are calculated with $\lambda_t = \lambda$.

Compare data, based on the application/use of hypotheses of harmony and stability, with the results of numerical calculations according to linear theory at subsonic speeds. In accordance with what has been said above under stability hypothesis let us understand the method of the calculation, during which in formulas (26.9) all coefficients of aerodynamic derivatives, except c_y^{α} and m_z^{α}, are reject/thrown. This comparison helps to establish/install the fields of the applicability of the hypotheses indicated.

In chapter of XXVII are given the aerodynamic characteristics of the rectangular and delta wings of different elongation λ in the incompressible medium ($M = 0$). Was examined the case of a change in

the angle of attack in the course of time according to the law

$$\alpha(\tau) = \alpha^{*}\tau. \qquad (26.19)$$

Figure 26.3-26.6 gives given data, that characterize the law of the increase of lift coefficient in time, and also the position of mean aerodynamic center of wing relative to the leading edge/nose of the mean aerodynamic chord.

As we see, the hypothesis of harmony in all cases gives more correct results, rather than stability hypothesis. An especially good agreement is obtained for the wings of very small elongation (λ = 0.5). With an increase λ an error in the approximation methods they grow/rise. This is explained by the facts that during small elongations the dependence of the coefficients aerodynamic derivative wings on Strouhal number is insignificant, and with an increase λ it becomes ever more noticeable.

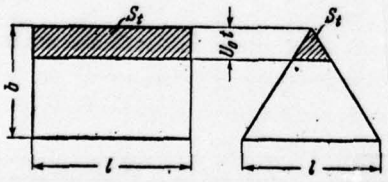


Fig. 26.2. On the calculation of the characteristics of rectangular and delta wings in the hypothesis of harmony upon the gradual entrance into gust.

Page 605.

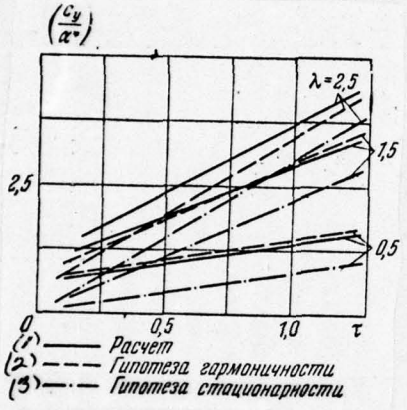


Fig. 26.3.

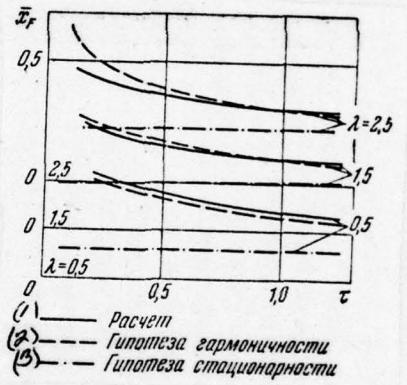


Fig. 26.4.

Fig. 26.3. Rectangular wings (M=0). Change in the lift during a change in the angle of attack in linear law.

Key: (1). Calculation. (2). Hypothesis of harmony. (3). Stability hypothesis.

Fig. 26.4. Rectangular wings (M=0). Position of focus during a change in the angle of attack in linear law.

Key: (1). Calculation. (2). Hypothesis of harmony. (3). Stability hypothesis.

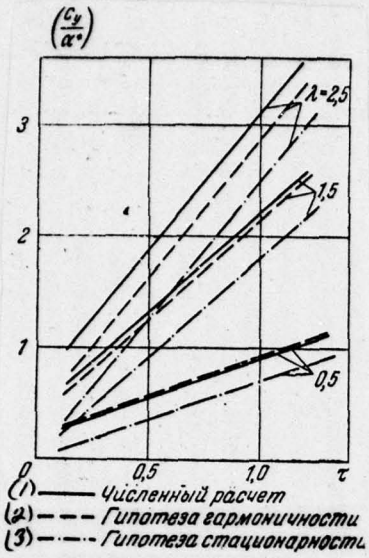


Fig 26.5.



Fig. 26.6.

Fig. 26.5. Delta wings (M=0). Lift during a change in the angle of

attack in linear law.

Key: (1). Numerical calculation. (2). Hypothesis of harmony. (3). Stability hypothesis.

Fig. 26.6. Delta wings (M-0) Position of focus during a change in the angle of attack in linear law.

Key: (1). Calculation. (2). Hypothesis of harmony. (3). Stability hypothesis.

Pages 606-607.

Examining the rotary motion of the wing, with which $\dot{\alpha} = \omega_z = \text{const}$, it is possible to write the following relationship/ratios on the hypothesis of harmonicity:

$$\left.\begin{aligned}(c_y)_{\alpha+\omega_z} &= c_y^{\alpha}\tau + c_y^{\dot{\alpha}} + c_y^{\omega_z},\\ (m_z)_{\alpha+\omega_z} &= m_z^{\alpha}\tau + m_z^{\dot{\alpha}} + m_z^{\omega_z},\end{aligned}\right\} \qquad (26.20)$$

and on stability hypothesis:

$$(c_y)_{\alpha+\omega_z} = c_y^{\alpha}\tau, \quad (m_z)_{\alpha+\omega_z} = m_z^{\alpha}\tau. \qquad (26.21)$$

Figures 26.7-26.9 depicts to the dependence of coefficients $(c_y)_{\alpha+\omega_z}$ and $(m_z)_{\alpha+\omega_z}$ on dimensionless time τ, obtained on the basis of numerical calculation, and also the hypotheses of harmony (26.20) and of stability (26.21). As an example are examined the delta wings of three elongations: $\lambda = 0.5$; 1.5; 5.0 - at subsonic speeds ($M = 0,6$). The hypothesis of harmony gives an especially good coincidence with numerical calculation during relatively small wing aspect ratio ($\lambda = 0.5$) and can serve good method of approximately determining aerodynamic characteristics, also, during the rotary motion of wing (see Fig. 26.7, 26.8).

At supersonic speeds ($M = 1,2$ and $M = 2$) analogous comparison is carried out for plates of infinite span. The more the number M, the the calculations according to the hypothesis of harmony they coincide with numerical calculations (see Fig. 26.9).

Is given below an example of the numerical calculation of the transient function of delta wing $\lambda = 0.5$ in the compressed medium ($M = 0,6$) during rotary motion. Values $(c_y)_{\alpha+\omega_z}$ and $(m_z)_{\alpha+\omega_z}$, determined by precise (numerical) calculation, are compared with the results of the approximate computations according to the hypotheses of harmony and stability. The coefficients of aerodynamic derivatives for the wing in question have the following values: $c_y^\alpha = 0,75$, $c_y^{\dot\alpha} = 0,199$, $c_y^{\omega_z} = 0,65$, $m_z^\alpha = -0,375$, $m_z^{\dot\alpha} = -0,12$, ($m_z^{\omega_z} = -0,375$.) As significant dimension is here undertaked root wing chord b; centering in the leading edge/nose of wing ($\bar{x}_T = 0$).

Table 26.1.

τ	0	0,143	0,286	0,429	0,571	0,714	0,857
$\left[\frac{c_y}{\alpha^\circ}\right]$	2	1,8297	0,7158	0,6995	0,6903	0,6943	0,6969
$(c_y)_{\dot{\alpha}}$	–	0,2734	0,4560	0,5564	0,6555	0,7541	0,8539
$\left[\frac{c_y}{\omega_z^\circ}\right]$	–	1,3618	0,6653	0,6529	0,6458	0,6486	0,6507
$(c_y)_{\dot{\alpha}+\omega_z}$	4,46	1,6352	1,1213	1,2093	1,3013	1,4027	1,5046
$(c_y)_{\text{гарм}}$	0,849	0,95625	1,0635	1,1707	1,27725	1,3845	1,49175
$(c_y)_{\text{стац}}$	0	0,10725	0,2145	0,32175	0,42825	0,5355	0,64275
$\left[\frac{m_z}{\alpha^\circ}\right]$	–1,3	–1,2457	–0,4426	–0,4279	–0,4229	–0,4265	–0,4279
$(m_z)_{\dot{\alpha}}$	–	–0,1818	–0,3028	–0,3645	–0,4252	–0,4857	–0,5470
$\left[\frac{m_z}{\omega_z^\circ}\right]$	–	–0,9924	–0,4607	–0,4489	–0,4449	–0,4474	–0,4487
$(m_z)_{\dot{\alpha}+\omega_z}$	–3,33	–1,1742	–0,7635	–0,8134	–0,8701	–0,9331	–0,9957
$(m_z)_{\text{гарм}}$	–0,493	–0,5466	–0,6002	–0,6538	–0,7071	–0,7607	–0,8143
$(m_z)_{\text{стац}}$	0	–0,05362	–0,1072	–0,16087	–0,2141	–0,2677	–0,3237

Table 26.1 (continued)

τ	1,0	1,143	1,286	1,429	1,571	1,714	1,857	2,0
$\left[\frac{c_y}{\alpha^\circ}\right]$	0,6966	0,6970	0,6972	0,6974	0,6974	0,6975	0,6976	0,6976
$(c_y)_{\dot{\alpha}}$	0,9538	1,0534	1,1531	1,2528	1,3507	1,4510	1,5513	1,6511
$\left[\frac{c_y}{\omega_z^\circ}\right]$	0,6505	0,6508	0,6510	0,6511	0,6512	0,6513	0,6514	0,6514
$(c_y)_{\dot{\alpha}+\omega_z}$	1,6043	1,7042	1,8041	1,9039	2,0019	2,1023	2,2027	2,3025
$(c_y)_{\text{гарм}}$	1,599	1,70625	1,8136	1,92075	2,0272	2,1345	2,24175	2,349
$(c_y)_{\text{стац}}$	0,75	0,85725	0,9645	1,07175	1,1782	1,2855	1,39275	1,5
$\left[\frac{m_z}{\alpha^\circ}\right]$	–0,4279	–0,4282	–0,4284	–0,4284	–0,4285	–0,4285	–0,4286	–0,4286
$(m_z)_{\dot{\alpha}}$	–0,6084	–0,6696	–0,7308	–0,7921	–0,8521	–0,9138	–0,9755	–1,0368
$\left[\frac{m_z}{\omega_z^\circ}\right]$	–0,4487	–0,4489	–0,4490	–0,1491	–0,4492	–0,1492	–0,4493	–0,4493
$(m_z)_{\dot{\alpha}+\omega_z}$	–1,0571	–1,1185	–1,1798	–1,2412	–1,3013	–1,3630	–1,4248	–1,4861
$(m_z)_{\text{гарм}}$	–0,868	–0,9216	–0,9752	–1,0288	–1,0761	–1,1357	–1,1893	–1,243
$(m_z)_{\text{стац}}$	–0,375	–0,4286	–0,4822	–0,5358	–0,5891	–0,6427	–0,6963	–0,750

Page 608.

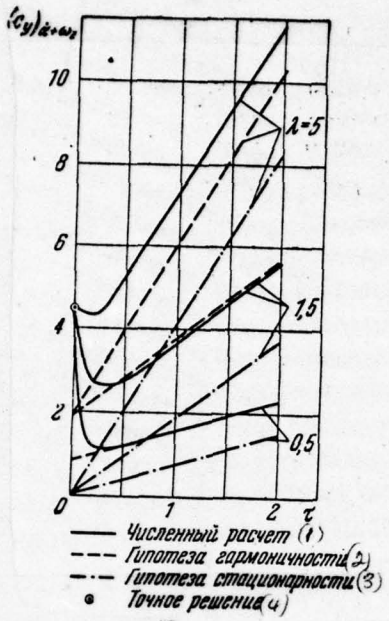


Fig. 26.7.

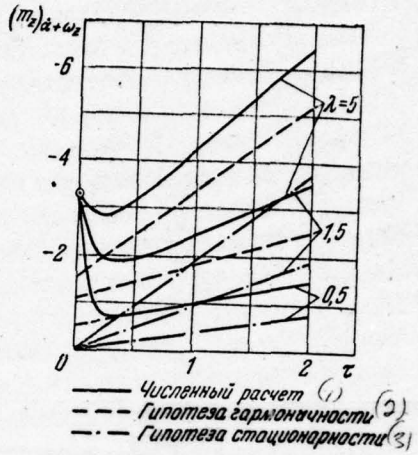


Fig. 26.8.

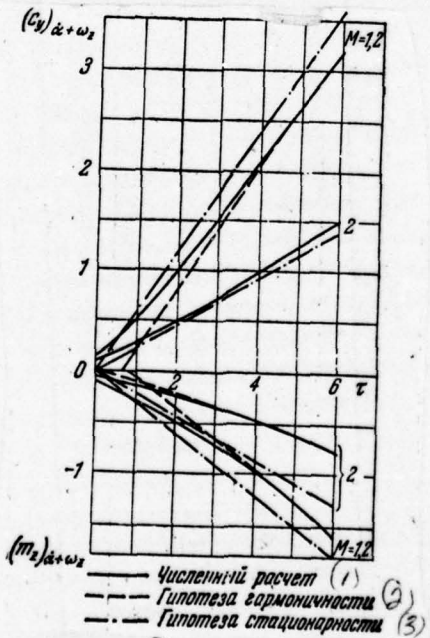


Fig. 26.9.

Fig. 26.7. Delta wing (M = 0.6).

Key: (1). Numerical calculation. (2). Hypothesis of harmonicity. (3). Stability hypothesis. (4). Exact solution.

Fig. 26.8. Delta wings (M = 0.6).

Key: (1). Numerical calculation. (2). Hypothesis of harmonicity. (3). Stability hypothesis.

Fig. 26.9. Infinite-span wing ($\lambda = \infty$).

Key: (1). Numerical calculation. (2). Hypothesis of harmonicity. (3). Stability hypothesis.

Page 609.

At zero time ($\tau = 0$) for transient functions we have the exact solutions:

$$(c_y(0))_{\alpha+\omega_z} = 4{,}46, \quad (m_z(0))_{\alpha+\omega_z} = -3{,}33.$$

The results of the calculations conducted are brought to table 26.1; the comparison of the different methods of the calculation given also in Fig. 26.7 and 26.8.

§4. Method of the local pressures. Method of tangential wedges.

Let us present according to (2.24) a difference in the pressure coefficient at the appropriate points of lower and suction sides of wing through the coefficients of the aerodynamic derivatives:

$$\Delta\bar{p} = \frac{p_- - p_+}{\rho\frac{U_0^2}{2}} = \sum_{i=1}^{4}\left(p^{q_i}q_i + p^{\dot{q}_i}\dot{q}_i\right) = p^{\alpha}\alpha + p^{\dot{\alpha}}\dot{\alpha} + p^{\omega_x}\omega_x +$$

$$+ p^{\dot{\omega}_x}\dot{\omega}_x + p^{\omega_z}\omega_z + p^{\dot{\omega}_z}\dot{\omega}_z + p^{\delta}\delta + p^{\dot{\delta}}\dot{\delta} + p^{\Delta}\Delta + p^{\dot{\Delta}}\dot{\Delta}. \quad (26.22)$$

The coefficients of the aerodynamic derivatives of lift and moments of the wing of symmetrical planform are connected with the coefficients of pressures by the relationship/ratios of form (2.5), namely:

$$\left.\begin{aligned}
c_y^{q_i} &= \lambda \frac{b}{l_4} \int_0^1 \int_{\bar{x}_1}^{\bar{x}_0} p^{q_i}\, d\bar{x}\, d\bar{z}, & c_y^{\dot{q}_i} &= \lambda \frac{b}{l} \int_0^1 \int_{\bar{x}_1}^{\bar{x}_0} p^{\dot{q}_i}\, d\bar{x}\, d\bar{z}, \\
m_x^{q_i} &= -\frac{\lambda}{2} \int_0^1 \int_{\bar{x}_1}^{\bar{x}_0} p^{q_i} \bar{z}\, d\bar{x}\, d\bar{z}, & m_x^{\dot{q}_i} &= -\frac{\lambda}{2} \int_0^1 \int_{\bar{x}_1}^{\bar{x}_0} p^{\dot{q}_i} \bar{z}\, d\bar{x}\, d\bar{z}, \\
m_z^{q_i} &= \lambda \frac{b}{l} \int_0^1 \int_{\bar{x}_1}^{\bar{x}_0} p^{q_i} \bar{x}\, d\bar{x}\, d\bar{z}, & m_z^{\dot{q}_i} &= \lambda \frac{b}{l} \int_0^1 \int_{\bar{x}_1}^{\bar{x}_0} p^{\dot{q}_i} \bar{x}\, d\bar{x}\, d\bar{z},
\end{aligned}\right\} \quad (26.23)$$

where $q_i = \alpha, \omega_x, \omega_z, \delta, \Delta$; $\bar{x} = \frac{x}{b}$, $\bar{z} = \frac{2z}{l}$, $\bar{x}_0$, $\bar{x}_1$ - the dimensionless coordinates of leading and trailing wing edges. If we in relationship/ratios (26.23) take the precise or approximate values of pressure coefficients, then also the coefficients of the aerodynamic derivatives of lift and torque/moments we will obtain by respectively precise or those which were approximated.

Page 610.

Let from the calculation or experiment during the steady motion

of this wing at the assigned number M be found the coefficients of pressure $\bar{p} = \bar{p}(\alpha)$. Let us find derivative

$$\left.\frac{d\bar{p}}{d\alpha}\right|_{\alpha=\alpha_0} = f(\alpha_0). \qquad (26.24)$$

Let us assume that this derivative during unsteady motion can be undertaked by the same as during steady flow (hypothesis of the local pressures). In this case the mutual effect of the different points of lifting surface is considered in the simplist form of motion - to steady flow.

During any unsteady motion along the method of the local pressures we have

$$\bar{p} = \frac{d\bar{p}}{d\alpha}\alpha_\Sigma, \qquad (26.25)$$

$$\alpha_\Sigma = -\frac{W_y}{U_0}, \qquad (26.26)$$

where α_Σ - instantaneous local total angle. The normal component of the relative disturbed speed of the medium W_y in the point (x, z) of surface is determined from boundary condition (3.56'). Thus, in standard system of coordinates we have

$$\alpha_\Sigma = \alpha + \omega_{x1}\bar{z} - \omega_z\bar{x} + \frac{\partial f_\delta}{\partial \bar{x}}\delta - f_{\dot{\delta}}\dot{\delta} + f_\Delta\Delta. \qquad (26.27)$$

Let us designate pressures on lower and suction sides of wing by indices respectively "-" and "+", then aerodynamic loading $\Delta\bar{p}$ at the points of lifting surface will be

$$\Delta\bar{p} = \bar{p}_- - \bar{p}_+. \qquad (26.28)$$

By substituting (26.27) in (26.25) and by comparing $\Delta\bar{p}$ with (26.22), we will obtain the coefficients of aerodynamic pressure derivatives in terms of the method of the local pressures:

$$\left.\begin{aligned} p^{\alpha} &= \left[\frac{d\bar{p}}{d\alpha}\Big|_{-} - \frac{d\bar{p}}{d\alpha}\Big|_{+}\right], \quad p^{\omega_{x1}} = \left[\frac{d\bar{p}}{d\alpha}\Big|_{-} - \frac{d\bar{p}}{d\alpha}\Big|_{+}\right]\bar{z}, \\ p^{\omega_z} &= \left[\frac{d\bar{p}}{d\alpha}\Big|_{-} - \frac{d\bar{p}}{d\alpha}\Big|_{+}\right]\bar{x}, \quad p^{\delta} = \left[\frac{d\bar{p}}{d\alpha}\Big|_{-} - \frac{d\bar{p}}{d\alpha}\Big|_{+}\right]\frac{\partial f_{\delta}}{\partial \bar{x}}, \\ p^{\delta} &= \left[\frac{d\bar{p}}{d\alpha}\Big|_{-} - \frac{d\bar{p}}{d\alpha}\Big|_{+}\right]f_{\delta}, \quad p^{\Delta} = \left[\frac{d\bar{p}}{d\alpha}\Big|_{-} - \frac{d\bar{p}}{d\alpha}\Big|_{+}\right]f_{\Delta}, \\ p^{\dot{\alpha}} &= p^{\dot{\omega}_{x1}} = p^{\dot{\omega}_z} = p^{\dot{\Delta}} = 0. \end{aligned}\right\} \quad (26.29)$$

By substituting these expressions in (26.23), we will obtain the coefficients aerodynamic derivative total characteristics.

In certain cases it is possible to obtain simple analytical expressions for function $d\bar{p}/d\alpha$.

Page 611.

Let us define pressures at the points of wing approximately according to the method of tangential wedges [1.22], i.e., by accepting $d\bar{p}/d\alpha$

by the same as of wedge. As is known [for 1.8], relative pressure on the surface of wedge in the linearized supersonic flow equally

$$\bar{p} = \frac{2\vartheta}{k}, \tag{26.30}$$

where ϑ is a wedge angle relative to the speed of undisturbed flow, whereupon $\vartheta < 0$ during the flow about the convex angle and $\vartheta > 0$ during the flow about the concave angle (Fig. 26.10). From (26.30) we obtain

$$\left.\frac{d\bar{p}}{d\alpha}\right|_{-} = \frac{d\bar{p}}{d\vartheta} = \frac{2}{k}, \quad \left.\frac{d\bar{p}}{d\alpha}\right|_{+} = -\frac{d\bar{p}}{d\vartheta} = -\frac{2}{k}. \tag{26.31}$$

For the coefficients of aerodynamic pressure derivative according to (26.31) let us have

$$\left.\begin{aligned} &p^{\alpha} = \frac{4}{k}, \quad p^{\omega_{x1}} = \frac{4}{k}\bar{z} \quad p^{\omega_z} = -\frac{4}{k}\bar{x}, \quad p^{\delta} = \frac{4}{k}\frac{\partial f_{\delta}}{\partial \bar{x}}, \\ &p^{\delta} = -\frac{4}{k}f_{\delta}, \quad p^{\Delta} = \frac{4}{k}f_{\Delta}, \quad p^{\dot{\alpha}} = p^{\dot{\omega}_{x1}} = p^{\dot{\omega}_z} = p^{\dot{\Delta}} = 0. \end{aligned}\right\} \tag{26.32}$$

By substituting these expressions in (26.23), we will obtain the values of the coefficients of the aerodynamic derivatives of lift and torque/moments for the wing of the assigned planform. It is easy to see that for all wings

$$c_y^{\dot{\alpha}} = c_y^{\dot{\omega}_z} = m_z^{\dot{\alpha}} = m_z^{\dot{\omega}_z} = m_{x1}^{\dot{\omega}_{x1}} = 0. \tag{26.33}$$

Let us find the expressions of the coefficients of aerodynamic derivatives without points for wings with direct/straight edges. The beginning of the axes let us place in the spout of root chord, and for significant dimensions let us accept the root chord b for m_z and

ω_z, and)

for m_{x_1} and ω_{x_1} - respectively 1 and 1/2 For such wings of the equation of leading and trailing edges in the adopted system of coordinates they will take the form (see §2 chapters I)

$$\left.\begin{aligned}\bar{x}_0 &= -\left(\frac{\eta+1}{\eta}\right)\frac{\lambda \operatorname{tg}\chi_0}{4}\bar{z},\\ \bar{x}_1 &= -1-\left(\frac{\eta-1}{\eta}+\frac{\eta+1}{\eta}\,\frac{\lambda \operatorname{tg}\chi_0}{4}\right)\bar{z}.\end{aligned}\right\} \tag{26.34}$$

Furthermore, let us consider that

$$\frac{b}{l}=\frac{2\eta}{\lambda(\eta+1)}.$$

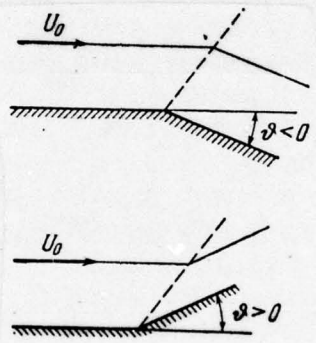


Fig. 26.10. On the calculation of according to the method of tangential wedges.

Page 612.

By substituting expressions for pressures (26.32) in (26.23) and by integrating within the limits indicated, we will obtain

$$\left.\begin{aligned} c_y^{\alpha} &= \frac{4}{k}, \\ c_y^{\omega_z} &= -m_z^{\alpha} = \frac{4}{k}\left[\frac{\eta^2+\eta+1}{3\eta(\eta+1)} + \frac{\eta+2}{3\eta}\,\frac{\lambda \operatorname{tg}\chi_0}{4}\right], \\ m_z^{\omega_z} &= -\frac{2}{3k}\left[\frac{\eta^2+1}{\eta^2} + \frac{\eta^2+2\eta+3}{\eta^2}\,\frac{\lambda \operatorname{tg}\chi_0}{4} + \right. \\ &\qquad \left. + \frac{\eta^2+4\eta+3}{\eta^2}\left(\frac{\lambda \operatorname{tg}\chi_0}{4}\right)^2\right], \\ m_{x1}^{\omega_{x1}} &= -\frac{1}{3k}\,\frac{\eta+3}{\eta+1}. \end{aligned}\right\} \qquad (26.35)$$

In the particular case of the rectangular wings

$$\left.\begin{aligned} c_y^{\alpha} &= \frac{4}{k}, \qquad m_z^{\alpha} = -\frac{2}{k}, \quad c_y^{\omega_z} = \frac{2}{k}, \\ m_z^{\omega_z} &= -\frac{4}{3k}, \quad m_{x1}^{\omega_{x1}} = -\frac{2}{3k}. \end{aligned}\right\} \qquad (26.36)$$

It is analogous, for direct/straight delta wings ($\eta = \infty, \lambda \operatorname{tg}\chi_0 = 4$)

$$\left.\begin{aligned} c_y^{\alpha} &= \frac{4}{k}, \qquad m_z^{\alpha} = -\frac{8}{3k}, \quad c_y^{\omega_z} = \frac{8}{3k}, \\ m_z^{\omega_z} &= -\frac{2}{k}, \quad m_{x1}^{\omega_{x1}} = -\frac{1}{3k}. \end{aligned}\right\} \qquad (26.37)$$

Comparing (26.36) with (22.13), a (26.37) with (22.32), we see that the method of tangential wedges gives the results, which coincide with exact solutions by linear theory for the infinite-span wing and delta wings with supersonic edges with $p^* \to 0$. The same is obtained for the distributed characteristics (loads). For the wings of the final elongation the results, obtained from the method of tangential wedges, will be precise solutions, than are more number/M

and wing aspect ratio.

One should again emphasize that everything said concerns only coefficients of aerodynamic derivatives without points.

§5. Piston theory.

In supersonic speeds frequently is applied so-called piston theory [1.26]. Let us give its basic condition/positions and the escape/ensuing of them relationship/ratios for aerodynamic wing characteristics.

Page 613.

Let us examine lifting surface by that consisting of the large number of separate trace elements. Then any unsteady motion of wing can be presented as totality of the motions of these cell/elements. In the general case of disturbance/perturbation at the particular point of wing they will be caused not only by the motion of the cell/element, to which belongs the point in question, but also by all remaining cell/elements of wing. However, in certain cases of disturbance/perturbation at the particular point from other

cell/elements they will be considerably less than those, that are caused by the motion of the cell/element itself. Let us assume that the disturbed pressure at the particular point is created only because of the disturbance/perturbations, introduced into current of traffic of the cell/element itself. In this case it is possible to count that the disturbance/perturbations from the motion of the examined element to sides are not spread, i.e., cell/element works as piston in duct. Therefore the theory, based on the assumption indicated, is called "piston".

Let us determine when making these assumptions the disturbed pressure, created by the motion of the cell/element of wing surface. For this let us examine the task of the unsteady isentropically flow of gas, included into cylindrical pipe and which is located on top above the piston (Fig. 26.11). Piston is moved upward with speed w, small as compared with the speed of sound in the undisturbed medium of gas. The velocity of propagation of slight disturbances (speed of sound) let us designate a', pressure p, density ρ. All these values change with removal/distance from piston. At sufficiently large distance from piston, gas is found in rest and w = 0. The speed of sound, the pressure and density in the undisturbed gas let us designate a, p_∞, ρ_∞. Let us select at certain distance from the piston two infinitely close sections m and m' at a distance dy = a' dt. Let in section m the pressure is equal to p, and in section m'

equally to p are dp. Let us compose momentum equation for the elementary mass of gas ρ dy, included between sections with single area. We consider that under the effect of disturbance/perturbation from piston this mass for time dt acquires the supplementary speed dw,

$$\rho\, dy\, dw = p\, dt - (p - dp)\, dt,$$

hence

$$dw = \frac{1}{\rho a'}\, dp. \qquad (26.38)$$

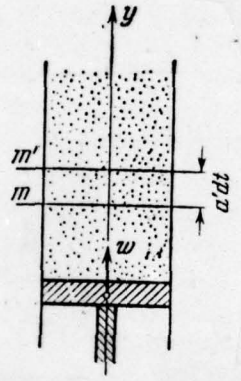


Fig. 26.11. To the derivation of the equation of motion of gas in moving piston.

Page 614.

For an isentropic process, as is known, occurs the dependence

$$\frac{p}{\rho^{\varkappa}} = \frac{p_\infty}{\rho_\infty^{\varkappa}} = \text{const}, \qquad (26.39)$$

while the speed of sound

$$a' = \sqrt{\varkappa \frac{p}{\rho}}. \qquad (26.40)$$

Here $\varkappa = c_p/c_v$ is relation of the heat capacities of gas. Equalities (26.38) and (26.40) give

$$dw = \frac{a'}{\varkappa p}\, dp. \qquad (26.41)$$

Utilizing (26.40), is expressed the speed of sound a' in the arbitrary section through the speed of sound a at infinity:

$$\frac{a'}{a} = \sqrt{\frac{p\rho_\infty}{\rho p_\infty}} = \left(\frac{p}{p_\infty}\right)^{\frac{\varkappa-1}{2\varkappa}}. \qquad (26.42)$$

Relationship/ratio (26.41) takes the form

$$dw = \frac{a}{\varkappa}\left(\frac{p}{p_\infty}\right)^{\frac{\varkappa-1}{2\varkappa}} \frac{dp}{p}. \qquad (26.43)$$

By integrating, we will obtain

$$w = \int_1^{p/p_\infty} \frac{a}{\varkappa}\left(\frac{p}{p_\infty}\right)^{\frac{-\varkappa-1}{2\varkappa}} d\left(\frac{p}{p_\infty}\right),$$

whence

$$w = \frac{2a}{\varkappa - 1}\left[\left(\frac{p}{p_\infty}\right)^{\frac{\varkappa-1}{2\varkappa}} - 1\right]. \qquad (26.44)$$

Further we have

$$\frac{p}{p_\infty} = \left(1 + \frac{\varkappa - 1}{2}\frac{w}{a}\right)^{\frac{2\varkappa}{\varkappa-1}}. \qquad (26.45)$$

If we pores p imply the gas pressure on piston, then in formula

(26.45) w it is necessary to take with plus sign during piston stroke upward (see Fig. 26.11) and with minus sign during piston stroke down. Counting w < a, is decomposed expression (26.45) in binomial series. Being limited to linear terms and taking into account that $\varkappa p_\infty = a^2\rho_\infty$, we find for the slight disturbances

$$p - p_\infty = \rho_\infty a w. \tag{26.46}$$

Page 615.

The pressure coefficient

$$\bar{p} = \frac{p - p_\infty}{\rho_\infty \frac{U_0^2}{2}} = \frac{2}{M}\frac{w}{U_0}, \tag{26.47}$$

where $M = U_0/a$ - Mach number.

Let us examine now the wing, which, besides forward motion along axis Ox at speed U_0, completes arbitrary motion. Then from boundary conditions (3.56') we have for a speed motions of cell/elements of wing on the lower surface

$$\frac{w}{U_0} = \alpha^* f(\tau) + \omega_x^* \bar{z} f(\tau) - \omega_z^* \bar{x} f(\tau) + \frac{\partial f_\delta}{\partial \bar{x}} \delta^* f(\tau) - f_\delta \dot{\delta}^* f(\tau). \tag{26.48}$$

Let f (τ) change according to the stepped law:

$$f(\tau) = \begin{cases} 0 & \text{(1) при} \quad \tau < 0, \\ 1 & \text{при} \quad \tau \geqslant 0. \end{cases} \tag{26.49}$$

Key: (1). with.

Then from (26.28) and (26.47) taking into account the fact that signs w for lower and suction sides of wing are different, we obtain

$$\left.\begin{aligned} &\left[\frac{\Delta\bar{p}}{\alpha^\circ}\right]=\frac{4}{M},\quad \left[\frac{\Delta\bar{p}}{\omega_z^\circ}\right]=-\frac{4}{M}\bar{x},\quad \left[\frac{\Delta\bar{p}}{\omega_x^\circ}\right]=\frac{4}{M}\bar{z},\\ &\left[\frac{\Delta\bar{p}}{\delta^\circ}\right]=\frac{4}{M}\frac{\partial f_\delta}{\partial\bar{x}},\quad \left[\frac{\Delta\bar{p}}{\dot{\delta}^\circ}\right]=-\frac{4}{M}f_\delta. \end{aligned}\right\} \qquad (26.50)$$

By substituting (26.50) into formulas of type (26.23) by performing the integration within the limits, determined by formulas (26.23), for wings with direct/straight edges we will obtain during change α

$$\left[\frac{c_y}{\alpha^\circ}\right]=\frac{4}{M},\quad \left[\frac{m_z}{\alpha^\circ}\right]=-\frac{4}{M}\left[\frac{\eta^2+\eta+1}{3\eta(\eta+1)}+\frac{\eta+2}{3\eta}\frac{\lambda\operatorname{tg}\chi_0}{4}\right]. \qquad (26.51)$$

During a change in the angular velocity Ω_z

$$\left.\begin{aligned} &\left[\frac{c_y}{\omega_z^\circ}\right]=\frac{4}{M}\left[\frac{\eta^2+\eta+1}{3\eta(\eta+1)}+\frac{\eta+2}{3\eta}\frac{\lambda\operatorname{tg}\chi_0}{4}\right],\\ &\left[\frac{m_z}{\omega_z^\circ}\right]=-\frac{2}{3M}\left[\frac{\eta^2+1}{\eta^2}+\frac{\eta^2+2\eta+3}{\eta^2}\frac{\lambda\operatorname{tg}\chi_0}{4}+\right.\\ &\qquad\left.+\frac{\eta^2+4\eta+3}{\eta^2}\left(\frac{\lambda\operatorname{tg}\chi_0}{4}\right)^2\right], \end{aligned}\right\} \qquad (26.52)$$

during rotation around axis Ox at angular velocity Ω_x

$$\left[\frac{m_{x1}}{\omega_{x1}^\circ}\right]=-\frac{1}{3M}\frac{\eta+3}{\eta+1}, \qquad (26.53)$$

and finally during the strains of the wing

$$\left.\begin{aligned}
\left[\frac{c_y}{\dot{\delta}^\circ}\right] &= -\frac{4}{M}\lambda\frac{b}{l}\int_0^1\int_{\bar{x}_0}^{\bar{x}_1}\frac{\partial f_\delta}{\partial\bar{x}}\,d\bar{x}\,d\bar{z},\\
\left[\frac{m_z}{\dot{\delta}^\circ}\right] &= -\frac{4}{M}\lambda\frac{b}{l}\int_0^1\int_{\bar{x}_0}^{\bar{x}_1}\frac{\partial f_\delta}{\partial\bar{x}}\,\bar{x}\,d\bar{x}\,d\bar{z},\\
\left[\frac{c_y}{\dot{\delta}^\circ}\right] &= \frac{4}{M}\lambda\frac{b}{l}\int_0^1\int_{\bar{x}_0}^{\bar{x}_1} f_\delta\,d\bar{x}\,d\bar{z},\\
\left[\frac{m_z}{\dot{\delta}^\circ}\right] &= \frac{4}{M}\lambda\frac{b}{l}\int_0^1\int_{\bar{x}_0}^{\bar{x}_1} f_\delta\bar{x}\,d\bar{x}\,d\bar{z}.
\end{aligned}\right\} \qquad (26.54)$$

Page 616.

In the particular case of rectangular wings ($\eta = 1$, $\lambda \operatorname{tg}\chi_0 = 0$) let us have with the beginning of the axes in the nose of the root chord

$$\left[\frac{c_y}{\dot{\alpha}^\circ}\right] = \frac{4}{M},\quad \left[\frac{m_z}{\dot{\alpha}^\circ}\right] = -\frac{2}{M},\quad \left[\frac{c_y}{\dot{\omega}_z^\circ}\right] = \frac{2}{M},\quad \left[\frac{m_z}{\dot{\omega}_z^\circ}\right] = -\frac{4}{3M},\quad \left[\frac{m_{x1}}{\dot{\omega}_{x1}^\circ}\right] = -\frac{2}{3M}. \qquad (26.55)$$

For delta wings ($\eta = \infty$, $\lambda \operatorname{tg}\chi_0 = 4$)

$$\left.\begin{aligned}
&\left[\frac{c_y}{\dot{\alpha}^\circ}\right] = \frac{4}{M},\quad \left[\frac{m_z}{\dot{\alpha}^\circ}\right] = -\frac{8}{3M},\quad \left[\frac{c_y}{\dot{\omega}_z^\circ}\right] = \frac{8}{3M},\\
&\left[\frac{m_z}{\dot{\omega}_z^\circ}\right] = -\frac{2}{M},\quad \left[\frac{m_{x1}}{\dot{\omega}_{x1}^\circ}\right] = -\frac{1}{3M}.
\end{aligned}\right\} \qquad (26.56)$$

Analogously, by utilizing (26.23), (26.29), it is possible to obtain the coefficients aerodynamic derivative loads and total characteristics. They will be determined by relationship/ratios (26.50) - (26.54), in which values $[c/q_i^*]$ one should replace by

$$c^{q_i}(c = p,\ c_y,\ m_z,\ m_{x1};\ q_i = \alpha,\ \omega_z,\ \omega_x,\ \delta,\ \dot{\delta}).$$

All coefficients of aerodynamic derivatives with the points of the total and distributed characteristics of rigid wing in terms of piston theory will be equal to zero. As concerns the wing being deformed that here they appear the coefficients, which stand with factor $d\delta/d\tau = \dot{\delta}$. This is connected with the fact that the corresponding factor is contained under boundary condition. Its appearance is caused by those supplementary angles of attack, which are caused by the velocities of the strain of the cell/element of wing in question.

One should expect, that piston theory will to give the the better/best results, the greater the specific useful load, caused by the local disturbances, in comparison with the loads, caused by the effect of other cell/elements of wing.

Earlier, in chapter IV, were obtained precise relationship/ratios for transient functions with $M \neq 0$ into the initial moment $(\tau \to 0)$ during a stepped variation in the boundary conditions. It is easy to ascertain that they coincide with those, that escape/ensue from piston theory. The reason for this coincidence is clear. Actually, during a stepped variation in the boundary conditions at the initial moment $(\tau \to 0)$ is observed an abrupt change in them. Disturbance/perturbations from the different cell/elements of wing at zero time still not manage to be propagated on wing, if the speed of sound is final $(M \neq 0)$, and each cell/element creates disturbance/perturbations independent of other. Thus, in this case all assumptions of piston theory are satisfied accurately.

In chapter VI the application/use of a Duhamel integral for the calculation of the coefficients of aerodynamic derivatives led to the precise relationship/ratio

$$A_{q_i}|_{\tau \to 0} = c^{q_i}(p^*)|_{p^* \to \infty}.$$

Hence it follows that all coefficients aerodynamic derivative total

and distributed wing characteristics with λ ($p^* \to \infty$) and λ ($M \neq 0$) are determined accurately from piston theory. This is connected with the fact that during the oscillations of wing with high frequency the local disturbances prevail above those, that are created at the particular point by the fluctuations of other points of wing.

Thus, piston theory gives the accurate results, in two cases indicated with $M \neq 0$: for transient functions at the initial moment Λ ($\tau \to 0$) and for the coefficients of aerodynamic derivatives with very large Strouhal numbers ($p^* \to \infty$).

Figure 26.12 in the form of an example gives the comparison of the transient functions of lift $[c_y/\alpha^*]$ the rectangular wings of different elongation at supersonic speeds, obtained by the calculations according to linear and piston theories. It is evident, that the greater the number M and Λ the lesser the elongation λ, the nearer the results, obtained from piston theory, to precise. It is possible to say that with all $M \neq 0$ the piston theory gives the correct results for the wings of any planform with $\tau \to 0$.

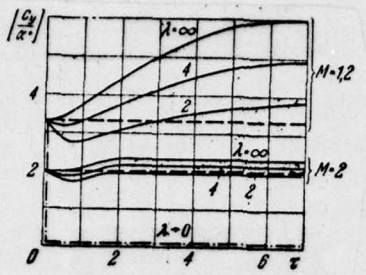


Fig. 26.12. Transient functions of the lift of rectangular wings. Comparison of linear (unbroken curves) and piston (dotted line) theories.

Page 618.

At supersonic speeds it the more precise in all range of change τ, the greater the number M.

In Fig. 26.13 and 26.14 given analogous comparisons for the coefficients of aerodynamic derivatives c_y^{α} and $c_y^{\dot{\alpha}}$ wing $\lambda = \infty$ with different Strouhal numbers. It is evident, that the greater the number M, the nearer the results of piston theory to datum, obtained

from strict linear theory. It is possible to draw the conclusion, that the greater the number M the more precise the results, determined according to piston theory. With $p^* \to \infty$ it gives accurate results for any wings with all $M \neq 0$.

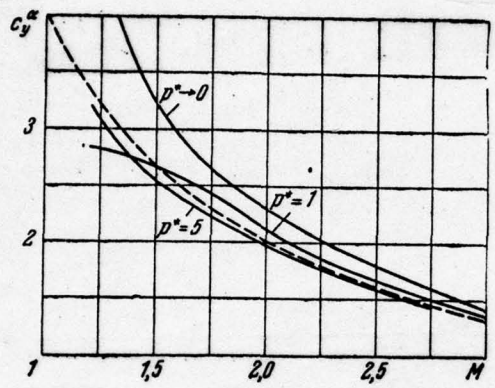


Fig. 26.13.

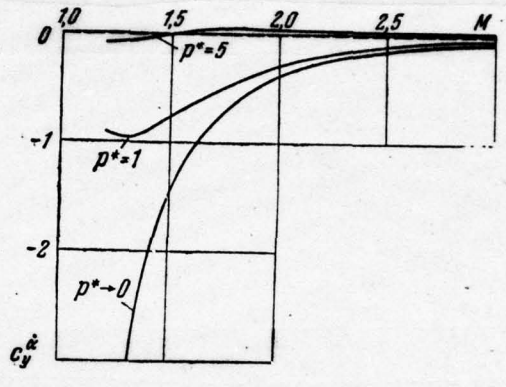


Fig. 26.14.

Fig. 26.13. The comparison of linear (unbroken curves) and piston (dotted line) theories for a derivative c_y^α covered λ = ∞.

Fig. 26.14. Comparison of linear (unbroken curves) and piston (dotted line) theories for a derived $c_y^{\dot\alpha}$ wing λ = ∞.

[Page 619] Chapter XXVII.

COEFFICIENTS OF THE AERODYNAMIC DERIVATIVE AND OF APPARENT ADDITIONAL MASSES.

§1. Coefficients of apparent additional masses.

The circuit of noncirculating flow makes it possible to simulate the phenomena, which occur at the average speed of motion U_0, of close to zero; therefore the given below material on the coefficients of apparent additional masses makes it possible to determine the total effect of the incompressible medium on wings during their evolutions on the spot, with the wind gusts, etc. Apparent additional masses are mainly necessary for the calculation in the incompressible medium of the dependences of the coefficients of aerodynamic derivatives of Strouhal number and during transition from some laws of motion to others on the basis of Duhamel integral.

The coefficients of apparent additional masses $(k_{22})_a$, $(k_{26})_a$, $(k_{66})_a$, $(k_{44})_a$ are connected with corresponding associated masses λ_{22}, λ_{26}, λ_{66}, λ_{44} as follows:

$$\left.\begin{aligned}(k_{22})_a &= \frac{\lambda_{22}}{\rho S b_a}, \quad (k_{26})_a = \frac{\lambda_{26}}{\rho S b_a^2},\\ (k_{66})_a &= \frac{\lambda_{66}}{\rho S b_a^3}, \quad (k_{44})_a = \frac{\lambda_{44}}{\rho S b_a l^2}.\end{aligned}\right\} \tag{27.1}$$

Here b_a, l, S are the mean aerodynamic chord, the spread/scope and wing area, ρ is density of the medium.

The forces and the torque/moments, which act on wing during noncirculating flow, are expressed as apparent additional masses by formulas (2.54) and (12.23). The coefficients of apparent additional masses were determined according to the procedure, presented in chapter XII, for the origin of coordinates, arrange/located in the leading edge/nose of the mean aerodynamic chord.

Page 620.

Table 27.1.

χ_0	η	λ	$(k_{22})_a$	$(k_{26})_a$	$(k_{66})_a$	$(k_{44})_a$
0	1	0,25	0,1605	−0,0803	0,0492	−0,0049
		0,5	0,2797	−0,1399	0,0832	−0,0094
		1,0	0,4283	−0,2142	0,1236	−0,0169
		1,5	0,5098	−0,2549	0,1452	−0,0228
		2,5	0,5905	−0,2953	0,1663	−0,0307
		5,0	0,6575	−0,3288	0,1836	−0,0399
		10	0,6893	−0,3447	0,1917	−0,0457
0	2	0,25	0,1462	−0,0486	0,0257	−0,0042
		0,5	0,2628	−0,0908	0,0468	−0,0080
		1,0	0,4211	−0,1516	0,0764	−0,0140
		1,5	0,5157	−0,1894	0,0945	−0,0188
		2,5	0,6142	−0,2295	0,1136	−0,0251
		5,0	0,6944	−0,2625	0,1293	−0,0324
		10	0,7278	−0,2764	0,1363	−0,0361
0	5	0,25	0,1173	−0,0250	0,0142	−0,0033
		0,5	0,2140	−0,0492	0,0265	−0,0057
		1,0	0,3571	−0,0913	0,0470	−0,0103
		1,5	0,4536	−0,1232	0,0623	−0,0135
		2,5	0,5696	−0,1653	0,0827	−0,0184
		5,0	0,6822	−0,2103	0,1054	−0,0234
		10	0,7364	−0,2340	0,1180	−0,0268
0	∞	0,25	0,0892	−0,0147	0,0099	−0,0024
		0,5	0,1656	−0,0304	0,0186	−0,0039
		1,0	0,2861	−0,0600	0,0336	−0,0071
		1,5	0,3757	−0,0859	0,0465	−0,0088
		2,5	0,4966	−0,1257	0,0658	−0,0122
		5,0	0,6378	−0,1788	0,0921	−0,0162
		10	0,7202	−0,2136	0,1104	−0,0195
30°	1	0,25	0,1593	−0,0785	0,0473	−0,0049
		0,5	0,2746	−0,1336	0,0772	−0,0093
		1,0	0,4109	−0,1949	0,1066	−0,0165
		1,5	0,4791	−0,2222	0,1187	−0,0219
		2,5	0,5401	−0,2411	0,1297	−0,0289
		5,0	0,5851	−0,2419	0,1680	−0,0363
		10	0,6040	−0,2126	0,3696	−0,0406
30°	2	0,25	0,1495	−0,0508	0,0266	−0,0042
		0,5	0,2719	−0,0984	0,0506	−0,0080
		1,0	0,4384	−0,1687	0,0838	−0,0144
		1,5	0,5306	−0,2101	0,1027	−0,0191
		2,5	0,6103	−0,2480	0,1211	−0,0249
		5,0	0,6518	−0,2755	0,1625	−0,0303
		10	0,6566	−0,2989	0,3541	−0,0328

Page 621.

Table 27.1 (continuation).

χ_0	η	λ	$(k_{xx})_a$	$(k_{xz})_a$	$(k_{zz})_a$	$(k_{yy})_a$
30°	5	0,25	0,1206	−0,0266	0,0145	−0,0033
		0,5	0,2241	−0,0552	0,0286	−0,0059
		1,0	0,3819	−0,1100	0,0528	−0,0106
		1,5	0,4882	−0,1543	0,0718	−0,0142
		2,5	0,6024	−0,2105	0,0965	−0,0189
		5,0	0,6764	−0,2614	0,1309	−0,0231
		10	0,6867	−0,2955	0,2457	−0,0248
30°	∞	0,25	0,0923	−0,0156	0,0096	−0,0025
		0,5	0,1738	−0,0336	0,0192	−0,0042
		1,0	0,3070	−0,0721	0,0362	−0,0070
		1,5	0,4078	−0,1087	0,0521	−0,0094
		2,5	0,5391	−0,1663	0,0761	−0,0129
		5,0	0,6600	−0.2361	0,1095	−0,0166
		10	0,6939	−0,2779	0,1691	−0,0184
45°	1	0,25	0,1571	−0,0766	0,0456	−0,0049
		0,5	0,2656	−0,1266	0,0713	−0,0091
		1,0	0,3812	−0,1738	0,0926	−0,0159
		1,5	0,4297	−0,1883	0,1004	−0,0206
		2,5	0,4668	−0,1914	0,1179	−0,0261
		5,0	0,4904	−0,1736	0,2338	−0,0314
		10	0,4983	−0,1244	0,7940	−0,0343
45°	2	0,25	0,1511	−0,0556	0,0302	−0.0042
		0,5	0,2753	−0,1036	0,0533	−0,0080
		1,0	0,4343	−0,1756	0,0883	−0,0143
		1,5	0,5069	−0,2105	0,1054	−0,0185
		2,5	0,5505	−0,2341	0,1279	−0,0230
		5,0	0,5559	−0,2485	0,2369	−0,0264
		10	0,5454	−0,2732	0,7538	−0,0278
45°	5	0,25	0,1226	−0,0277	0,0148	−0,0033
		0,5	0,2291	−0,0601	0,0299	−0,0061
		1,0	0,3909	−0,1245	0,0588	−0,0107
		1,5	0,4925	−0,1746	0,0820	−0,0142
		2,5	0,5770	−0,2264	0,1116	−0,0181
		5,0	0,5966	−0,2576	0,1804	−0,0205
		10	0,5787	−0,2862	0,5037	−0,0212
45°	∞	0,25	0,0940	−0,0162	0,0103	−0,0025
		0,5	0,1783	−0,0367	0,0196	−0,0042
		1,0	0,3168	−0,0828	0,0397	−0,0072
		1,5	0,4197	−0.1270	0,0588	−0,0096
		2,5	0,5398	−0,1921	0,0897	−0,0127
		5,0	0,6063	−0,2476	0,1375	−0,0151
		10	0,5962	−0,2745	0,3003	−0,0160

Table 27.1. Con't.

χ_0	η	λ	$(k_{22})_a$	$(k_{24})_a$	$(k_{44})_a$	$(k_{46})_a$
60°	1	0,25	0,1514	−0,0726	0,0421	−0,0048
		0,5	0,2446	−0,1124	0,0610	−0,0088
		1,0	0,3165	−0,1347	0,0724	−0,0144
		1,5	0,3367	−0,1341	0,0829	−0,0177
		2,5	0,3487	−0,1239	0,1324	−0,0211
		5,0	0,3545	−0,0940	0,4267	−0,0239
		10	0,3545	−0,0300	1,6931	−0,0255
60°	2	0,25	0,1526	−0,0521	0,0294	−0,0042
		0,5	0,2750	−0,1111	0,0577	−0,0080
		1,0	0,3959	−0,1702	0,0884	−0,0134
		1,5	0,4220	−0,1836	0,1020	−0,0163
		2,5	0,4189	−0,1860	0,1459	−0,0185
		5,0	0,3919	−0,2069	0,2877	−0,0197
		10	0,3722	−0,2724	1,9541	−0,0207
60°	5	0,25	0,1248	−0,0302	0,0158	−0,0033
		0,5	0,2338	−0,0694	0,0334	−0,0061
		1,0	0,3902	−0,1463	0,0714	−0,0106
		1,5	0,4575	−0,1896	0,0972	−0,0136
		2,5	0,4689	−0,1922	0,1286	−0,0149
		5,0	0,4382	−0,2108	0,2898	−0,0154
		10	0,4120	−0,2434	1,0488	−0,0161
60°	∞	0,25	0,0961	−0,0175	0,0100	−0,0026
		0,5	0,1830	−0,0426	0,0214	−0,0042
		1,0	0,3241	−0,1015	0,0472	−0,0072
		1,5	0,4185	−0,1548	0,0748	−0,0095
		2,5	0,4816	−0,1800	0,1026	−0,0112
		5,0	0,4625	−0,2125	0,1875	−0,0117
		10	0,4291	−0,2302	0,5847	−0,0123
86° 25′	∞	0,25	0,0892	−0,0447	0,0331	−0,0024
82° 52′	∞	0,5	0,1656	−0,0799	0,0465	−0,0041
75° 57′	∞	1,0	0,2861	−0,1306	0,0724	−0,0071
69° 28′	∞	1,5	0,3757	−0,1644	0,0886	−0,0089
58° 00′	∞	2,5	0,4966	−0,2052	0,1071	−0,0122
38° 40′	∞	5,0	0,6378	−0,2463	0,1239	−0,0162
21° 48′	∞	10	0,7201	−0,2664	0,1312	−0,0195

Page 622.

With the displacement of the origin of axial coordinates Ox up to distance ξ_a from this centering and recalculation for another characteristic linear dimension (for example, root wing chord b) they use the following by the formulas:

$$\left.\begin{aligned} &k_{22} = \frac{b_a}{b}(k_{22})_a, \quad k_{26} = \frac{b_a}{b}\left[\frac{b_a}{b}(k_{26})_a - \xi_a (k_{22})_a\right], \\ &k_{66} = \frac{b_a}{b}\left[\left(\frac{b_a}{b}\right)^2 (k_{66})_a - 2\frac{b_a}{b}\xi_a (k_{26})_a + \xi_a^2 (k_{22})_a\right], \\ &k_{44} = \frac{b_a}{b}(k_{44})_a. \end{aligned}\right\} \qquad (27.2)$$

Page 623.

For the wings of different planform with the direct/straight edges of value ξ_a and b_a/b they are determined from relationship/ratios (see Fig. 2.3)

$$\xi_a = \frac{h_a}{b} = \frac{\lambda \operatorname{tg} \chi_0}{12} \frac{\eta+2}{\eta}, \quad \frac{b_a}{b} = \frac{2}{3} \frac{\eta^2+\eta+1}{\eta(\eta+1)}. \qquad (27.3)$$

The coefficients of the apparent additional masses of rigid wing were designed for the following range of a change in the geometric parameters: elongation λ = 0.25-10, sweep angle on leading edge χ_0 = 0-60°, contraction η = 1-∞. Table 27.1 gives the numerical values of the coefficients of apparent additional masses depending on the geometric parameters of wing, which characterize wing planform, at centering $\bar{x}_{b_a} = 0$. In this case are isolated the data, that relate to delta wings (λ = 0.25-10). The calculations of the coefficients of associated masses are carried out E. P. Kapustinoy. Let us note that the systematic materials for rectangular and delta wings were given above in the form of curve/graphs (Fig. 14.25-14.55), but for centering $\bar{x}_T$ = 0.5.

§2. Common/general/total relationship/ratios for the coefficients of aerodynamic derivatives.

Are given below systematic data on the coefficients of aerodynamic derivatives at subsonic ($0 \leqslant M \leqslant 1$) and supersonic ($M > 1$) speeds. All these materials are obtained on the basis of the numerical methods of the calculation (see chapters X, XI, XV, XX) and of exact solutions (in that field, where they are, see chapters XIII, XVIII, XXI) it corresponds to very small Strouhal numbers ($p^* \to 0$).

The aerodynamic lift coefficients, of the pitching moment and moment of roll are introduced as follows:

$$c_y = \frac{2Y}{\rho S U_0^2}, \quad m_z = \frac{2M_z}{\rho S U_0^2 b_a}, \quad m_{x1} = \frac{2M_r}{\rho S U_0^2 l}. \tag{27.4}$$

Coefficients c_y, m_z, m_{x1} rigid wing can be (see Chapter II) presented in the form

$$\left.\begin{aligned} c_y &= c_{y0} + c_y^{\alpha}\alpha + c_y^{\dot{\alpha}}\dot{\alpha}_a + c_{ya}^{\omega_{za}}\omega_{za} + c_{ya}^{\dot{\omega}_{za}}\dot{\omega}_{za}, \\ m_z &= m_{z0} + m_{za}^{\alpha}\alpha + m_{za}^{\dot{\alpha}_a}\dot{\alpha}_a + m_{za}^{\omega_{za}}\omega_{za} + m_{za}^{\dot{\omega}_{za}}\dot{\omega}_{za}, \\ m_{x1} &= m_{x0} + m_{x1}^{\omega_{x1}}\omega_{x1} + m_{x1}^{\dot{\omega}_{x1}}\dot{\omega}_{x1}. \end{aligned}\right\} \tag{27.5}$$

Here c_{y0}, m_{z0}, m_{x0} are coefficients at mean incidence α_0. With the accuracy, accepted in linear theory for a fine/thin wing, the

coefficients of aerodynamic derivatives do not depend on α_0.

Page 624.

From the calculations by ETsVM [digital computer] are obtained the following aerodynamic characteristics:

$$kc_y^{\alpha},\ kc_{ya}^{\dot{\omega}_{za}},\ km_{za}^{\alpha},\ km_{za}^{\omega_{za}},\ km_{x1}^{\omega_{x1}},\ k^3c_{ya1}^{\dot{\alpha}_a},\ k^3c_{ya2}^{\dot{\alpha}_a},\ k^3c_{ya1}^{\dot{\omega}_{za}},\ k^3c_{ya2}^{\dot{\omega}_{za}},$$
$$k^3m_{za1}^{\dot{\alpha}_a},\ k^3m_{za2}^{\dot{\alpha}_a},\ k^3m_{za1}^{\dot{\omega}_{za}},\ k^3m_{za2}^{\dot{\omega}_{za}},\ k^2\left(m_{x1}^{\dot{\omega}_{x1}}\right)_1,\ k^2\left(m_{x1}^{\dot{\omega}_{x1}}\right)_2.$$

In this case at subsonic speeds $k=\sqrt{1-M^2}$, at supersonic speeds $k=\sqrt{M^2-1}$.

The coefficients of aerodynamic derivatives are determined by the relationship/ratios

$$\left.\begin{aligned}
c_y^{\alpha}&=\frac{1}{k}\left(kc_y^{\alpha}\right),\quad c_{ya}^{\omega_{za}}=\frac{1}{k}\left(kc_{ya}^{\omega_{za}}\right),\quad m_{za}^{\alpha}=\frac{1}{k}\left(km_{za}^{\alpha}\right),\\
m_{za}^{\omega_{za}}&=\frac{1}{k}\left(km_{za}^{\omega_{za}}\right),\quad m_{x1}^{\omega_{x1}}=\frac{1}{k}\left(km_{x1}^{\omega_{x1}}\right),\\
c_{ya}^{\dot{\alpha}_a}&=\frac{1}{k^3}\left[\left(k^3c_{ya1}^{\dot{\alpha}_a}\right)+M^2\left(k^3c_{ya2}^{\dot{\alpha}_a}\right)\right],\\
c_{ya}^{\dot{\omega}_{za}}&=\frac{1}{k^3}\left[\left(k^3c_{ya1}^{\dot{\omega}_{za}}\right)+M^2\left(c_{ya2}^{\dot{\omega}_{za}}\right)\right],\\
m_{za}^{\dot{\alpha}_a}&=\frac{1}{k^3}\left[\left(k^3m_{za1}^{\dot{\alpha}_a}\right)+M^2\left(k^3m_{za2}^{\dot{\alpha}_a}\right)\right],\\
m_{za}^{\dot{\omega}_{za}}&=\frac{1}{k^3}\left[\left(k^3m_{za1}^{\dot{\omega}_{za}}\right)+M^2\left(k^3m_{za2}^{\dot{\omega}_{za}}\right)\right],\\
m_{x1}^{\dot{\omega}_{x1}}&=\frac{1}{k^2}\left[k^2\left(m_{x1}^{\dot{\omega}_{x1}}\right)_1+M^2k^2\left(m_{x1}^{\dot{\omega}_{x1}}\right)_2\right].
\end{aligned}\right\}\qquad(27.6)$$

For significant dimension for the kinematic parameters $\dot{\alpha}_a, \omega_{za}, \dot{\omega}_{za}$ and the moment coefficient m_{za} is undertaked the mean aerodynamic chord of wing b_a, that it makes the dependence of the coefficients of aerodynamic derivatives on the geometric parameters of wing more stable it draws together it with the appropriate dependences for rectangular wings. During the calculation of the rolling-moment coefficient m_{xl} for characteristic linear dimension is undertaked the spread/scope of wing l, a for the kinematic parameters ω_{xl} and $\dot{\omega}_{xl}$ - semirange $l/2$.

Dimensionless kinematic parameters:

$$\left.\begin{aligned} &\omega_{x1}=\frac{\Omega_x l}{2U_0}, \qquad \omega_{za}=\frac{\Omega_z b_a}{U_0}, \\ &\dot{\alpha}_a=\frac{d\alpha}{dt}\frac{b_a}{U_0}, \quad \dot{\omega}_{x1}=\frac{d\Omega_x}{dt}\frac{l^2}{4U_0^2}, \quad \dot{\omega}_{za}=\frac{d\Omega_z}{dt}\frac{b_a^2}{U_0^2}. \end{aligned}\right\} \tag{27.7}$$

The origin of coordinates was arranged on the axis of symmetry, whereupon so that axis Oz it passed through the leading edge/nose MAC ($\bar{x}_{b_a}=0$), as this shown in Fig. to 27.1.

Page 625.

Recalculation for another significant dimension, for example root wing chord b, and another centering ξ_a was realized by the formulas

$$\left.\begin{aligned} &c_y^{\alpha}=c_{ya}^{\alpha}, \quad c_y^{\dot{\alpha}}=\frac{b_a}{b}c_{ya}^{\dot{\alpha}}, \\ &c_y^{\omega_z}=\frac{b_a}{b}\left(c_{ya}^{\omega_{za}}+\xi_a c_{ya}^{\alpha}\right), \quad c_y^{\dot{\omega}_z}=\left(\frac{b_a}{b}\right)^2\left(c_{ya}^{\dot{\omega}_{za}}+\xi_a c_{ya}^{\dot{\alpha}_a}\right), \\ &m_z^{\alpha}=\frac{b_a}{b}\left(m_{za}^{\alpha}-\xi_a c_{ya}^{\alpha}\right), \quad m_z^{\dot{\alpha}}=\left(\frac{b_a}{b}\right)^2\left(m_{za}^{\dot{\alpha}_a}-\xi_a c_{ya}^{\dot{\alpha}_a}\right), \\ &m_z^{\omega_z}=\left(\frac{b_a}{b}\right)^2\left[m_{za}^{\omega_{za}}+\xi_a\left(m_{za}^{\alpha}-c_{ya}^{\omega_{za}}\right)-\xi_a^2 c_{ya}^{\alpha}\right], \\ &m_z^{\dot{\omega}_z}=\left(\frac{b_a}{b}\right)^3\left[m_{za}^{\dot{\omega}_{za}}+\xi_a\left(m_{za}^{\dot{\alpha}_a}-c_{ya}^{\dot{\omega}_{za}}\right)-\xi_a^2 c_{ya}^{\dot{\alpha}_a}\right]. \end{aligned}\right\} \tag{27.8}$$

For the wings of constant sweepback on leading and trailing edges were applied formulas (27.3). Coefficient with index "a" is related to the mean aerodynamic chord of wing b_a, without index - to the root chord b. The coefficients of the aerodynamic derivatives of rigid wing at subsonic speeds were determined according to the procedure, presented in chapters X and XV.

At supersonic speeds were examined three ranges of the Mach numbers, in which for a wing are satisfied the following conditions.

Wing with supersonic leading and trailing edges:

$$k\lambda \geqslant \lambda \operatorname{tg} \chi_0. \qquad (27.9)$$

Wing with the subsonic leading and supersonic trailing edges:

$$\left[\lambda \operatorname{tg} \chi_0 - \frac{4(\eta-1)}{\eta+1}\right] < k\lambda < \lambda \operatorname{tg} \chi_0. \qquad (27.10)$$

Wing with the subsonic leading and trailing edges:

$$k\lambda < \left[\lambda \operatorname{tg} \chi_0 - \frac{4(\eta-1)}{\eta+1}\right]. \qquad (27.11)$$

In the first case are obtained the exact solutions for the coefficients of the aerodynamic derivatives (see Chapter of XXI), in the second and third it was conducted the numerical calculation of these coefficients (see Chapter of XX).

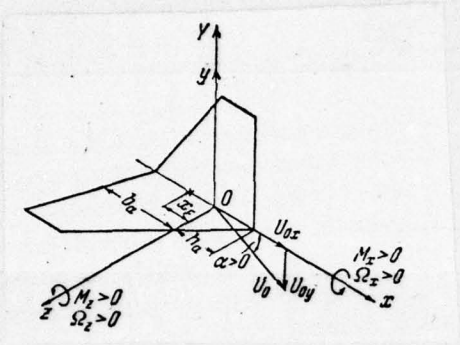


Fig. 27.1. Standard system of axes.

Page 626.

The results of the calculations, just as at subsonic speeds, are given depending on the parameters of similarity $k\lambda$, $\lambda \operatorname{tg} \chi_0$, η at very small Strouhal number ($p^* \to 0$).

§3. Coefficients of aerodynamic derivatives at subsonic speeds.

V. Ya. Gordinsk, E. B. Kozlovskaya and L. A. Strel'tsova designed the total coefficients of aerodynamic derivatives at subsonic speeds($0 \leqslant M < 1$). From numerical calculations were obtained the coefficients

$$kc_y^{\alpha}, \quad kc_{ya}^{\omega_{za}}, \quad km_{za}^{\alpha}, \quad km_{za}^{\omega_{za}}, \quad km_{x1}^{\omega_{x1}}, \quad k^3c_{ya1}^{\dot{\alpha}_a}, \quad k^3c_{ya2}^{\dot{\alpha}_a},$$
$$k^3c_{ya1}^{\dot{\omega}_{za}}, \quad k^3c_{ya2}^{\dot{\omega}_{za}}, \quad k^3m_{za1}^{\dot{\alpha}_a}, \quad k^3m_{za2}^{\dot{\alpha}_a}, \quad k^3m_{za1}^{\dot{\omega}_{za}}, \quad k^3m_{za2}^{\dot{\omega}_{za}},$$
$$k^2\left(m_{x1}^{\dot{\omega}_{x1}}\right)_1, \quad k^2\left(m_{x1}^{\dot{\omega}_{x1}}\right)_2.$$

Table 27.2 gives the systematic results of the calculations with $\bar{x}_{\mathfrak{I}_a} = 0$. These characteristics are constructed in the function of the parameters of similarity $k\lambda$, $\lambda \operatorname{tg} \chi_0$, η, $(k = \sqrt{1 - M^2})$. Is examined the following range of a change in these parameters: $k\lambda = 0 - 10$, $\lambda \operatorname{tg} \chi_0 = 0 - 8{,}0$, $\eta = 1 - \infty$ - with very small Strouhal number $(p^* \to 0)$.

Figure 27.2-27.61 gives the diagrams indicated, constructed for $k\lambda$; as parameters here serve value $\lambda \operatorname{tg} \chi_0$ and η. With the aid of these graphs it is possible to determine the coefficients aerodynamic derivative wings for entire range of subsonic numbers M by including the case of the incompressible medium $(M = 0)$.

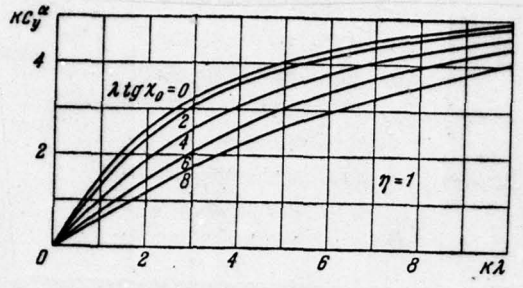


Fig. 27.2. Dependence of derivative c_y^α of the parameters of similarity $(M<1)$.

Page 627.

Table 27.2.

$\eta = 1,\ \lambda \operatorname{tg} \chi_0 = 0$

$k\lambda$	0,25	0,5	1,0	1,5	2,5	5,0	10,0
kc_y^{α}	0,4078	0,8046	1,5149	2,0928	2,9325	4,0618	4,9619
$kc_{ya}^{\omega_{za}}$	0,3751	0,7073	1,2532	1,6778	2,2849	3,0981	3,7410
km_{za}^{α}	−0,0326	−0,0973	−0,2617	−0,4150	−0,6476	−0,9637	−1,2109
$km_{za}^{\omega_{za}}$	−0,1714	−0,3090	−0,5119	−0,6566	−0,8520	−1,0999	−1,2877
$km_{x1}^{\omega_{x1}}$	−0,0265	−0,0531	−0,1058	−0,1567	−0,2489	−0,4207	−0,6129
$k^3 c_{ya1}^{\dot{\alpha}_a}$	0,3404	0,5909	0,8438	0,8596	0,5139	−0,9081	−3,2842
$k^3 c_{ya1}^{\dot{\omega}_{za}}$	0,1723	0,2982	0,4095	0,3762	0,0705	−1,0309	−2,8216
$k^3 m_{za1}^{\dot{\alpha}_a}$	−0,1681	−0,2927	−0,4343	−0,4834	−0,4434	−0,1228	0,4626
$k^3 m_{za1}^{\dot{\omega}_{za}}$	−0,1044	−0,1770	−0,2532	−0,2719	−0,2230	0,0327	0,4775
$k^2 \left(m_{x1}^{\dot{\omega}_{x1}}\right)_1$	−0,1896	−0,1838	−0,1677	−0,1503	−0,1179	−0,0585	−0,0017
$k^3 c_{ya2}^{\dot{\alpha}_a}$	−0,3425	−0,6099	−0,9915	−1,2628	−1,6373	−2,1345	−2,5301
$k^3 c_{ya2}^{\dot{\omega}_{za}}$	−0,1774	−0,3309	−0,5849	−0,7872	−1,0844	−1,4954	−1,8296
$k^3 m_{za2}^{\dot{\alpha}_a}$	0,1651	0,2791	0,4067	0,4756	0,5529	0,6391	0,7006
$k^3 m_{za2}^{\dot{\omega}_{za}}$	0,1031	0,1730	0,2566	0,3075	0,3709	0,4478	0,5056
$k^2 \left(m_{x1}^{\dot{\omega}_{x1}}\right)_2$	0,1896	0,1839	0,1635	0,1537	0,1307	0,0970	0,0654

$\eta = 1,\ \lambda \operatorname{tg} \chi_0 = 2$

$k\lambda$	0,25	0,5	1,0	1,5	2,5	5,0	10,0
kc_y^{α}	0,3780	0,7330	1,3623	1,8913	2,7091	3,9031	4,8833
$kc_{ya}^{\omega_{za}}$	0,2598	0,5040	0,9363	1,2999	1,8652	2,7146	3,4641
km_{za}^{α}	−0,0641	−0,1240	−0,2327	−0,3300	−0,4958	−0,7762	−1,0454
$km_{za}^{\omega_{za}}$	−0,1109	−0,2131	−0,3875	−0,5281	−0,7398	−1,0616	−1,3773
$km_{x1}^{\omega_{x1}}$	−0,0264	−0,0527	−0,1041	−0,1531	−0,2420	−0,4114	−0,6064

Table 27.2 Continued

$k\lambda$	0,25	0,5	1,0	1,5	2,5	5,0	10,0
$k^3 c_{ya1}^{\dot{\alpha}_a}$	0,1857	0,3412	0,5332	0,5763	0,3499	−0,8935	−3,2327
$k^3 c_{ya1}^{\dot{\omega}_{za}}$	0,0890	0,1615	0,2422	0,2417	0,0661	−0,7686	−2,3722
$k^3 m_{za1}^{\dot{\alpha}_a}$	−0,0731	−0,1381	−0,2356	−0,2918	−0,3139	−0,1443	0,2831
$k^3 m_{za1}^{\dot{\omega}_{za}}$	−0,0495	−0,0936	−0,1608	−0,2017	−0,2249	−0,1227	0,1995
$k^2 \left(m_{x1}^{\dot{\omega}_{x1}}\right)_1$	−0,1485	−0,1462	−0,1382	−0,1276	−0,1043	−0,0543	−0,0012
$k^3 c_{ya2}^{\dot{\alpha}_a}$	−0,1958	−0,3800	−0,7035	−0,9699	−1,3694	−1,9384	−2,4187
$k^3 c_{ya2}^{\dot{\omega}_{za}}$	−0,0982	−0,1965	−0,3884	−0,5654	−0,8618	−1,6318	−1,7443
$k^3 m_{za2}^{\dot{\alpha}_a}$	0,0714	0,1337	0,2279	0,2904	0,3616	0,4369	0,5167
$k^3 m_{za2}^{\dot{\omega}_{za}}$	0,0496	0,0946	0,1690	0,2255	0,3039	0,4132	0,5265
$k^2 \left(m_{x1}^{\dot{\omega}_{x1}}\right)_2$	0,1484	0,1463	0,1400	0,1325	0,1180	0,0916	0,0634

$\eta = 1,\ \lambda \operatorname{tg} \chi_0 = 4$

$k\lambda$	0,25	0,5	1,0	1,5	2,5	5,0	10,0
kc_y^{α}	0,2603	0,5162	1,0043	1,4522	2,2180	3,5032	4,6842
$kc_{ya}^{\omega_{za}}$	0,1376	0,2746	0,5441	0,8022	1,2682	2,1266	3,0444
km_{za}^{α}	−0,0517	−0,1016	−0,1937	−0,2762	−0,4161	−0,6686	−0,9360
$km_{za}^{\omega_{za}}$	−0,0993	−0,1966	−0,3812	−0,5508	−0,8454	−1,3839	−2,0100
$km_{x1}^{\omega_{x1}}$	−0,0239	−0,0477	−0,0943	−0,1389	−0,2214	−0,3865	−0,5882
$k^3 c_{ya1}^{\dot{\alpha}_a}$	0,0788	0,1487	0,2452	0,2736	0,1435	−0,8288	−3,0650
$k^3 c_{ya1}^{\dot{\omega}_{za}}$	0,0410	0,0790	0,1387	0,1690	0,1367	−0,3292	−1,6565
$k^3 m_{za1}^{\dot{\alpha}_a}$	−0,0229	−0,0436	−0,0751	−0,0932	−0,0941	0,0186	0,3197
$k^3 m_{za1}^{\dot{\omega}_{za}}$	−0,0454	−0,0888	−0,1656	−0,2275	−0,3082	−0,3300	−0,0544
$k^2 \left(m_{x1}^{\dot{\omega}_{x1}}\right)_1$	−0,1012	−0,1001	−0,0965	−0,0913	−0,0784	−0,0442	0,0003

Page 629.

Table 27.2 (continuation).

$k\lambda$	0,25	0,5	1,0	1,5	2,5	5,0	10,0
$k^3 c_{ya2}^{\dot{\alpha}_0}$	−0,0859	−0,1730	−0,3504	−0,5260	−0,8521	−1,4580	−2,1082
$k^3 c_{ya2}^{\dot{\omega}_{za}}$	−0,0447	−0,0927	−0,2020	−0,3242	−0,5800	−1,1093	−1,6698
$k^3 m_{za2}^{\dot{\alpha}_a}$	0,0208	0,0397	0,0687	0,0874	0,1013	0,1063	0,1676
$k^3 m_{za2}^{\dot{\omega}_{za}}$	0,0454	0,0897	0,1720	0,2450	0,3628	0,5559	0,7801
$k^2 \left(m_{x1}^{\dot{\omega}_{x1}}\right)_2$	0,1013	0,1009	0,0994	0,0972	0,0920	0,0780	0,0581

$\eta = 1,\ \lambda \operatorname{tg} \chi_0 = 6$

$k\lambda$	0,25	0,5	1,0	1,5	2,5	5,0	10,0
kc_y^{α}	0,1917	0,3821	0,7556	1,1147	1,7748	3,0454	4,4006
$kc_{ya}^{\omega_{za}}$	0,0799	0,1602	0,3230	0,4882	0,8179	1,5608	2,5608
km_{za}^{α}	−0,0434	−0,0861	−0,1681	−0,2442	−0,3775	−0,6188	−0,8783
$km_{za}^{\omega_{za}}$	−0,1220	−0,2431	−0,4805	−0,7089	−1,1325	−1,9962	−3,1212
$km_{x1}^{\omega_{x1}}$	−0,0205	−0,0409	−0,0812	−0,1206	−0,1954	−0,3537	−0,5615
$k^3 c_{ya1}^{\dot{\alpha}_a}$	0,0300	0,0565	0,0912	0,0937	−0,0086	−0,7642	−2,8382
$k^3 c_{ya1}^{\dot{\omega}_{za}}$	0,0348	0,0688	0,1321	0,1854	0,2480	0,1188	−0,8227
$k^3 m_{za1}^{\dot{\alpha}_a}$	0,0062	0,0131	0,0297	0,0510	0,1060	0,2706	0,5286
$k^3 m_{za1}^{\dot{\omega}_{za}}$	−0,0618	−0,1220	−0,2344	−0,3328	−0,4827	−0,6180	−0,3169
$k^2 \left(m_{x1}^{\dot{\omega}_{x1}}\right)_1$	−0,0666	−0,0663	−0,0645	−0,0619	−0,0547	−0,0327	0,0023
$k^3 c_{ya2}^{\dot{\alpha}_a}$	−0,0365	−0,0741	−0,1550	−0,2440	−0,4404	−0,9420	−1,6825
$k^3 c_{ya2}^{\dot{\omega}_{za}}$	−0,0372	−0,0756	−0,1585	−0,2505	−0,4554	−0,9720	−1,6442
$k^3 m_{za2}^{\dot{\alpha}_a}$	−0,0105	−0,0213	−0,0446	−0,0705	−0,1272	−0,2464	−0,2738
$k^3 m_{za2}^{\dot{\omega}_{za}}$	0,0630	0,1252	0,2459	0,3587	0,5564	0,9053	1,2983
$k^2 \left(m_{x1}^{\dot{\omega}_{x1}}\right)_2$	0,0677	0,0677	0,0674	0,0672	0,0661	0,0614	0,0505

Page 630.

Table 27.2 (continuation).

$\eta = 1$, $\lambda \operatorname{tg} \chi_0 = 8$

$k\lambda$	0,25	0,5	1,0	1,5	2,5	5,0	10,0
kc_y^{α}	0,1521	0,3037	0,6038	0,8977	1,4570	2,6331	4,0791
$kc_{ya}^{\omega_{za}}$	0,0510	0,1024	0,2072	0,3150	0,5394	1,1156	2,0835
km_{za}^{α}	−0,0387	−0,0770	−0,1517	−0,2230	−0,3525	−0,5969	−0,8567
$km_{za}^{\omega_{za}}$	−0,1585	−0,3164	−0,6292	−0,9360	−1,5234	−2,8036	−4,6142
$km_{x1}^{\omega_{x1}}$	−0,0177	−0,0354	−0,0704	−0,1050	−0,1719	−0,3202	−0,5301
$k^3 c_{ya1}^{\dot{\alpha}_a}$	0,0044	0,0072	0,0037	−0,0169	−0,1208	−0,7338	−2,6053
$k^3 c_{ya1}^{\dot{\omega}_{za}}$	0,0413	0,0823	0,1623	0,2378	0,3670	0,4990	0,0045
$k^3 m_{za1}^{\dot{\alpha}_a}$	0,0261	0,0525	0,1059	0,1604	0,2712	0,5298	0,8390
$k^3 m_{za1}^{\dot{\omega}_{za}}$	−0,0830	−0,1646	−0,3206	−0,4631	−0,6979	−0,9756	−0,6227
$k^2 \left(m_{x1}^{\dot{\omega}_{x1}}\right)_1$	−0,0431	−0,0429	−0,0420	−0,0406	−0,0365	−0,0222	0,0047
$k^3 c_{ya2}^{\dot{\alpha}_a}$	−0,0123	−0,0254	−0,0554	−0,0920	−0,1869	−0,5187	−1,2268
$k^3 c_{ya2}^{\dot{\omega}_{za}}$	−0,0437	−0,0877	−0,1776	−0,2705	−0,4644	−0,9581	−1,6926
$k^3 m_{za2}^{\dot{\alpha}_a}$	−0,0324	−0,0648	−0,1290	−0,1924	−0,3143	−0,5637	−0,7427
$k^3 m_{za2}^{\dot{\omega}_{za}}$	0,0878	0,1752	0,3471	0,5127	0,8178	1,4039	2,0616
$k^2 \left(m_{x1}^{\dot{\omega}_{x1}}\right)_2$	0,0458	0,0458	0,0459	0,0460	0,0462	0,0458	0,0419

$\eta = 2$, $\lambda \operatorname{tg} \chi_0 = 0$

$k\lambda$	0,25	0,5	1,0	1,5	2,5	5,0	10,0
kc_y^{α}	0,4072	0,8005	1,5070	2,0905	2,9690	4,1600	5,0824
$kc_{ya}^{\omega_{za}}$	0,3399	0,6522	1,2002	1,6390	2,3007	3,1716	3,8464
km_{za}^{α}	−0,0324	−0,0930	−0,2508	−0,4048	−0,6569	−1,0003	−1,2593
$km_{za}^{\omega_{za}}$	−0,1451	−0,2715	−0,4850	−0,6445	−0,8770	−1,1566	−1,3618
$km_{x1}^{\omega_{x1}}$	−0,0265	−0,0531	−0,1053	−0,1551	−0,2431	−0,4008	−0,5657

Page 631.

Table 27.2 (continuation).

$k\lambda$	0,25	0,5	1,0	1,5	2,5	5,0	10,0
$k^3 c_{ya1}^{\dot{\alpha}_a}$	0,3055	0,5402	0,8087	0,8531	0,5646	−0,8654	−3,3451
$k^3 c_{ya1}^{\bar{\omega}_{za}}$	0,1508	0,2705	0,4014	0,3951	0,1342	−0,9805	−2,8832
$k^3 m_{za1}^{\dot{\alpha}_a}$	−0,1415	−0,2559	−0,4123	−0,4804	−0,4737	−0,1513	0,4771
$k^3 m_{za1}^{\bar{\omega}_{za}}$	−0,0860	−0,1552	−0,2483	−0,2845	−0,2627	−0,0051	0,4821
$k^2 \left(m_{x1}^{\bar{\omega}_{x1}}\right)_1$	−0,1541	−0,1499	−0,1356	−0,1204	−0,0910	−0,0385	0,0084
$k^3 c_{ya2}^{\dot{\alpha}_a}$	−0,3075	−0,5592	−0,9495	−1,2342	−1,6438	−2,1714	−2,5871
$k^3 c_{ya2}^{\bar{\omega}_{za}}$	−0,1542	−0,2993	−0,5598	−0,7766	−1,1139	−1,5753	−1,9464
$k^3 m_{za2}^{\dot{\alpha}_a}$	0,1389	0,2440	0,3857	0,4675	0,5647	0,6587	0,7255
$k^3 m_{za2}^{\bar{\omega}_{za}}$	0,0838	0,1510	0,2480	0,3120	0,3955	0,4892	0,5589
$k^2 \left(m_{x1}^{\bar{\omega}_{x1}}\right)_2$	0,1541	0,1500	0,1370	0,1250	0,1057	0,0774	0,0510

$\eta = 2,\ \lambda \operatorname{tg} \chi_0 = 2$

$k\lambda$	0,25	0,5	1,0	1,5	2,5	5,0	10,0
kc_y^{α}	0,4027	0,7849	1,4630	2,0278	2,8839	4,0932	5,0467
$kc_{ya}^{\bar{\omega}_{za}}$	0,3513	0,6693	1,1992	1,6192	2,2339	3,0918	3,7813
km_{za}^{α}	−0,0954	−0,1869	−0,3495	−0,4852	−0,6948	−0,9986	−1,2416
$km_{za}^{\bar{\omega}_{za}}$	−0,1728	−0,3196	−0,5434	−0,7019	−0,9158	−1,1942	−1,4178
$km_{x1}^{\bar{\omega}_{x1}}$	−0,0265	−0,0530	−0,1048	−0,1538	−0,2406	−0,3976	−0,5632
$k^3 c_{ya1}^{\dot{\alpha}_a}$	0,2486	0,4504	0,6879	0,7381	0,4756	−0,8746	−3,3253
$k^3 c_{ya1}^{\bar{\omega}_{za}}$	0,1342	0,2373	0,3322	0,3107	0,0467	−1,0011	−2,8088
$k^3 m_{za1}^{\dot{\alpha}_a}$	−0,1224	−0,2193	−0,3395	−0,3856	−0,3545	−0,0547	0,4984
$k^3 m_{za1}^{\bar{\omega}_{za}}$	−0,0793	−0,1400	−0,2085	−0,2279	−0,1878	0,0462	0,4673
$k^2 \left(m_{x1}^{\bar{\omega}_{x1}}\right)_1$	−0,1413	−0,1374	−0,1263	−0,1132	−0,0869	−0,0373	0,0086

Page 632.

Table 27.2 (continuation).

$k\lambda$	0,25	0,5	1,0	1,5	2,5	5,0	10,0
$k^3 c_{ya2}^{\dot{\alpha}_a}$	−0,2559	−0,4824	−0,8497	−1,1340	−1,5390	−2,0932	−2,5397
$k^3 c_{ya2}^{\dot{\omega}_{za}}$	−0,1428	−0,2756	−0,5058	−0,7020	−1,0031	−1,4465	−1,8117
$k^3 m_{za2}^{\dot{\alpha}_a}$	0,1205	0,2137	0,3354	0,4034	0,4702	0,5248	0,5640
$k^3 m_{za2}^{\dot{\omega}_{za}}$	0,0797	0,1423	0,2276	0,2803	0,3408	0,4069	0,4593
$k^2 \left(m_{x1}^{\dot{\omega}_{x1}}\right)_2$	0,1411	0,1375	0,1280	0,1183	0,1017	0,0756	0,0503

$\eta = 2,\ \lambda \operatorname{tg} \chi_0 = 4$

$k\lambda$	0,25	0,5	1,0	1,5	2,5	5,0	10,0
kc_y^{α}	0,3023	0,5959	1,1475	1,6383	2,4490	3,7486	4,8850
$kc_{ya}^{\omega_{za}}$	0,2183	0,4301	0,8291	1,1826	1,7627	2,6990	3,5558
km_{za}^{α}	−0,0949	−0,1859	−0,3478	−0,4859	−0,7019	−1,0158	−1,2605
$km_{za}^{\omega_{za}}$	−0,1338	−0,2632	−0,4965	−0,6975	−1,0169	−1,5021	−1,9599
$km_{x1}^{\omega_{x1}}$	−0,0246	−0,0490	−0,0962	−0,1408	−0,2214	−0,3751	−0,5482
$k^3 c_{ya1}^{\dot{\alpha}_a}$	0,1135	0,2118	0,3495	0,3930	0,2395	−0,8355	−3,1914
$k^3 c_{ya1}^{\dot{\omega}_{za}}$	0,0540	0,0985	0,1529	0,1495	−0,0018	−0,7789	−2,4350
$k^3 m_{za1}^{\dot{\alpha}_a}$	−0,0370	−0,0690	−0,1089	−0,1197	−0,0726	0,2122	0,7116
$k^3 m_{za1}^{\dot{\omega}_{za}}$	−0,0393	−0,0747	−0,1261	−0,1528	−0,1501	0,0200	0,4414
$k^2 \left(m_{x1}^{\dot{\omega}_{x1}}\right)_1$	−0,0923	−0,0909	−0,0861	−0,0796	−0,0647	−0,0298	0,0093
$k^3 c_{ya2}^{\dot{\alpha}_a}$	−0,1234	−0,2443	−0,4813	−0,6967	−1,0608	−1,6832	−2,2953
$k^3 c_{ya2}^{\dot{\omega}_{za}}$	−0,0625	−0,1267	−0,2673	−0,4096	−0,6741	−1,1803	−1,6664
$k^3 m_{za2}^{\dot{\alpha}_a}$	0,0362	0,0701	0,1215	0,1562	0,1902	0,1905	0,2061
$k^3 m_{za2}^{\dot{\omega}_{za}}$	0,0402	0,0800	0,1489	0,2069	0,2967	0,4102	0,5241
$k^2 \left(m_{x1}^{\dot{\omega}_{x1}}\right)_2$	0,0928	0,0920	0,0896	0,0864	0,0797	0,0648	0,0463

Page 633.

Table 27.2 (continuation).

$\eta = 2$, $\lambda \operatorname{tg} \chi_0 = 6$

$k\lambda$	0,25	0,5	1,0	1,5	2,5	5,0	10,0
kc_y^{α}	0,2179	0,4335	0,8531	1,2510	1,9707	3,2867	4,6111
$kc_{ya}^{\omega_{za}}$	0,1323	0,2643	0,5254	0,7792	1,2552	2,1748	3,1920
km_{za}^{α}	−0,0779	−0,1544	−0,2996	−0,4318	−0,6553	−1,0139	−1,3008
$km_{za}^{\omega_{za}}$	−0,1349	−0,2682	−0,5264	−0,7697	−1,2050	−2,0150	−2,9290
$km_{x1}^{\omega_{x1}}$	−0,0204	−0,0408	−0,0810	−0,1199	−0,1929	−0,3417	−0,5234
$k^3 c_{ya1}^{\dot{\alpha}_a}$	0,0478	0,0905	0,1511	0,1654	0,0618	−0,7737	−2,9711
$k^3 c_{ya1}^{\dot{\omega}_{za}}$	0,0211	0,0405	0,0697	0,0795	0,0269	−0,4466	−1,8395
$k^3 m_{za1}^{\dot{\alpha}_a}$	0,0083	0,0183	0,0459	0,0865	0,1987	0,5473	1,0596
$k^3 m_{za1}^{\dot{\omega}_{za}}$	−0,0365	−0,0711	−0,1314	−0,1763	−0,2172	−0,1208	0,3645
$k^2 \left(m_{x1}^{\dot{\omega}_{x1}}\right)_1$	−0,0545	−0,0540	−0,0523	−0,0495	−0,0421	−0,0203	0,0104
$k^3 c_{ya2}^{\dot{\alpha}_a}$	−0,0544	−0,1099	−0,2259	−0,3475	−0,5999	−1,1609	−1,8912
$k^3 c_{ya2}^{\dot{\omega}_{za}}$	−0,0249	−0,0529	−0,1215	−0,2059	−0,4052	−0,9027	−1,5082
$k^3 m_{za2}^{\dot{\alpha}_a}$	−0,0104	−0,0212	−0,0449	−0,0714	−0,1289	−0,2457	−0,2856
$k^3 m_{za2}^{\dot{\omega}_{za}}$	0,0373	0,0745	0,1476	0,2166	0,3368	0,5476	0,7904
$k^2 \left(m_{x1}^{\dot{\omega}_{x1}}\right)_2$	0,0555	0,0556	0,0557	0,0555	0,0546	0,0499	0,0399

$\eta = 2$, $\lambda \operatorname{tg} \chi_0 = 8$

$k\lambda$	0,25	0,5	1,0	1,5	2,5	5,0	10,0
kc_y^{α}	0,1692	0,3377	0,6699	0,9929	1,6006	2,8412	4,2867
$kc_{ya}^{\omega_{za}}$	0,0888	0,1777	0,3564	0,5355	0,8895	1,6894	2,7749
km_{za}^{α}	−0,0664	−0,1322	−0,2604	−0,3820	−0,6005	−0,9936	−1,3377
$km_{za}^{\omega_{za}}$	−0,1572	−0,3138	−0,6232	−0,9246	−1,4947	−2,6877	−4,2319
$km_{x1}^{\omega_{x1}}$	−0,0173	−0,0345	−0,0687	−0,1023	−0,1668	−0,3064	−0,4930

Page 634.

Table 27.2 (continuation).

$k\lambda$	0,25	0,5	1,0	1,5	2,5	5,0	10,0
$k^3 c_{ya1}^{\dot{\alpha}_a}$	0,0144	0,0266	0,0386	0,0284	−0,0712	−0,7366	−2,7291
$k^3 c_{ya1}^{\dot{\omega}_{za}}$	0,0166	0,0327	0,0614	0,0825	0,0906	−0,1263	−1,1657
$k^3 m_{za1}^{\dot{\alpha}_a}$	0,0378	0,0761	0,1555	0,2392	0,4178	0,8720	1,4767
$k^3 m_{za1}^{\dot{\omega}_{za}}$	−0,0487	−0,0961	−0,1840	−0,2591	−0,3633	−0,3678	0,2075
$k^2 \left(m_{x1}^{\dot{\omega}_{x1}}\right)_1$	−0,0318	−0,0315	−0,0306	−0,0290	−0,0251	−0,0115	0,0119
$k^3 c_{ya2}^{\dot{\alpha}_a}$	−0,0224	−0,0455	−0,0960	−0,1535	−0,2891	−0,6958	−1,4372
$k^3 c_{ya2}^{\dot{\omega}_{za}}$	−0,0210	−0,0432	−0,0933	−0,1523	−0,2960	−0,7226	−1,3908
$k^3 m_{za2}^{\dot{\alpha}_a}$	−0,0416	−0,0831	−0,1649	−0,2444	−0,3929	−0,6726	−0,8521
$k^3 m_{za2}^{\dot{\omega}_{za}}$	0,0521	0,1041	0,2064	0,3052	0,4877	0,8406	1,2589
$k^2 \left(m_{x1}^{\dot{\omega}_{x1}}\right)_2$	0,0345	0,0345	0,0347	0,0349	0,0353	0,0354	0,0324

$\eta = 5,\ \lambda \operatorname{tg} \chi_0 = 0$

$k\lambda$	0,25	0,5	1,0	1,5	2,5	5,0	10,0
kc_y^{α}	0,4037	0,7852	1,4568	2,0055	2,8634	4,0632	4,9117
$kc_{ya}^{\omega_{za}}$	0,2676	0,5242	0,9897	1,3822	2,0099	2,8930	3,6231
km_{za}^{α}	−0,0320	−0,0840	−0,2100	−0,3514	−0,5837	−0,9172	−1,2654
$km_{za}^{\omega_{za}}$	−0,1027	−0,1981	−0,3732	−0,5278	−0,7582	−1,0764	−1,3702
$km_{x1}^{\omega_{x1}}$	−0,0265	−0,0528	−0,1032	−0,1507	−0,2293	−0,3642	−0,5022
$k^3 c_{ya1}^{\dot{\alpha}_a}$	0,2331	0,4199	0,6496	0,6974	0,5135	−0,6364	−2,7252
$k^3 c_{ya1}^{\dot{\omega}_{za}}$	0,1082	0,2033	0,3248	0,3443	0,2079	−0,6302	−2,2238
$k^3 m_{za1}^{\dot{\alpha}_a}$	−0,0987	−0,1842	−0,3168	−0,3930	−0,4338	−0,2343	0,3405
$k^3 m_{za1}^{\dot{\omega}_{za}}$	−0,0593	−0,1134	−0,1986	−0,2475	−0,2773	−0,1277	0,3109
$k^2 \left(m_{x1}^{\dot{\omega}_{x1}}\right)_1$	−0,1142	−0,1092	−0,0961	−0,0870	−0,0621	−0,0208	0,0124

Page 635.

Table 27.2 (continuation).

$k\lambda$	0,25	0,5	1,0	1,5	2,5	5,0	10,0
$k^3 c_{ya2}^{\dot{\alpha}_a}$	−0,2355	−0,4402	−0,7797	−1,0309	−1,4262	−1,9758	−2,3576
$k^3 c_{ya2}^{\dot{\omega}_z}$	−0,1114	−0,2246	−0,4423	−0,6277	−0,9538	−1,4386	−1,8444
$k^3 m_{za2}^{\dot{\alpha}_a}$	0,0967	0,1767	0,2990	0,3810	0,4926	0,6097	0,7214
$k^3 m_{za2}^{\dot{\omega}_{za}}$	0,0582	0,1109	0,1976	0,2619	0,3622	0,4783	0,6036
$k^2 \left(m_{x1}^{\dot{\omega}_{x1}}\right)_2$	0,1142	0,1096	0,0990	0,0934	0,0787	0,0576	0,0394

$\eta = 5,\ \lambda \operatorname{tg} \chi_0 = 2$

$k\lambda$	0,25	0,5	1,0	1,5	2,5	5,0	10,0
kc_y^{α}	0,4061	0,7954	1,4896	2,0656	2,9296	4,1226	5,0496
$kc_{ya}^{\omega_{za}}$	0,3643	0,6920	1,2383	1,6689	2,2952	3,1476	3,8122
km_{za}^{α}	−0,1049	−0,2098	−0,4001	−0,5572	−0,7887	−1,0970	−1,3209
$km_{za}^{\omega_{za}}$	−0,1837	−0,3389	−0,5737	−0,7394	−0,9566	−1,2174	−1,3966
$km_{x1}^{\omega_{x1}}$	−0,0265	−0,0530	−0,1042	−0,1516	−0,2324	−0,3674	−0,4954
$k^3 c_{ya1}^{\dot{\alpha}_a}$	0,2540	0,4570	0,6985	0,7590	0,5418	−0,6483	−2,8536
$k^3 c_{ya1}^{\dot{\omega}_{za}}$	0,1421	0,2490	0,3538	0,3424	0,1092	−0,8480	−2,5248
$k^3 m_{za1}^{\dot{\alpha}_a}$	−0,1352	−0,2388	−0,3623	−0,4082	−0,3753	−0,0811	0,4526
$k^3 m_{za1}^{\dot{\omega}_{za}}$	−0,0891	−0,1536	−0,2221	−0,2381	−0,1905	−0,0506	0,4579
$k^2 \left(m_{x1}^{\dot{\omega}_{x1}}\right)_1$	−0,1203	−0,1155	−0,1031	−0,0898	−0,0647	−0,0217	0,0128

Page 636.

Table 27.2 (continuation).

$k\lambda$	0,25	0,5	1,0	1,5	2,5	5,0	10,0
$k^3 c_{ya2}^{\dot{\alpha}_a}$	−0,2594	−0,4822	−0,8382	−1,1118	−1,5065	−2,0507	−2,4913
$k^3 c_{ya2}^{\dot{\omega}_{za}}$	−0,1481	−0,2797	−0,5064	−0,6980	−0,9906	−1,4252	−1,7925
$k^3 m_{za2}^{\dot{\alpha}_a}$	0,1335	0,2336	0,3613	0,4350	0,5125	0,5821	0,6171
$k^3 m_{za2}^{\dot{\omega}_{za}}$	0,0892	0,1555	0,2424	0,2957	0,3573	0,4203	0,4559
$k^2 \left(m_{x1}^{\dot{\omega}_{x1}}\right)_2$	0,1203	0,1157	0,1054	0,0959	0,0811	0,0590	0,0383

$\eta = 5,\ \lambda \operatorname{tg} \chi_0 = 4$

$k\lambda$	0,25	0,5	1,0	1,5	2,5	5,0	10,0
kc_y^{α}	0,3428	0,6707	1,2661	1,7806	2,6036	3,8669	4,9279
$kc_{ya}^{\omega_{za}}$	0,2982	0,5789	1,0728	1,4826	2,1101	3,0295	3,7841
km_{za}^{α}	−0,1420	−0,2731	−0,4955	−0,6713	−0,9238	−1,2492	−1,4560
$km_{za}^{\omega_{za}}$	−0,1852	−0,3547	−0,6367	−0,8534	−1,1547	−1,5391	−1,8178
$km_{x1}^{\omega_{x1}}$	−0,0251	−0,0497	−0,0967	−0,1400	−0,2153	−0,3489	−0,4841
$k^3 c_{ya1}^{\dot{\alpha}_a}$	0,1461	0,2718	0,4401	0,4996	0,3682	−0,6280	−2,7702
$k^3 c_{ya1}^{\dot{\omega}_{za}}$	0,0776	0,1396	0,2023	0,1886	−0,0019	−0,8591	−2,4931
$k^3 m_{za1}^{\dot{\alpha}_a}$	−0,0654	−0,1190	−0,1828	−0,1964	−0,1287	0,2137	0,7564
$k^3 m_{za1}^{\dot{\omega}_{za}}$	−0,0477	−0,0856	−0,1265	−0,1290	−0,0651	0,2083	0,6458
$k^2 \left(m_{x1}^{\dot{\omega}_{x1}}\right)_1$	−0,0821	−0,0802	−0,0741	−0,0664	−0,0501	−0,0175	0,0130
$k^3 c_{ya2}^{\dot{\alpha}_a}$	−0,1562	−0,3058	−0,5772	−0,8113	−1,1864	−1,7803	−2,3282
$k^3 c_{ya2}^{\dot{\omega}_{za}}$	−0,0876	−0,1748	−0,3433	−0,4992	−0,7671	−1,2200	−1,6337
$k^3 m_{za2}^{\dot{\alpha}_a}$	0,0666	0,1252	0,2134	0,2691	0,3221	0,3451	0,3504
$k^3 m_{za2}^{\dot{\omega}_{za}}$	0,0506	0,0966	0,1707	0,2236	0,2875	0,3506	0,3929
$k^2 \left(m_{x1}^{\dot{\omega}_{x1}}\right)_2$	0,0828	0,0817	0,0783	0,0742	0,0664	0,0518	0,0357

Page 637.

Table 27.2 (continuation).

$\eta = 5,\ \lambda \operatorname{tg} \chi_0 = 6$

$k\lambda$	0,25	0,5	1,0	1,5	2,5	5,0	10,0
kc_y^{α}	0,2408	0,4785	0,9369	1,3649	2,1153	3,4331	4,6901
$kc_{ya}^{\omega_{za}}$	0,1872	0,3722	0,7290	1,0615	1,6408	2,6441	3,5893
km_{za}^{α}	—0,1098	—0,2171	—0,4190	—0,5990	—0,8901	—1,3115	—1,5767
$km_{za}^{\omega_{za}}$	—0,1515	—0,3001	—0,5818	—0,8369	—1,2619	—1,9410	—2,5384
$km_{x1}^{\omega_{x1}}$	—0,0200	—0,0399	—0,0788	—0,1161	—0,1844	—0,3163	—0,4625
$k^3 c_{ya1}^{\dot{\alpha}_a}$	0,0692	0,1318	0,2242	0,2639	0,1884	—0,5839	—2,6017
$k^3 c_{ya1}^{\dot{\omega}_{za}}$	0,0263	0,0484	0,0720	0,0624	—0,0552	—0,7084	—2,2257
$k^3 m_{za1}^{\dot{\alpha}_a}$	—0,0058	—0,0085	0,0003	0,0306	0,1450	0,5506	1,1471
$k^3 m_{za1}^{\dot{\omega}_{za}}$	—0,0182	—0,0338	—0,0524	—0,0518	—0,0004	0,2693	0,7873
$k^2 \left(m_{x1}^{\dot{\omega}_{x1}}\right)_1$	—0,0450	—0,0444	—0,0423	—0,0392	—0,0314	—0,0110	0,0134
$k^3 c_{ya2}^{\dot{\alpha}_a}$	—0,0775	—0,1551	—0,3100	—0,4625	—0,7507	—1,3326	—2,0126
$k^3 c_{ya2}^{\dot{\omega}_{za}}$	—0,0334	—0,0692	—0,1503	—0,2428	—0,4452	—0,9067	—1,4312
$k^3 m_{za2}^{\dot{\alpha}_a}$	0,0058	0,0109	0,0177	0,0189	0,0070	—0,0446	—0,0687
$k^3 m_{za2}^{\dot{\omega}_{za}}$	0,0202	0,0406	0,0811	0,1196	0,1857	0,2920	0,4049
$k^2 \left(m_{x1}^{\dot{\omega}_{x1}}\right)_2$	0,0466	0,0465	0,0464	0,0460	0,0446	0,0397	0,0309

$\eta = 5,\ \lambda \operatorname{tg} \chi_0 = 8$

$k\lambda$	0,25	0,5	1,0	1,5	2,5	5,0	10,0
kc_y^{α}	0,1843	0,3674	0,7266	1,0728	1,7142	2,9798	4,3832
$kc_{ya}^{\omega_{za}}$	0,1298	0,2590	0,5144	0,7634	1,2332	2,1885	3,2833
km_{za}^{α}	—0,0914	—0,1818	—0,3566	—0,5206	0,8086	—1,2976	—1,6637
$km_{za}^{\omega_{za}}$	—0,1519	—0,3027	—0,5979	—0,8808	—1,3992	—2,3970	—3,4871
$km_{x1}^{\omega_{x1}}$	—0,0163	—0,0325	—0,0646	—0,0960	—0,1556	—0,2803	—0,4346

Page 638.

Table 27.2 (continuation).

$k\lambda$	0,25	0,5	1,0	1,5	2,5	5,0	10,0
$k^3 c_{ya1}^{\dot{\alpha}_a}$	0,0310	0,0589	0,0991	0,1124	0,0480	−0,5547	−2,3973
$k^3 c_{ya1}^{\dot{\omega}_{za}}$	0,0058	0,0104	0,0129	−0,0024	−0,0682	−0,5134	−1,8192
$k^3 m_{za1}^{\dot{\alpha}_a}$	0,0280	0,0572	0,1219	0,1962	0,3712	0,8658	1,5681
$k^3 m_{za1}^{\dot{\omega}_{za}}$	−0,0124	−0,0236	−0,0393	−0,0436	−0,0149	0,2207	0,8441
$k^2 \left(m_{x1}^{\dot{\omega}_{x1}}\right)_1$	−0,0234	−0,0232	−0,0223	−0,0209	−0,0169	−0,0046	0,0140
$k^3 c_{ya2}^{\dot{\alpha}_a}$	−0,0383	−0,0772	−0,1578	−0,2429	−0,4246	−0,8909	−1,6196
$k^3 c_{ya2}^{\dot{\omega}_{za}}$	−0,0111	−0,0242	−0,0586	−0,1055	−0,2313	−0,6199	−1,2162
$k^3 m_{za2}^{\dot{\alpha}_a}$	−0,0289	−0,0579	−0,1156	−0,1724	−0,2786	−0,4723	−0,5845
$k^3 m_{za2}^{\dot{\omega}_{za}}$	0,0150	0,0304	0,0620	0,0946	0,1602	0,3055	0,5134
$k^2 \left(m_{x1}^{\dot{\omega}_{x1}}\right)_2$	0,0259	0,0259	0,0262	0,0264	0,0270	0,0273	0,0249

$\eta = \infty$, $\lambda \operatorname{tg} \chi_0 = 0$

$k\lambda$	0,25	0,5	1,0	1,5	2,5	5,0	10,0
kc_y^{α}	0,3835	0,7248	1,3165	1,8087	2,5952	3,7212	4,9054
$kc_{ya}^{\omega_{za}}$	0,1999	0,3927	0,7540	1,0777	1,6267	2,4929	3,3974
km_{za}^{α}	−0,0241	−0,0604	−0,1544	−0,2574	−0,4487	−0,7749	−1,1035
$km_{za}^{\omega_{za}}$	−0,0717	−0,1420	−0,2750	−0,3966	−0,5997	−0,9286	−1,2437
$km_{x1}^{\omega_{x1}}$	−0,0254	−0,0490	−0,0912	−0,1299	−0,1892	−0,2869	−0,3656
$k^3 c_{ya1}^{\dot{\alpha}_a}$	0,1728	0,3127	0.4996	0,5792	0,5265	−0,1619	−2,1016
$k^3 c_{ya1}^{\dot{\omega}_{za}}$	0,0784	0,1485	0,2535	0,3058	0,2858	−0,1731	−1,5721
$k^3 m_{za1}^{\dot{\alpha}_a}$	−0,0692	−0,1330	−0,2394	−0,3155	−0,3932	−0,3425	0,0613
$k^3 m_{za1}^{\dot{\omega}_{za}}$	−0,0425	−0,0827	−0,1528	−0,2056	−0,2661	−0,2405	0,0534
$k^2 \left(m_{x1}^{\dot{\omega}_{x1}}\right)_1$	−0,0727	−0,0691	−0,0609	−0,0532	−0,0386	−0,0136	0,0065

Page 639.

Table 27.2 (continuation).

$k\lambda$	0,25	0,5	1,0	1,5	2,5	5,0	10,0
$k^3 c_{ya2}^{\dot{\alpha}_a}$	−0,1759	−0,3322	−0,5996	−0,8203	−1,1779	−1,7180	−2,2939
$k^3 c_{ya2}^{\dot{\omega}_{za}}$	−0,0806	−0,1616	−0,3229	−0,4758	−0,7565	−1,2360	−1,7777
$k^3 m_{za2}^{\dot{\alpha}_a}$	0,0682	0,1287	0,2273	0,3021	0,4088	0,5516	0,6726
$k^3 m_{za2}^{\dot{\omega}_{za}}$	0,0418	0,0810	0,1504	0,2084	0,3009	0,4392	0,5670
$k^2 \left(m_{x1}^{\dot{\omega}_{x1}}\right)_2$	0,0733	0,0708	0,0655	0,0610	0,0534	0,0409	0,0270

$\eta = \infty$, $\lambda \operatorname{tg} \chi_0 = 2$

$k\lambda$	0,25	0,5	1,0	1,5	2,5	5,0	10,0
kc_y^{α}	0,4004	0,7724	1,4238	1,9520	2,7432	3,8976	4,8104
$kc_{ya}^{\omega_{za}}$	0,2997	0,5761	1,0640	1,4400	2,0127	2,9028	3,5627
km_{za}^{α}	−0,1023	−0,1987	−0,3711	−0,5092	−0,7163	−1,0258	−1,2421
$km_{za}^{\omega_{za}}$	−0,1355	−0,2575	−0,4665	−0,6086	−0,8137	−1,1205	−1,2919
$km_{x1}^{\omega_{x1}}$	−0,0263	−0,0514	−0,0969	−0,1359	−0,1973	−0,2915	−0,3787
$k^3 c_{ya1}^{\dot{\alpha}_a}$	0,1927	0,3550	0,5800	0,6558	0,5681	−0,1857	−1,9380
$k^3 c_{ya1}^{\dot{\omega}_{za}}$	0,1007	0,1846	0,2969	0,3123	0,2017	−0,4098	−1,7438
$k^3 m_{za1}^{\dot{\alpha}_a}$	−0,0944	−0,1743	−0,2948	−0,3460	−0,3653	−0,2324	0,1876
$k^3 m_{za1}^{\dot{\omega}_{za}}$	−0,0592	−0,1088	−0,1832	−0,2069	−0,2048	−0,0896	0,2329
$k^2 \left(m_{x1}^{\dot{\omega}_{x1}}\right)_1$	−0,0796	−0,0767	−0,0685	−0,0597	−0,0431	−0,0151	0,0073
$k^3 c_{ya2}^{\dot{\alpha}_a}$	−0,1974	−0,3774	−0,6928	−0,9310	−1,2964	−1,8770	−2,3206
$k^3 c_{ya2}^{\dot{\omega}_{za}}$	−0,1044	−0,2058	−0,4014	−0,5698	−0,8251	−1,2979	−1,6803
$k^3 m_{za2}^{\dot{\alpha}_a}$	0,0937	0,1728	0,2974	0,3693	0,4638	0,5928	0,6416
$k^3 m_{za2}^{\dot{\omega}_{za}}$	0,0591	0,1105	0,1956	0,2464	0,3176	0,4250	0,4728
$k^2 \left(m_{x1}^{\dot{\omega}_{x1}}\right)_2$	0,0796	0,0775	0,0723	0,0674	0,0585	0,0432	0,0285

Page 640.

Table 27.2 (continuation).

$\eta = \infty$, $\lambda \operatorname{tg} \chi_0 = 4$

$k\lambda$	0,25	0,5	1,0	1,5	2,5	5,0	10,0
kc_y^{α}	0,3719	0,7100	1,2972	1,7920	2,5585	3,7403	4,7548
$kc_{ya}^{\omega_{za}}$	0,3485	0,6509	1,1454	1,5408	2,1142	2,9686	3,6688
km_{za}^{α}	−0,1720	−0,3161	−0,5423	−0,7075	−0,9440	−1,2283	−1,4221
$km_{za}^{\omega_{za}}$	−0,2196	−0,3973	−0,6635	−0,8459	−1,0990	−1,3811	−1,5717
$km_{x1}^{\omega_{x1}}$	−0,0243	−0,0471	−0,0880	−0,1238	−0,1827	−0,2793	−0,3718
$k^3 c_{ya1}^{\dot{\alpha}_a}$	0,1685	0,3066	0,4886	0,5758	0,5055	−0,1972	−1,9243
$k^3 c_{ya1}^{\dot{\omega}_{za}}$	0,1009	0,1770	0,2548	0,2685	0,1193	−0,5271	−1,8877
$k^3 m_{za1}^{\dot{\alpha}_a}$	−0,0917	−0,1605	−0,2421	−0,2694	−0,2418	−0,0028	0,4461
$k^3 m_{za1}^{\dot{\omega}_{za}}$	−0,0651	−0,1108	−0,1559	−0,1628	−0,1118	0,0972	0,4535
$k^2 \left(m_{x1}^{\dot{\omega}_{x1}}\right)_1$	−0,0706	−0,0673	−0,0595	−0,0518	−0,0379	−0,0136	0,0074
$k^3 c_{ya2}^{\dot{\alpha}_a}$	−0,1765	−0,3348	−0,6030	−0,8332	−1,1702	−1,7398	−2,2466
$k^3 c_{ya2}^{\dot{\omega}_{za}}$	−0,1089	−0,2072	−0,3765	−0,5326	−0,7594	−1,1878	−1,5734
$k^3 m_{za2}^{\dot{\alpha}_a}$	0,0928	0,1666	0,2715	0,3359	0,4142	0,4738	0,4975
$k^3 m_{za2}^{\dot{\omega}_{za}}$	0,0672	0,1208	0,1970	0,2473	0,3078	0,3658	0,3946
$k^2 \left(m_{x1}^{\dot{\omega}_{x1}}\right)_2$	0,0713	0,0689	0,0639	0,0594	0,0521	0,0399	0,0273

$\eta = \infty$, $\lambda \operatorname{tg} \chi_0 = 6$

$k\lambda$	0,25	0,5	1,0	1,5	2,5	5,0	10,0
kc_y^{α}	0,2544	0,5037	0,9768	1,4082	2,1418	3,3869	4,5707
$kc_{ya}^{\omega_{za}}$	0,2248	0,4434	0,8514	1,2141	1,8082	2,7580	3,6067
km_{za}^{α}	−0,1251	−0,2458	−0,4670	−0,6558	−0,9499	−1,3353	−1,5681
$km_{za}^{\omega_{za}}$	−0,1593	−0,3123	−0,5902	−0,8249	−1,1859	−1,6676	−2,0071
$km_{x1}^{\omega_{x1}}$	−0,0172	−0,0342	−0,0673	−0,0984	−0,1534	−0,2531	−0,3564

Page 641.

Table 27.2 (continuation).

$k\lambda$	0,25	0,5	1,0	1,5	2,5	5,0	10,0
$k^3 c_{ya1}^{\dot{\alpha}_a}$	0,0918	0,1754	0,3038	0,3760	0,3666	0,1995	1,8302
$k^3 c_{ya1}^{\bar{\omega}_{za}}$	0,0445	0,0828	0,1300	0,1362	0,0388	−0,5301	−1,8457
$k^3 m_{za1}^{\dot{\alpha}_a}$	−0,0336	−0,0622	−0,0975	−0,1025	−0,0529	0,2451	0,7495
$k^3 m_{za1}^{\bar{\omega}_{za}}$	−0,0244	−0,0446	−0,0670	−0,0651	−0,0122	0,2342	0,6440
$k^2 \left(m_{x1}^{\bar{\omega}_{x1}}\right)_1$	−0,0403	−0,0396	−0,0373	−0,0341	−0,0268	−0,0103	0,0076
$k^3 c_{ya2}^{\dot{\alpha}_a}$	−0,0997	−0,1977	−0,3844	−0,5583	−0,8583	−1,4228	−2,0386
$k^3 c_{ya2}^{\bar{\omega}_{za}}$	−0,0521	−0,1052	−0,2132	−0,3223	−0,5258	−0,9464	−1,4102
$k^3 m_{za2}^{\dot{\alpha}_a}$	0,0349	0,0673	0,1219	0,1610	0,2124	0,2353	0,2373
$k^3 m_{za2}^{\bar{\omega}_{za}}$	0,0271	0,0532	0,1012	0,1408	0,2032	0,2735	0,3243
$k^2 \left(m_{x1}^{\bar{\omega}_{x1}}\right)_2$	0,0418	0,0416	0,0410	0,0401	0,0379	0,0323	0,0243

$\eta = \infty$, $\lambda \operatorname{tg} \chi_0 = 8$

$k\lambda$	0,25	0,5	1,0	1,5	2,5	5,0	10,0
kc_y^{α}	0,1914	0,3809	0,7506	1,1043	1,7481	2,9764	4,2989
$kc_{ya}^{\omega_{za}}$	0,1574	0,3130	0,6158	0,9052	1,4272	2,4010	3,4007
km_{za}^{α}	−0,0990	−0,1969	−0,3852	−0,5588	−0,8565	−1,3343	−1,6710
$km_{za}^{\omega_{za}}$	−0,1356	−0,2698	−0,5289	−0,7697	−1,1900	−1,9091	−2,5545
$km_{x1}^{\omega_{x1}}$	−0,0134	−0,0267	−0,0530	−0,0786	−0,1265	−0,2230	−0,3355
$k^3 c_{ya1}^{\dot{\alpha}_a}$	0,0511	0,0982	0,1748	0,2234	0,2243	−0,2050	−1,7023
$k^3 c_{ya1}^{\bar{\omega}_{za}}$	0,0166	0,0303	0,0461	0,0442	0,0224	−0,4637	−1,6690
$k^3 m_{za1}^{\dot{\alpha}_a}$	0,0007	0,0028	0,0159	0,0431	0,1358	0,4814	1,0635
$k^3 m_{za1}^{\bar{\omega}_{za}}$	−0,0062	−0,0110	−0,0132	−0,0033	0,0508	0,2970	0,7730
$k^2 \left(m_{x1}^{\bar{\omega}_{x1}}\right)_1$	−0,0223	−0,0221	−0,0212	−0,0199	−0,0163	−0,0061	0,0079

Table 27.2 (continuation).

kλ	0,25	0,5	1,0	1,5	2,5	5,0	10,0
$k^3 c^{\dot{\alpha}_a}_{ya2}$	−0,0584	−0,1161	−0,2307	−0,3464	−0,5707	−1,0667	−1,7296
$k^3 c^{\bar{\omega}_{za}}_{ya2}$	−0,0231	−0,0467	−0,0986	−0,1609	−0,3030	−0,6748	−1,1902
$k^3 m^{\dot{\alpha}_a}_{za2}$	−0,0001	−0,0002	−0,0019	−0,0071	−0,0237	−0,0736	−0,1079
$k^3 m^{\bar{\omega}_{za}}_{za2}$	0,0086	0,0176	0,0368	0,0556	0,0930	0,1714	0,2747
$k^2 \left(m^{\bar{\omega}_{x1}}_{x1}\right)_z$	0,0243	0,0243	0,0244	0,0245	0,0244	0,0236	0,0204

Page 642.

At the low speeds, when $M = 0$ and k = 1, the given materials can be directly utilized during the analysis of the effect of the geometric parameters of wing on the value of aerodynamic derivatives in the incompressible medium, since the wing planform in this case is determined by three geometric parameters: λ, χ_0, η.

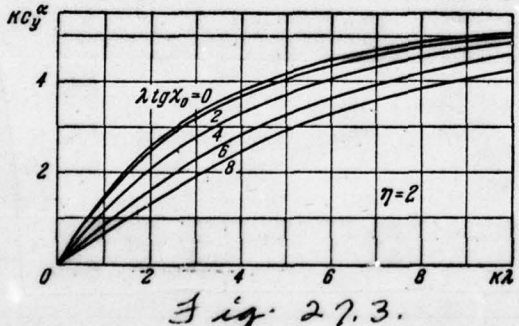


Fig. 27.3.

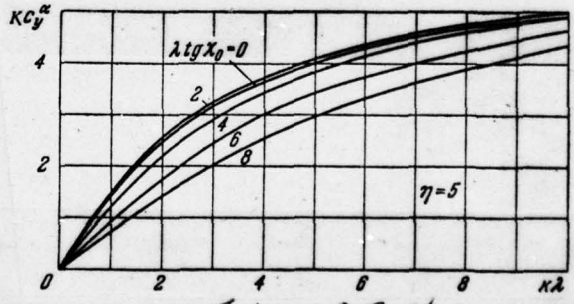


Fig 27.4

Fig. 27.3. Dependences of derivative c_y^α of the parameters of similarity ($M < 1$).

Fig. 27.4. Dependence of derivative c_y^α of the parameters of similarity ($M < 1$).

Page 643.

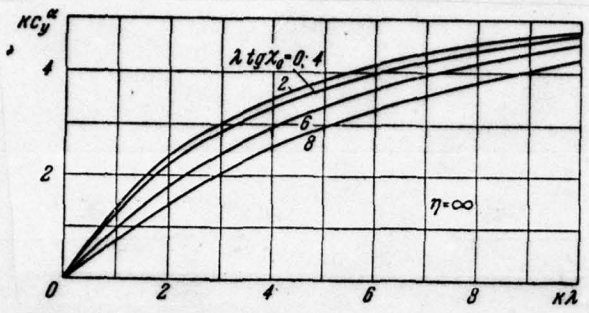


Fig. 27.5. Dependence of derivative c_y^{α} of the parameters of similarity ($M < 1$).

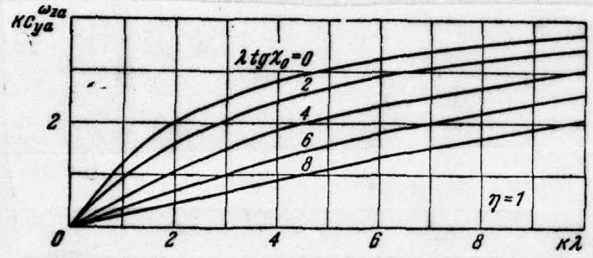


Fig. 27.6. Dependence of derivative $c_{ya}^{\omega_{za}}$ of the parameters of similarity ($M < 1$).

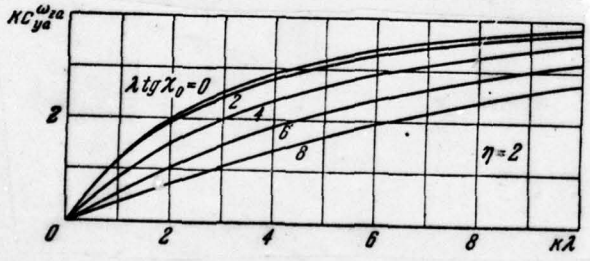


Fig. 27.7. Dependence of derivative $c_{ya}^{\omega_{za}}$ of the parameters of similarity ($M < 1$).

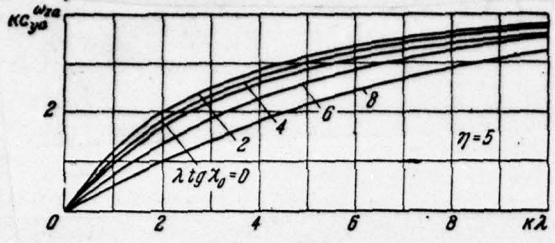


Fig. 27.8. Dependence of derivative $c_{ya}^{\omega_{za}}$ of the parameters of similarity (M < 1).

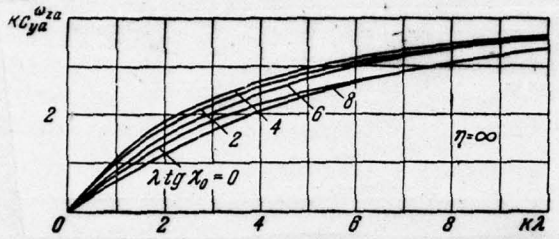


Fig. 27.9. Dependence of derivative $c_{ya}^{\omega_{za}}$ of the parameters of similarity (M < 1).

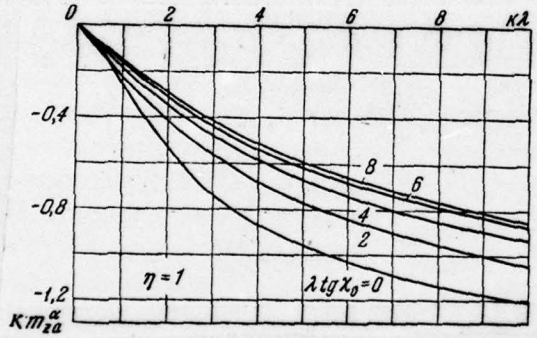


Fig. 27.10. Dependence of derivative m_{za}^{α} of the parameters of similarity (M < 1)

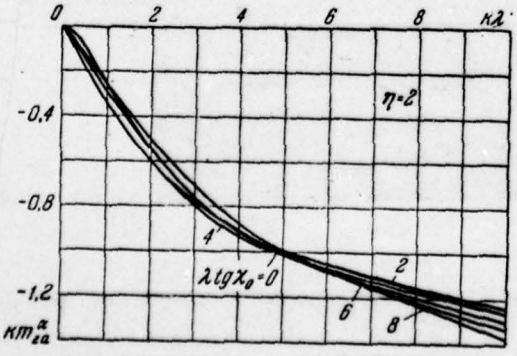


Fig. 27.11. Dependence of derivative m_{za}^{α} of the parameters of similarity (M < 1).

Page 645.

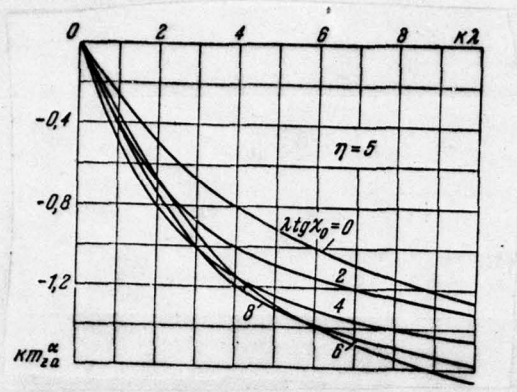


Fig. 27.12. Depenience of derivative m_{za}^{α} of the parameters of similarity (M < 1).

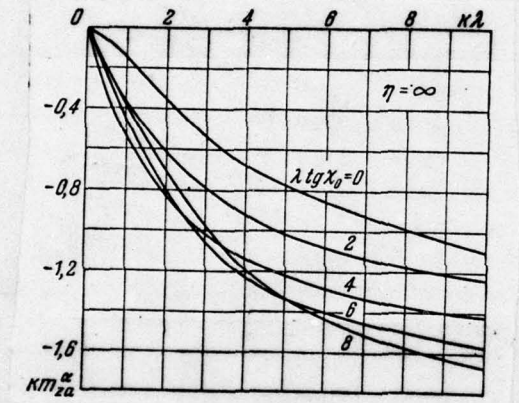


Fig. 27.13. Dependence of derivative m_{za}^{α} of the parameters of similarity (M < 1).

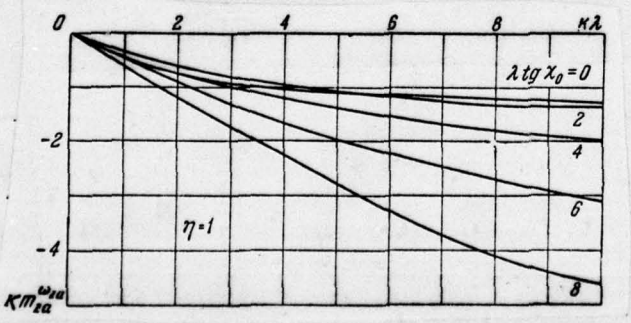


Fig. 27.14. Dependence of derivative $m_{za}^{\omega_{za}}$ of the parameters of similarity (M < 1).

Page 646.

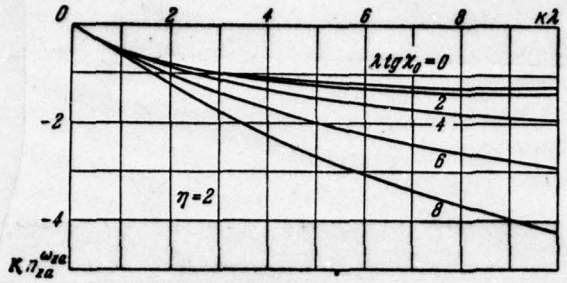


Fig. 27.15. Dependence of derivative $m_{za}^{\omega_{za}}$ of the parameters of similarity (M < 1).

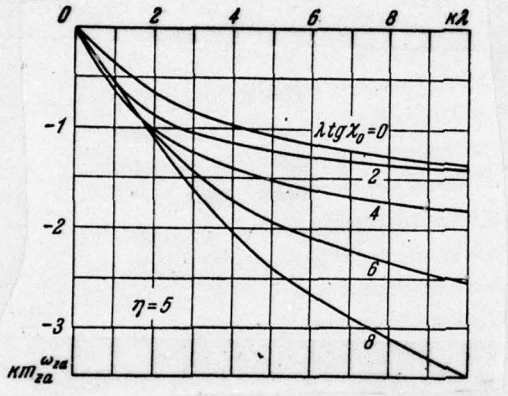


Fig. 27.16. Dependence of derivative $m_{za}^{\omega_{za}}$ of the parameters of similarity (M < 1).

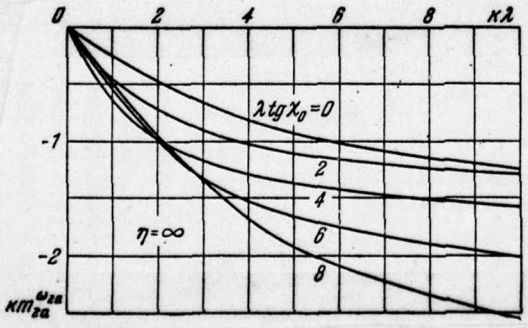


Fig. 27.17. Dependence of derivative $m_{za}^{\omega_{za}}$ of the parameters of similarity (M < 1).

Page 647.

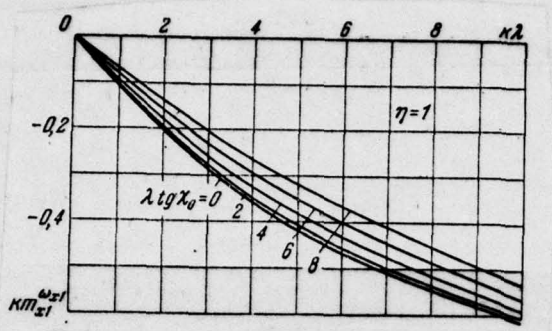


Fig. 27.18. Dependence of derivative $m^{\omega_{x1}}_{x1}$ of the parameters of similarity (M < 1).

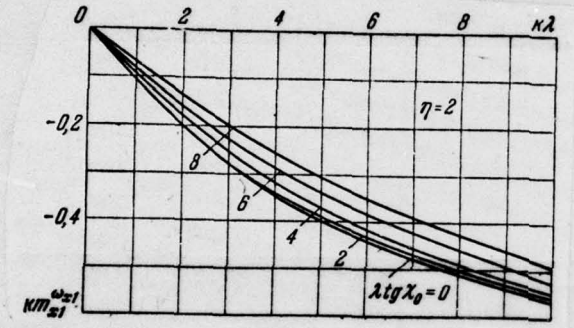


Fig. 27.19. Dependence of derived $m^{\omega_{x1}}_{x1}$ on the parameters of similarity (M < 1).

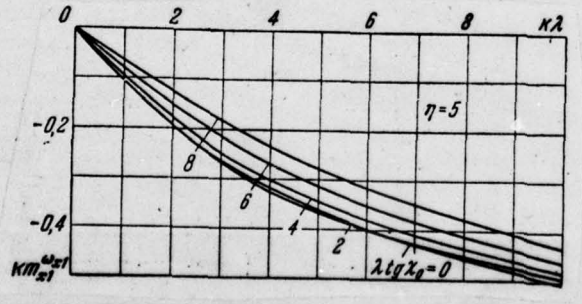


Fig. 27.20. Dependence of derivative $m^{\omega_{x1}}_{x1}$ of the parameters of similarity (M < 1).

Page 648.

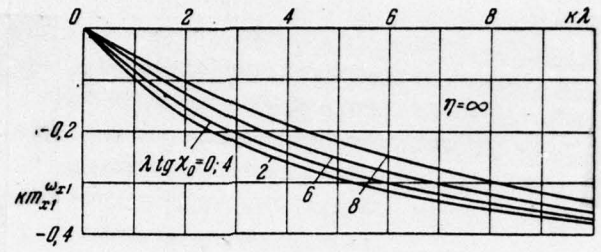


Fig. 27.21. Dependence of derived $m^{\omega_{x1}}_{x1}$ on the parameters of similarity (M < 1).

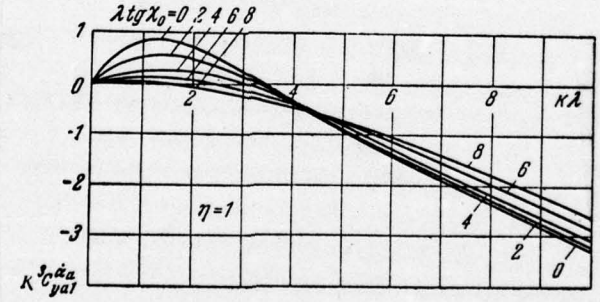


Fig. 27.22 Caption next page.

Fig. 27.22. Dependence of derivative $c_{y\alpha 1}^{\alpha_a}$ of the parameters of similarity (M < 1).

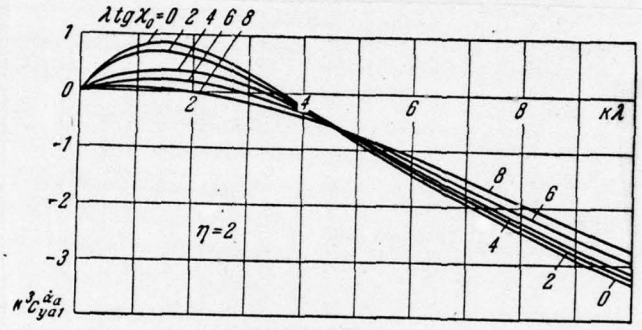


Fig. 27.23. Dependence of derivative $c_{y\alpha 1}^{\alpha_a}$ of the parameters of similarity (M < 1).

Page 649.

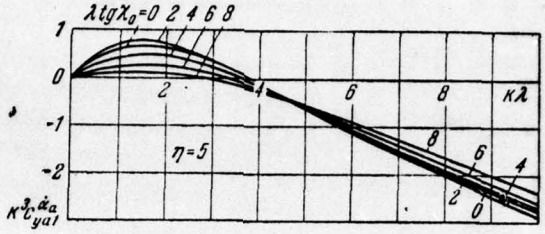


Fig. 27.24. Dependence of derivative $c_{ya1}^{\alpha_a}$ of the parameters of similarity (M < 1).

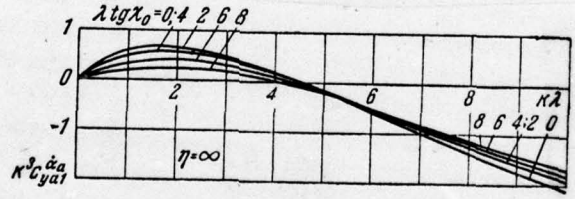


Fig. 27.25. Dependence of derivative $c_{ya1}^{\alpha_a}$ of the parameters of similarity (M < 1).

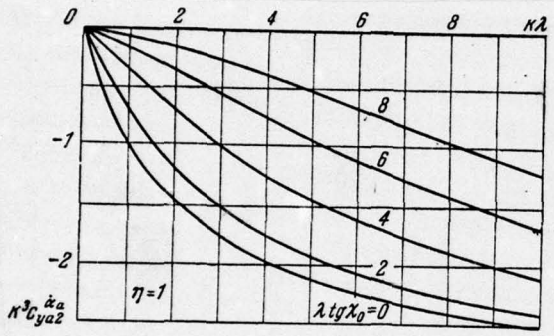


Fig 27.26

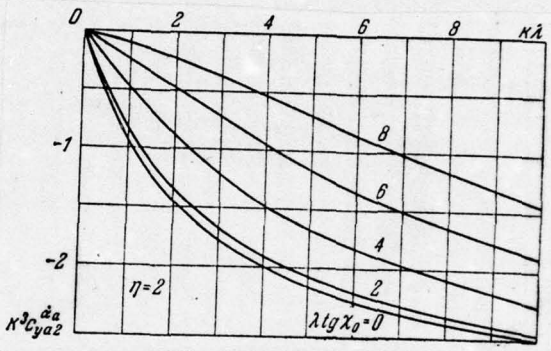


Fig. 27.27

Fig. 27.26. Dependence of derivative $c_{ya2}^{\dot{\alpha}_a}$ of the parameters of similarity (M < 1).

Fig. 27.27. Dependence of derivative $c_{ya2}^{\dot{\alpha}_a}$ of the parameters of similarity (M < 1).

Page 650.

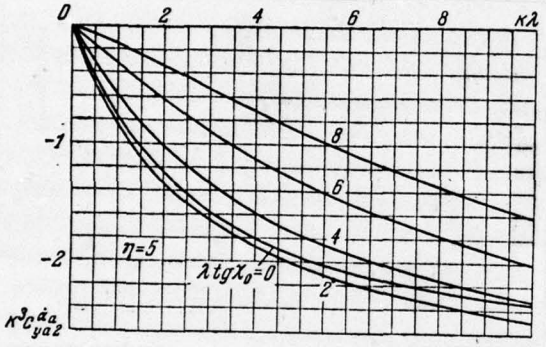


Fig 27.28

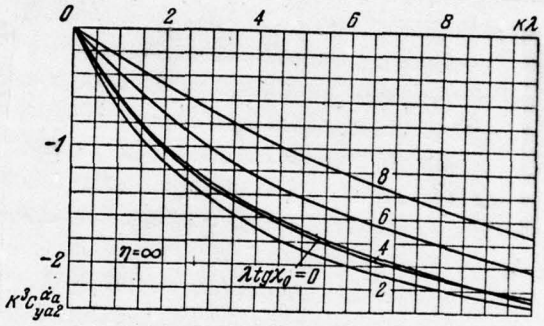


Fig 27.29

Fig. 27.28. Dependence of derivative $c_{ya2}^{\alpha_a}$ of the parameters of similarity (M < 1).

Fig. 27.29. Dependence of derivative $c_{ya2}^{\alpha_a}$ of the parameters of similarity (M < 1).

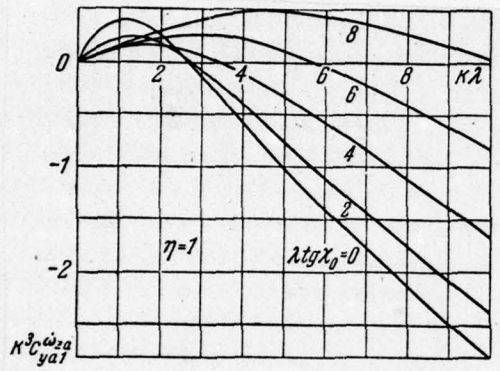


Fig 27.30

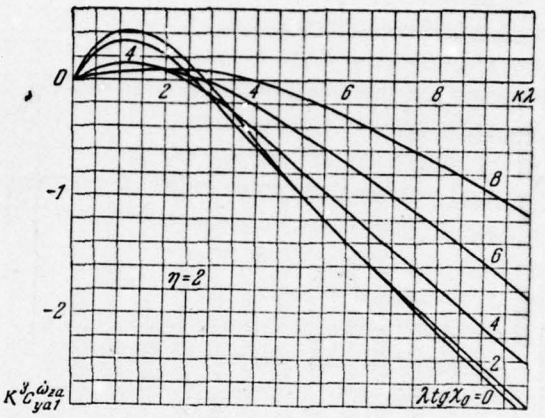


Fig. 27.31.

Fig. 27.30. Dependence of derivative $c^{\dot{\omega}_{zn}}_{ya1}$ of the parameters of similarity (M < 1).

Fig. 27.31. Dependence of derivative $c^{\dot{\omega}_{za}}_{ya1}$ of the parameters of similarity (M < 1).

Page 651.

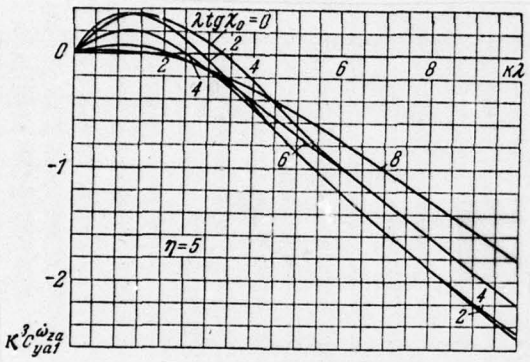


Fig 27.32

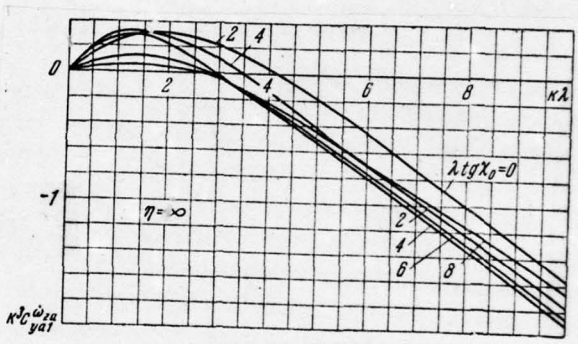


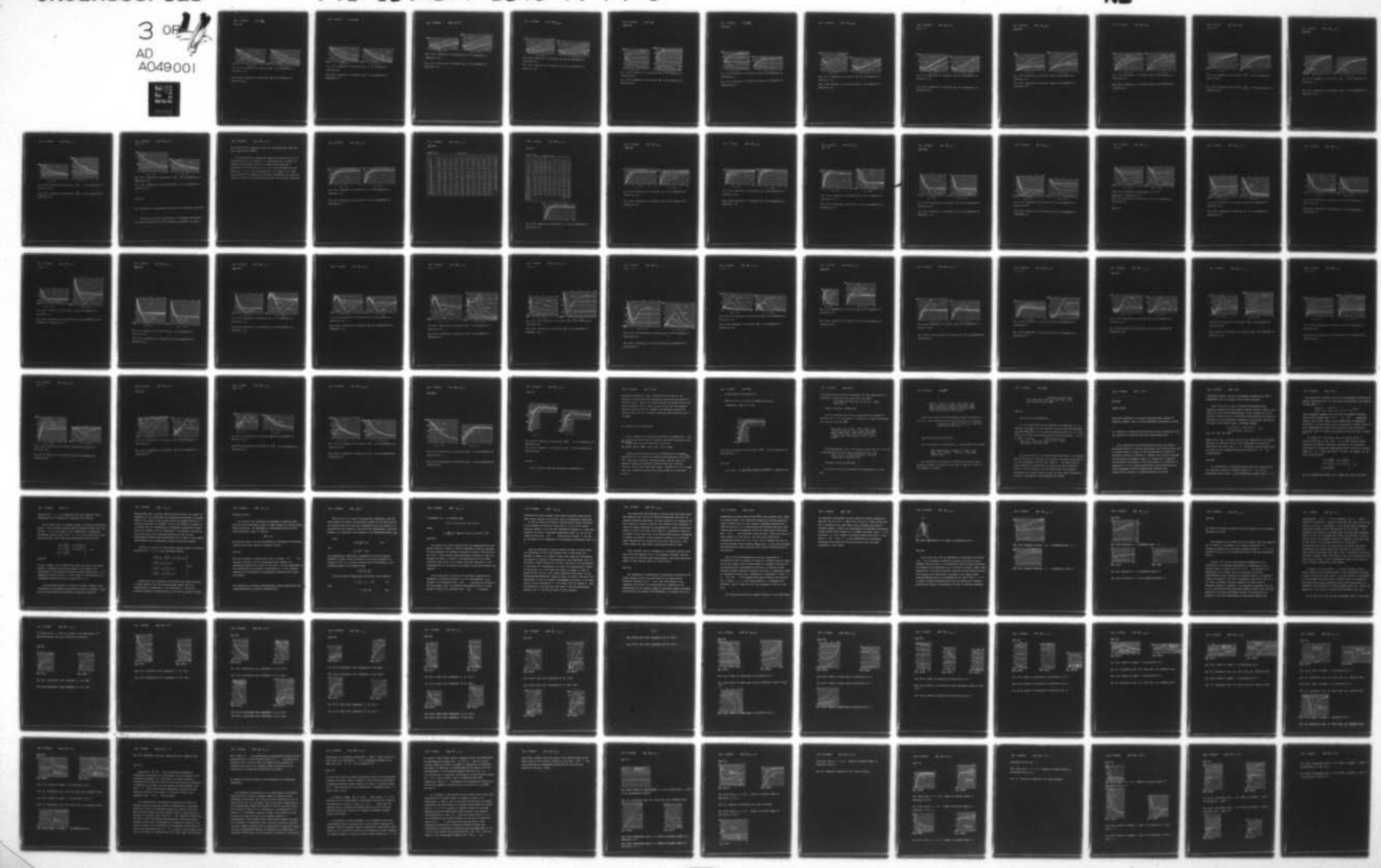
Fig 27.33

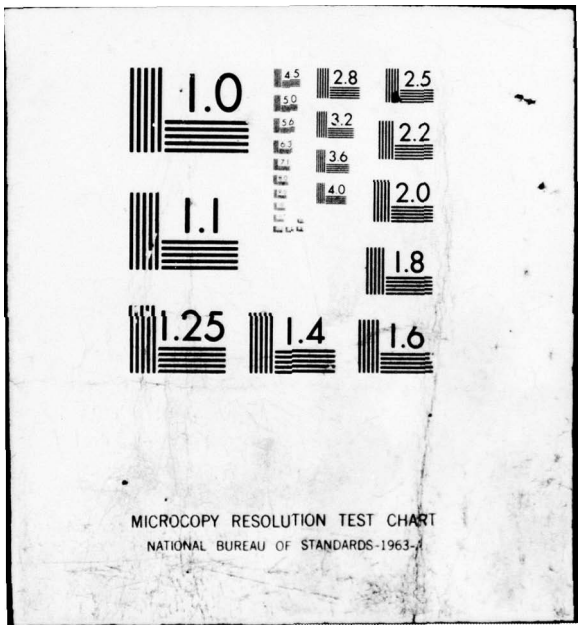
Fig. 27.32. Dependence of derivative $c^{\dot{\omega}_{za}}_{yal}$ of the parameters of similarity (M < 1).

Fig. 27.33. Dependence of derivative $c^{\dot{\omega}_{za}}_{yal}$ of the parameters of similarity (M < 1).

AD-A049 001 FOREIGN TECHNOLOGY DIV WRIGHT-PATTERSON AFB OHIO F/G 1/3
A WING IN AN UNSTEADY GAS FLOW. PART 3,(U)
SEP 77 S M BELOTSERKOVSKIY, B K SKRIPACH
UNCLASSIFIED FTD-ID(RS)T-1543-77-PT-3 NL

3 OF
AD
A049001




1.0
1.1
1.25
1.4
1.6
1.8
2.0
2.2
2.5
2.8
3.2
3.6
4.0
4.5
5.0
5.6
MICROCOPY RESOLUTION TEST CHART
NATIONAL BUREAU OF STANDARDS-1963-A

Page 652.

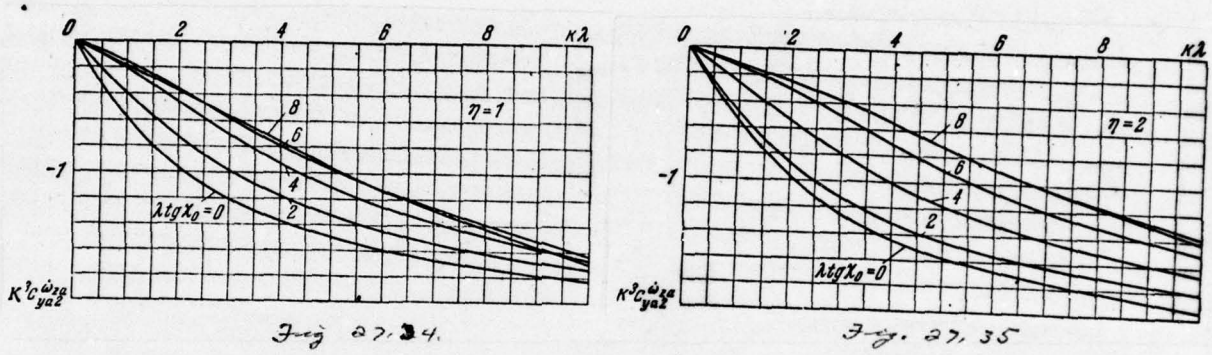


Fig. 27.34. Fig. 27.35.

Fig. 27.34. Dependence of derivative $c^{\omega_{za}}_{ya2}$ of the parameters of similarity (M < 1).

Fig. 27.35. Dependence of derivative $c^{\omega_{za}}_{ya2}$ of the parameters of similarity (M < 1).

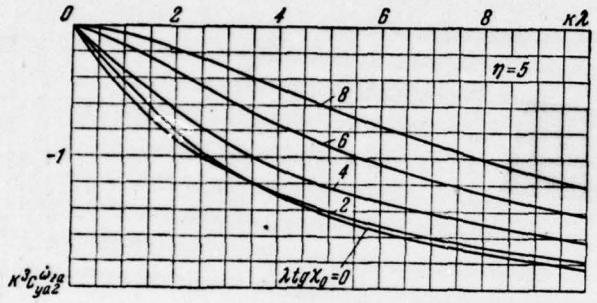


Fig. 27.36.

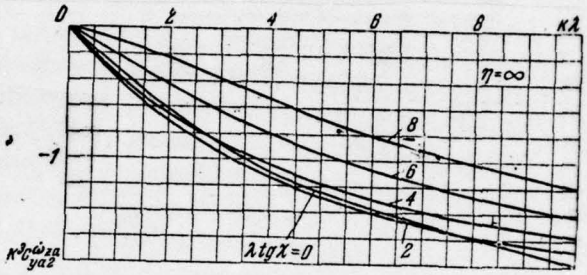


Fig. 27.37.

Fig. 27.36. Dependence of derivative $c_{ya2}^{\bar{\omega}_{za}}$ of the parameters of similarity (M < 1).

Fig. 27.37. Dependence of derivative $c_{ya2}^{\bar{\omega}_{za}}$ of the parameters of similarity (M > 1).

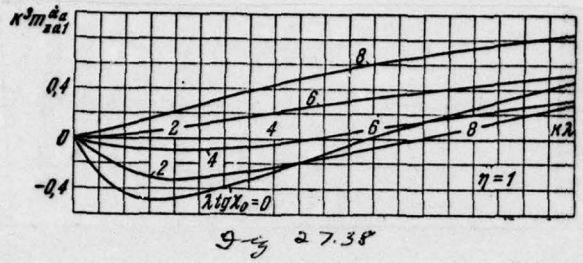


Fig. 27.38

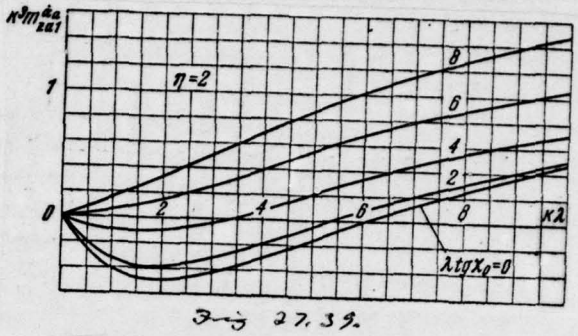
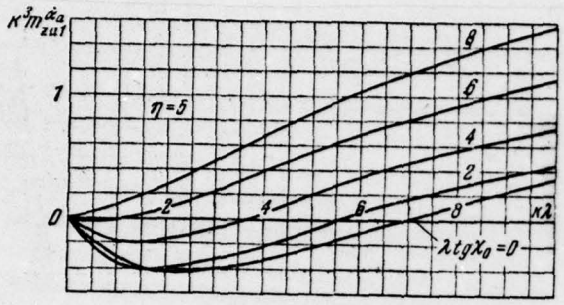


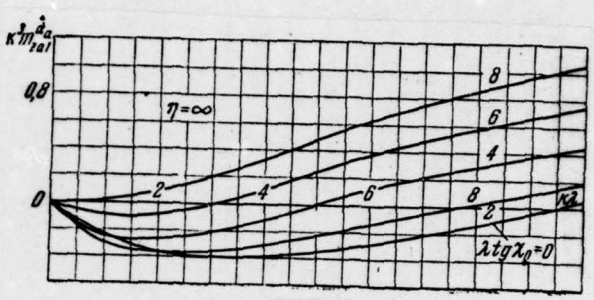
Fig. 27.39.

Fig. 27.38. Dependence of derivative $m^{\alpha_a}_{zal}$ of the parameters of similarity (M < 1).

Fig. 27.39. Dependence of derivative $m^{\alpha_a}_{zal}$ of the parameters of similarity (M < 1).



Фиг 27.40



Фиг 27.41.

Fig. 27.40. Dependence of derivative $m_{zal}^{\dot{\alpha}_a}$ of the parameters of similarity ($M < 1$).

Fig. 27.41. Dependence of derivative $m_{zal}^{\dot{\alpha}_a}$ of the parameters of similarity ($M < 1$).

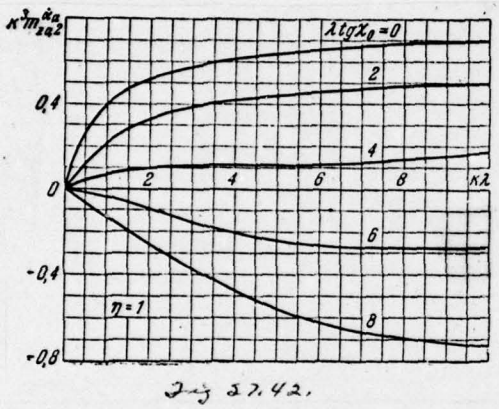


Fig 27.42.

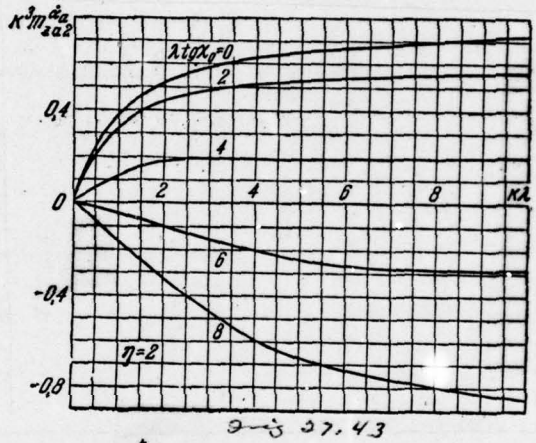


Fig 27.43

Fig. 27.42. Dependence of derivative $m^{\dot{\alpha}_a}_{za2}$ of the parameters of similarity (M < 1).

Fig. 27.43. Dependence of derivative $m^{\dot{\alpha}_a}_{za2}$ of the parameters of similarity (M < 1).

Page 655.

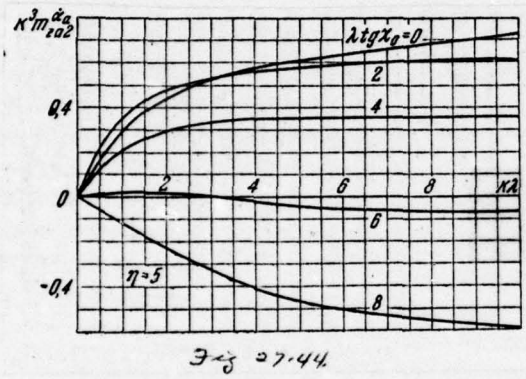


Fig 27.44

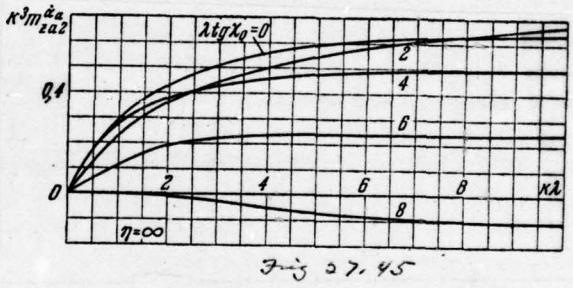
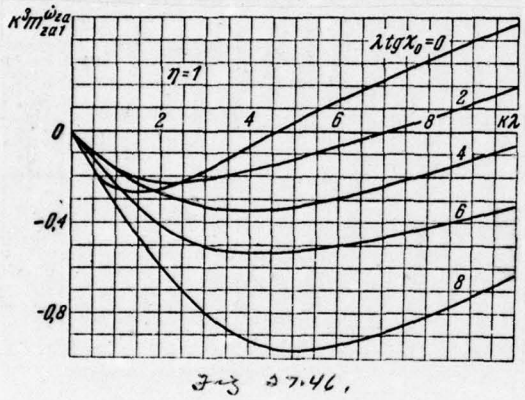


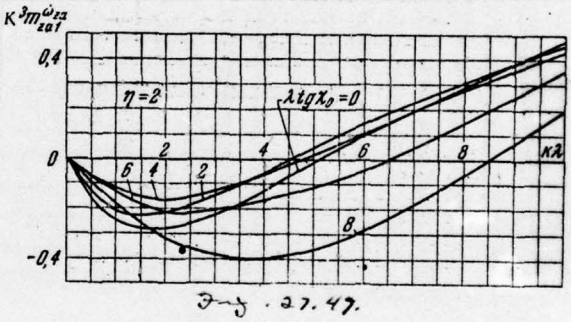
Fig 27.45

Fig. 27.44. Dependence of derivative $m^{\dot{\alpha}_a}_{za2}$ of the parameters of similarity (M < 1).

Fig. 27.45. Dependence of derivative $m^{\dot{\alpha}_a}_{za2}$ of the parameters of similarity (M < 1).



Фиг 27.46.

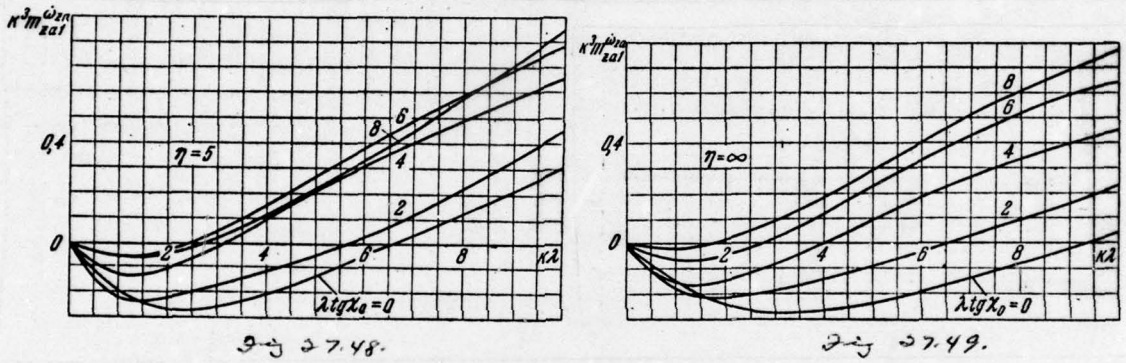


Фиг. 27.47.

Fig. 27.46. Dependence by derivative $m^{\dot{\omega}_{za}}_{za1}$ of the parameters of similarity (M < 1).

Fig. 27.47. Dependence of derivative $m^{\dot{\omega}_{za}}_{za1}$ of the parameters of similarity (M < 1).

page 656.



Фиг 27.48. Фиг 27.49.

Fig. 27.48. Dependence of derivative $m^{\dot{\omega}_{za}}_{za}$ of the parameters of similarity (M < 1).

Fig. 27.49. Dependence of derivative $m^{\dot{\omega}_{za}}_{za}$ of the parameters of similarity (M < 1).

Page 657.

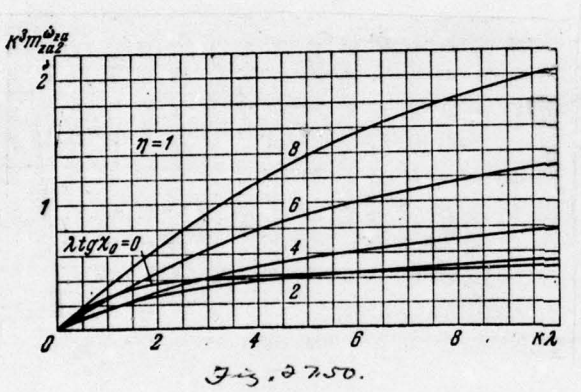


Fig. 27.50.

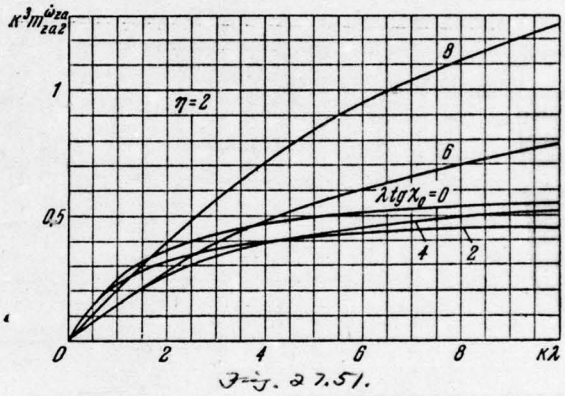


Fig. 27.51.

Fig. 27.50. Dependence of derivative $m^{\dot{\omega}_{za}}_{za2}$ of the parameters of similarity (M < 1).

Fig. 27.51. Dependence of derivative $m^{\dot{\omega}_{za}}_{za2}$ of the parameters of similarity (M < 1).

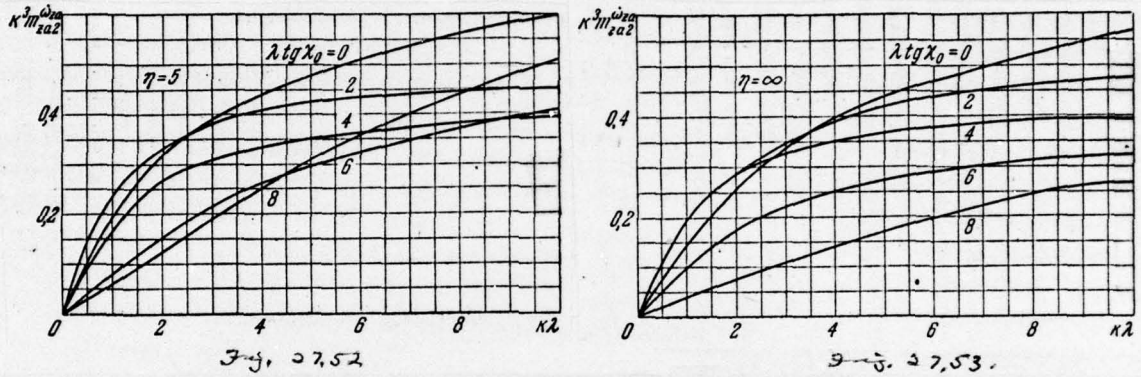
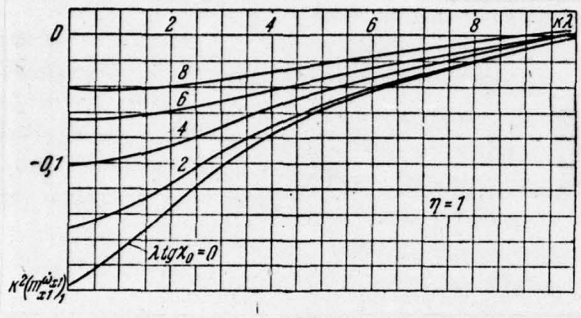
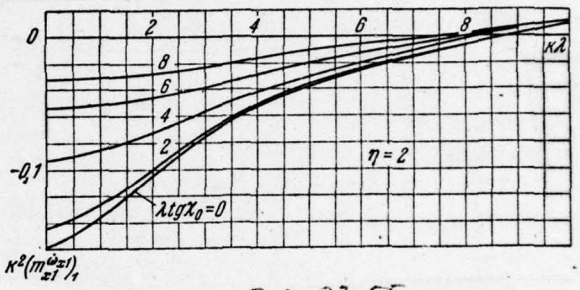


Fig. 27.52. Dependence of derivative $m^{\dot{\omega}_{za}}_{za2}$ of the parameters of similarity (M < 1).

Fig. 27.53. Dependence of derivative $m^{\dot{\omega}_{za}}_{za2}$ of the parameters of similarity (M < 1).



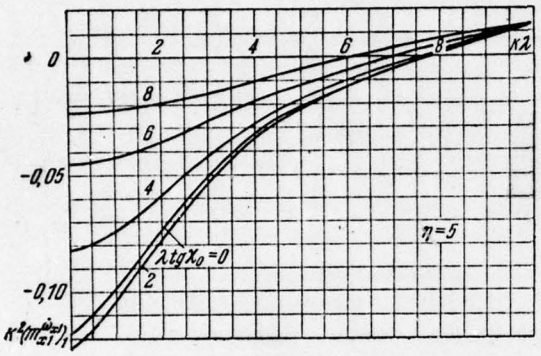
Эф. 27.54.



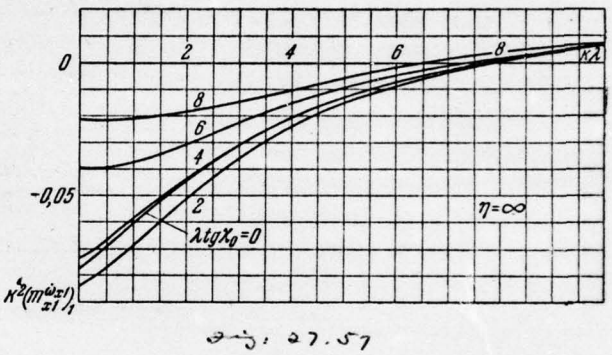
Эф. 27.55.

Fig. 27.54. Dependence of derivative $\left(m_{x1}^{\dot{\omega}_{x1}}\right)_1$ of the parameters of similarity (M < 1).

Fig. 27.55. Dependence of derivative $\left(m_{x1}^{\dot{\omega}_{x1}}\right)_1$ of the parameters of similarity (M < 1).



Фиг. 27.56



Фиг. 27.57

Fig. 27.56. Dependence of derivative $\left(m_{x1}^{\dot{\omega}_{x1}}\right)_1$ of the parameters of similarity $(M < 1)$.

Fig. 27.57. Dependence of derivative $\left(m_{x1}^{\dot{\omega}_{x1}}\right)_1$ of the parameters of similarity $(M < 1)$.

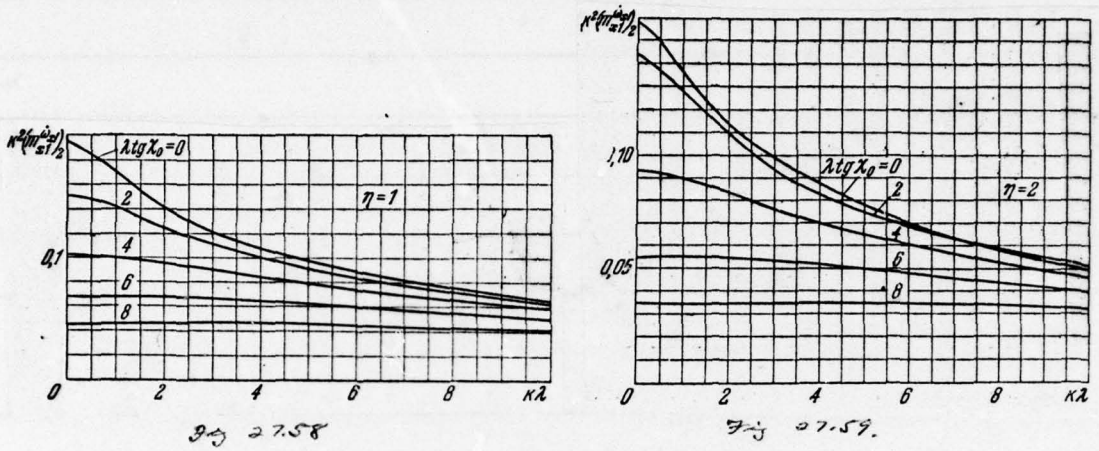
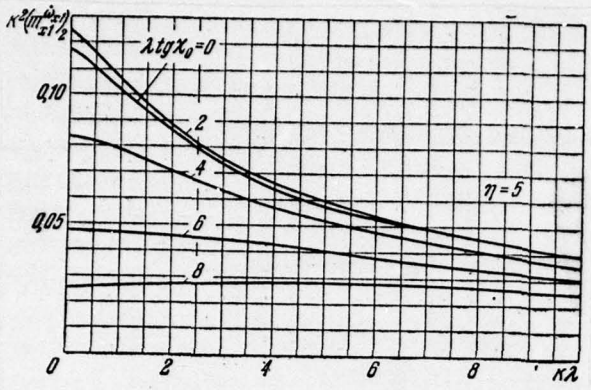


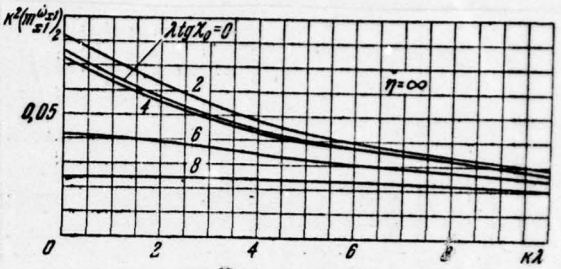
Fig 27.58 Fig 27.59.

Fig. 27.58. Dependence of derivative $\left(m^{\omega}_{x1}\right)_2$ of the parameters of similarity ($M < 1$).

Fig. 27.59. Dependence of derivative $\left(m^{\omega}_{x1}\right)_2$ of the parameters of similarity ($M < 1$).



Эф. 27.60.



Эф. 27.61.

Fig. 27.60. Dependence of derivative $\left(m^{\bar{\omega}_{xz}}_{x1}\right)_2$ of the parameters of similarity (M < 1).

Fig. 27.61. Dependence of derivative $\left(m^{\bar{\omega}_{xz}}_{x1}\right)_2$ of the parameters of similarity (M < 1).

Page 661.

§4. Coefficients of aerodynamic derivatives at supersonic velocities.

The given on diagrams coefficients of aerodynamic derivatives are obtained depending on three similarity parameters: $k\lambda$, $\lambda tg\chi_0$, η,

that determine the geometry of wing with direct/straight edges and Mach number Maxa ($k = \sqrt{M^2 - 1}$).

The calculations at supersonic speeds are carried out by N. A. Kudryavtsevoy, N. G. Lavrenko, V. G. Tabachnikov, M. K. Fursov. Is examined the following range of a change in the similarity parameters: $k\lambda = 0 \div 20$, $\lambda \operatorname{tg} \chi_0 = 0 \div 8$, $\eta = 1 \div \infty$ - with very small Strouhal number (p * $\rightarrow$ 0). For rectangular ($k\lambda = 1 \div \infty$, $\lambda \operatorname{tg} \chi_0 = 0$, $\eta = 1$) and triangular ($k\lambda = 0{,}1 \div \infty$; $\lambda \operatorname{tg} \chi_0 = 4$; $\eta = \infty$) wings, furthermore, are given the numerical values of the derivatives (tables 27.3 and 27.4) indicated.

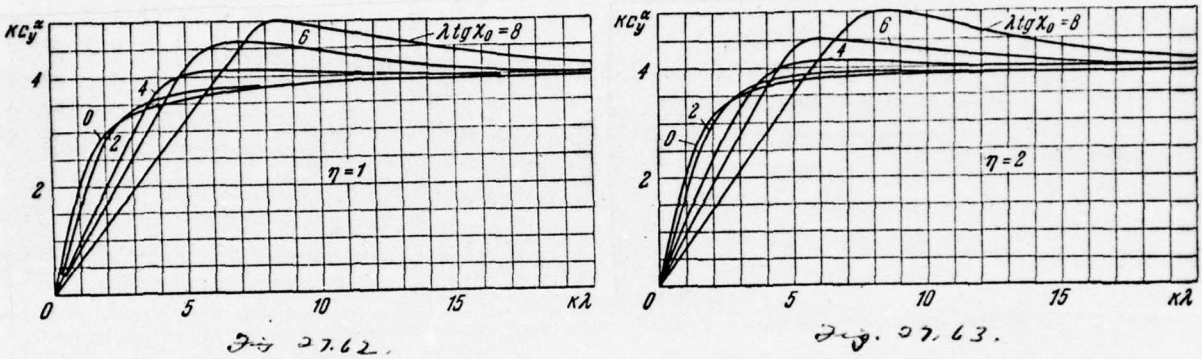


Fig. 27.62. Dependence of derivative c_y^α of the parameters of similarity (M > 1).

Fig. 27.63. Dependence of derivative c_y^α of the parameters of similarity (M > 1).

Page 662.

Table 27.3.

$\lambda \operatorname{tg} \chi_0 = 0,\ \eta = 1$

$b\lambda$	1	2	3	4	6	8	10	12	15	20	∞
kc_y^{α}	2,000	3,000	3,333	3,500	3,667	3,750	3,800	3,833	3,867	3,900	4,000
$kc_{ya}^{\omega_{za}}$	1,333	1,667	1,778	1,833	1,889	1,917	1,933	1,944	1,956	1,967	2,000
km_{za}^{α}	−0,6667	−1,333	−1,556	−1,667	−1,778	−1,833	−1,867	−1,889	−1,911	−1,933	−2,000
$km_{za}^{\omega_{za}}$	−0,8333	−1,083	−1,167	−1,208	−1,250	−1,271	−1,283	−1,292	−1,300	−1,308	−1,333
$km_{x1}^{\omega_{x1}}$	−0,103	−0,268	−0,381	−0,442	−0,504	0,543	−0,558	0,569	−0,584	−0,591	−0,591
$k^3 c_{ya1}^{\dot{\alpha}_a}$	−1,333	−1,667	−1,778	−1,833	−1,889	−1,917	−1,933	−1,944	−1,956	−1,967	−2,000
$k^3 c_{ya2}^{\dot{\alpha}_a}$	0,6667	0,3333	0,2222	0,1667	0,1111	0,0833	0,0667	0,0556	0,0444	0,0333	0,000
$k^3 c_{ya1}^{\dot{\omega}_{za}}$	−0,5000	−0,5834	−0,6111	−0,6250	−0,6389	−0,6459	−0,650	−0,6528	−0,6556	−0,6584	−0,6667
$k^3 c_{ya2}^{\dot{\omega}_{za}}$	0,1667	0,0833	0,0556	0,0417	0,0278	0,0208	0,0167	0,0139	0,0111	0,0083	0,000
$k^3 m_{za1}^{\dot{\alpha}_a}$	0,8333	1,083	1,167	1,208	1,250	1,271	1,283	1,292	1,300	1,308	1,333
$k^3 m_{za2}^{\dot{\alpha}_a}$	−0,500	−0,250	−0,1667	−0,1250	−0,0838	−0,0625	−0,0500	−0,0417	−0,0333	−0,0250	0,000
$k^3 m_{za1}^{\dot{\omega}_{za}}$	0,3667	0,4333	0,4556	0,4666	0,4778	0,4833	0,4867	0,4889	0,4911	0,4933	0,5000
$k^3 m_{za2}^{\dot{\omega}_{za}}$	−0,1333	−0,0667	−0,0444	−0,0333	−0,0222	−0,0167	−0,0133	−0,0111	−0,0089	−0,0067	0,000
$k^2 \left(m_{x1}^{\dot{\omega}_{x1}}\right)_1$	0,200	0,1897	0,1547	0,1277	0,0932	0,0699	0,0602	0,0510	0,0414	0,0316	0
$k^2 \left(m_{x1}^{\dot{\omega}_{x1}}\right)_2$	−0,223	−0,1187	−0,0605	−0,0362	−0,0169	−0,0097	−0,0064	−0,0044	−0,0029	−0,0017	0

Page 663.

Table 27.4. $\lambda \operatorname{tg} \chi_0 = 4,\ \eta = \infty$

$k\lambda$	0,1	0,25	0,50	1	2	3	4	∞
kc_y^{α}	0,1568	0,3896	0,7672	1,464	2,594	3,410	4,000	4,000
$kc_{ya}^{\omega_{za}}$	0,1548	0,3824	0,7252	1,251	1,791	1,943	2,000	2,000
km_{za}^{α}	−0,0784	−0,1948	−0,3836	−0,7322	−1,297	−1,705	−2,000	−2,000
$km_{za}^{\omega_{za}}$	−0,1066	−0,2634	−0,5012	−0,8737	−1,281	−1,428	−1,500	−1,500
$km_{x1}^{\omega_{x1}}$	−0,005	−0,025	−0,050	−0,103	−0,192	−0,267	−0,334	−0,334
$k^3 c_{ya1}^{\dot{\alpha}_a}$	−0,0784	−0,1948	−0,3835	−0,7322	−1,297	−1,705	−2,000	−2,000
$k^3 c_{ya2}^{\dot{\alpha}_a}$	0,0764	0,1876	0,3416	0,5192	0,4936	0,2384	0,0000	0,0000
$k^3 c_{ya1}^{\dot{\omega}_{za}}$	−0,482	−0,1190	−0,2240	−0,3777	−0,5093	−0,5156	−0,5000	−0,5000
$k^3 c_{ya2}^{\dot{\omega}_{za}}$	0,0595	0,1208	0,1793	0,1092	0,0600	0,0248	0,000	0,0000
$k^3 m_{za1}^{\dot{\alpha}_a}$	0,0490	0,1218	0,2398	0,4576	0,8106	1,066	1,250	1,250
$k^3 m_{za2}^{\dot{\alpha}_a}$	−0,0478	−0,1172	−0,2135	−0,3245	−0,3085	−0,1490	0,0000	0,0000
$k^3 m_{za1}^{\dot{\omega}_{za}}$	0,0367	0,0906	0,1712	0,2919	0,4052	0,4248	0,4250	0,4250
$k^3 m_{za2}^{\dot{\omega}_{za}}$	−0,0445	−0,0917	−0,1384	−0,1656	−0,0602	−0,0263	0,0000	0,0000
$k^2 \left(m_{x1}^{\dot{\omega}_{x1}}\right)_1$	—	—	—	—	—	—	0,0666	0,0666
$k^2 \left(m_{x1}^{\dot{\omega}_{x1}}\right)_2$	—	—	—	—	—	—	0	0

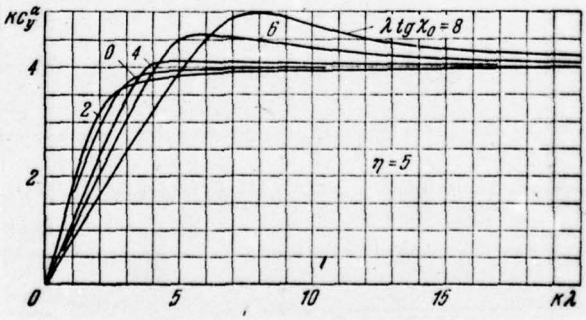


Fig. 27.64. Dependence of derivative c_y^{α} of the parameters of similarity ($M > 1$).

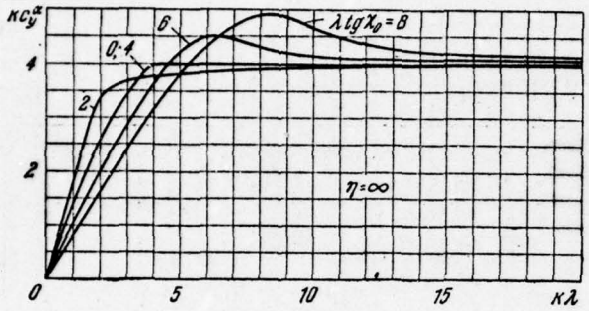


Fig 27.65

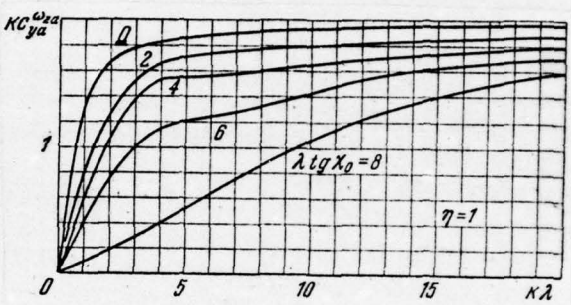


Fig. 27.66

Fig. 27.65. Dependence of derivative c_y^{α} of the parameters of similarity (M > 1).

Fig. 27.66. Dependence of derivative $c_{ya}^{\omega_{za}}$ of the parameters of similarity (M > 1).

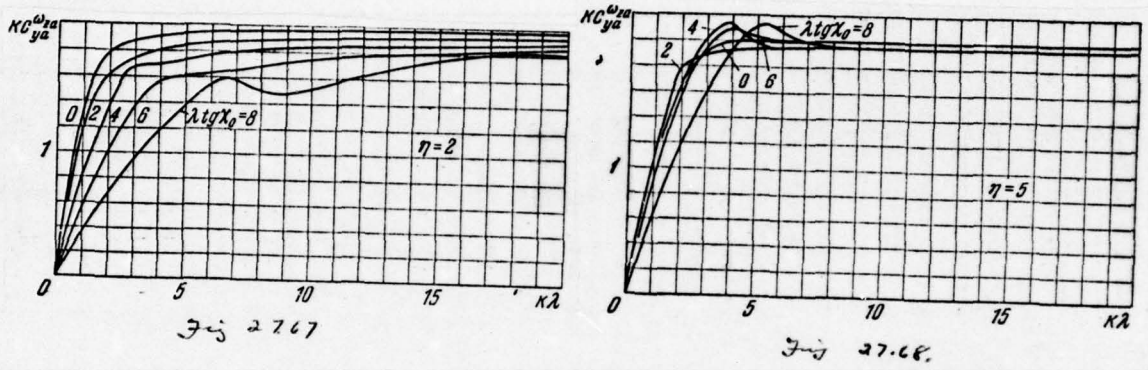
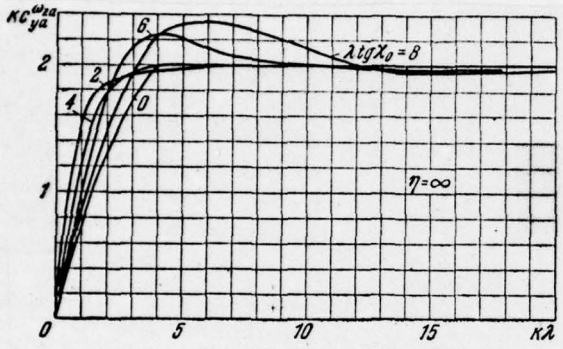


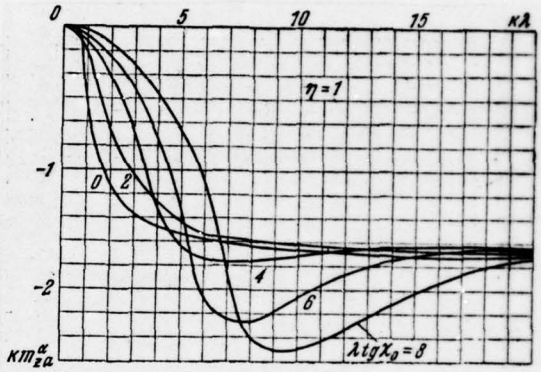
Fig 27.67 Fig 27.68.

Fig. 27.67. Dependence of derivative $c^{\omega_{za}}_{y\alpha}$ of the parameters of similarity (M > 1).

Fig. 27.68. Dependence of derivative $c^{\omega_{za}}_{y\dot{\alpha}}$ of the parameters of similarity (M > 1).



Фиг. 27.69.



Фиг. 27.70.

Fig. 27.69. Dependence of derivative $c_{ya}^{\omega_{za}}$ of the parameters of similarity (M > 1).

Fig. 27.70. Dependence of derivative m_{za}^{α} of the parameters of similarity (M > 1).

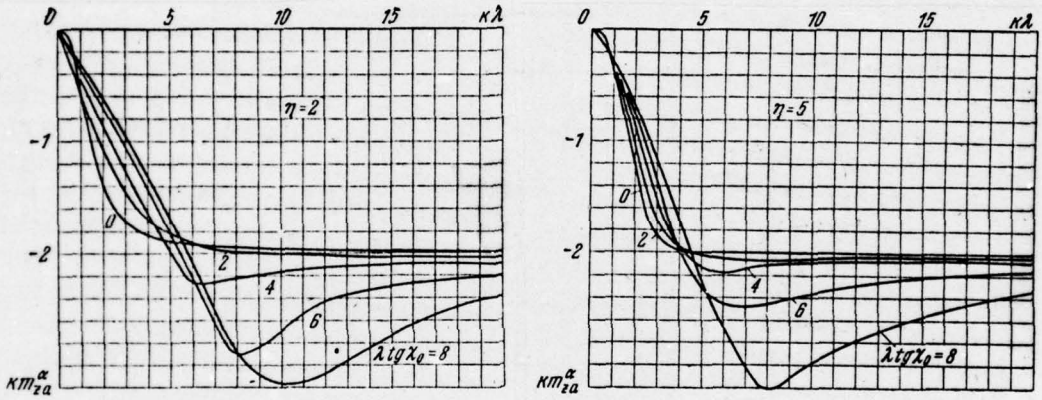


Fig. 27.71. Fig. 27.72.

Fig. 27.71. Dependence of derivative m_{za}^{α} of the parameters of similarity (M > 1).

Fig. 27.72. Dependence of derivative m_{za}^{α} of the parameters of similarity (M > 1).

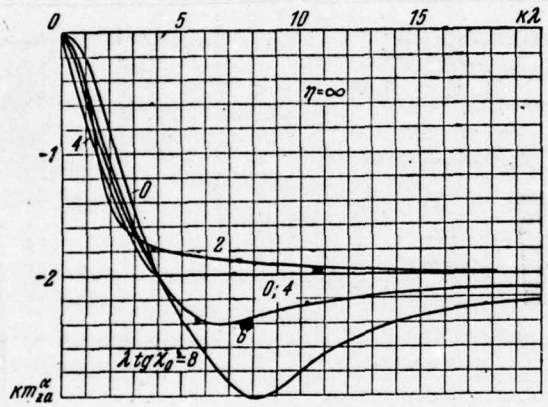


Fig. 27.73.

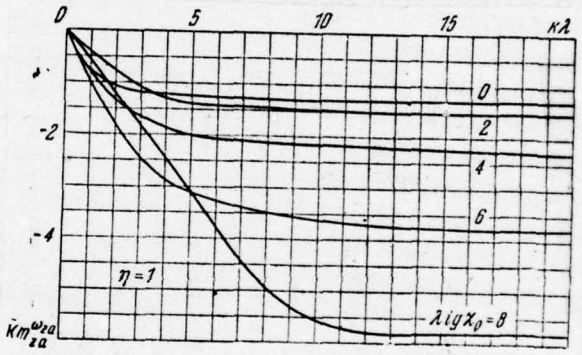


Fig 27.74

Fig. 27.73. Dependence of derivative m_{za}^{α} of the parameters of similarity (M > 1).

Fig. 27.74. Dependence of derivative $m_{za}^{\omega_{za}}$ of the parameters of similarity (M > 1).

Page 667.

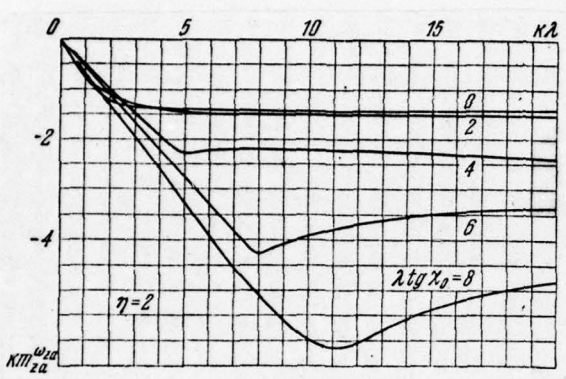


Fig 27.75

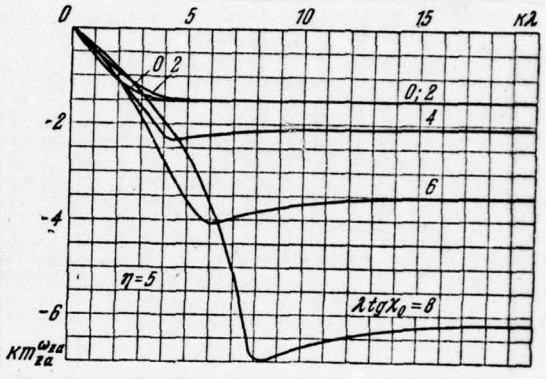


Fig 27.76.

Fig. 27.75. Dependence of derivative $m^{\omega_{za}}_{za}$ of the parameters of similarity (M > 1).

Fig. 27.76. Dependence of derivative $m^{\omega_{za}}_{za}$ of the parameters of similarity (M > 1).

Page 668.

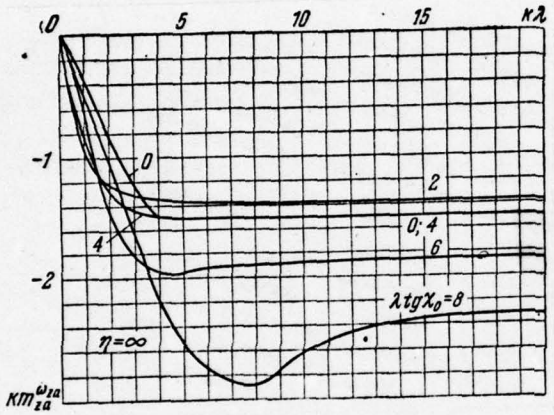


Fig. 27.77.

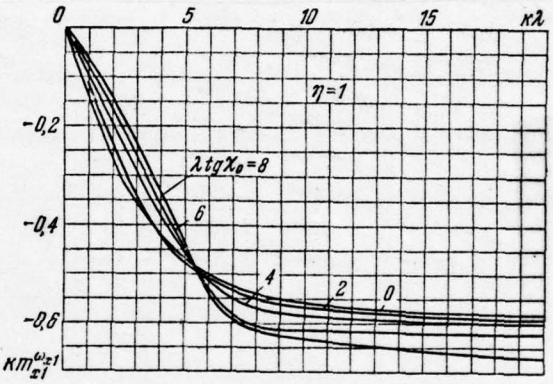


Fig. 27.78

Fig. 27.77. Dependence of derivative $m_{za}^{\omega_{za}}$ of the parameters of similarity (M > 1).

Fig. 27.78. Dependence of derivative $m_{x1}^{\omega_{x1}}$ of the parameters of similarity (M > 1).

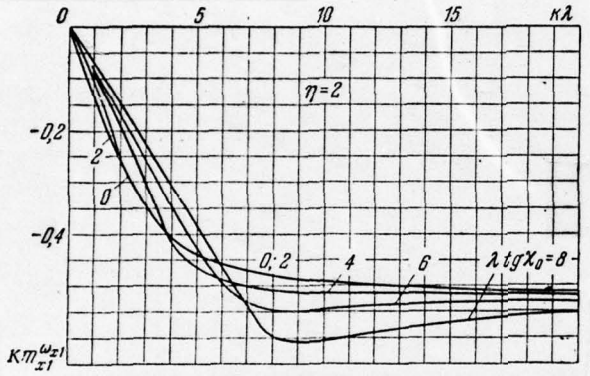


Fig. 27.79.

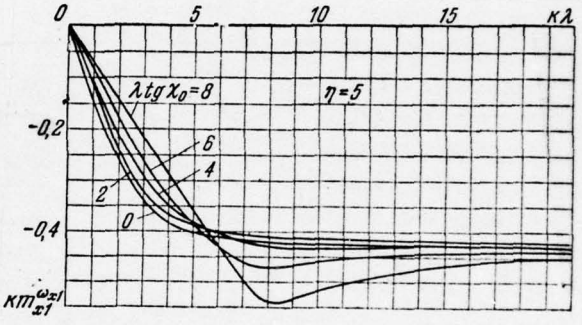


Fig. 27.80.

Fig. 27.79. Dependence of derivative $m_{x1}^{\omega_{x1}}$ of the parameters of similarity (M > 1).

Fig. 27.80. Dependence of derivative $m_{x1}^{\omega_{x1}}$ of the parameters of similarity (M > 1).

Page 669.

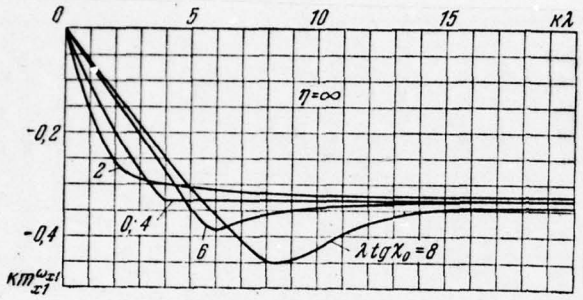


Fig. 27.81.

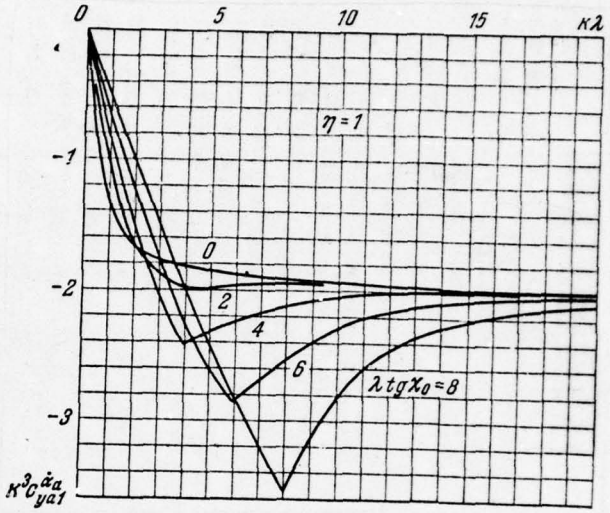


Fig. 27.82.

Fig. 27.81. Dependence of derivative $m_{x1}^{\omega_{x1}}$ of the parameters of similarity (M > 1).

Fig. 27.82. Dependence of derivative $c_{ya1}^{\dot{\alpha}_a}$ of the parameters of the parameters of similarity (M > 1).

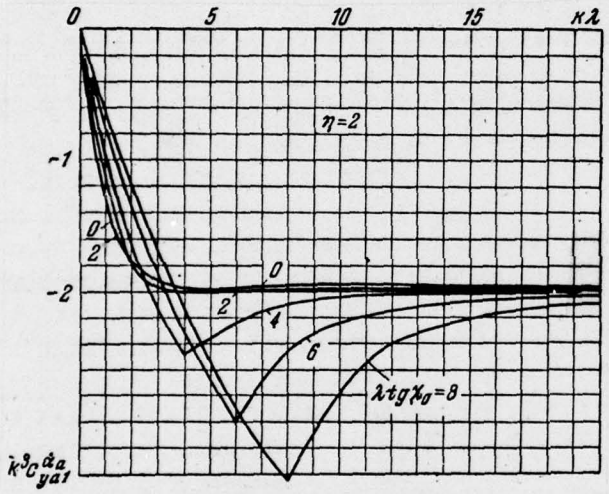


Fig. 27.83

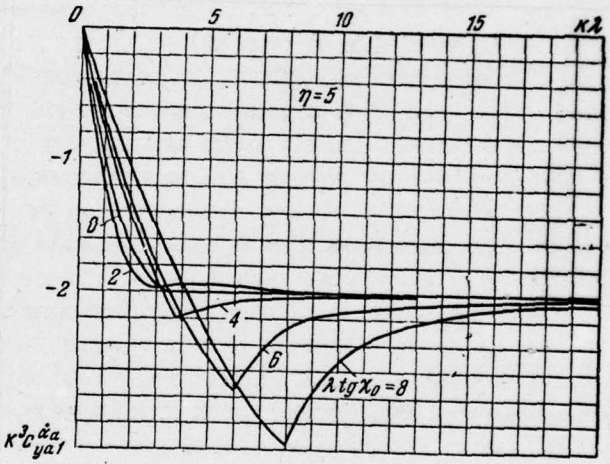
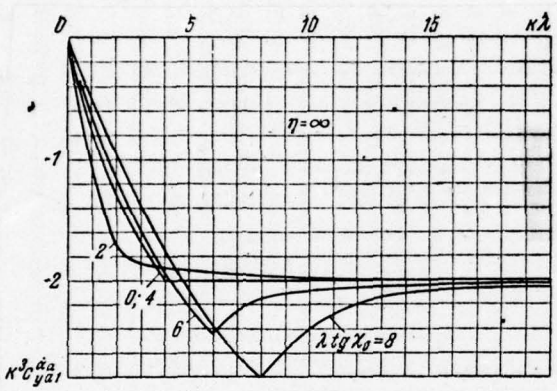


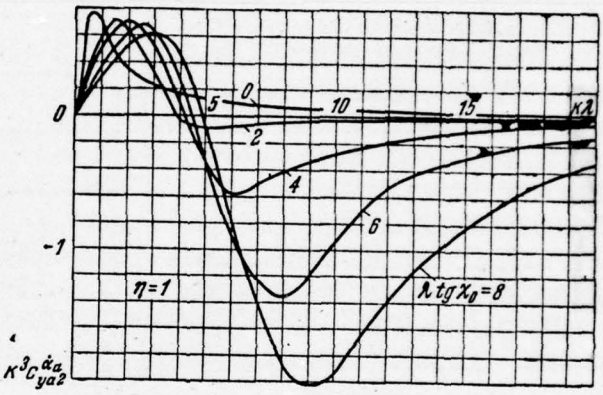
Fig. 27.84

Fig. 27.83. Dependence of derivative $c^{\alpha_a}_{ya1}$ of the parameters of similarity (M > 1).

Fig. 27.84. Dependence of derivative $c^{\alpha_a}_{ma1}$ of the parameters of similarity (M > 1).



Фиг 27.85.



Фиг. 27.86.

Fig. 27.85. Dependence of derivative $c^{\alpha_a}_{ya1}$ of the parameters of similarity (M > 1).

Fig. 27.86. Dependence of derivative $c^{\alpha_a}_{ya2}$ of the parameters of similarity (M > 1).

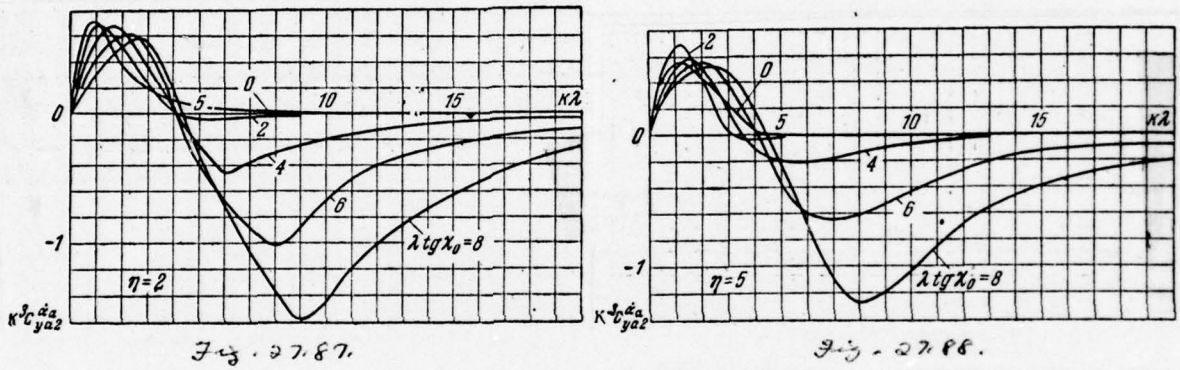


Fig. 27.87. Fig. 27.88.

Fig. 27.87. Dependence of derivative $c^{\dot{\alpha}_a}_{ya2}$ of the parameters of similarity (M > 1).

Fig. 27.88. Dependence of derivative $c^{\dot{\alpha}_a}_{ya2}$ of the parameters of similarity (M > 1).

Page 672.

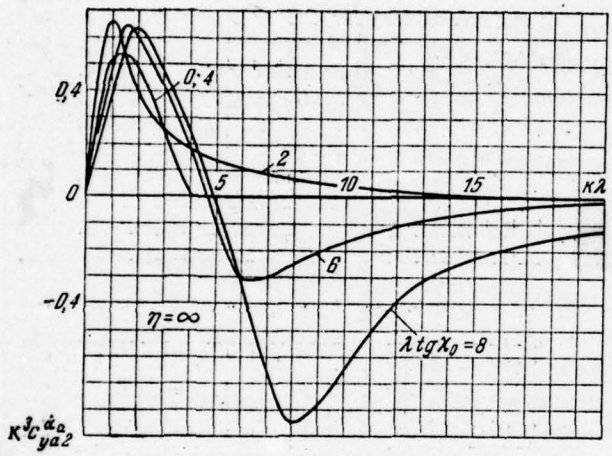


Fig. 27.89.

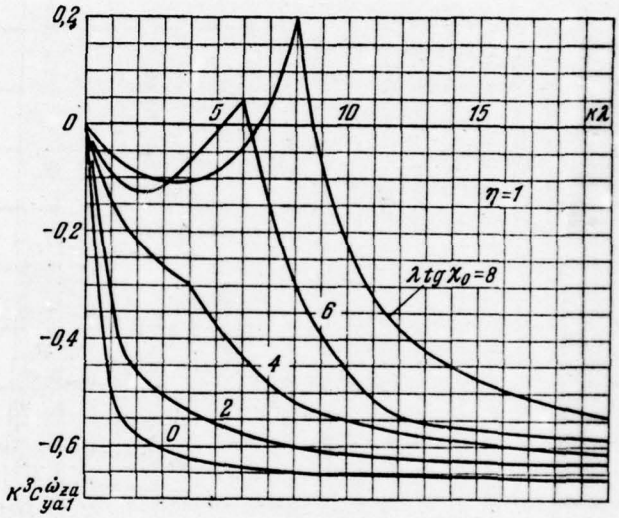


Fig. 27.90.

Fig. 27.89. Dependence of derivative $c^{\dot{\alpha}_a}_{ya2}$ of the parameters of similarity (M > 1).

Fig. 27.90. Dependence of derivative $c^{\dot{\omega}_{za}}_{ya1}$ of the parameters of similarity (M > 1).

Page 673.

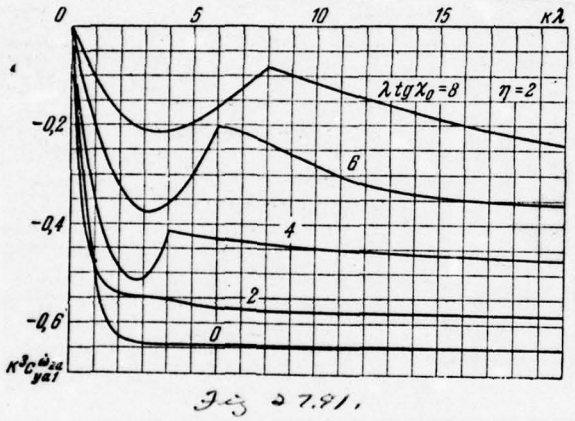


Fig 27.91.

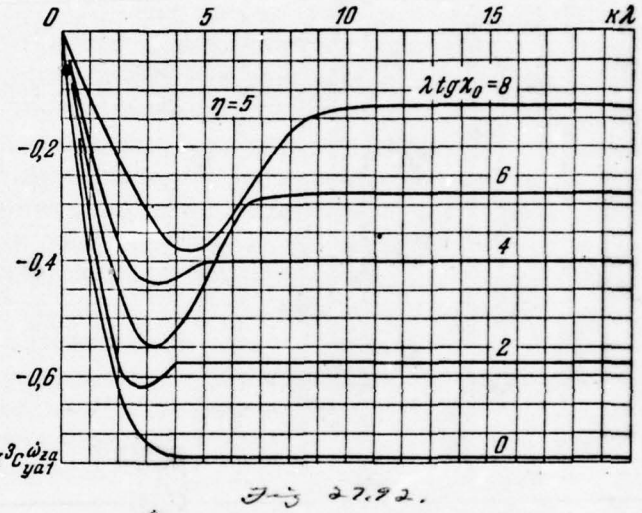


Fig 27.92.

Fig. 27.91. the dependence of derivative $c^{\omega_{za}}_{ya1}$ of the parameters of similarity (M > 1).

Fig. 27.92. Dependence of derivative $c^{\omega_{za}}_{ya1}$ of the parameters of similarity (M > 1).

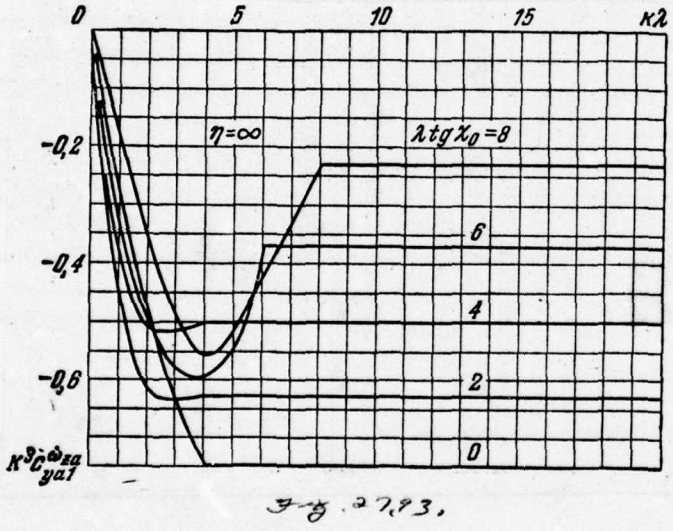


Fig. 27.93.

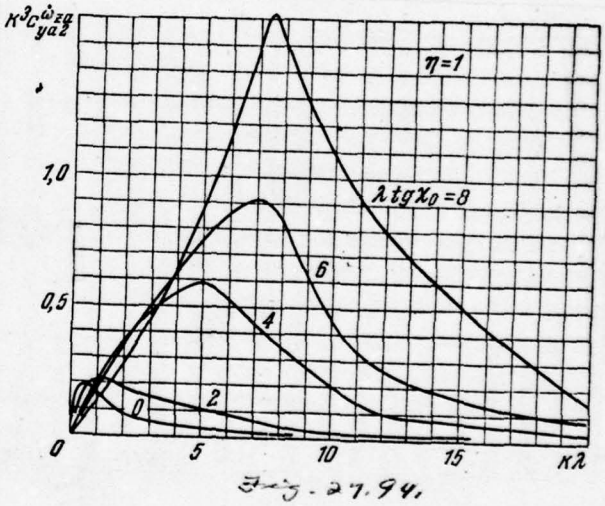


Fig. 27.94.

Fig. 27.93. the dependence of derivative $c^{\dot{\omega}_{za}}_{ya1}$ of the parameters of similarity (M > 1).

Fig. 27.94. Dependence of the derivative $c^{\dot{\omega}_{za}}_{ya2}$ on parameters of similarity (M > 1).

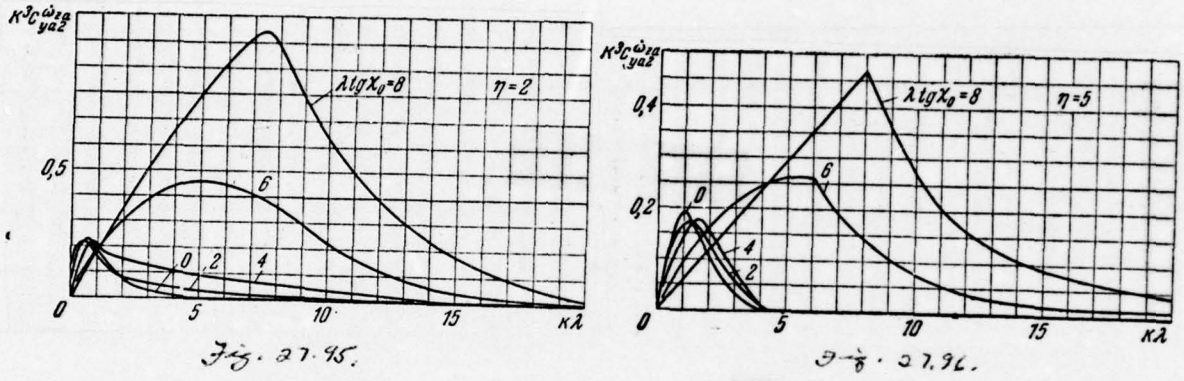


Fig. 27.95. Фиг. 27.96.

Fig. 27.95. the dependence of derivative $c^{\omega_{za}}_{ya2}$ of the parameters of similarity (M > 1).

Fig. 27.96. Dependence of derivative $c^{\omega_{za}}_{ya2}$ of the parameters of similarity (M > 1).

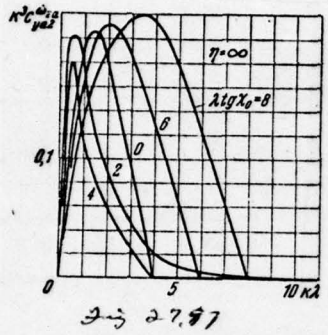


Fig 27.97

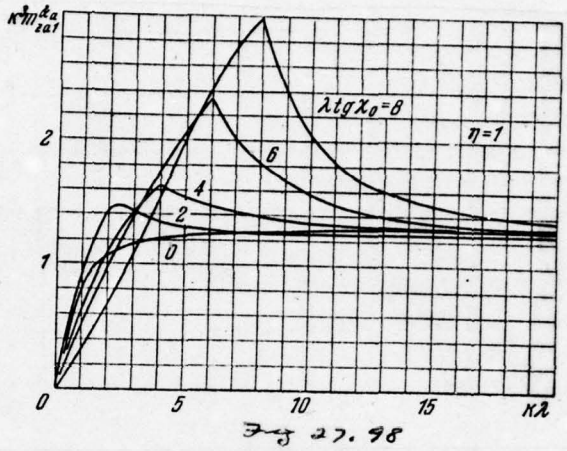
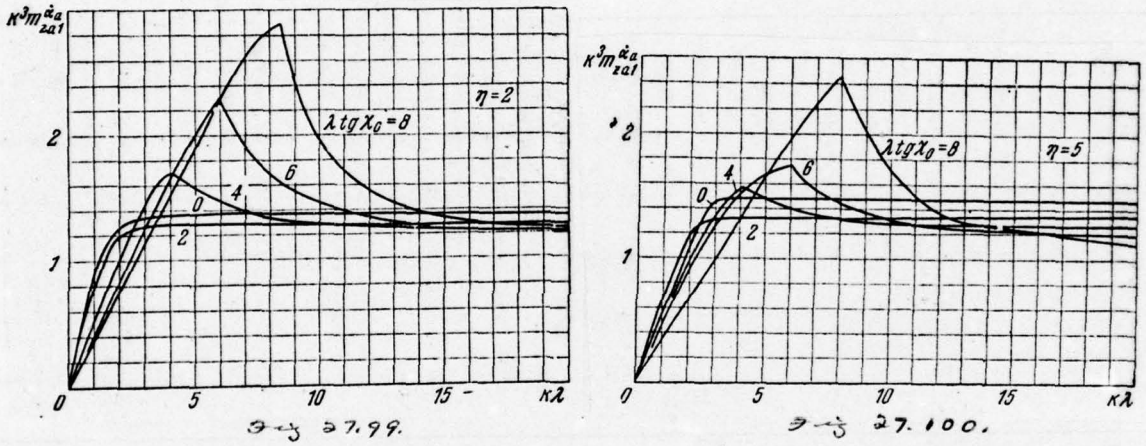


Fig 27.98

Fig. 27.97. Dependence of derivative $\frac{\omega_{za}}{c_{ya2}}$ of the parameters of similarity (M > 1).

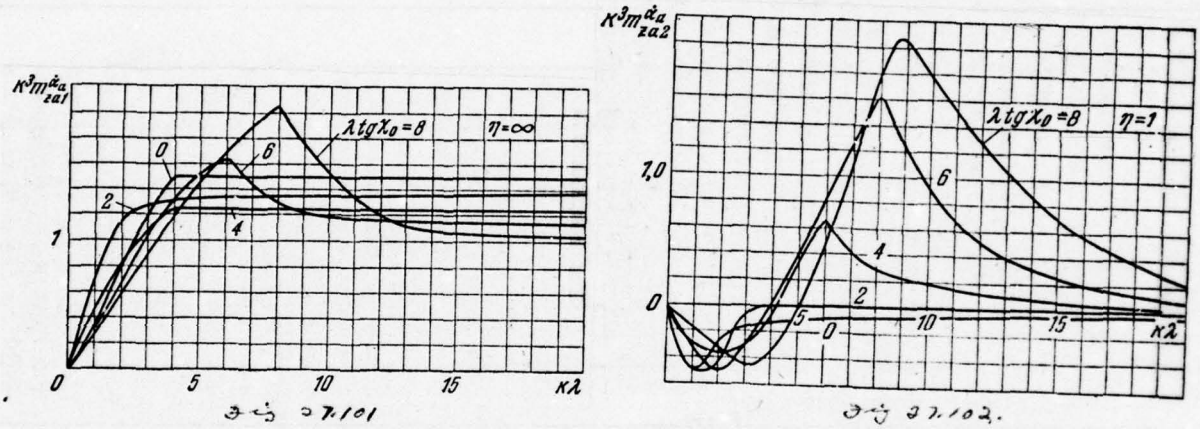
Fig. 27.98. Dependence of derivative $m^{\alpha_a}_{za1}$ of the parameters of similarity (M > 1).



Э-3 27.99. Э-3 27.100.

Fig. 27.99. Dependence of derivative $m^{\dot{\alpha}_a}_{za1}$ of the parameters of similarity (M>1).

Fig. 27.100. the dependence of derivative $m^{\dot{\alpha}_a}_{za1}$ of the parameters of similarity (M>1).



Фиг. 27.101 Фиг. 27.102.

Fig. 27.101. Dependence of derivative $m^{\dot{\alpha}_a}_{za1}$ of the parameters of similarity (M>1).

Fig. 27.102. Dependence of derivative $m^{\dot{\alpha}_a}_{za2}$ of the parameters of similarity (M>1).

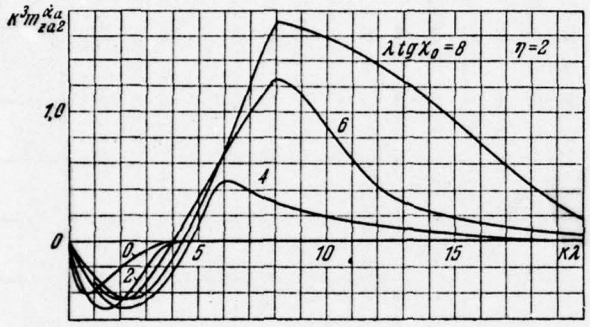


Fig 27.103

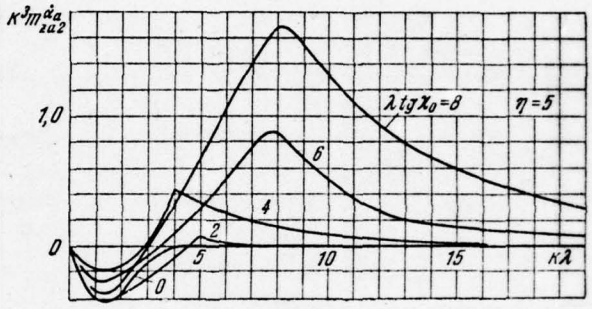
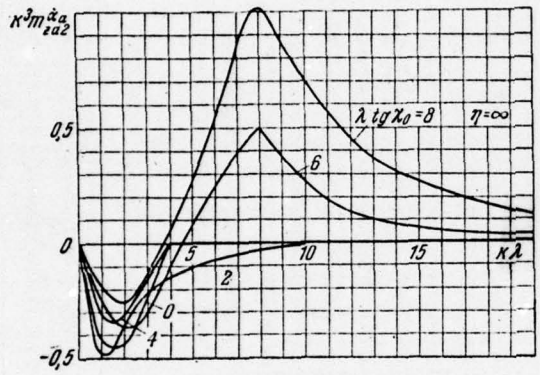


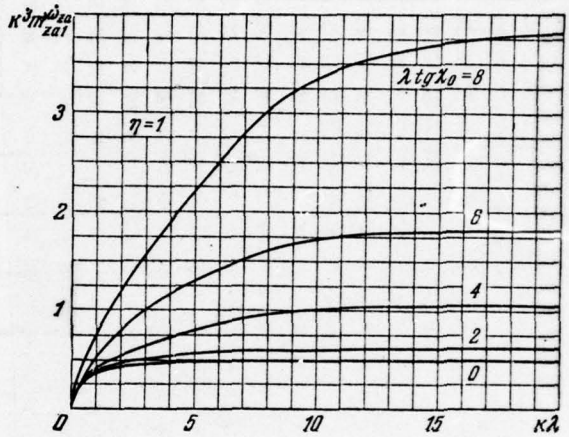
Fig 27.104

Fig. 27.103. Dependence of derivative $m^{\dot{\alpha}_a}_{za2}$ of the parameters of similarity (M>1).

Fig. 27.104. Dependence of derivative $m^{\dot{\alpha}_a}_{za2}$ of the parameters of similarity (M>1).



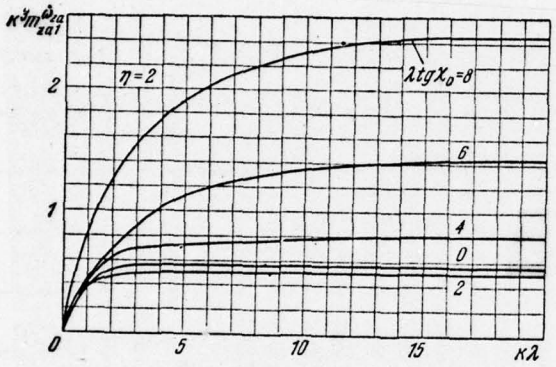
Эд. 27.105.



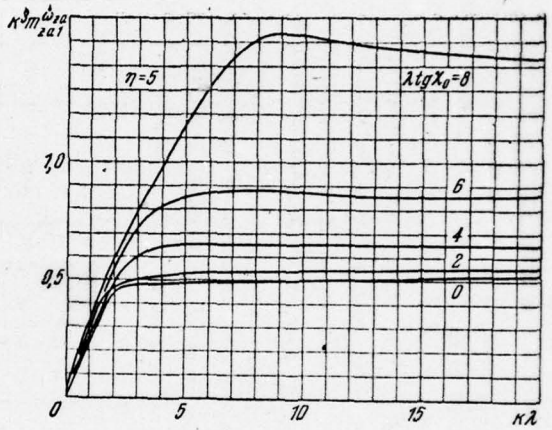
Эд. 27.106.

Fig. 27.105. Dependence of derivative $m^{\dot{\alpha}_a}_{za2}$ of the parameters of similarity (M>1).

Fig. 27.106. the dependence of derivative $m^{\dot{\omega}_{za}}_{za1}$ of the parameters of similarity (M>1).



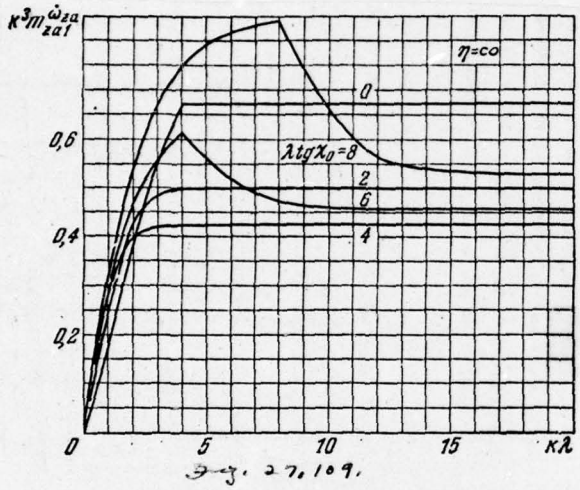
Эз. 27.107.



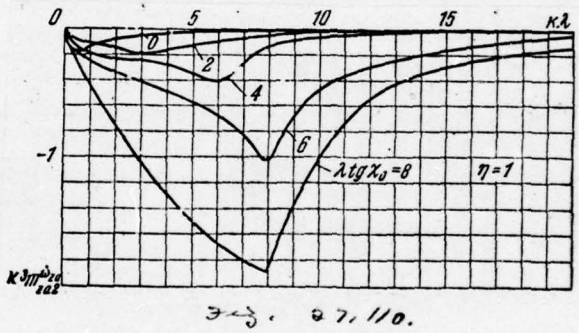
Эз. 27.108.

Fig. 27.107. Dependence of derivative $m^{\omega_{za}}_{zal}$ of the parameters of similarity (M>1).

Fig. 27.108. Dependence of derivative $m^{\omega_{za}}_{zal}$ of the parameters of similarity (M>1).



Фиг. 27.109.

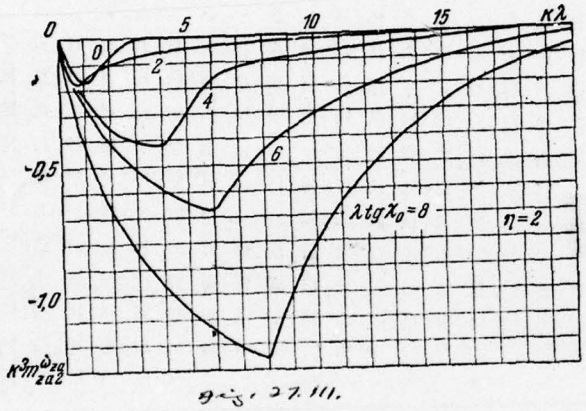


Фиг. 27.110.

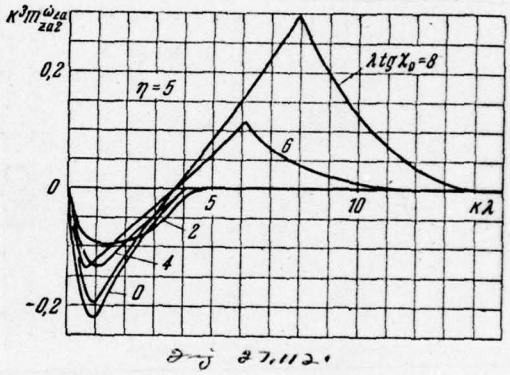
Fig. 27.109. Dependence of derivative $m^{\dot{\omega}_{za}}_{za1}$ of the parameters of similarity (M>1).

Fig. 27.110. Dependence of derivative $m^{\dot{\omega}_{za}}_{za2}$ of the parameters of similarity (M>1).

Page 681.



Фиг. 27.111.



Фиг. 27.112.

Fig. 27.111. Dependence of derivative $m^{\dot{\omega}_{za}}_{za2}$ of the parameters of similarity (M>1).

Fig. 27.112. Dependence of derivative $m^{\dot{\omega}_{za}}_{za2}$ of the parameters of similarity (M>1).

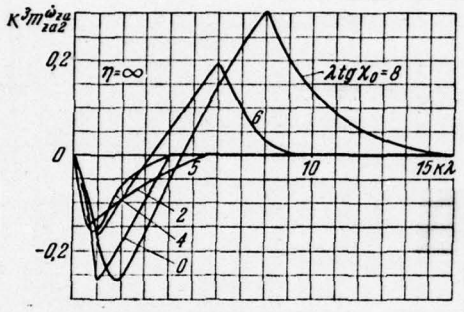


Fig 27.113.

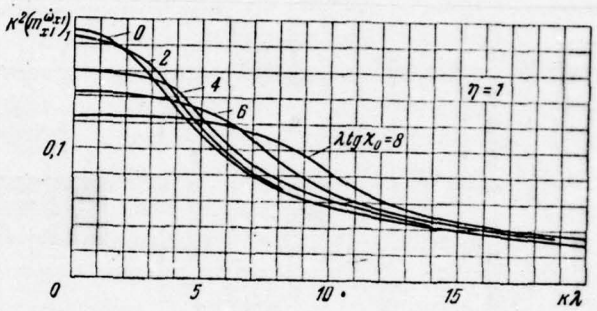
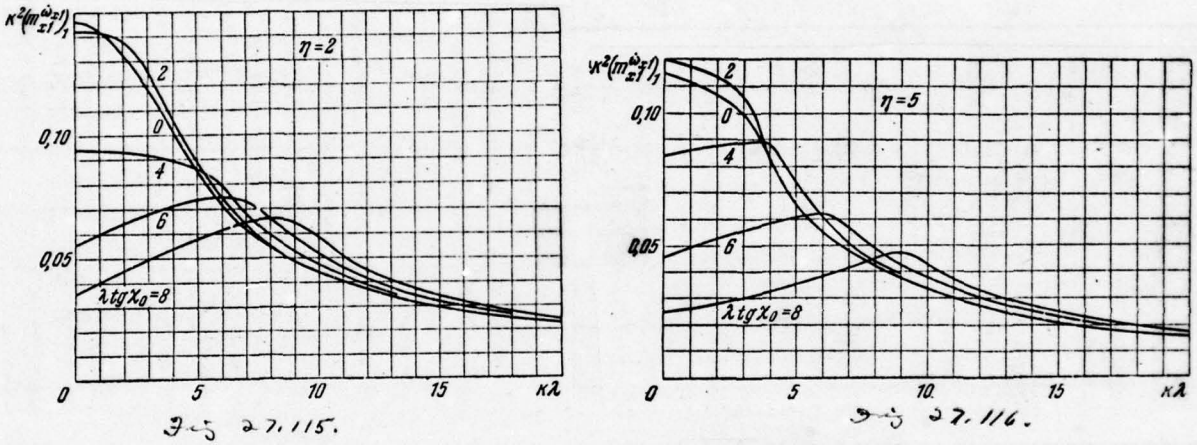


Fig. 27.114

Fig. 27.113. Dependence of derivative $m^{\dot{\omega}_{za}}_{za^2}$ of the parameters of similarity (M>1).

Fig. 27.114. Dependence of derivative $\left(m^{\dot{\omega}_{x1}}_{x1}\right)_1$ of the parameters of similarity (M>1).

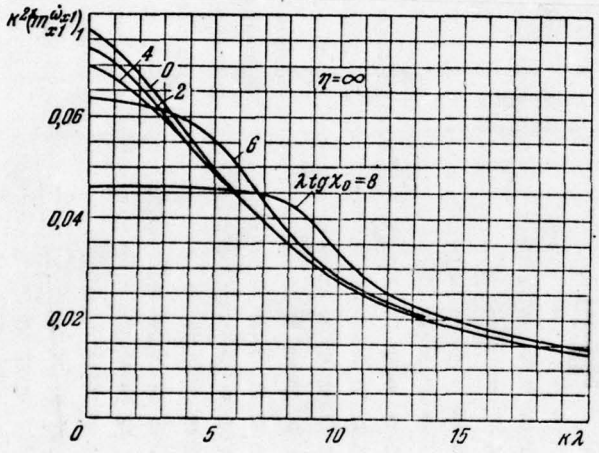


Э-5 27.115. Э-5 27.116.

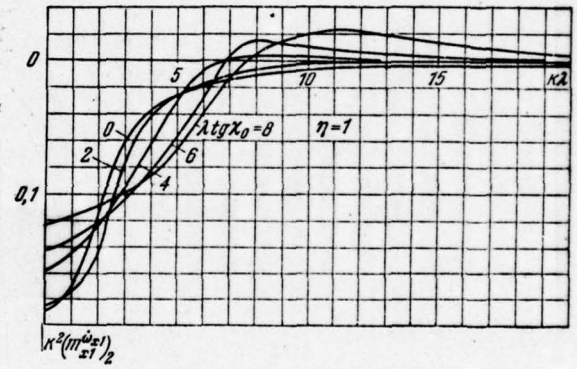
Fig. 27.115. Dependence of derivative $\left(m_{x1}^{\bar{\omega}_{x1}}\right)_1$ of the parameters of similarity (M>1).

Fig. 27.116. Dependence of derivative $\left(m_{x1}^{\bar{\omega}_{x1}}\right)_1$ of the parameters of similarity (M>1).

Page 683.



Фиг. 27.117.

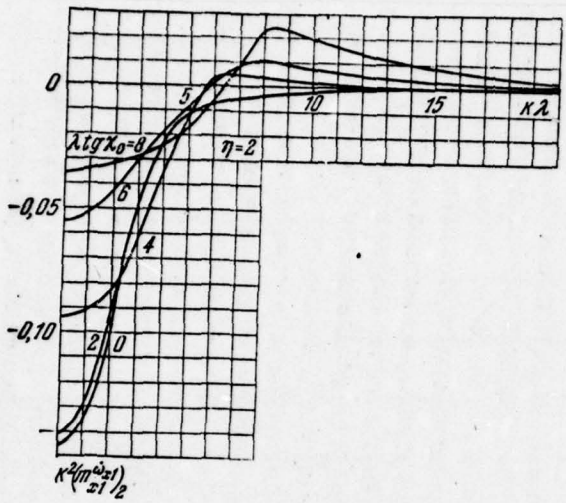


Фиг. 27.118.

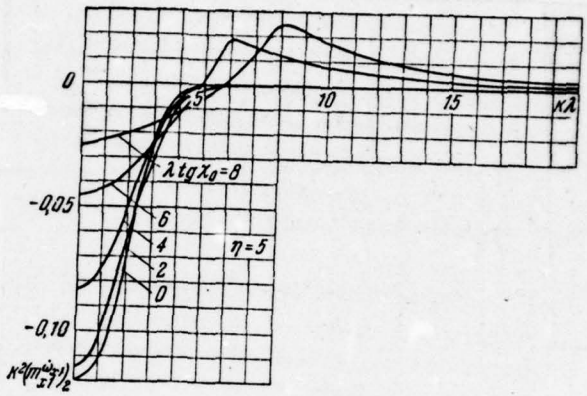
Fig. 27.117. Dependence of derivative $\left(m_{x1}^{\dot{\omega}_{x1}}\right)_1$ of the parameters of similarity (M>1).

Fig. 27.118. Dependence of derivative $\left(m_{x1}^{\dot{\omega}_{x_1}}\right)_2$ of the parameters of similarity (M>1).

Page 684.



Эд. 27.119.



Эд. 27.120.

Fig. 27.119. Dependence of derivative $\left(m^{\omega}_{x1}\right)_2$ of the parameters of similarity (M>1).

Fig. 27.120. Dependence of derivative $\left(m^{\omega}_{x1}\right)_2$ of the parameters of similarity (M>1).

Page 685.

All the obtained from the calculation coefficients of

aerodynamic derivatives (Fig. 27.62-27.121) are given in the standard, connected with wing coordinate system and are related to centering $\bar{x}_{b_a}=0$ (axis Oz it passes through the leading edge of the mean aerodynamic chord of wing b_a). Let us note that the designed versions contain wings with subsonic and supersonic leading and trailing wing edges with constant sweepback [see conditions (27.9) - (27.11)].

§5. Example of the calculation.

Let us examine the triangular rigid wing of lengthening $\lambda = 2.5$. Let us find the coefficients of apparent additional masses $(k_{22})_a$, $(k_{26})_a$, $(k_{66})_a$, $(k_{44})_a$. For this wing from table 27.1 we obtain;

$(k_{22})_a = 0{,}4967$, $(k_{26})_a = -0{,}2054$, $(k_{66})_a = 0{,}1071$, $(k_{44})_a = -0{,}0122$.

During the determination of the coefficients of aerodynamic derivatives let us examine two subsonic mode/conditions: $M = 0$ and $M = 0{,}8$ - even three supersonic mode/conditions; $M = 1{,}28$ (wing with subsonic leading and supersonic trailing edges is a condition (27.10)); $M = 1{,}9$ (wing with sonic edges - condition $k\lambda = 4$); $M = 2{,}28$ (wing with supersonic leading and trailing edges is a condition (27.9)).

Incompressible medium, $M=0$, $k=1$

From table 27.2 we obtain: $c_y^{\alpha}=2{,}5585$, $c_{ya}^{\omega_{za}}=2{,}1142$, $m_{za}^{\alpha}=$ $-0{,}9440$, $m_{za}^{\omega_{za}}=-1{,}099$, $m_{x1}^{\omega_{x1}}=-0{,}1827$.

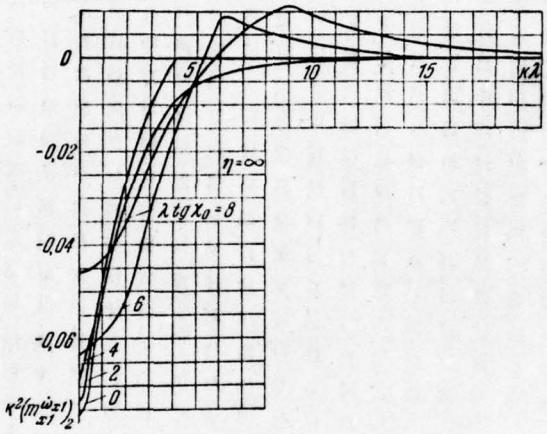


Fig. 27.121. dependence of derivative $\left(m_{x1}^{\dot{\omega}_{x1}}\right)_2$ of the parameters of similarity (M>1).

Page 686.

With $M=0$ we have $M^2c_{ya2}^{\dot{\alpha}_a}=0$, $M^2m_{za2}^{\dot{\alpha}_a}=0$, $M^2\left(m_{x1}^{\dot{\omega}_{x1}}\right)_2=0$, therefore for

the incompressible medium are determined the only coefficients of aerodynamic derivatives with points with the index

1: $c_{ya}^{\dot{\alpha}_a} = 0{,}5055$, $c_{ya}^{\bar{\omega}_{za}} = 0{,}1193$, $m_{za}^{\bar{\omega}_{za}} = -0{,}1118$, $m_{xl}^{\bar{\omega}_{xl}} = -0{,}0379$, $m_{za}^{\dot{\alpha}_a} = -0{,}2418$.

Subsonic velocity, $M = 0{,}8$, $k = 0{,}6$

For the mode/conditions being investigated the parameter of similarity $k\lambda = 1.5$; therefore it is possible to utilize immediately the tabulated data $kc_y^{\alpha} = 1{,}7920$,

$kc_{ya}^{\bar{\omega}_{za}} = 1{,}5408$, $km_{za}^{\alpha} = -0{,}7075$, $km_{za}^{\bar{\omega}_{za}} = -0{,}8459$, $km_{xl}^{\bar{\omega}_{xl}} = -0{,}1238$, $k^3 c_{ya1}^{\dot{\alpha}_a} = 0{,}5758$, $k^3 c_{ya2}^{\dot{\alpha}_a} = -0{,}8322$, $k^3 c_{ya1}^{\bar{\omega}_{za}} = 0{,}2685$, $k^3 c_{ya2}^{\bar{\omega}_{za}} = -0{,}5326$, $k^3 m_{za1}^{\dot{\alpha}_a} = -0{,}2694$, $k^3 m_{za2}^{\dot{\alpha}_a} = 0{,}3359$, $k^3 m_{za1}^{\bar{\omega}_{za}} = -0{,}1628$, $k^3 m_{za2}^{\bar{\omega}_{za}} = 0{,}2473$, $k^2 \left(m_{xl}^{\bar{\omega}_{xl}}\right)_1 = -0{,}0518$, $k^2 \left(m_{xl}^{\bar{\omega}_{xl}}\right)_2 = 0{,}0594$.

Utilizing formulas (27.6) and bearing in mind that $k^2 = 0.36$, $k^3 = 0.216$, $M^2 = 0{,}64$, we will obtain: $c_y^{\alpha} = 2{,}99$, $c_{ya}^{\bar{\omega}_{za}} = 2{,}57$, $m_{za}^{\alpha} = -1{,}18$, $m_{za}^{\bar{\omega}_{za}} = -1{,}41$, $m_{xl}^{\bar{\omega}_{xl}} = -0{,}206$, $c_y^{\dot{\alpha}_a} = 0{,}1945$, $c_{ya}^{\bar{\omega}_{za}} = -0{,}332$, $m_{za}^{\dot{\alpha}_a} = 0{,}2545$, $m_{za}^{\bar{\omega}_{za}} = -0{,}0208$, $m_{xl}^{\bar{\omega}_{xl}} = 0{,}0375$.

Supersonic speed, $M = 1{,}28$, $k = 0{,}8$

From table 27.4 for the parameter of similarity $k\lambda = 2.0$ we have:

$kc_y^{\alpha} = 2{,}594$, $kc_{ya}^{\omega_{za}} = 1{,}791$, $km_{za}^{\alpha} = -1{,}297$, $km_{za}^{\omega_{za}} = -1{,}281$, $km_{x1}^{\omega_{x1}} = -0{,}192$, $k^3 c_{ya1}^{\dot{\alpha}_a} = -1{,}297$, $k^3 c_{ya2}^{\dot{\alpha}_a} = 0{,}4936$, $k^3 c_{ya1}^{\dot{\omega}_{za}} = -0{,}5093$, $k^3 c_{ya2}^{\dot{\omega}_{za}} = 0{,}0600$, $k^3 m_{za1}^{\dot{\alpha}_a} = 0{,}8106$, $k^3 m_{za2}^{\dot{\alpha}_a} = -0{,}3085$, $k^3 m_{za1}^{\dot{\omega}_{za}} = 0{,}4052$, $k^3 m_{za2}^{\dot{\omega}_{za}} = -0{,}0602$, $k^2 \left(m_{x1}^{\dot{\omega}_{x1}}\right)_1 = 0{,}095$, $k^2 \left(m_{x1}^{\dot{\omega}_{x1}}\right)_2 = 0$.

Taking into account relationship/ratio (27.6) and values $k^2 = 0.64$, $k^3 = 0.512$, $M^2 = 1{,}64$, we find: $c_y^{\alpha} = 3{,}24$, $c_{ya}^{\dot{\omega}_{za}} = 2{,}24$, $m_{za}^{\alpha} = -1{,}622$, $m_{za}^{\omega_{za}} = -1{,}603$, $m_{x1}^{\omega_{x1}} = -0{,}24$, $c_{ya}^{\dot{\alpha}_a} = -0{,}952$, $c_{ya}^{\dot{\omega}_{za}} = -0{,}802$, $m_{za}^{\dot{\alpha}_a} = 0{,}601$, $m_{za}^{\dot{\omega}_{za}} = 0{,}6$, $m_{x1}^{\dot{\omega}_{x1}} = 0{,}148$.

Supersonic speed, $M = 1{,}9$, $k = 1{,}615$

For the parameter of similarity $k\lambda \approx 4.0$ of table 27.4 we have:

$kc_y^{\alpha} = 4{,}0$, $kc_{ya}^{\omega_{za}} = 2{,}0$, $km_{za}^{\alpha} = -2{,}0$, $km_{za}^{\omega_{za}} = -1{,}5$, $km_{x1}^{\omega_{x1}} = -0{,}334$, $k^3 c_{ya}^{\dot{\alpha}_a} = -2{,}0$, $k^3 c_{ya1}^{\dot{\omega}_{za}} = 0{,}5$, $k^3 m_{za1}^{\dot{\alpha}_a} = 1{,}25$, $k^3 m_{za1}^{\dot{\omega}_{za}} = 0{,}425$, $k^2 \left(m_{x1}^{\dot{\omega}_{x1}}\right)_1 = 0{,}0666$.

All coefficients with points for index 2 are equal to zero. Taking into account of formula (27.6) and of value $k^2 = 2.61$, $k^3 = 4.28$, $M^2 = 3{,}61$, we obtain:

$c_y^{\alpha}=2{,}49$, $c_{ya}^{\omega_{za}}=1{,}245$, $m_{za}^{\alpha}=-1{,}245$,
$m_{a}^{\omega_{za}}=-0{,}932$, $m_{x1}^{\omega_{x1}}=-0{,}207$, $c_{ya}^{\dot{\alpha}_a}=-0{,}478$, $c_{ya}^{\bar{\omega}_{za}}=-0{,}1195$,
$m_{a}^{\dot{\alpha}_a}=0{,}3$, $m_{za}^{\bar{\omega}_{za}}=0{,}102$, $m_{x1}^{\bar{\omega}_{x1}}=0{,}0256$.

Page 687.

Supersonic speed, $M=2{,}24$, $k=2$

For this mode/conditions the parameter of similarity $k\lambda = 5$; therefore from table 27.4 are obtained the same values $kc_{ya}^{q_a}$, $km_{za}^{q_a}$, $km_{x1}^{\omega_{x1}}$, $k^3c_{ya}^{\dot{q}_a}$, $k^3m_{za}^{\dot{q}_a}$, $k^2m_{x1}^{\dot{\omega}_{x1}}$, that also for the preceding/previous case ($k\lambda \approx 4$). Thus, taking into account relationship/ratio (27.6) and values $k^2 = 4$, $k^3 = 8$, $M^2=5$, we obtain: $c_y^{\alpha}=2{,}0$, $c_{ya}^{\omega_{za}}=1$, $m_{za}^{\alpha}=-1$,
$m_{za}^{\omega_{za}}=-0{,}75$, $m_{x1}^{\omega_{x1}}=-0{,}167$, $c_{ya}^{\dot{\alpha}_a}=-0{,}25$, $c_{ya}^{\bar{\omega}_{za}}=-0{,}0625$,
$m_{za}^{\dot{\alpha}_a}=0{,}1563$, $m_{za}^{\bar{\omega}_{za}}=0{,}532$, $m_{x1}^{\bar{\omega}_{x1}}=0{,}0167$.

Let us note that for all examined mode/conditions it was assumed that the origin of coordinates is located in the leading edge/nose of the mean aerodynamic chord of wing $b_a(\bar{x}_{b_a}=0)$. For characteristic linear dimension is undertaked the value of the mean aerodynamic chord b_a. The recalculation of the coefficients of aerodynamic derivatives for another centering (with the same linear dimension b_a) is made on the basis of relationship/ratios (27.8).

Chapter XXVIII.

SOME COMMON PROPERTIES OF UNSTEADY CHARACTERISTICS. EFFECT OF PLANFORM, NUMBERS M AND p* ON THE AERODYNAMIC DERIVATIVES OF WINGS.

§1. Properties of unsteady characteristics, which escape/ensue from the analysis of common/general/total relationship/ratios.

Most completely and concrete/specific/actually the special feature/peculiarity of unsteady aerodynamic wing characteristics will be studied further by means of the interpretation of results of systematic numerical calculations. However, this analysis possesses the determined limitedness, since it is cabled only to specific characteristics and wings; in this case usually it is important to supplement it by the common/general/total conclusion/derivations, which escape/ensue from the mathematical setting of the boundary-value problem: by limited solutions, by precise

relationship/ratios, and also the physical considerations, which escape/ensue from the essence of the studied phenomena.

First of all let us turn to precise relationship/ratios, obtained in chapter VI on the basis of Duhamel integral. There it was shown, that the momentum/impulse/pulse of the unsteady part of any transient function (total or distributed characteristic) was equal to the value of the corresponding coefficient of aerodynamic derivative with point with Strouhal number, vanishing, namely:

$$\left.\begin{aligned} c^{q_i}|_{p^*\to 0} &= \int_0^\infty [A_{q_i}(\tau) - A_{q_i}(\infty)]\,d\tau + 2\mu k_{q_i}, \\ \mu = 0 \overset{(1)}{\text{при}}\ M \neq 0 &\overset{(2)}{\text{и}}\ \mu = 1 \overset{(1)}{\text{при}}\ M = 0. \end{aligned}\right\} \qquad (28.1)$$

Key: (1). with. (2). and.

Hence, by the way, it follows that with the equalization of transient functions the absolute values of the coefficients of aerodynamic derivatives with point with $p^* \longrightarrow 0$ decrease, turning within limit into zero for the compressed medium and striving to $2k_{q_i}$ for incompressible.

Page 689.

All coefficients of aerodynamic derivatives with points during the unlimited increase in Strouhal number ($p^* \longrightarrow \infty$) in the compressed medium vanish. In the incompressible medium with $p^* \longrightarrow \infty$

they approach the doubled value of the corresponding coefficient of apparent additional mass. For the total characteristics, for example, we have with $M = 0$

$$\left.\begin{aligned} &c_y^{\alpha}(\infty) = 2k_{22}, \qquad m_z^{\alpha}(\infty) = 2k_{26}, \\ &c_y^{\bar{\omega}_z}(\infty) = -2k_{26}, \quad m_z^{\bar{\omega}_z}(\infty) = -2k_{66}, \quad m_{x1}^{\bar{\omega}_{x1}}(\infty) = -2k_{44}. \end{aligned}\right\} \tag{28.2}$$

These asymptotic formulas show that with an increase of Strouhal number during passage from $M = 0$ to $M \neq 0$ occurs ever sharper, more intense change in the coefficients of aerodynamic derivatives. In other words, during an increase in Strouhal number p^* the compressibility effect of the medium on these derivatives increases, which is exhibited especially strongly with small numbers M.

In chapter IV it was shown, that the limiting values of transient functions at zero time $\tau \longrightarrow 0$, when occurs an abrupt change in the boundary conditions, are equal to the appropriate coefficients of aerodynamic derivatives without points with Strouhal number $p^* \longrightarrow \infty$. Thus, with any M we have, for example, for the total characteristics

$$\left.\begin{aligned} &c_y^{\alpha}(\infty) = \left[\frac{c_y(0)}{\alpha^*}\right], \quad m_z^{\alpha}(\infty) = \left[\frac{m_z(0)}{\alpha^*}\right], \\ &c_y^{\omega_z}(\infty) = \left[\frac{c_y(0)}{\omega_z^*}\right], \quad m_z^{\omega_z}(\infty) = \left[\frac{m_z(0)}{\omega_z^*}\right], \\ &m_{x1}^{\omega_{x1}}(\infty) = \left[\frac{m_{x1}(0)}{\omega_{x1}^*}\right]. \end{aligned}\right\} \tag{28.3}$$

In the incompressible medium $(M = 0)$ under the value of transient

function with $\tau \longrightarrow 0$ is understood the finite quantity, which corresponds to the regular part transiently of function.

On the other hand, the limiting values of transient functions at values τ, when transient process ended (at subsonic speeds this will be with $\tau \longrightarrow \infty$), are equal to the coefficients of aerodynamic derivatives without points with $p^* \longrightarrow 0$. If are studied the total characteristics, then these relationship/ratios take the form

$$\left.\begin{aligned} c_y^{\alpha}(0) &= \left[\frac{c_y(\infty)}{\alpha^*}\right], \quad m_z^{\alpha}(0) = \left[\frac{m_z(\infty)}{\alpha^*}\right], \\ c_y^{\omega_z}(0) &= \left[\frac{c_y(\infty)}{\omega_z^*}\right], \quad m_z^{\omega_z}(0) = \left[\frac{m_z(\infty)}{\omega_z^*}\right], \\ m_{x1}^{\omega_{x1}}(0) &= \left[\frac{m_{x1}(\infty)}{\omega_{x1}^*}\right]. \end{aligned}\right\} \qquad (28.4)$$

Page 690.

In such a manner, as is evident from (28.3) and (28.4), the finite values of transient functions are equal to the values of the coefficients of aerodynamic derivatives without points with $p^* = 0$, [illegible], and initial values - to the values of the coefficients of aerodynamic derivatives without points with $p^* = \infty$.

From the given formulas it follows that small changes in the coefficients of aerodynamic derivatives in terms of Strouhal numbers and the stable behavior of transient functions in terms of

dimensionless time τ closely related with each other. The lesser the dependence of the coefficients of aerodynamic derivatives of Strouhal number, that nearer to the constant value of transient function. If transient functions are constant, then of the formulas of chapter VI it follows that the coefficients of aerodynamic derivatives without points are constant, and the coefficients of aerodynamic derivatives with points turn in the compressed medium into zero (in the incompressible medium these coefficients will be equal to the doubled coefficients of the corresponding apparent additional masses).

Earlier, in chapter IV, were derived precise values of transient functions with $\tau \longrightarrow 0$ in the compressed medium:

$$\left.\begin{aligned}
&\left[\frac{c_y(0)}{\alpha^*}\right]=\frac{4}{M},\quad \left[\frac{m_z(0)}{\alpha^*}\right]=-\frac{4}{M}\lambda\frac{b}{l}\int_0^1\int_{\bar{x}_0}^{\bar{x}_1}\bar{x}\,d\bar{x}\,d\bar{z},\\
&\left[\frac{c_y(0)}{\omega_z^*}\right]=\frac{4}{M}\lambda\frac{b}{l}\int_0^1\int_{\bar{x}_0}^{\bar{x}_1}\bar{x}\,d\bar{x}\,d\bar{z},\\
&\left[\frac{m_z(0)}{\omega_z^*}\right]=-\frac{4}{M}\lambda\frac{b}{l}\int_0^1\int_{\bar{x}_0}^{\bar{x}_1}\bar{x}^2\,d\bar{x}\,d\bar{z},\\
&\left[\frac{m_{x1}(0)}{\omega_{x1}^*}\right]=-\frac{2}{M}\lambda\frac{b}{l}\int_0^1\int_{\bar{x}_0}^{\bar{x}_1}\bar{z}^2\,d\bar{x}\,d\bar{z}.
\end{aligned}\right\}\qquad(28.5)$$

Formulas for the calculation of the total wing characteristics of simple planform with the direct/straight edges, which are characterized by lengthening λ, by contraction η and by the constant sweepback of leading edge χ_0, are given in chapter of XXII

[formula (22.34)].

The values of the coefficients aerodynamic derivative these wings with the sufficiently large M, when leading and trailing edges become supersonic, are determined by relationship/ratios (26.35). With sufficiently large M we have

$$\sqrt{M^2-1}\to M$$

and formulas (26.35) for the coefficients of aerodynamic derivatives without points they convert to formulas (20.52).

Page 691.

From the aforesaid it follows that with an increase $M>1$ the transient functions will be increasingly less changed in τ, approaching steady-state values in all range τ, and the dependence of the coefficients of aerodynamic derivatives of p^* will decrease, whereupon the coefficients of aerodynamic derivatives with points will vanish.

§2. Properties of unsteady characteristics, which escape/ensue from common/general/total physical considerations.

First of all let us give the qualitative explanation, when one should expect the larger compressibility effect of the medium during the unsteady motion of wing. The compressibility of the medium it is exhibited the more powerful, the greater the supplementary (agitated) pressure p in comparison with pressure in the undisturbed medium p_∞.

Since

$$\frac{q_\infty}{p_\infty} = \frac{\rho_\infty U_0^2}{2p_\infty} = \frac{\varkappa}{2} M^2, \tag{28.6}$$

then

$$\frac{p'}{p_\infty} = \frac{\varkappa}{2} M^2 \bar{p}, \quad \bar{p} = \frac{p'}{p_\infty}.$$

The dimensionless coefficient of pressure $\bar{p}$ with the accuracy, accepted in linear theory, according to the Cauchy integral of - Lagrange (3.17) is as follows connected with the potential of the disturbed speeds in the standard axes:

$$\bar{p} = \frac{2}{U_0^2}\left(U_0 \frac{\partial \varphi}{\partial x} - \frac{\partial \varphi}{\partial t}\right).$$

Let us introduce dimensionless quantities, after assuming

$$\varphi = U_0 b \bar{\varphi}, \quad \xi = \frac{x}{b}, \quad \tau = \frac{U_0 t}{b}; \tag{28.7}$$

then

$$\bar{p} = 2\left(\frac{\partial \bar{\varphi}}{\partial \xi} - \frac{\partial \bar{\varphi}}{\partial \tau}\right). \tag{28.8}$$

If dependence on τ is harmonic, then

$$\bar{\varphi}(\bar{x}, \bar{y}, \bar{z}, \tau) = \varphi_1(\xi, \eta, \zeta)\cos p^*\tau + \varphi_2(\xi, \eta, \zeta)\sin p^*\tau,$$

whence

$$\bar{p} = 2\left(\frac{\partial\bar{\varphi}_1}{\partial\xi}\cos p^*\tau + \frac{\partial\varphi_2}{\partial\xi}\sin p^*\tau + \bar{\varphi}_1 p^*\sin p^*\tau - \bar{\varphi}_2 p^*\cos p^*\tau\right). \quad (28.9)$$

Page 692.

From (28.6) and (28.8) follows that the compressibility of the medium (effect of number M) will be exhibited, generally speaking, the more powerful, the greater the absolute values of derivatives $\bar{\varphi}$ and ξ and τ. With harmonic time dependences according to (28.9) an increase in number p * leads to the amplification of the effect indicated. From (28.6) it is evident that with identical p * the compressibility of the medium will manifest itself more powerful the large M.

Let us note that of the wing of very small lengthening the dependence of velocity potential φ on ξ is insignificant. To an increase in the absolute value $\partial\bar{\varphi}/\partial\xi$ contribute an increase in the wing aspect ratio, an increase common/general/total or local angles of attack, etc. Absolute value $\partial\bar{\varphi}/\partial\tau$ is directly

connected with those changes, which undergo boundary conditions on body. Abrupt changes in the latter lead to considerable change $\partial\bar{\varphi}/\partial\tau$.

It must be noted that during an instantaneous stepped variation in the boundary conditions at zero time ($\tau \longrightarrow 0$) the transient functions undergo I will eat more substantial changes in τ, than less number M. By this is explained considerable effect M on all the characteristics near $M = 0$ during abrupt changes q_i, and also at the values of the coefficients of aerodynamic derivatives with p * → ∞.

Near the end/faces of wing at positive angles of attack occurs the overflowing of flow from pressure side of wing (where the pressure in essence is raised) to upper. The lesser the lengthening, the greater the specific gravity/weight of end overflowing. This, in particular, lowers airfoil lift during a decrease in its lengthening λ. The lesser the lengthening, the weaker the compressibility effect of the medium, i.e., the lesser the effect of number M. This is connected with the fact that, other conditions being equal, of the disturbance/perturbations, caused by wing, the weaker, the lesser the lengthening. At the low values of lengthening the effect of the sweep angle χ_0 and of contraction η it is small with all numbers M. This is explained by the facts that with small λ even the considerable change χ_0 and η has little effect on wing planform.

The reasons for the deviation of precise data from those which were obtained with the aid of stability hypothesis (and even the expanded stability hypothesis, in which correctly are considered the local angles of attack in statics) they consist in the following. A change of flight conditions is accompanied by a change in the local angles of attack and loads. This leads to a circulation control of the speed in this place that in the ideal medium must be accompanied by descent and escape of free vortices. According to the theorems about conservation of circulation, the total circulation on the locked liquid duct must remain constant/invariable in time.

Thus, unsteady flow is accompanied by continuous motion along wing and by the descent from it of transverse transient vortices (their axes are directed along spread/scope). They cause additional tapers on wing, change loads on it and so forth.

Page 693.

The appearance of coefficients of aerodynamic derivatives with points closely related with the effect of the eddy/vortices indicated. Moreover, if $p^* \longrightarrow 0$, then circulations in the parameters with points are located from the condition of the compensation for the tapers, caused by transverse (purely unsteady) free vortices. The greater the lengthening, the greater the total

spread/scope of these eddy/vortices and the more powerful their effect at subsonic speeds. With supersonic speeds and trailing supersonic edges an effect have the only unsteady transverse eddy/vortices, which go over wing. If trailing edges have subsonic sections, wing affects only the corresponding section of vortex sheet after wing. With $M > 1$ and supersonic edges the flow about the section $z =$ const affects the only part of the wing, which lies within reverse/inverse Mach cone (it on Fig. 28.1 is shaded). The more M, the less the mach angle (already shaded part). In this case decreases the spread/scope of free vortices, which affect characteristics in this section.

Give in the preceding/previous and this paragraphs of consideration make it possible to examine in general terms the effect of the wing aspect ratio and Mach number on transient functions and the coefficients of aerodynamic derivatives. At subsonic speeds transient process continues infinitely for long, at supersonic speeds it concludes in finite time. Independent of lengthening λ, when $\tau \to 0$, $[c_y/\alpha^*] \to 4/M$ of low-aspect-ratio wing transient functions for all τ, except $\tau \longrightarrow 0$, will weakly depend on τ. Therefore with different λ and M they take the form, depicted on Figs. 28.2 and 28.3.

Let us pass with the aid of Duhamel integral to the coefficients

of aerodynamic derivatives. We will obtain the result, depicted on Figs. 28.4 and 28.5 for c_y^a and on Fig. 28.6 for $c_y^{\dot{a}}$. Let us note that with a decrease in the wing aspect ratio increases the range of Strouhal numbers, in whom the coefficients of aerodynamic derivatives without points weakly depend on p *. Within the limit, when $\lambda \longrightarrow 0$, derivative c_y^a is not depend on Strouhal numbers with final p * and equal to 4/M with p * = ∞. The coefficients of aerodynamic derivatives with points the faster turn into zero, the lesser lengthening λ (Fig. 28.6).

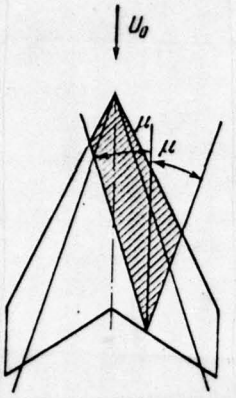


Fig. 28.1. Determination of ranges of integration with M>1.

Page 694.

Let us note also that the dependence of aerodynamic derivatives $c^{q_i}|_{p^*\to 0}$ of the different parameters indicates the role of purely unsteady characteristics at the different values of these parameters. For harmonic time dependences and low values of Strouhal number these coefficients, as already mentioned, they have purely unsteady nature. With harmonic time dependences, according to the theorem about momentum/impulse/pulses, the coefficient with point with $p^* \to 0$ is equal to momentum/impulse/pulse from the appropriate transient function and integral characterizes the role of unsteady phenomena.

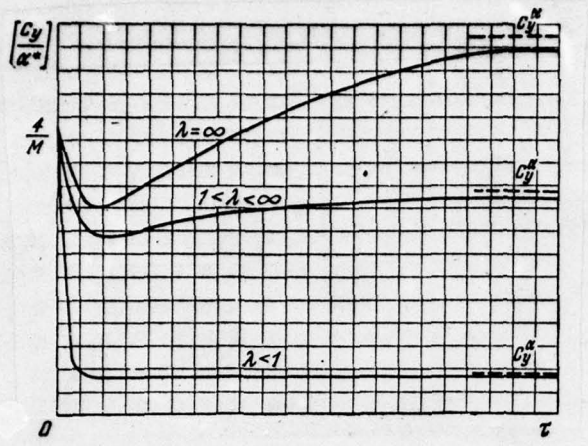


Fig. 28.2. Transient function $[c_y/\alpha^\circ]$ **in subsonic range** $(0<M<1)$.

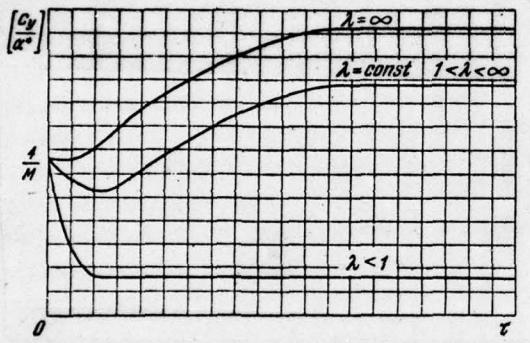


Fig. 28.3. Transient function $[c_y/\alpha^\circ]$ **in supersonic range** $(M>1)$.

Page 695.

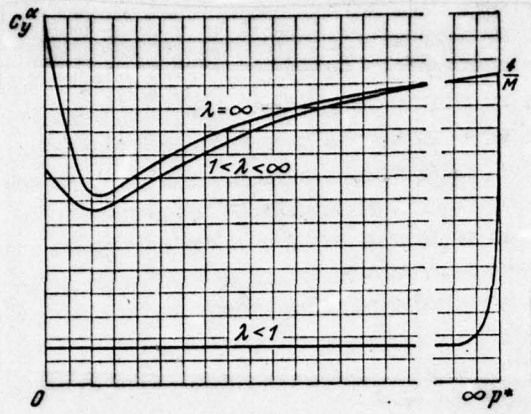


Fig. 28.4. Derivative c_y^α in subsonic range $(0<M<1)$.

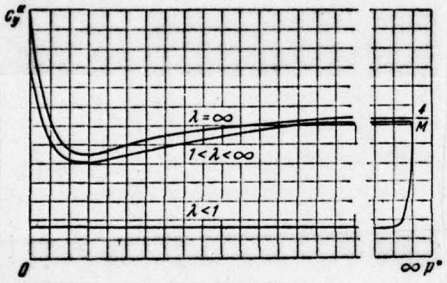


Fig. 28.5.

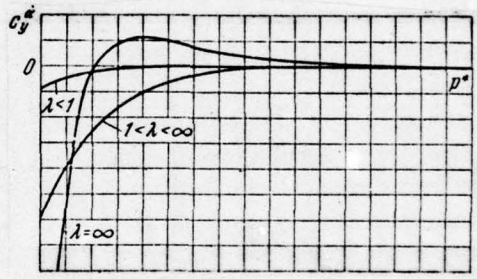


Fig. 28.6.

Fig. 28.5. Derivative c_y^α in supersonic range $(M>1)$.

Fig. 28.6. Derivative c_y^α in the compressed medium $(M>0)$.

§3. Effect of geometric parameters and Mach number on the aerodynamic derivatives of wing.

The analysis of the effect of the wing aspect ratio and number M let us conduct in an example of the wings of rectangular and triangular planform with very small Strouhal number ($p^* \longrightarrow 0$) and position of axis Oz on the leading edge/nose of the mean aerodynamic chord b_a.

On Figs. 28-7-28.26 are depicted the dependences of the coefficients of aerodynamic derivatives of lengthening λ at the constant values of number $M (M = 0; 0,8; 1,4; 3,0)$. An increase in the lengthening, as is known, leads to an increase in the lift effectiveness of wing, especially at subsonic speeds. At supersonic speeds an increase in the lift of rectangular wing occurs only to λ = 3-4, then c_y^a remains virtually constant. For delta wings at supersonic speeds the constancy c_y^a is observed, beginning with $k\lambda \geqslant 4$, i.e., when leading wing edges they become at first sonic, and then supersonic. The given curve/graphs confirm the known fact of an increase in the lift effectiveness of wing during passage from

incompressible $(M = 0)$ to the compressed $(M = 0,8)$ medium according to prandtlya - Glauert's known rule (see about this in more detail in part III). Analogously c_y^α are changed other aerodynamic coefficients without points (derivatives $c_{ya}^{\omega_{za}}$, m_{za}^{α}, $m_{za}^{\omega_{za}}$, $m_{x1}^{\omega_{x1}}$). The analysis of the effect of the sweep angle and wing taper although is carried out for the incompressible medium, qualitatively it can be common also for high subsonic speeds. An increase in the sweep angle of wing leads to a noticeable reduction in the derived c_y^α high-aspect-ratio wing. It is qualitative, and during very great lengthenings and quantitatively this described by the diagram of yawing wing. During small wing aspect ratio λ the effect of angle χ_0 virtually is absent (Figs. 28.27-28.32). This can be explained by the facts that with small λ even a considerable change in the angle χ_0 does not affect substantially wing planform.

A change in the wing taper η at constant values λ and χ_0 weakly affects the lift effectiveness of wing, especially with small λ (Figs. 28.33-28.38). This result it is not difficult to understand, if one considers that basic part of subsonic lift is concentrated near leading wing edges, especially during small lengthenings. An increase in the contraction at constant sweep angles (χ_0 = const) had reduced as to the cutting of certain feed backbone of the wing.

Let us note also, that the mean aerodynamic center of wing with

its steady motion $\bar{x}_F$ with an increase in the sweep angle it is displaced back/ago the more noticeably, the more χ_0.

Page 697.

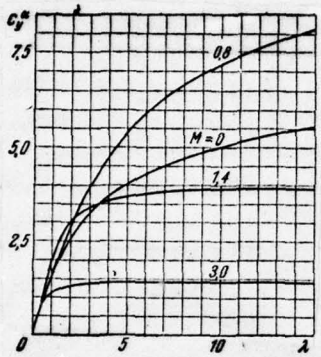


Fig. 28.7.

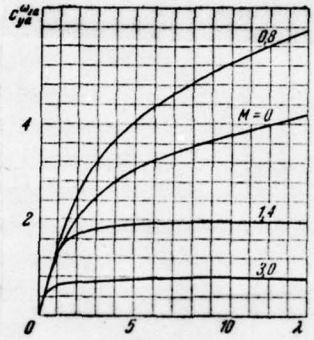


Fig. 28.8.

Fig. 28.7. Rectangular wing. Dependence c_y^α on λ and M.

Fig. 28.8. Rectangular wing. Dependence $c_{ya}^{\omega_{za}}$ on λ and M.

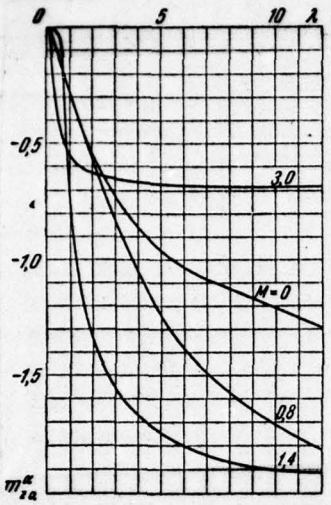


Fig. 28.9.

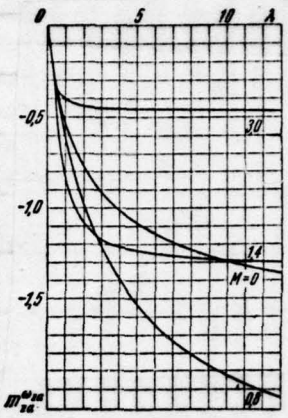


Fig. 28.10.

Fig. 28.9. Rectangular wing. Dependence m^{α}_{za} on λ and M.

Fig. 28.10. Rectangular wing. Dependence $m^{\omega_{za}}_{za}$ on λ and M.

Page 698.

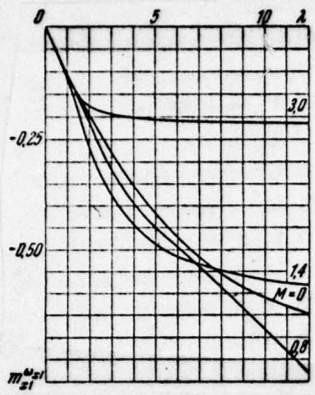


Fig. 28.11.

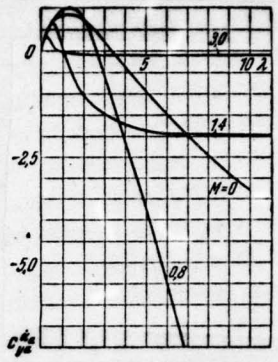


Fig. 28.12.

Fig. 28.11. Rectangular wing. Dependence $m_{x1}^{\omega_{x1}}$ on λ and M.

Fig. 28.12. Rectangular wing. Dependence $c_{ya}^{\dot{\alpha}_a}$ on λ and M.

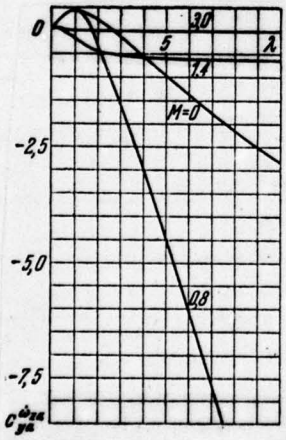


Fig. 28.13.

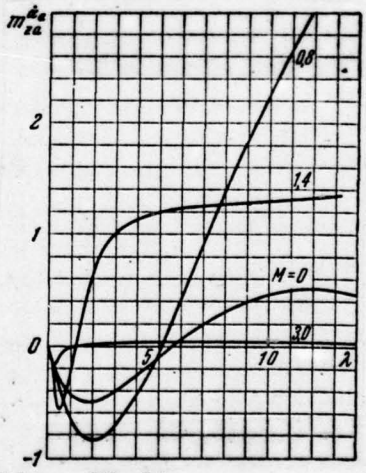


Fig. 28.14.

Fig. 28.13. Rectangular wing. Dependence $c_{ya}^{\omega_{za}}$ on λ and M.

Fig. 28.14. Rectangular wing. Dependence $m_{za}^{\dot{\alpha}_a}$ on λ and M.

Page 699.

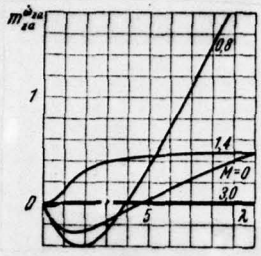


Fig. 28.15.

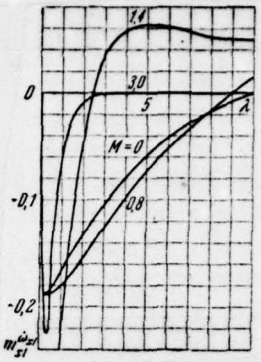


Fig. 28.16.

Fig. 28.15. Rectangular wing. Dependence $m_{za}^{\dot{\omega}_{za}}$ on λ and M.

Fig. 28.16. Rectangular wing. Dependence $m_{x1}^{\dot{\omega}_{x1}}$ on λ and M.

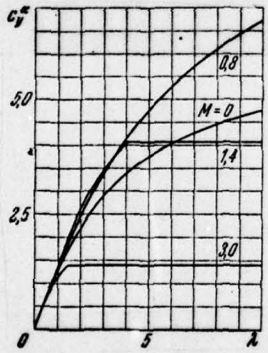


Fig. 28.17.

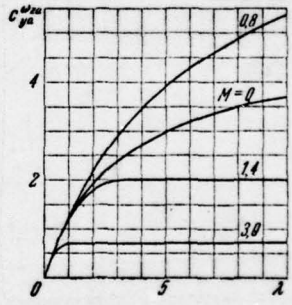


Fig. 28.18.

Fig. 28.17. Delta wing. Dependence c_y^{α} on λ and M.

Fig. 28.18. Delta wing. Dependence $c_{ya}^{\omega_{za}}$ on λ and M.

Page 700.

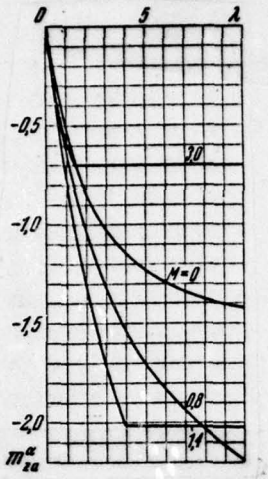


Fig. 28.19.

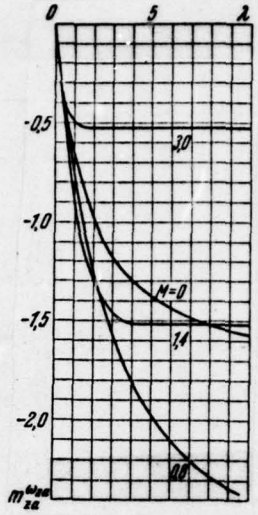


Fig. 28.20.

Fig. 28.19. Delta wing. Dependence m_{za}^{α} on λ and M.

Fig. 28.20. Delta wing. Dependence $m_{za}^{\omega_{za}}$ on λ and M.

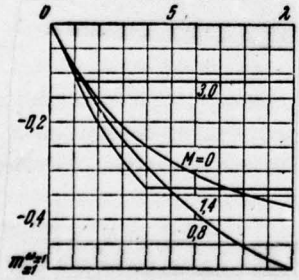


Fig. 28.21.

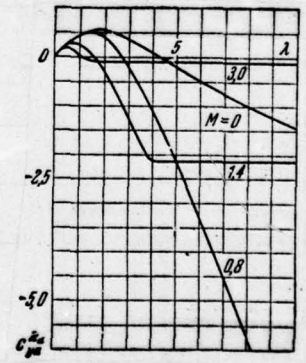


Fig. 28.22.

Fig. 28.21. Delta wing. Dependence $m_{x1}^{\omega_{x1}}$ on λ and M.

Fig. 28.22. Delta wing. Dependence $c_{ya}^{\dot{\alpha}_a}$ on λ and M.

Page 701.

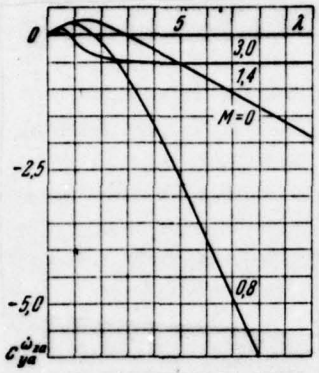


Fig. 28.23.

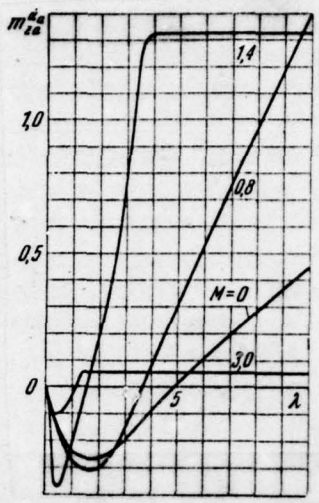


Fig. 28.24.

Fig. 28.23. Delta wing. Dependence $c_{y\alpha}^{\dot{\omega}_{za}}$ on λ and M.

Fig. 28.24. Delta wing. Dependence of $m_{z\dot{\alpha}}^{\dot{\alpha}_a}$ from λ and M.

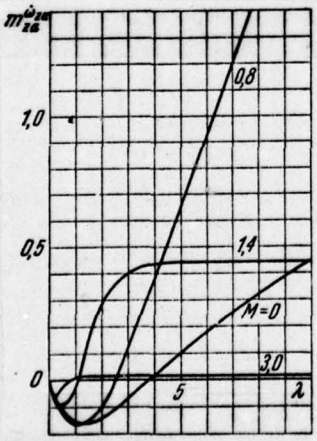


Fig. 28.25.

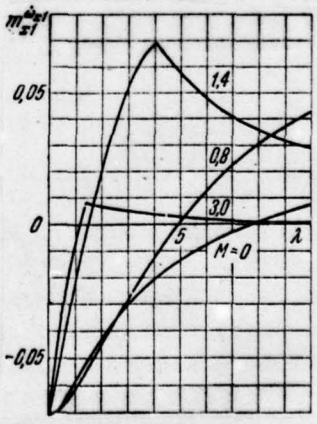


Fig. 28.26.

Fig. 28.25. Delta wing. Dependence $m_{za}^{\Phi_{za}}$ on λ and M.

Fig. 28.26. Delta wing. Dependence $m_{x1}^{\Phi_{x1}}$ on λ and M.

Page 702.

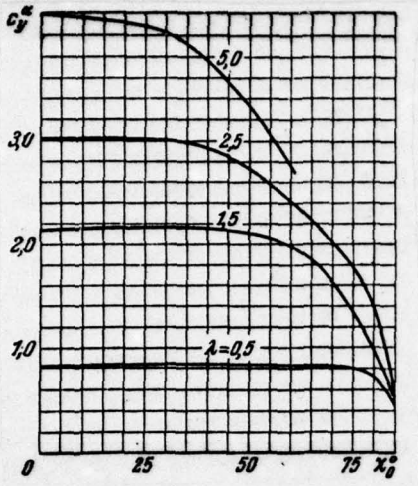


Fig. 28.27.

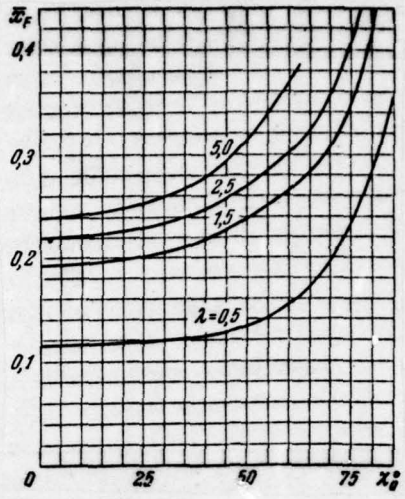


Fig. 28.28.

Fig. 28.27. Effect of sweep angle on derivative c_y^α (η-2).

Fig. 28.28. Effect of sweep angle on mean aerodynamic center of wing $\bar{x}_F$ (η-2).

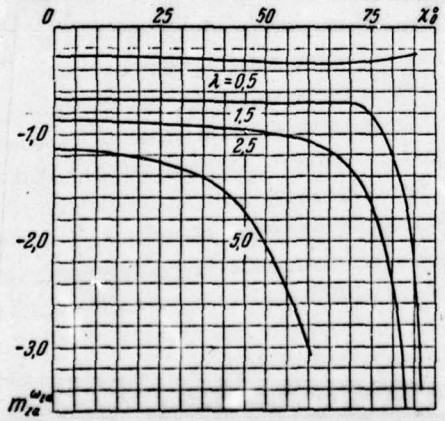


Fig. 28.29. Effect of sweep angle on derivative $m_{z\alpha}^{\omega_{z\alpha}}$ (η-2).

Page 703.

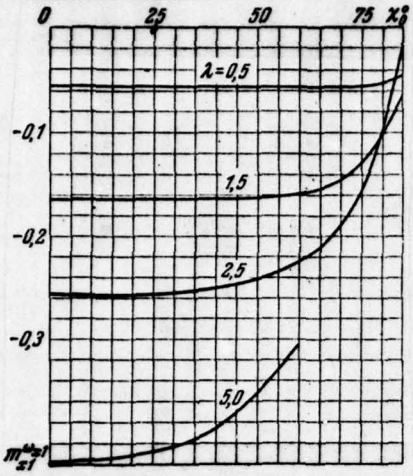


Fig. 28.30.

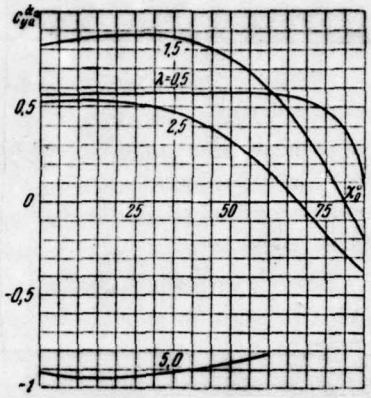


Fig. 28.31.

Fig. 28.30. Effect of sweep angle to derivative $m_{x1}^{\omega_{x1}}$ ($\eta=2$).

Fig. 28.31. Effect of sweep angle on derivative $c_{ya}^{\alpha_a}$ ($\eta=2$).

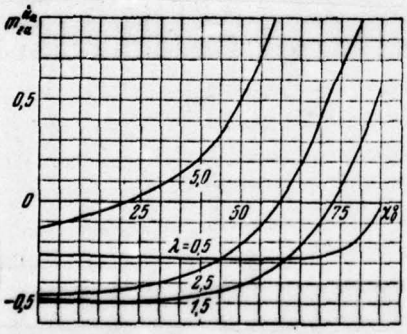


Fig. 28.32. Effect of sweep angle on derivative $m_{za}^{\dot{\alpha}_a}$ ($\eta=2$).

Page 704.

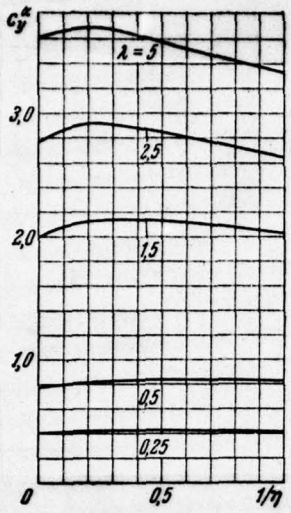


Fig. 28.33.

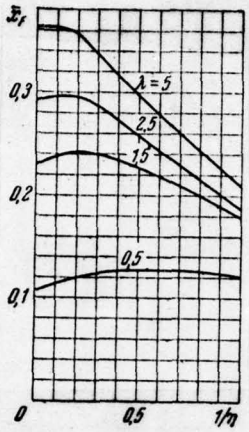


Fig. 28.34.

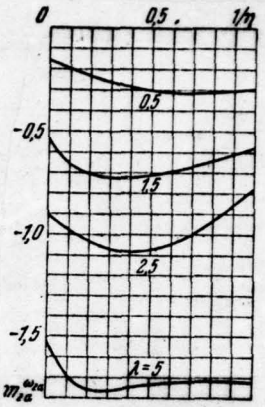


Fig. 28.35.

Fig. 28.33. Effect of contraction on derivative c_y^α ($\chi_0 = 45°$).

Fig. 28.34. Effect of contraction on mean aerodynamic center of wing $\bar{x}_F$ ($\chi_0 = 45°$).

Fig. 28.35. Effect of contraction on derivative $m_{za}^{\omega_z b_a}$ ($\chi_0 = 45°$).

Page 705.

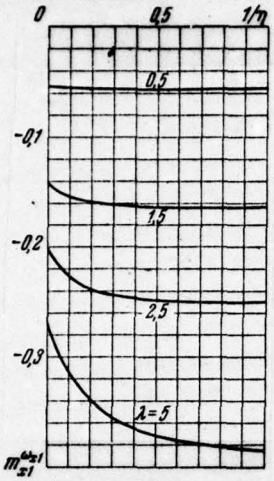


Fig. 28.36.

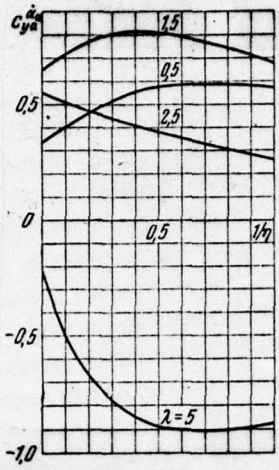


Fig. 28.37.

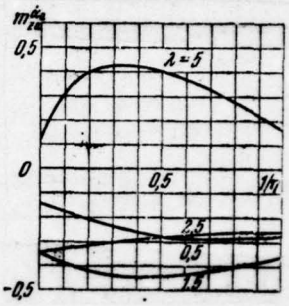


Fig. 28.38.

Fig. 28.36. Effect of contraction on derivative $m_{x1}^{\omega_{x1}}$ ($\chi_0 = 45°$).

Fig. 28.37. Effect of contraction on derivative $c_{ya}^{\dot{\alpha}_a}$ ($\chi_0 = 45°$).

Fig. 28.38. Effect of contraction on derivative $m_{za}^{\dot{\alpha}_a}$ ($\chi_0 = 45°$).

Page 706.



Fig. 28.39.

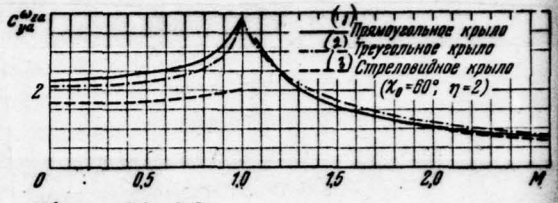


Fig. 28.40.

Fig. 28.39. Effect of number M on derivative c_y^{α} (λ = 2,5).

Key: (1). Rectangular wing. (2). Delta wing. (3). Sweptback wing.

Fig. 28.40. Effect of number M derivative $c_{ya}^{\omega_z a}$ (λ = 2,5).

Key: (1). Rectangular wing. (2). Delta wing. (3). Sweptback wing.



Fig. 28.41.

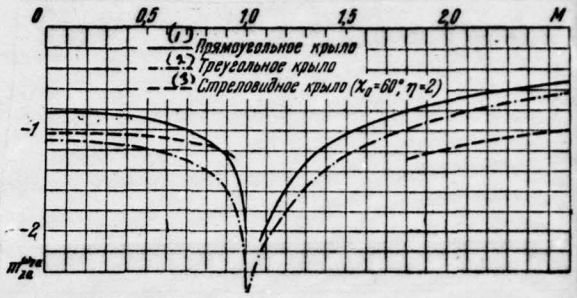


Fig. 28.42.

Fig. 28.41. Effect of number M on derivative m_{za}^{α} ($\lambda = 2,5$).

Key: (1). Rectangular wing. (2). Delta wing. (3). Sweptback wing.

Fig. 28.42. Effect of number M on derivative $m_{za}^{\omega_{za}}$ ($\lambda = 2,5$).

Key: (1). Rectangular wing. (2). Delta wing. (3). Sweptback wing.

Page 707.

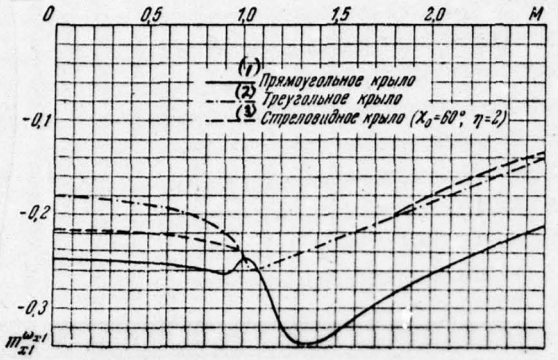


Fig. 28.43.

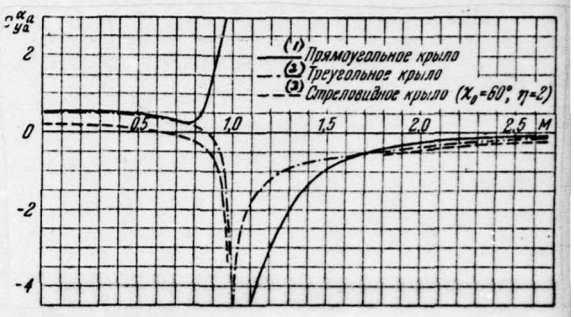


Fig. 28.44.

Fig. 28.43. Effect of number M on derivative $m_{x1}^{\omega_{x1}}$ ($\lambda = 2,5$).

Key: (1). Rectangular wing. (2). Delta wing. (3). Sweptback wing.

Fig. 28.44. Effect of number M on derivative $c_{ya}^{\alpha_a}$ ($\lambda = 2,5$).

Key: (1). Rectangular wing. (2). Delta wing. (3). Sweptback wing.

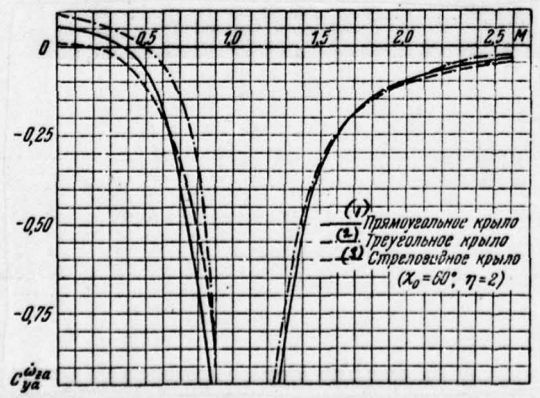


Fig. 28.45. Effect of number M derivative $c_{ya}^{\omega_{za}}$ ($\lambda = 2,5$).

Key: (1). Rectangular wing. (2). Delta wing. (3). Sweptback wing.

Page 708.

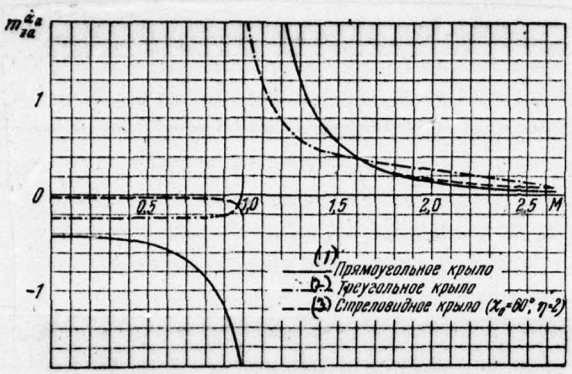


Fig. 28.46.

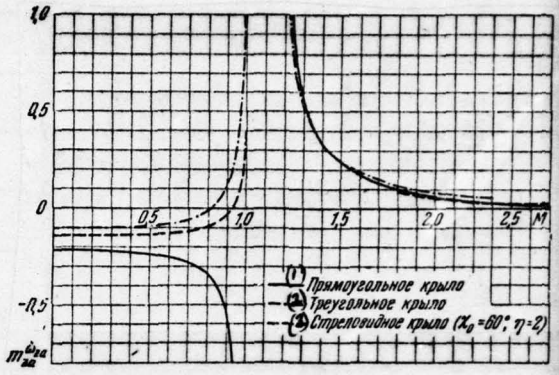


Fig. 28.47.

Fig. 28.46. Effect of number M on derivative $m_{za}^{\dot{\alpha}_a}$ ($\lambda = 2,5$).

Key: (1). Rectangular wing. (2). Delta wing. (3). Sweptback wing.

Fig. 28.47. Effect of number M on derivative $m_{za}^{\bar{\omega}_{za}}$ ($\lambda = 2,5$).

Key: (1). Rectangular wing. (2). Delta wing. (3). Sweptback wing.

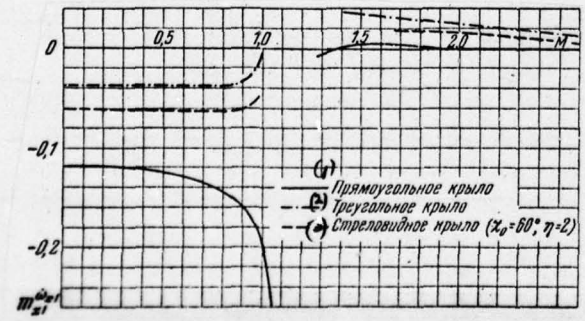


Fig. 28.48. Effect of number M on derivative $m_{xl}^{\bar{\omega}_{xl}}$ ($\lambda = 2,5$).

Key: (1). Rectangular wing. (2). Delta wing. (3). Sweptback wing.

Page 709.

Derivatives $m_{za}^{\omega_{za}}$, $m_{x1}^{\omega_{x1}}$, that characterize respectively longitudinal attenuation and roll damping, with an increase in the lengthening increase, i.e., attenuation is raised. Moreover on low-aspect-ratio wings the effect of the sweep angle and contraction is exhibited very weakly. The derivatives indicated together with value m_{za}^{α}, which characterizes longitudinal stability factor, during an increase in the number M increase at first, then, especially with $M \geqslant 3,0$, they decrease.

The coefficients of aerodynamic derivatives with points in subsonic range also strongly depend on lengthening. At supersonic speeds the effect of lengthening proves to be smaller. With very small Strouhal numbers the most powerful effect of Mach number is observed at transonic speed (near $M = 1$). Here especially grow/rises the role of those aerodynamic characteristics, which have purely unsteady nature. This is exhibited in an essential increase in the absolute values of the coefficients of aerodynamic derivatives with points near mode/conditions $M = 1$, in a change in their signs in the area of the value M indicated and of so forth (Figs. 28.39-28.48).

With $M \geqslant 2{,}5 \div 3{,}0$ the coefficients of aerodynamic derivatives with points decrease, striving for zero with $M \to \infty$. One should turn attention also to the fact that the effect of wing planform is exhibited most powerful in transonic range, especially for the coefficients of aerodynamic derivatives with points.

§4. Effect of Strouhal number on the coefficients of aerodynamic derivatives.

The immediate determination of the coefficients of aerodynamic derivatives with arbitrary Strouhal number is reduced to very cumbersome calculations. This task was solved numerically by Ye. M. Moiseyev only for the rectangular wings of the final lengthening in the incompressible medium (see Chapter of XIV) and for delta wings with supersonic edges of O. N. Sokolovoy, V. G. Tabachnikov, M. K. Pursov, A. I. Shevchenko (chapter of XXII). More effective is the solution of problem with the aid of Duhamel integral. It render/showed to much simpler solve task during a stepped variation in the kinematic parameters in time, and then, utilizing transient function, Duhamel integral and the coefficients of associated masses (for the incompressible medium), to determine the coefficients of aerodynamic derivatives. By this method, in particular, obtained the

coefficients of aerodynamic derivatives $c_y^{\omega_x}$ and $c_y^{\omega_y}$ (Fig. 28.49) for three wings with lengthening $\lambda = 2.5$: rectangular, triangular and swept ($\chi_0 = 60°$, $\eta = 2$) - at low speeds ($M = 0$).

Page 710.

As the initial materials during calculations served the corresponding transient functions, given in chapter of XXIX, and the coefficients of apparent additional masses (chapter of XXVII). At subsonic speeds ($M < 1$) these derivatives are determined for a rectangular wing $\lambda = 1$ (Figs. 28.50, 28.51).

At subsonic speeds ($M = 0; 0,1; 0,6; 0,9$) for a plate ($\lambda = \infty$) are obtained also the coefficients of aerodynamic derivatives, caused by the deflection of rudder or flap, $c_y^{\delta_p}, \ldots, m_z^{\delta_p}$. These data are acquired also by numerical calculation with the aid of transient functions during the solution of δ-problem and Duhamel integral (Figs. 28.52-28.59).

By analyzing the given materials, it is possible to draw the common/general/total conclusion that on the speeds in question the greatest effect of Strouhal number is observed at comparatively small values of p *. Attention is drawn to the interesting result, obtained for subsonic speeds. If with very small Strouhal numbers (p * $\longrightarrow 0$)

the effect of Mach number begins to manifest itself the coefficients of aerodynamic derivatives with $M \approx 0,6 \div 0,7$, then with large Strouhal numbers the effect of number M especially is substantial near small M, whereupon is observed jump during passage from that incompressible to the compressed medium. Even with $M \approx 0,1 \div 0,2$ the coefficients of aerodynamic derivatives on large Strouhal numbers ($p^* \longrightarrow \infty$) change several times in comparison with these coefficients with $M = 0$. Subsequently this difference, remaining in value large, somewhat decreases during an increase in the number M ($0 < M < 1$).

Let us examine in more detail curves to Figs. 28.60, 28.61, that characterize the combined effect of numbers M and p^* on coefficients c_y^{α} and $c_{y'}^{\alpha}$. Let us note that for the plate of infinite lengthening the coefficients of aerodynamic derivatives with points with $p^* \longrightarrow 0$ go to infinity at subsonic speeds. In this same mode/conditions the coefficients without points have a special feature/peculiarity near $M = 1$ (see Fig. 28.60). With $p^* \longrightarrow \infty$ the coefficients with points are equal to zero for all numbers M, except $M = 0$. In the latter case they are equal to the appropriate coefficients of apparent additional masses. The coefficients of aerodynamic derivatives without points with $p^* \longrightarrow \infty$ do not have special feature/peculiarities, when $M = 1$, but they appear in the incompressible medium. With $M = 0$ the

coefficients without points are equal to the initial values of the regular part of the transient function. In the case $M \neq 0$ for the coefficients of aerodynamic derivatives are valid precise formulas of the type const/M.

Page 711.

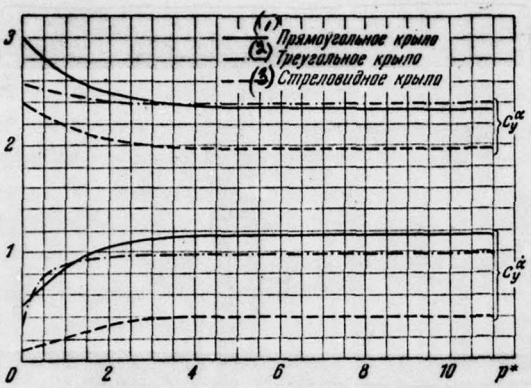


Fig. 28.49. Effect of wing planform (λ = 2.5) on derivatives c_y^α and $c_y^{\dot\alpha}$ in the incompressible medium.

Key: (1). Rectangular wing. (2). Delta wing. (3). Sweptback wing.

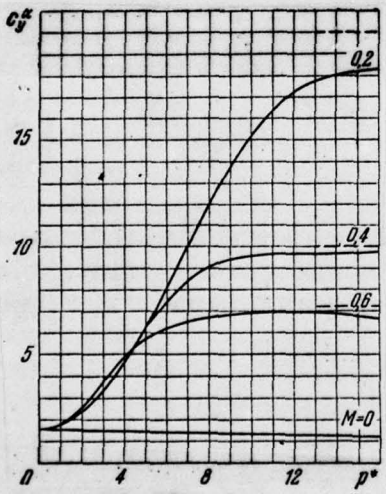


Fig. 28.50.

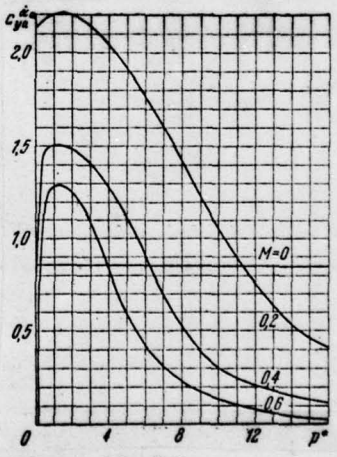


Fig. 28.51.

Fig. 28.50. Rectangular wing λ = 1. Effect of Strouhal number on c_y^α derivative $(0 \leqslant M < 1)$.

Fig. 28.51. Rectangular wing λ = 1. Effect of Strouhal number on derivative $c_{y_a}^{\dot\alpha_a}(0 \leqslant M < 1)$.

Page 712.

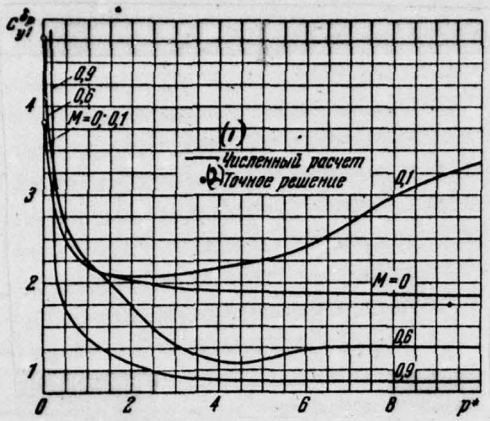


Fig. 28.52.

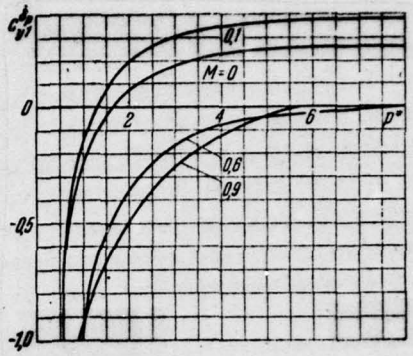


Fig. 28.53.

Fig. 28.52. Wing $\lambda = \infty$, $b_p = 0{,}25$. Effect of Strouhal number on derivative $c_{y1}^{\delta_p}$ $(0 \leq M < 1)$.

Key: (1). Numerical calculation. (2). Exact solution.

Fig. 28.53. Wing $\lambda = \infty$, $b_p = 0{,}25$. Effect of Strouhal number on derivative $c_{y1}^{\delta_p}$ $(0 \leq M < 1)$.

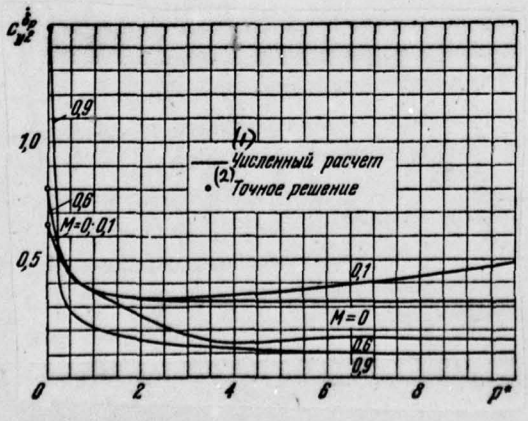


Fig. 28.54.

Fig. 28.54. Wing $\lambda = \infty$, $c_p = 0.25$. Effect of Strouhal number on derivative $c_{y\bar{z}}^{\delta_p}$ $(0 \leq M < 1)$.

Key: (1). Numerical calculation. (2). Exact solution.

Page 713.

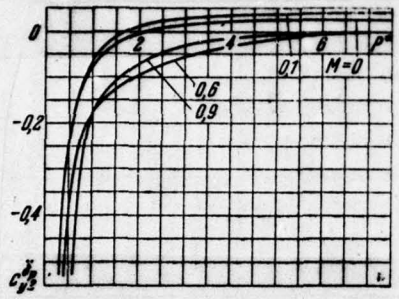


Fig. 28.55.

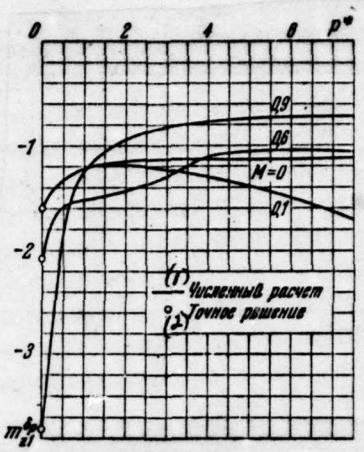


Fig. 28.56.

Fig. 28.55. Wing $\lambda = \infty$, $b_p = 0,25$. Effect of Strouhal number on derivative $c_{y^2}^{\delta_p}$ $(0 \leq M < 1)$.

Fig. 28.56. Wing $\lambda = \infty$ $b_p = 0,25$. Effect of Strouhal number on derivative $m_{z1}^{\delta_p}$ $(0 \leq M < 1,\ \bar{x}_T = 0)$.

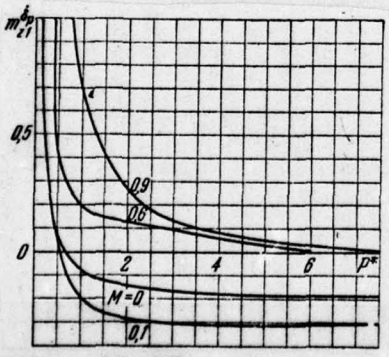


Fig. 28.57.

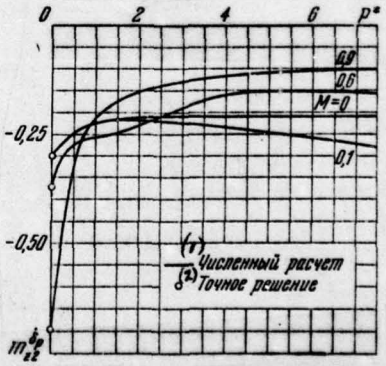


Fig. 28.58.

Fig. 28.57. Wing $\lambda = \infty$, $b_p = 0,25$. Effect of Strouhal number on

derivative $m_{z\bar{z}}^{\delta_p}$ $(0 \leqslant M < 1,\ \bar{x}_T = 0)$.

Fig. 28.58. Wing $\lambda = \infty$, $\delta_p = 0{,}25$. Effect of Strouhal number on derivative $m_{z\bar{z}}^{\delta_p}$ $(0 \leqslant M < 1,\ \bar{x}_T = 0)$.

Key: (1). Numerical calculation. (2). Exact solution.

Page 714.

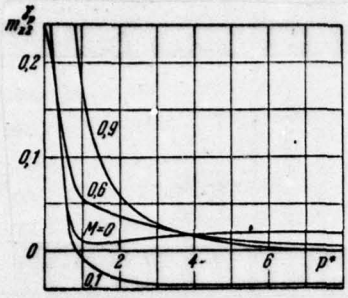


Fig. 28.59. Wing λ = ∞, δ_p = 0,25. Effect of Strouhal number on derivative $m_{z2}^{\delta p}$ $(0 \leqslant M < 1,\ \bar{x}_T = 0)$.

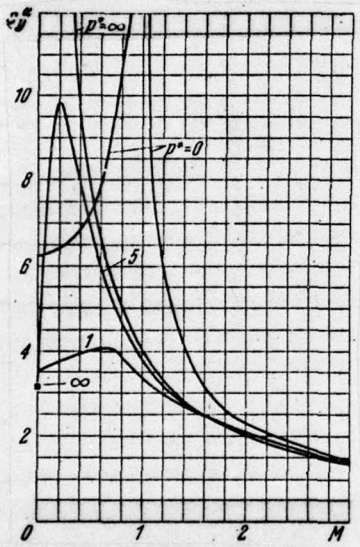


Fig. 28.60.

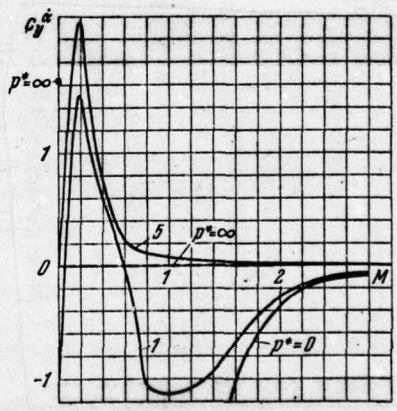


Fig. 28.61.

Fig. 28.60. Effect of numbers M and p * on derivative c_y^{α} for a wing λ = ∞.

Fig. 28.61. Effect of numbers M and p * on derivative c_y^{α} for a wing λ = ∞.

Page 715.

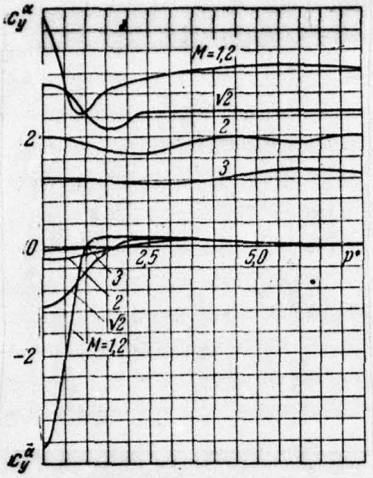


Fig. 28.62.

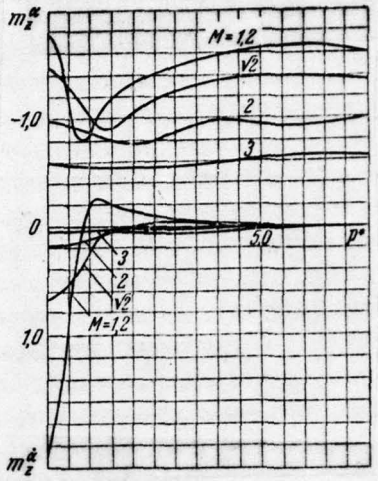


Fig. 28.63.

Fig. 28.62. Rectangular wing λ = 2.5. Effect of numbers M and p * on derivatives c_y^{α} and $c_y^{\dot{\alpha}}$.

Fig. 28.63. Rectangular wing λ = 2.5. Effect of numbers M and p * to derivatives m_z^{α} and $m_z^{\dot{\alpha}}(\bar{x}_T=0)$.

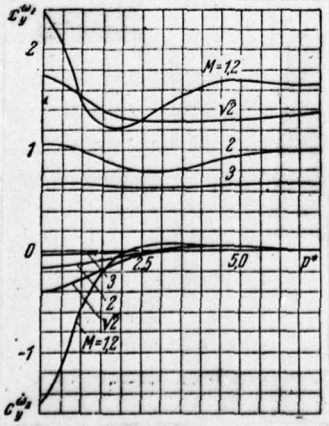


Fig. 28.64.

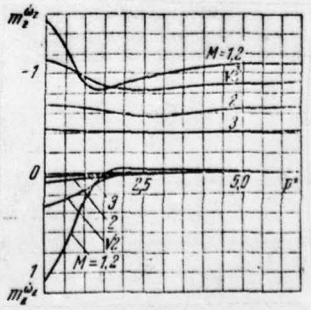


Fig. 28.65.

Fig. 28.64. Rectangular wing λ = 2.5. Effect of numbers M and p * on derivatives $c_y^{\bar{\omega}_z}$ and $c_y^{\bar{\omega}_z}(\bar{x}_T=0)$.

Fig. 28.65. Rectangular wing λ = 2.5. Effect of numbers M and p * on derivative $m_z^{\bar{\omega}_z}$ and $m_z^{\bar{\omega}_z}(\bar{x}=0)$.

AD-A049 001 FOREIGN TECHNOLOGY DIV WRIGHT-PATTERSON AFB OHIO F/G 1/3
A WING IN AN UNSTEADY GAS FLOW. PART 3,(U)
SEP 77 S M BELOTSERKOVSKIY, B K SKRIPACH
UNCLASSIFIED FTD-ID(RS)T-1543-77-PT-3 NL



IFIED

4 OF

AD

A049001

1.0 1.1 1.25 1.4 1.6 2.8 3.2 3.6 4.0 2.5 2.2 2.0 1.8

MICROCOPY RESOLUTION TEST CHART
NATIONAL BUREAU OF STANDARDS-1963-A

Page 716.

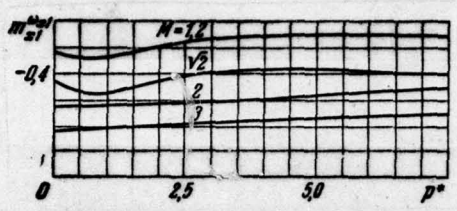


Fig. 28.66. Rectangular wing $\lambda = 2.5$. Effect of numbers M and p * on derivative $m_{x1}^{\omega_{x1}}$.

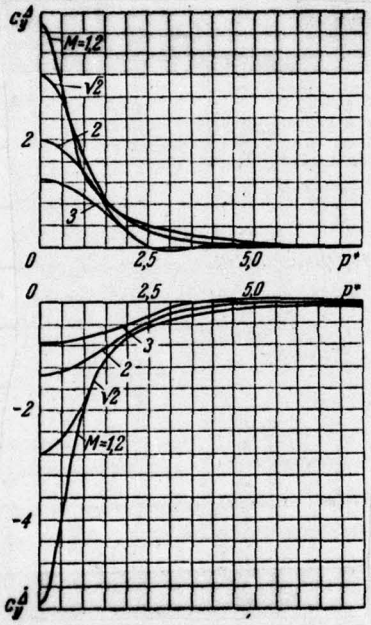


Fig. 28.67.

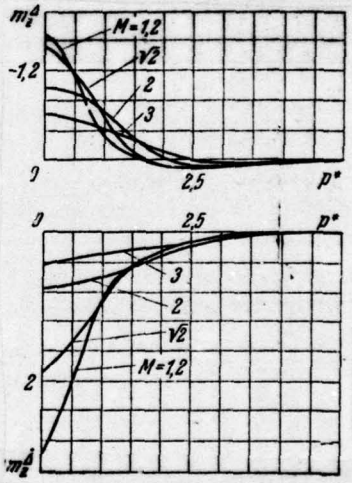


Fig. 28.68.

Fig. 28.67. Rectangular wing $\lambda = 2.5$. Effect of numbers M and p * on derivatives c_y^{Δ} and $c_y^{\dot{\Delta}}(\bar{x}_T=0)$.

Fig. 28.68. Rectangular wing $\lambda = 2.5$. Effect of numbers M and p * on derivatives m_z^{Δ} and $m_z^{\dot{\Delta}}(\bar{x}_T=0)$.

Page 717.

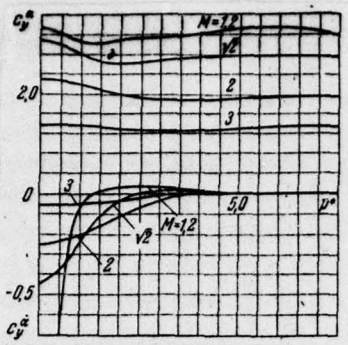


Fig. 28.69.

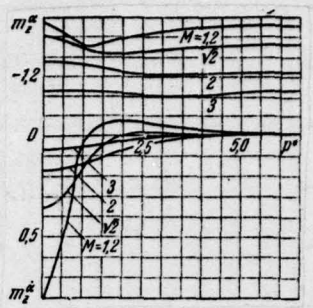


Fig. 28.70.

Fig. 28.69. Delta wing $\lambda = 2.5$. Effect of numbers M and p * on derivatives c_y^{α} and $c_y^{\dot{\alpha}}$.

Fig. 28.70. Delta wing $\lambda = 2.5$. Effect of numbers M and p * on derivatives m_z^{α} and $m_z^{\dot{\alpha}}{}_{(\bar{x}_T=0)}$.

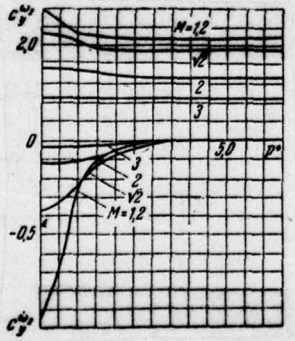


Fig. 28.71.

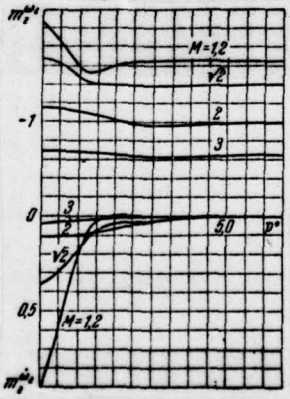


Fig. 28.72.

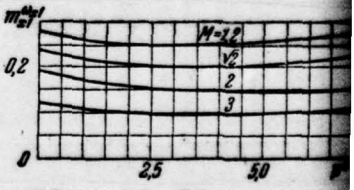


Fig. 28.73.

Fig. 28.71. Delta wing $\lambda = 2.5$. Effect of numbers M and p * on

derivatives $c_y^{\omega_z}$ and $c_y^{\dot{\omega}_z}(\bar{x}_T=0)$.

Fig. 28.72. Delta wing λ = 2.5. Effect of numbers M and p * on derivatives $m_z^{\omega_z}$ and $m_z^{\dot{\omega}_z}(\bar{x}_T=0)$.

Fig. 28.73. Delta wing λ = 2.5. Effect of numbers M and p * on derivative $m_{x1}^{\omega_{x1}}$.

Page 718.

The dependences of aerodynamic derivatives of Strouhal number at supersonic speeds (M = 1,2; $\sqrt{2}$; 2,0; 3,0) for the rectangular and delta wings of lengthening λ = 2.5 are given in Fig. 28.62-28.77. Are examined the cases of harmonic oscillations (derivatives c_y^{α}, $c_y^{\dot{\alpha}}$, m_z^{α}, $m_z^{\dot{\alpha}}$, $c_y^{\omega_z}$, $c_y^{\dot{\omega}_z}$, $m_z^{\omega_z}$, $m_z^{\dot{\omega}_z}$, $m_{x1}^{\omega_{x1}}$, $m_{x1}^{\dot{\omega}_{x1}}$) and of harmonic gust (derivatives c_y^{Δ}, $c_y^{\dot{\Delta}}$, m_z^{Δ}, $m_z^{\dot{\Delta}}$). The derivatives indicated, besides $m_{x1}^{\omega_{x1}}$, noticeably depend on Strouhal number in the range of the low values p *. With p * $\longrightarrow$ - the coefficients without points $(c_y^{\alpha}, c_y^{\omega_z}, m_z^{\alpha}, m_z^{\omega_z}, m_{x1}^{\omega_{x1}})$ approach some finite values, coefficients with points - for zero.

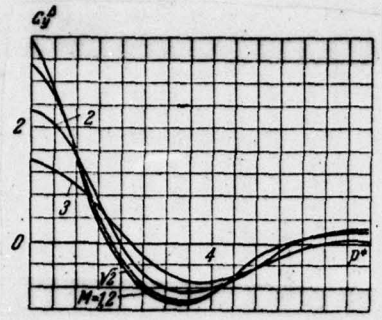


Fig. 28.74.

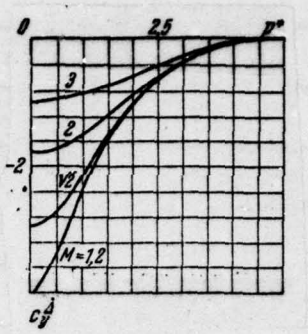


Fig. 28.75.

Fig. 28.74. Delta wing λ = 2.5. Effect of numbers M and p * on derivative c_y^{Δ}.

Fig. 28.75. Delta wing λ = 2.5. Effect of numbers M and p * on derivative $c_y^{\dot{\Delta}}$.

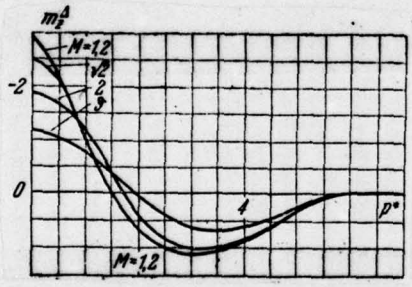


Fig. 28.76.

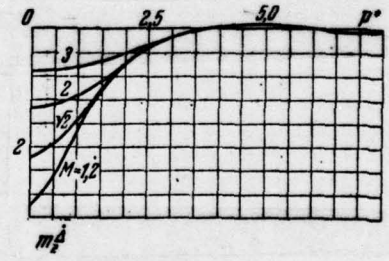


Fig. 28.77.

Fig. 28.76. Delta wing λ = 2.5. Effect of numbers M and p * on derivative $m_z^{\Delta}(\bar{x}_T=0)$.

Fig. 28.77. Delta wing λ = 2.5. Effect of numbers M and p * on derivative $m_z^{\dot{\Delta}}(\bar{x}_T=0)$.

Page 719.

In the case of harmonic gust at supersonic speeds the coefficients of aerodynamic derivatives without points $(c_y^{\Delta}, m_z^{\Delta})$ during the unlimited increase in Strouhal number $(p^* \to \infty)$ vanish, but coefficients with points, just as are earlier, they turn into zero. Passage from the supersonic to transonic speed produces an increase in the absolute values of the wing characteristics, connected with lift effectiveness, static stability level and the attenuating properties of wing. Increase also the coefficients of purely unsteady nature (coefficients with points).

Comparing the appropriate coefficients of aerodynamic derivatives without points for rectangular and delta wings with very small Strouhal number we see that qualitatively the wing characteristics of the forms in question differ from each other by supersonic speeds approximately just as for the incompressible medium $(M = 0)$.

§5. Effect of centering on the coefficients of aerodynamic

derivatives.

The given in chapter XXVII systematic data on the coefficients of aerodynamic derivatives are related to the determined centering. This is related also to some coefficients of apparent additional masses. The problem of the recalculation of aerodynamic coefficients for other centering is solved with the aid of relationship/ratios (27.3) and (27.8).

The analysis of the effect of centering on the coefficients of aerodynamic derivatives was carried out on an example of delta wing (λ = 2.5). On Figs. 28.78-28.85 are represented the results of the made recalculations, by which the position of the origin of coordinates was displaced along the mean aerodynamic chord b_a (see Fig. 28.78). Coefficients are given depending on $\bar{x}_T = x_T/b_a$ (x_T — distance from leading edge/nose b_a to the new origin of coordinates). The point $\bar{x}_T$ is the center of bringing forces, and through it it passes axis Oz, relative to which occurs rotation. Were studied five characteristic cases: the incompressible medium ($M = 0$), high subsonic speeds ($M = 0,8$) and three supersonic mode/conditions. For supersonic speeds ($M > 1$) is investigated the wing with subsonic leading edge ($k\lambda = 2$, $M = 1,28$), sonic leading edge ($k\lambda = 4$, $M = 1,9$) and supersonic leading edge ($k\lambda = 5$, $M = 2,24$).

Derivatives c_y^α and $c_y^{\dot{\alpha}_a}$ do not depend on centering. The coefficients of aerodynamic derivatives $c_{ya}^{\omega_{za}}$, m_{za}^α depend on centering linearly, whereupon the angles of the slope of the dependences $c_{ya}^{\omega_{za}}$, m_{za}^α on $\bar{x}_T$ are determined by value c_y^α. These angles are opposite on sign in the characteristics indicated in consequence of which always it is possible to find centering, for which $c_{ya}^{\omega_{za}} = 0$ or $m_{za}^\alpha = 0$.

Page 720.

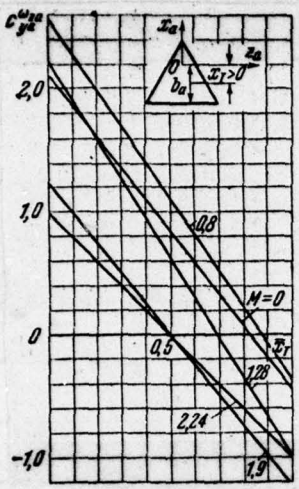


Fig. 28.78.

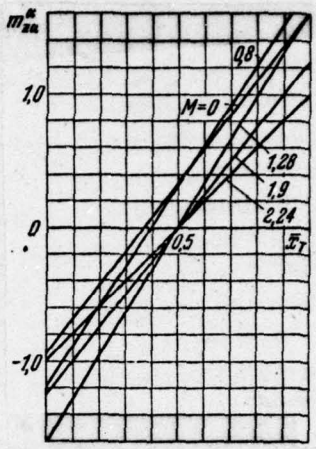


Fig. 28.79.

Fig. 28.78. Delta wing $\lambda = 2.5$. Effect of centering on derivative $c^{\omega_{za}}_{ya}$.

Fig. 28.79. Delta wing $\lambda = 2.5$. Effect of centering on derivative m^{α}_{za}.

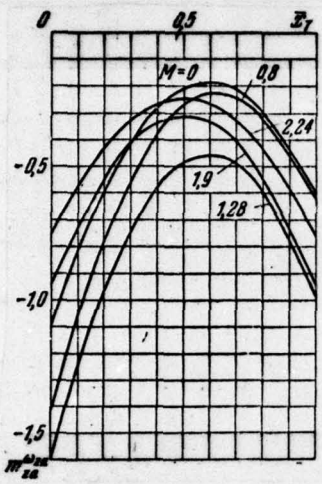


Fig. 28.80.

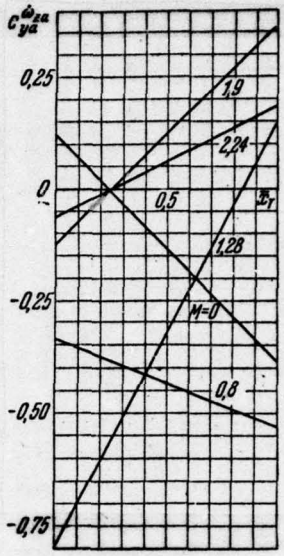


Fig. 28.81.

Fig. 28.80. Delta wing $\lambda = 2.5$. Effect of centering on derivative $m_{za}^{\omega_{za}}$.

Fig. 28.81. Delta wing $\lambda = 2.5$. Effect of centering on derivative $c_{ya}^{\omega_{za}}$.

Page 721.

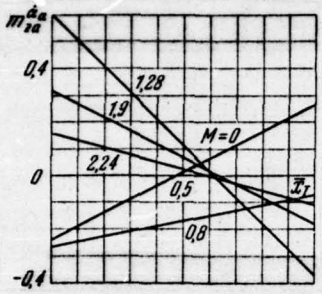


Fig. 28.82.

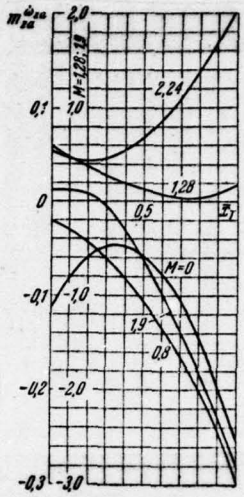


Fig. 28.83.

Fig. 28.82. Delta wing $\lambda = 2.5$. Effect of centering on derivative $m_{za}^{\dot{\alpha}_a}$.

Fig. 28.83. Delta wing $\lambda = 2.5$. effect of centering on derivative $m_{za}^{\omega_{za}}$.

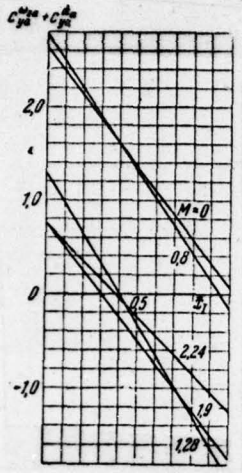


Fig. 28.84.

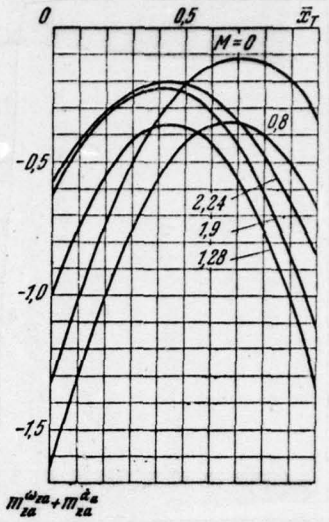


Fig. 28.85.

Fig. 28.84. Delta wing $\lambda = 2.5$. Effect of centering on combination $c_{ya}^{\omega_{za}} + c_{ya}^{\dot{\alpha}_a}$.

Fig. 28.85. Delta wing $\lambda = 2.5$. Effect of centering on combination $m_{za}^{\omega_{za}} + m_{za}^{\dot{\alpha}_a}$.

Page 722.

Similar pattern is observed for coefficients $c_{ya}^{\omega_{za}}$ and $m_{za}^{\dot{\alpha}_a}$, only here the slope angles are determined by the value of derivative $c_{ya}^{\dot{\alpha}_a}$. The dependence $m_{za}^{\omega_{za}}$, just as $m_{za}^{\dot{\omega}_{za}}$, on centering is quadratic. The

more the lift effectiveness of wing, the more the curvature of the parabola with a given $\bar{x}_T$ (see Fig. 28.80). Most interesting are the curves for combinations $c^{\omega_{za}}_{y_a} + c^{\dot{\alpha}_a}_{y_a}$ and $m^{\omega_{za}}_{z_a} + m^{\dot{\alpha}_a}_{z_a}$ (see Figs. 28.84 and 28.85), which characterize the damping and the attenuating pitching moment during the rotary oscillations of wing relative to axis Oz. If $m^{\omega_{za}}_{z_a} + m^{\dot{\alpha}_a}_{z_a} > 0$, then instead of that which attenuate appears the torque/moment, which increases the amplitude of oscillations.

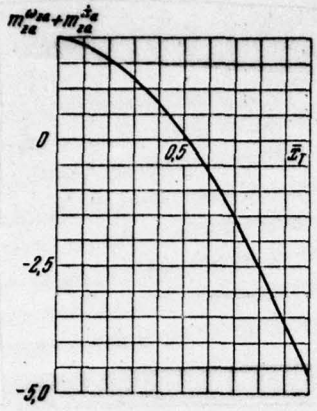


Fig. 28.86.

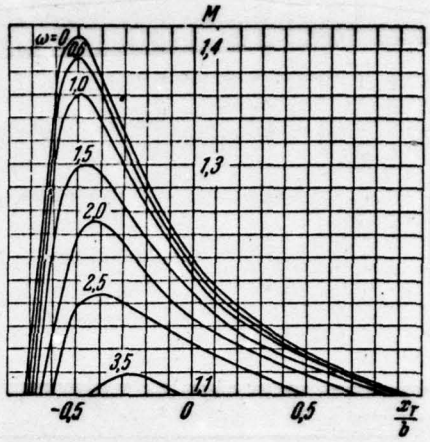


Fig. 28.87.

Fig. 28.86. Delta wing $\lambda = 7.5$ (M-1,2). Ranges of negative damping.

Fig. 28.87. Ranges of negative damping for delta wings with supersonic edges (λ tg $\chi_0 = 4$, $\chi_1 = 0$, $\eta-\infty$).

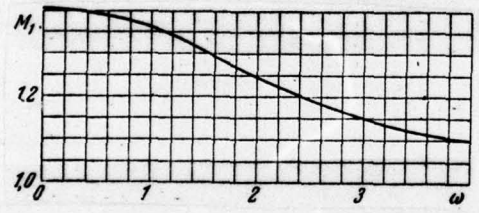


Fig. 28.88. Range of negative damping for delta wings with supersonic edges.

In all designed mode/conditions the delta wing (λ = 2.5) possesses attenuation. At the low speeds ($M = 0$) the wing of any planform does not have negative damping ($m_{za}^{\omega_{za}} + m_{za}^{\dot{\alpha}_a} \leqslant 0$). For the rectangular wing of very small lengthening with $M = 0$ $m_{za}^{\omega_{za}} + m_{za}^{\dot{\alpha}_a} = 0$ on trailing wing edge ($\bar{x}_T = 1$). For a delta wing with supersonic leading edges ($k\lambda > 4$) are vast ranges of the negative attenuation, which appear with the relatively small values of supersonic speed or large wing aspect ratio. The coefficient of the attenuation of longitudinal vibrations with certain determined centering reaches the greatest value, which corresponds to the minimum of the attenuating properties of wing.

The given to Fig. 28.86 dependences $m_{za}^{\omega_{za}} + m_{za}^{\dot{\alpha}_a}$ on the position of axis Oz (from centering of wing $\bar{x}_T$) for a delta wing ($\lambda = 7{,}5$, $M = 1{,}2$) show that with bow heavinesses ($\bar{x}_T \leqslant 0{,}5$) the wing is swought by flow ($m_{za}^{\omega_{za}} + m_{za}^{\dot{\alpha}_a} > 0$). During a decrease in the number M ($M < 1{,}2$) or an increase in lengthening this wing of the range of negative damping they will be expanded and moved to trailing wing edge. For the wings indicated these ranges depend even on given Strouhal number $\omega = p^* \frac{M^2}{k^2}$. The range of negative damping for each value ω lie/rests below corresponding curve. The given to Figs. 28.87, 28.88 curves indicate with datum ω and any centering this number M, higher than which negative damping, according to the data of linear theory, is impossible.

Chapter XXIX.

Effect of planform, the Mach numbers and laws of motion for transient functions.

§1. Some relationship/ratios for transient functions.

For the solution to the problem, in which the kinematic parameters change with arbitrary form in time, sufficient to examine a stepped variation in these parameters. As a result of the solution of this problem are determined the transient functions during an instantaneous change in the kinematic parameters (α-, ω_z-, ω_x- problems), and also at the gradual entrance of wing into step gust (Δ- problem).

If they change immediately several parameters, then the general case is represented as the linear combination examine/considered. For example, for the lift coefficients c_y, of the pitching moment m_z, of the moment of roll m_x we have

$$\left.\begin{aligned} c_y(\tau) &= \left[\frac{c_y(\tau)}{\alpha^*}\right]\alpha^* + \left[\frac{c_y(\tau)}{\omega_z^*}\right]\omega_z^*, \\ m_z(\tau) &= \left[\frac{m_z(\tau)}{\alpha^*}\right]\alpha^* + \left[\frac{m_z(\tau)}{\omega_z^*}\right]\omega_z^*, \\ m_{x1}(\tau) &= \left[\frac{m_{x1}(\tau)}{\omega_{x1}^*}\right]\omega_{x1}^*. \end{aligned}\right\} \qquad (29.1)$$

Here value included into brackets, transient functions for α-, ω_z- and ω_x-problems: α^*, ω_z^*, ω_x^* – the amplitude values of the corresponding kinematic parameters.

Especially let us examine the case, when wing completes rotation around axis Oz as solid body; here

$$\omega_z = \dot{\alpha} = \frac{\Omega_z b}{U_0}. \qquad (29.2)$$

In order to obtain transient functions in this case, it is necessary to examine two problems. one of them, in which ω_z is changed according to stepped law, was studied higher according to (29.2) the dimensionless derivative of angle of attack in terms of time $\dot{\alpha}(\tau)$ must in this case also change in terms of stepped law.

Page 725.

Consequently, it is necessary additionally to find aerodynamic wing characteristics, including $c_{y_\alpha}(\tau)$ and $m_{z_\alpha}(\tau)$, for the law

$$\frac{\alpha(\tau)}{\alpha^*} = \tau. \qquad (29.3)$$

Then, after accepting $\omega_z^\circ = \alpha^\circ$, we will obtain

$$\left.\begin{aligned} c_y(\tau) &= \left\{ c_{y_\alpha}(\tau) + \left[\frac{c_y(\tau)}{\omega_z^\circ}\right] \right\} \omega_z^\circ, \\ m_z(\tau) &= \left\{ m_{z_\alpha}(\tau) + \left[\frac{m_z(\tau)}{\omega_z^\circ}\right] \right\} \omega_z^\circ. \end{aligned}\right\} \qquad (29.4)$$

Analogously it is possible to determine the distributed characteristics. The calculation of functions $c_{y_\alpha}(\tau)$ and $m_{z_\alpha}(\tau)$ is most convenient produced with the aid of Duhamel integral (about this in more detail - in chapter VI). According to (6.45) we have

$$\left.\begin{aligned} c_{y_\alpha}(\tau) &= 2\mu k_{22} + \int_0^\tau \left[\frac{c_y(\tau_1)}{\alpha^\circ}\right] d\tau_1, \\ m_{z_\alpha}(\tau) &= 2\mu k_{26} + \int_0^\tau \left[\frac{m_z(\tau_1)}{\alpha^\circ}\right] d\tau_1, \\ \mu &= \begin{cases} 0 & \text{with } M \neq 0, \\ 1 & \text{with } M = 0. \end{cases} \end{aligned}\right\} \qquad (29.5)$$

Is carried out below the analysis of the effect of the geometric parameters of wing, number M on the laws of motion for the transient functions

$$\left[\frac{c_y}{\alpha^\circ}\right], \quad \bar{x}_\alpha, \quad \left[\frac{c_y}{\omega_z^\circ}\right], \quad \bar{x}_{\omega_z}, \quad \left[\frac{m_{x1}}{\omega_{x1}^\circ}\right]$$

during a stepped variation in the kinematic parameters and

$$\left[\frac{c_y}{\omega_{y\Delta}^\circ}\right], \quad \bar{x}_{\omega_{y\Delta}}$$

at the gradual entrance of wing into gust. Aerodynamic coefficients are introduced as follows:

$$c_y = \frac{2Y}{\rho S U_0^2}, \quad m_z = \frac{2M_z}{\rho S U_0^2 b}, \quad m_{x1} = \frac{2M_x}{\rho S U_0^2 l}, \quad \bar{x}_{q_l} = \frac{x_{q_l}}{b}; \quad (29.6)$$

b - root wing chord $\bar{x}_\alpha$, $\bar{x}_{\omega_z}$ — the coordinate of unsteady mean aerodynamic centers of wing relative to the leading edge/nose of its root chord ($\bar{x}_{q_l} > 0$, if focus lie/rests behind leading edge/nose).

Page 726.

A stepped variation in the kinematic parameters is conducted in such a way that at the initial moment $\tau = 0$ kinematic parameters α, ω_z, ω_{x1}, $\omega_{y\Delta}$ are changed by jump to amplitude values α^*, ω_z^*, ω_{x1}^*, $\omega_{y\Delta}^*$ and retain them with $\tau > 0$ (see Fig. 6.3). The obtained from the calculations transient functions $[c_y/\alpha^*]$, $\bar{x}_\alpha$, $[m_{x1}/\omega_{x1}^*]$ do not depend on centering $\bar{x}_T$, $[c_y/\omega_z^*]$, $\bar{x}_{\omega_z}$ they depend on the position of axis Oz. According to these data it is not difficult to find in the general case moment coefficient relative to another position of axis Oz, for example, passing through the leading edge/nose the root chord:

$$[m_z] = -\left[\frac{c_y}{\alpha^*}\right]\alpha^*\bar{x}_\alpha - \left[\frac{c_y}{\omega_z^*}\right]\omega_z^*\bar{x}_{\omega_z}. \quad (29.7)$$

Transient functions for ω_z-problems are obtained for the case, when beginning of coordinates is arranged in the leading edge/nose of root wing chord ($\bar{x}_T = 0$). Recalculation for another

centering is conducted according to the following formulas:

$$\left.\begin{aligned}
&\left[\frac{c_y}{\alpha^\circ}\right]_1=\left[\frac{c_y}{\alpha^\circ}\right],\quad \left[\frac{c_y}{\omega_z^\circ}\right]_1=\left[\frac{c_y}{\omega_z^\circ}\right]+\xi_0\left[\frac{c_y}{\alpha^\circ}\right],\\
&\left[\frac{m_z}{\alpha^\circ}\right]_1=\left[\frac{m_z}{\alpha^\circ}\right]-\xi_0\left[\frac{c_y}{\alpha^\circ}\right],\\
&\left[\frac{m_z}{\omega_z^\circ}\right]_1=\left[\frac{m_z}{\omega_z^\circ}\right]+\xi_0\left\{\left[\frac{m_z}{\alpha^\circ}\right]-\left[\frac{c_y}{\omega_z^\circ}\right]\right\}-\xi_0^2\left[\frac{c_y}{\alpha^\circ}\right].
\end{aligned}\right\} \qquad (29.8)$$

Here ξ_0 - the dimensionless coordinate new began relatively old.

For wings with constant sweepback the distance from the leading edge/nose of root chord to leading edge/nose MAC is determined from the formula

$$\frac{h_a}{b}=\frac{\lambda\,\mathrm{tg}\,\chi_0}{12}\,\frac{\eta+2}{\eta}. \qquad (29.9)$$

Mean aerodynamic center of wing relative to leading edge/nose $b_a\,\bar{x}_F=x_F/b_a$ can be obtained, by utilizing a value of the focus $\bar{x}_{q_l}=x_{q_l}/b$, undertaked relative to leading edge/nose b:

$$\left.\begin{aligned}
&\bar{x}_F=\frac{b}{b_a}\left(\bar{x}_{q_l}-\bar{z}_a\frac{l}{2b}\,\mathrm{tg}\,\chi_0\right),\\
&\bar{z}_a=\frac{1}{3}\,\frac{\eta+2}{\eta+1},\quad \frac{l}{b}=\frac{\lambda}{2}\left(1+\frac{1}{\eta}\right).
\end{aligned}\right\} \qquad (29.10)$$

Page 727.

§2. Special feature/peculiarities of a change in the transient functions.

Let us note some special feature/peculiarities of a change in the transient function of aerodynamic wing characteristics, when the kinematic parameters are changed in the course of time according to stepped law.

During a change in the angle of attack and angular velocities at the initial moment $\tau = 0$ derivatives $\dot{\alpha}$, $\dot{\omega}_z, \dot{\omega}_{x1}$ have infinite values. This leads to a sharp, abrupt change in the aerodynamic wing characteristics.

In the incompressible medium $(M = 0)$ disturbance/perturbation they are spread instantly; therefore they cover entire mass of liquid. At torque/moment $\tau = 0$ on wing is realized noncirculating flow, since free vortices on wing and after it to converge still not began. But in this case forces and torque/moments on wing will be equal to infinity, because they are proportional to the derivatives (see about this in more detail in §9 chapters II and §5 of chapter VI) indicated. At the following torque/moment $(\tau > 0)$ on an entire wing surface will occur the departure/withdrawal of free vortices from those which were connected and will arise the circulation scheme of flow with the execution of chaplygina - Joukowski's hypothesis on trailing wing edges. Forces and torque/moments instantly accept the finite values, but further begins the regular part of the transient process.

In the compressed medium ($M \neq 0$) disturbance/perturbation they are spread at the final speed, equal to the speed of sound. In connection with this with $\tau = 0$ aerodynamic forces and moments take the finite values, the lesser, the greater the number M. Then they decrease, but not abruptly, as in the incompressible medium, and gradually, but the more intensely, the less M. The subsequent part of the transient process in compressed and incompressible the media is qualitatively identical.

Although the boundary conditions on wing in α-, ω_{x1}- and ω_z- problems with $\tau > 0$ do not change in the course of time however occurs at first readjustment of vortex/eddy system on wing and after it. A circulation control of bound vortexes on wing is accompanied by the removal/drift of equally contrasted/opposed free vortices with those direction of axes. Thus far trace affects wing, producing on it unsteady tapers, is changed and the circulation of bound vortexes, but that means change all the aerodynamic characteristics. At subsonic speeds ($M < 1$) this will occur theoretically infinite time. Therefore transient process here bears asymptotic character. At supersonic speeds ($M > 1$) disturbance/perturbation they are spread only downstream from perturbation source. To flow around of the wing in this case affect the only transient vortices, which go

over wing, but with subsonic trailing edges - and certain limited part of the wing wake.

Page 728.

Transient process continues finite time and concludes with certain $\tau = \tau_k$. It is not difficult to see that according to the termination of the transient process of function $[c_y/\alpha^*]$, $[c_y/\omega_z^*]$, $[m_{x1}/\omega_{x1}^*]$ are taken respectively the values of aerodynamic derivatives c_y^α, $c_y^{\omega_z}$, $m_{x1}^{\omega_{x1}}$, found at the same numbers M for $p^* \longrightarrow 0$.

Upon the gradual entrance of the wing-plate of arbitrary planform into the gust of disturbance/perturbation they appear for the first time with $\tau = 0$, when begins the entrance of wing into gust. At the initial moment, obviously, the lift and torque/moment are equal to zero. With a entrance of wing into gust and an increase in the range, which experience/tests its direct effect, the lift and torque/moment in absolute value increase at first. The limiting values, which correspond $\tau \longrightarrow \infty$ with $M < 1$ and $\tau = \tau_k$ with $M > 1$, will be equal to c_y^α for $[c_y/w_{y\Delta}^*]$ and m_z^α for $[m_z/w_{y\Delta}^*]$, since $w_{y\Delta}^* = W_{y\Delta}^*/U_0 = \alpha^*$.

§3. Effect of the geometric parameters of wing on transient

functions.

Common/general/total considerations on the effect of the geometry of wing on its aerodynamic characteristics are presented in the preceding/previous chapter. Much from the aforesaid about the effect of geometric parameters wing on the coefficients of aerodynamic derivatives almost completely can be attributed to transient functions, if one compares wing characteristics at the fixed values of the moments of time τ = const. Therefore we will not give the in detail indicated data, but in addition to the aforesaid, above let us test of transient functions in all range of a change in the dimensionless time τ.

On Figs 29.1-29.4 for subsonic speeds are given transition functions $[c_y/\alpha^*]$ and the corresponding to them coordinates of focus $\bar{x}_\alpha$ for three wings of the simplest planform with lengthening λ = 2.5: 1 - rectangular, 2 - triangular and 3 - swept (χ_0 = 60°, - two wings of complex planform (see Fig. 2.5): 4 - λ = 7.4, $\chi_0^{(1)}$ = 72°,5, $\chi_0^{(2)}$ = 15° and 5 - λ = 3.2, $\chi_0^{(1)}$ = 72°,5, $\chi_0^{(2)}$ = 60°.

In the incompressible medium (M = 0) during an instantaneous change in the kinematic parameters q_i at the initial moment τ = 0 transient functions $[c_y/q_i^*]$, $[m_z/q_i^*]$, $[m_{x1}/\omega_{x1}^*]$ go to infinity. Then their

values in absolute value instantly fall, reaching finite quantity. Subsequently occurs smooth approach/approximation to the steady-state values, which correspond $\tau \longrightarrow \infty$ (dot-dash line on curve/graphs).

Page 729.

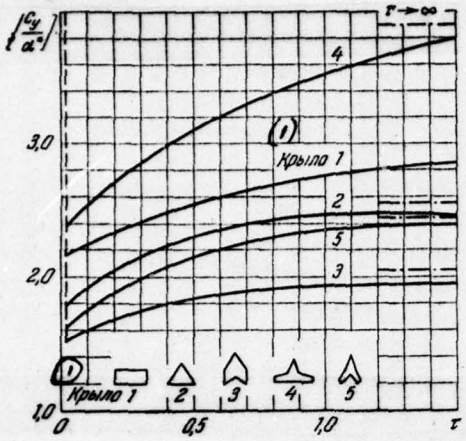


Fig. 29.1. Dependence of transient function $[c_y/\alpha^\circ]$ of dimensionless time $\tau_{(M=0)}$.

Key: (1). Wing.

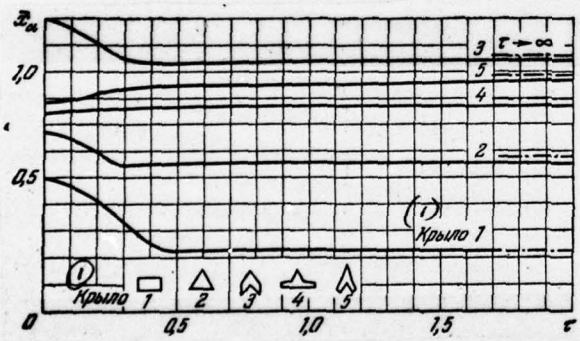


Fig. 29.2. Dependence of unsteady focus $\bar{x}_\alpha$ on dimensionless time $\tau_{(M=0)}$.

Key: (1). Wing.

Page 730

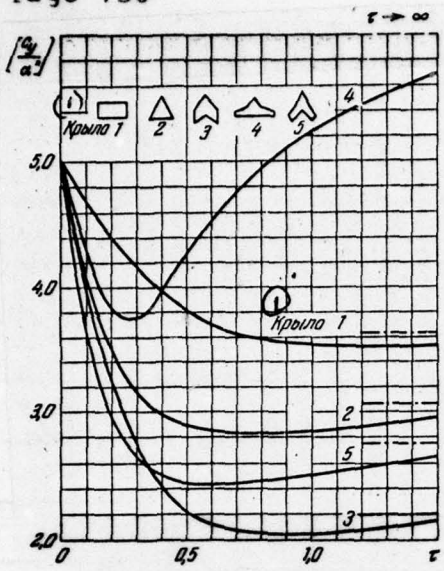


Fig. 29.3. Dependence of transient function $[c_y/\alpha^\circ]$ of dimensionless time $\tau_{(M=0,8)}$.

Key: (1). Wing.

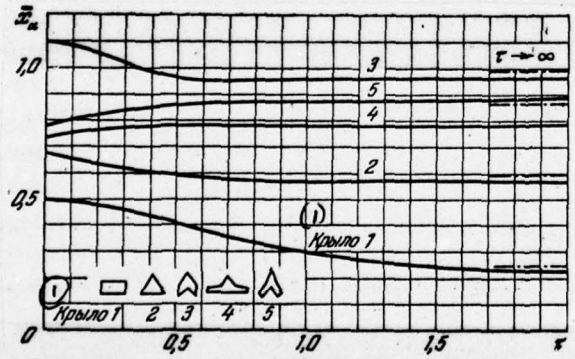


Fig. 29.4. Dependence of unsteady focus $\bar{x}_\alpha$ on dimensionless time $\tau_{(M=0,8)}$.

Upon the gradual entrance of wing into the gust, which for rectangular and delta wings begins with $\tau = 0$ and concludes into torque/moment $\tau = 1$, transient functions $[c_y/w^*_{y\Delta}]$ and $[m_z/w^*_{y\Delta}]$ they grow/rise in absolute value from zero to steady-state value. Transient process with $M \leqslant 1$ continues infinitely for long, and with $M > 1$ - finite time.

At high subsonic speeds $(M = 0,8)$ and an with instantaneous change in the kinematic parameters into torque/moment $\tau = 0$ transient function $[c_y/\alpha^*]$ takes the finite value. It is identical for all wing planforms and in the case in question $(M = 0,8)$ is equal to $[c_y/\alpha^*]$ $= 4/M = 5,0$ (see Fig. 29.3).

The given materials (see Figs. 29.1-29.4) they show also, as affects wing planform the transient function $[c_y/\alpha^*]$ and the position of focus $\bar{x}_\alpha$ in subsonic range $(0 < M < 1)$.

Characteristic from the viewpoint of the effect of wing aspect ratio to transient functions are the curve/graphs, on which are constructed the relations of form $|c_y(\tau)/q^*_i|/|c_y(\infty)/q^*_i|$ depending on dimensionless quantity τ. The greatest effect of lengthening is observed at low values τ - in the beginning of transient process,

then during increase τ the value of this the relationship approaches unity. On diagrams (Figs. 29.5-29.8) are depicted the dependences of transient functions with $M = 0$ for different lengthenings of rectangular wing, including the limiting case of the wing of very small lengthening ($\lambda \longrightarrow 0$) dotted line on curve/graphs).

At high subsonic speeds more visually the effect of wing aspect ratio can be traced on the curve/graphs, where are depicted transient functions themselves, but not their relation. This is connected with the fact that with $\tau = 0$ functions in question do not depend on wing aspect ratio λ and all the curves begin at cne point (Figs. 29.9-29.11). As is evident, with $\lambda \longrightarrow 0$ transient functions approach the limiting values, indicated by dotted line. For a Δ-problem these values are everywhere equal to zero (Fig. 29.12). In α-, ω_z- and ω_{x1}-problems within limit is obtained interruption the function. With $\tau = 0$ it is equal to the finite quantity, determined by formulas §3 chapter IV, while with $\tau > 0$ it turns into zero.

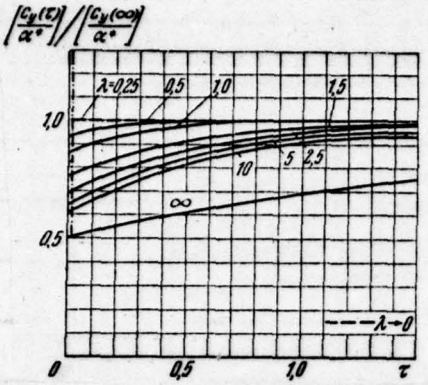


Fig. 29.5. Effect of lengthening rectangular wing on transient function $[c_y/\alpha^\circ]$ with M=0.

Page 732.

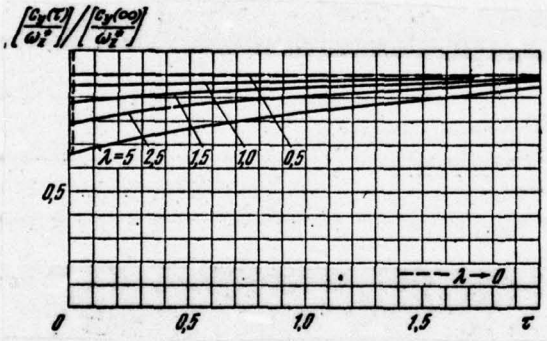


Fig. 29.6.

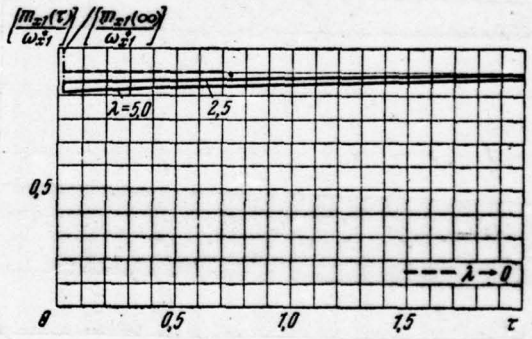


Fig. 29.7.

Fig. 29.6. Effect of lengthening rectangular wing on transient function $[c_y/\omega_z^\circ]$ with M=0, $\bar{x}_T$=0.

Fig. 29.7. Effect of lengthening rectangular wing on transient function $[m_{x1}/\omega_{x1}^\circ]$ with M=0.

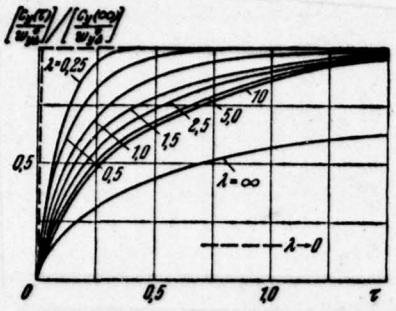


Fig. 29.8. Effect of lengthening rectangular wing on transient function $[c_y/\omega^{\circ}_{y\Delta}]$ with M=0.

Page 733.

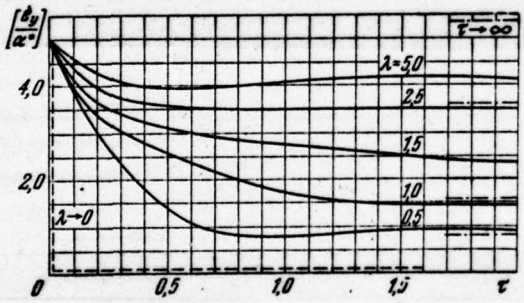


Fig. 29.9.

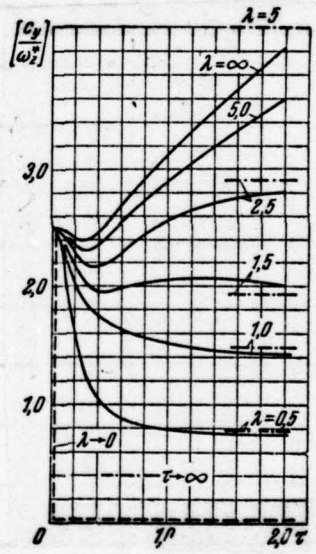


Fig. 29.10.

Fig. 29.9. Effect of lengthening rectangular wing on transient function $[c_y/\alpha^{\circ}]$ with M=0,8.

Fig. 29.10. Effect of lengthening rectangular wing on transient function $[c_y/\omega^{\circ}_z]$ with M=0,8, $\bar{x}_T$=0.

Page 734.

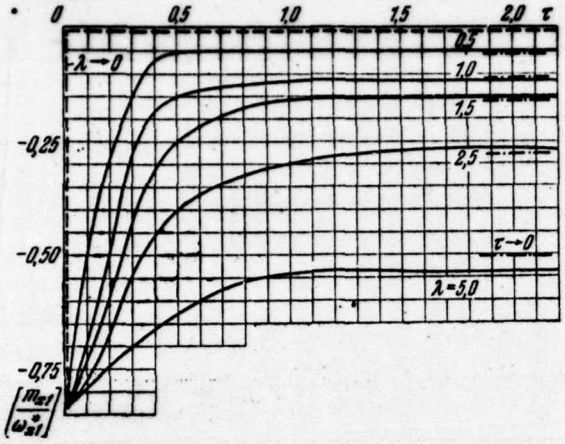


Fig. 29.11. Effect of lengthening rectangular wing on transient function $[m_{x1}/\omega^{\circ}_{x1}]$ with M=0.8.

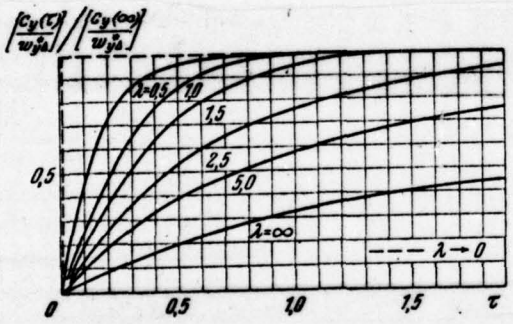


Fig. 29.12.

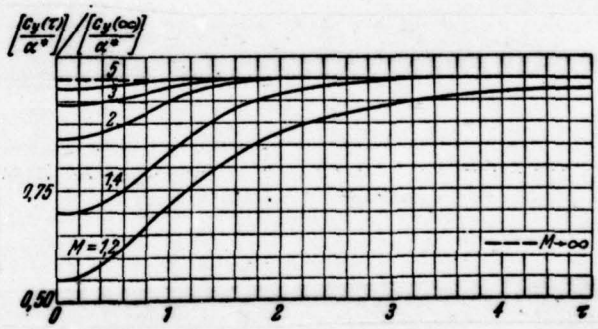


Fig. 29.13.

Fig. 29.12. Effect of lengthening rectangular wing on transient function $[c_y/\omega^{\circ}_{y\Delta}]$ with M=0.8.

Fig. 29.13. Effect of number M on transient function $[c_y/\alpha^{\circ}]$ delta wing with supersonic edges.

Page 735.

At supersonic speeds ($M>1$) and with instantaneous change in the kinematic parameters, when the number M grow/rises within limit $\frac{4}{\sqrt{M^2-1}} \to \frac{4}{M}$, transient functions will be virtually constant in all range τ (Figs. 29.13, 29.14).

§4. Effect of number M on transient functions.

In addition to the materials, given above, let us examine the transient functions of the rigid rectangular and delta wings of one and the same lengthening ($\lambda = 2.5$) with different most characteristic Mach numbers ($M = 0$; 0.8; 1.2; $\sqrt{2}$; 2.0; 3.0). Is studied the gradual entrance of wing into step gust (Δ-problem) and a stepped variation in the kinematic parameters of rigid wing (α-, ω_z- and ω_{x1}-problems). The effect of numbers M on the characteristics of the deforming wings in many respects is analogous with the cases indicated. In order to illustrate the basic special

feature/peculiarities of the transient process of flexible wing, to Figs. 29.15-29.18 are given the curve/graphs of the transient functions of airfoil/profile with control ($\bar{b}_p = 0{,}25$). These functions, obtained by direct/straight calculation also according to reciprocity theorem, correspond to centering $\bar{x}_T = 0$ and to numbers $M = 0.1$ 0.6 and 0.9. Let us note that with $M > 1$ the deflection of control does not produce disturbance/perturbations on the front part of the airfoil/profile. Therefore the transient functions of airfoil/profile with control do not require special examination and can be obtained by the simple recalculation of the corresponding characteristics of rigid wing.

For the cases of the value of transient functions indicated at $\tau = 0$, obtained by precise formulas §3 chapters IV, are represented in the form of Tables 29.1, 29.2 and 29.3.

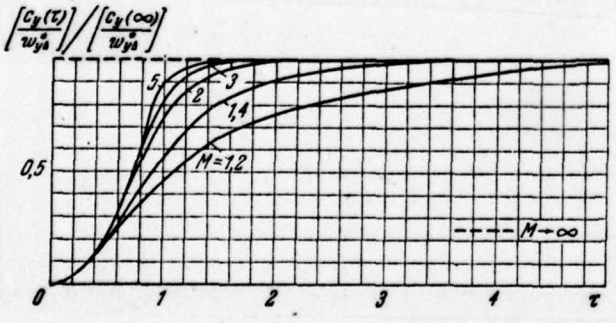


Fig. 29.14. Effect of M number on transient function $[c_y/w^*_{y\Delta}]$ of a delta wing with supersonic edges.

Page 736.

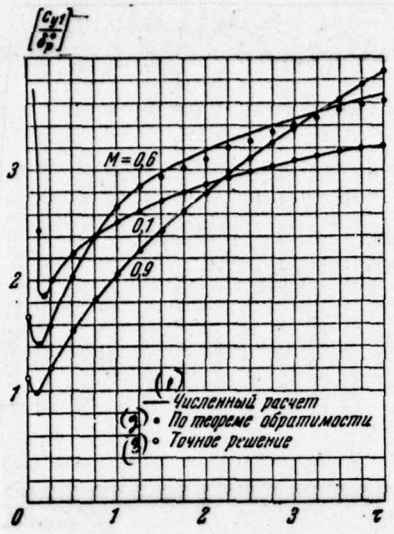


Fig. 29.15.

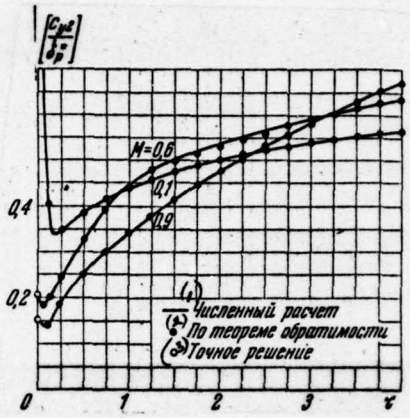


Fig. 29.16.

Fig. 29.15. Effect of number M on transient function $[c_{y1}/\delta_p^\circ]$ wing λ = ∞.

Key: (1). Numerical calculation. (2). According to reciprocity theorem. (3). Exact solution.

Fig. 29.16. Effect of number M on transient function $[c_{y2}/\delta_p^\circ]$ wing λ = ∞.

Key: (1). Numerical calculation. (2). According to reciprocity theorem. (3). Exact solution.

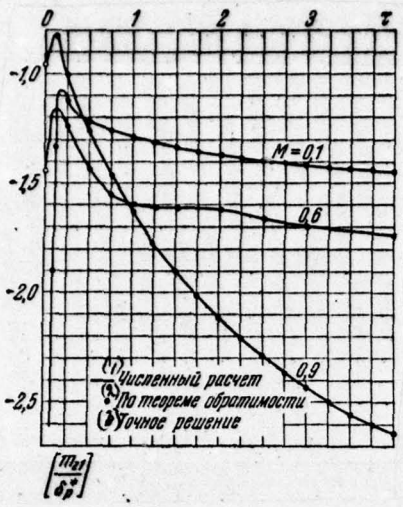


Fig. 29.17.

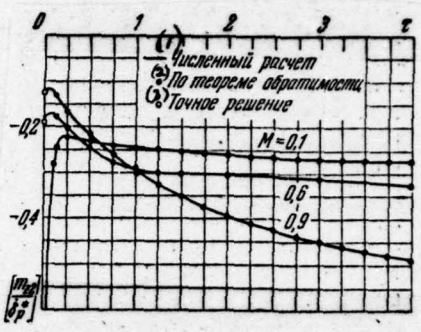


Fig. 29.18.

Fig. 29.17. Effect of number M on transient function $[m_{z1}/\delta_p^*]$ wing λ = ∞, $\bar{x}_T = 0$.

Key: (1). Numerical calculation. (2). According to reciprocity theorem. (3). Exact solution.

Fig. 29.18. Effect of number M on transient function $[m_{z2}/\delta_p^*]$ wing λ = ∞, x_T=0.

Page 737.

On curve/graphs (Figs. 29.19-29.32) dotted line showed the limiting

values of the transient functions, which at subsonic speeds are reached asymptotically at $\tau \longrightarrow \infty$, while on supersonic - at $\tau = \tau_k$.

Given data (Figs. 29.19-29.32) confirm common/general/total considerations about the compressibility effect of the medium (number M) on the character of transient process, expressed earlier. Let us note one fact, very important for practical application/appendices. During an increase in the number M at supersonic speeds transient functions increasingly less differ from their steady-state values, which correspond $\tau = \tau_k$. During increase M the role of purely unsteady aerodynamic characteristics decreases. Most substantially their role is exhibited at subsonic and transonic speed.

Table 29.1. Values of the transient functions of airfoil/profile with control at the initial moment $\tau = 0$ $(\bar{b}_p = 0{,}25,\ \bar{x}_\tau = 0)$

M	0,1	0,6	0,9
$\left[\frac{c_{y1}}{\dot{\delta}_p^*}\right]$	10,00	1,67	1,155
$\left[\frac{c_{y2}}{\dot{\delta}_p^*}\right]$	1,25	0,209	0,139
$\left[\frac{m_{z1}}{\dot{\delta}_p^*}\right]$	−8,75	−1,46	−0,975
$\left[\frac{m_{z2}}{\dot{\delta}_p^*}\right]$	−1,14	−0,190	−0,127

Table 29.2. Values of the transient functions of rectangular wings at the initial moment $\tau = 0$ $(\bar{x}_\tau = 0)$

M	0,8	1,2	1,41	2,0	3,0
$\left[\frac{c_y}{\alpha^*}\right]$	5,0	3.33	2,83	2,0	1,33
$\left[\frac{c_y}{\omega_z^*}\right]$	2,5	1,5	1,42	1,0	0,666
$\left[\frac{m_{x1}}{\omega_{x1}^*}\right]$	−0,833	−0,555	−0,473	−0,334	−0,223
$\bar{x}_\alpha$	0,5	0,5	0,5	0,5	0,5
$\bar{x}_{\omega_z}$	0,666	0,666	0,666	0,666	0,666

Page 738.

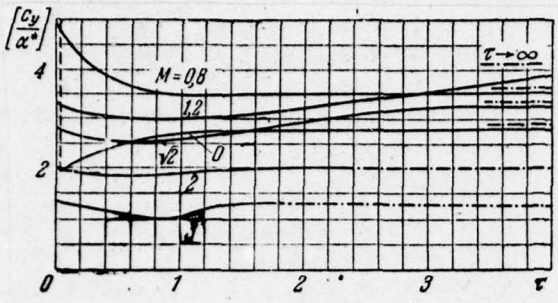


Fig. 29.19.

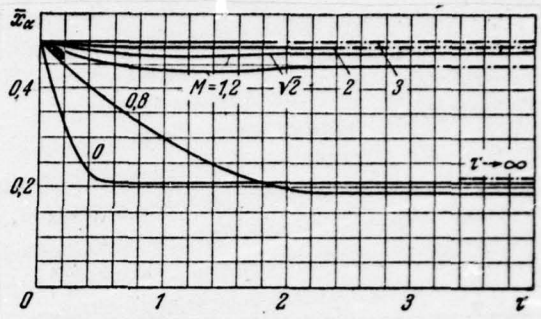


Fig. 29.20.

Fig. 29.19. Effect of number M on transient function $[c_y/\alpha^\circ]$ rectangular wing $\lambda = 2.5$.

Fig. 29.20. Effect of number M on the unsteady focus of the $\bar{x}_\alpha$ of rectangular wing $\lambda = 2.5$.

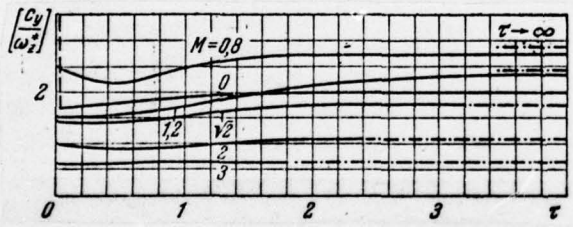


Fig. 29.32. Effect of number M on transient function $[c_y/\omega_z^\circ]$ rectangular wing $\lambda = 2.5$, $\bar{x}_T = 0$.

Page 739.

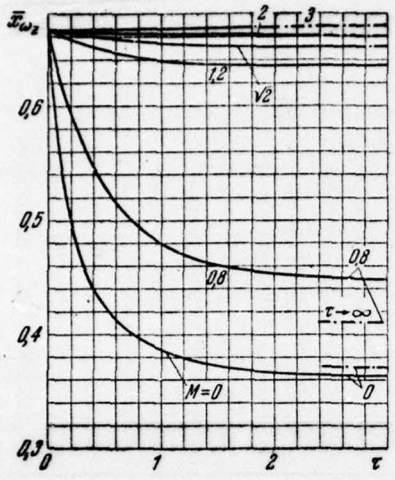


Fig. 29.22.

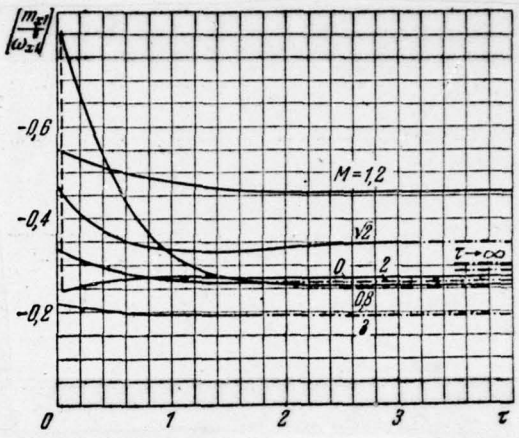


Fig. 29.23.

Fig. 29.22. Effect of number M on unsteady focus $\bar{x}_{\omega_z}$ rectangular wing $\lambda = 2.5$.

Fig. 29.23. Effect of number M on transient function $[m_{x1}/\omega_x^*]$ rectangular wing $\lambda = 2.5$.

Page 740.

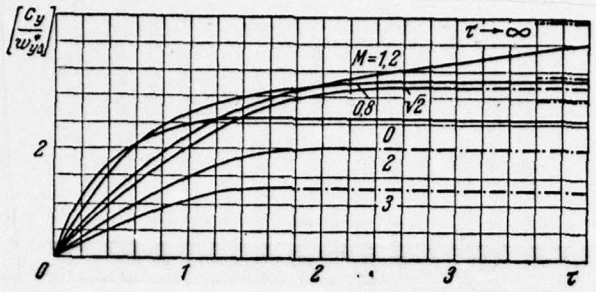


Fig. 29.24. Effect of number M on transient function $[c_y/w^{\circ}_{y\Delta}]$ rectangular wing $\lambda = 2.5$.

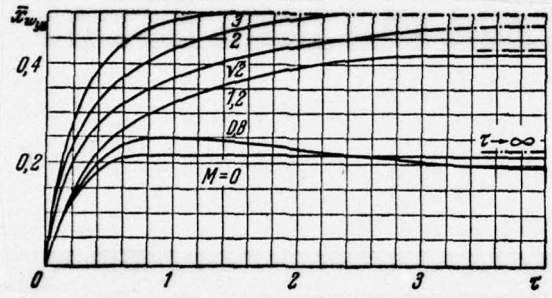


Fig. 29.25.

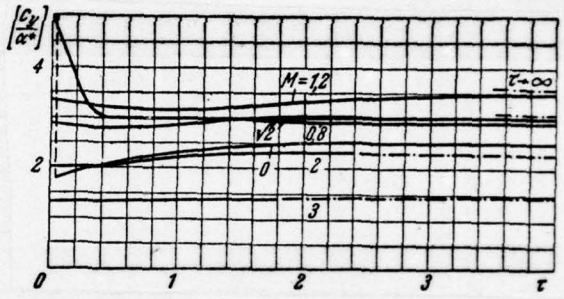


Fig. 29.26.

Fig. 29.25. Effect of number M on unsteady focus $\bar{x}_{w_{y\Delta}}$ rectangular wing $\lambda = 2.5$.

Fig. 29.26. Effect of number M on transient function $[c_y/\alpha^{\circ}]$ delta wing $\lambda = 2.5$.

Page 741.

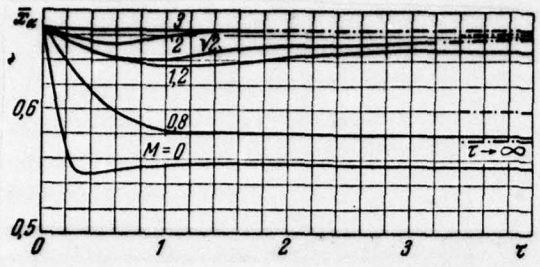


Fig. 29.27. Effect of number M on unsteady focus $\bar{x}_\alpha$ delta wing λ = 2.5.

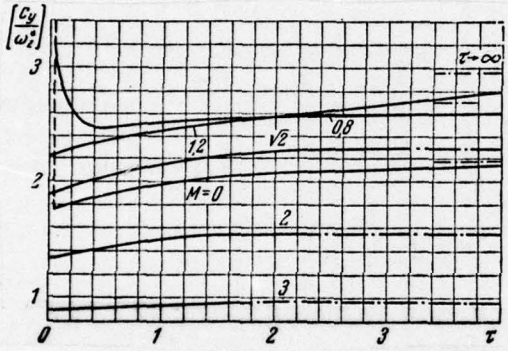


Fig. 29.28.

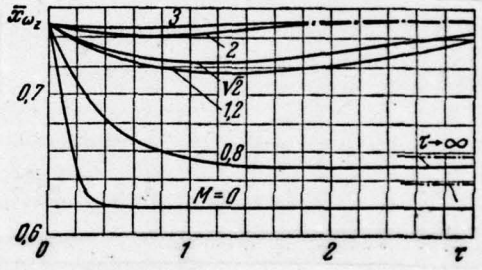


Fig. 29.29.

Fig. 29.28. Effect of number M on transient function $[c_y/\omega_z^*]$ delta wing λ = 2.5, $\bar{x}_T$=0.

Fig. 29.29. Effect of number M unsteady focus $\bar{x}_{\omega_z}$ delta wing λ = 2.5.

Page 742.

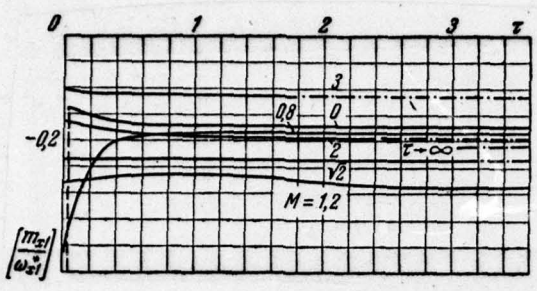


Fig. 29.30.

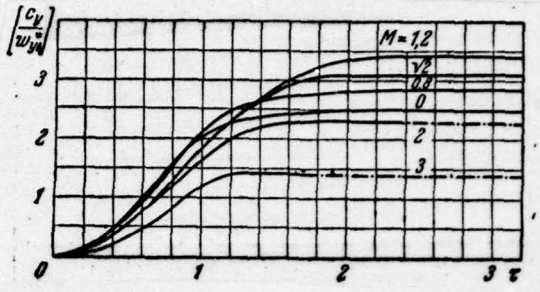


Fig. 29.31.

Fig. 29.30. Effect of number M on transient function $[m_{x1}/\omega_{x1}^{\circ}]$ delta wing $\lambda = 2.5$.

Fig. 29.31. Effect of number M on transient function $[c_y/\omega_{y\Delta}^{\circ}]$ delta wing $\lambda = 2.5$.

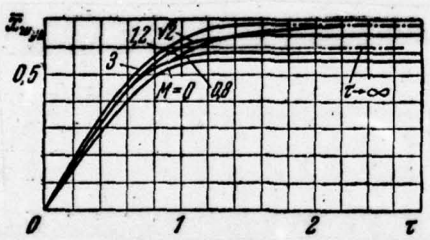


Fig. 29.32. Effect of number M on unsteady focus $\bar{x}_{\omega_{y\Delta}}$ delta wing $\lambda = 2.5$.

Page 743.

§5. Effect of the laws of motion for transient functions.

Knowing the reaction of wing for single step function, with the aid of this transient function and Duhamel integral can be passed to the arbitrary law of a change in the kinematic parameters.

Let us examine the law, which satisfies the conditions:

$$f(\tau)=\begin{cases} k\tau & \text{with } 0\leqslant\tau\leqslant\tau_0, \\ 1 & \text{with } \tau\geqslant\tau_0. \end{cases} \qquad (29.11)$$

Let parameter k, which characterizes the law of motion ($k = \operatorname{tg}\gamma = 1/\tau_0$), it is changed from 0 to ∞. Then case $k = 0$ ($\tau_0 = \infty$) will correspond to a very slow change in the parameter, when is valid stability hypothesis; case $k = \infty$ ($\tau_0 = 0$) - to the stepped law of a change in the kinematic parameters. Besides the enumerated limiting cases let us examine intermediate values of k = 0.2; 1.0; 5.0 (Fig. 29.33). For entire range of change k = 0-∞ are given transient functions for a delta wing $\lambda = 2.5$ in the incompressible medium (Figs. 29.34 and 29.35), at high subsonic speeds $M = 0{,}8$ (Fig. 29.36) and supersonic speeds $M = 3{,}0$ (Fig. 29.37).

Is given also change in the transient function $(c_y/\omega^{\cdot}_{y\Delta})$ upon

the gradual entrance of wing into the gust: for a rectangular wing with $M = 0,8$ (Fig. 29.38) and triangular with $M = 3$ (Fig. 29.39).

Table 29.3. Values of the transient functions of delta wings at the initial moment $\tau = 0$ ($\bar{x}_\tau = 0$)

M	0,8	1,2	1,41	2,0	3,0
$\left[\frac{c_y}{\alpha^*}\right]$	5,0	3,33	2,83	2,0	1,33
$\left[\frac{c_y}{\omega_z^*}\right]$	3,33	2,23	1,89	1,34	0,89
$\left[\frac{m_{x1}}{\omega_{x1}^*}\right]$	−0,416	−0,277	−0,236	−0,167	−0,111
$\bar{x}_\alpha$	0,666	0,666	0,666	0,666	0,666
$\bar{x}_{\omega_z}$	0,75	0,75	0,75	0,75	0,75

Page 744.

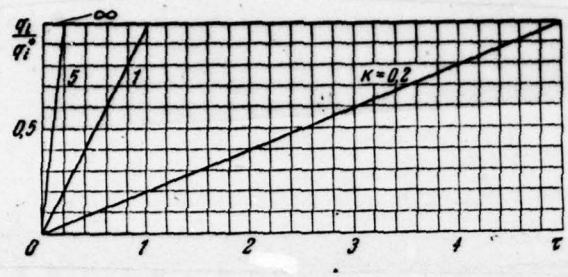


Fig. 29.33. Investigated laws of the motion of wing.

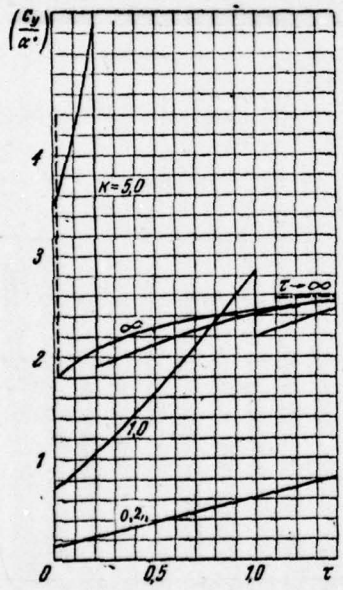


Fig. 29.34.

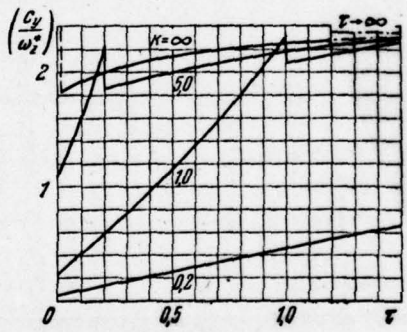


Fig. 29.35.

Fig. 29.34. Transient function (c_y/α^0) for the different laws of the motion of delta wing $\lambda=2,5$ $(M=0)$.

Fig. 29.35. Transient function (c_y/ω_z^0) for the different laws of the motion of delta wing $\lambda=2,5$ $(M=0,\ x_T=0)$.

Page 734.

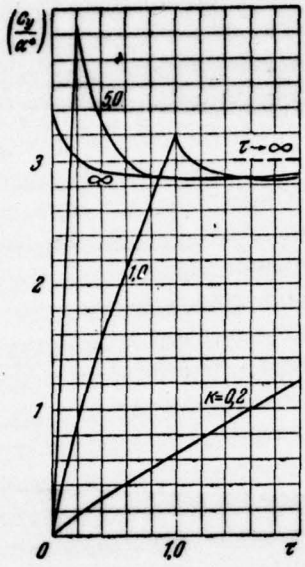


Fig. 29.36.

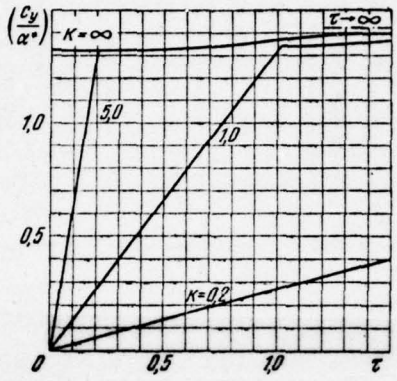


Fig. 29.37.

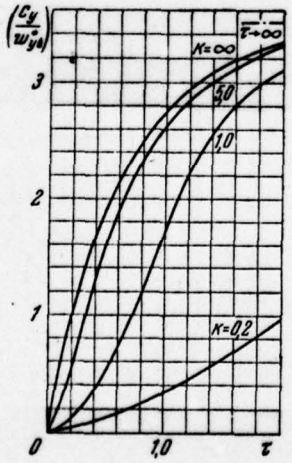


Fig. 29.38.

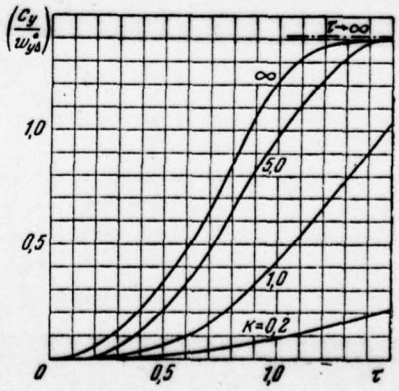


Fig. 29.39.

Fig. 29.36.
Transient function (c_y/α^*) for the different laws of the motion of delta wing $\lambda = 2,5$ $(M = 0,8)$.

Fig. 29.37. Transient function (c_y/α^*) for the different laws of the motion of delta wing with supersonic edges $(M = 3)$.

Fig. 29.38. Transient function $(c_y/\omega^*_{y\Delta})$ for the different laws of the motion of rectangular wing $\lambda = 2,5$ $(M = 0,8)$.

Fig. 29.39. Transient function $(c_y/\omega^*_{y\Delta})$ for the different laws of the motion of delta wing with supersonic edges $(M = 3)$.

Page 746.

Law f (τ) has two characteristic sections: the first for the values of dimensionless time $0 < \tau < \tau_0$ and the second for an interval $\tau_0 < \tau < \infty$. During an instantaneous change in the kinematic parameters aerodynamic characteristics have a fracture with $\tau = \tau_0 = 1/k$. The peak of aerodynamic characteristics is observed at the same values τ, for which occurs the fracture in the law of a change in the kinematic parameters in τ. The value of peak the more greater, the more powerful this fracture. With $k = \infty$ in the incompressible medium

this peak for torque/moment $\tau \to 0$ approaches ∞. With an increase of number M the maximum value of this peak descends. Upon the gradual entrance of wing into gust aerodynamic characteristics are changed smoothly in time from zero value with $\tau = 0$. With $\tau \to \infty$ all the characteristics approach maximum steady-state values (dotted line on diagrams).

Page 747.

1. Literature in the Russian language.

1.1. N. Ye, Joukowski, on bound vortexes. Collected works, Vol. IV, the State Technical Press, Moscow, 1949.

1.2. N. Ye. Joukowski, ~~Teoreticheskiyes the~~ Theoretical basis of aeronautics. Collected works, Vol. V, the State Technical Press, Moscow, 1950.

1.3. N. Ye. Zhukovsiy, the vortex conception of screw propeller. Collected works, Vol. IV, the State Technical Press, Moscow, 1949.

1.4. S. A. Chaplygin, Results of theoretical studies about the motion of airplanes. Collected works, Vol. II, the State Technical Press, Moscow, 1948.

1.5. S. A. Chaplygin, about the pressure of plane-parallel flow to the obstructing bodies (to the theory of airplane). Collected works, Vol. II, the State Technical Press, Moscow, 1948.

1.6. S. A. Chaplygin, about the effect of plane-parallel airflow to the driving in it cylindrical body. Collected works, Vol. II, Gostekhnizdat, Moscow, 1948.

1.7. A. I. Nekrasov airfoil theory in unsteady flow, the publishing house of the AS USSR, Moscow, 1947.

1.8. R. Zauyer, ~~Vvedeniyes~~ Introduction into gas dynamics, the trans. with Ger., the State Technical Press, Moscow, 1947.

1.9. F. I. Frankl', Ye. A. Karpovich, ~~Gazodinamik~~ gasdynamics, the State Technical Press, Moscow, 1948.

1.10. L. Prandtl. , ~~Gidromekhanik~~ Fluid mechanics, trans. ~~with~~ from Ger., IL, Moscow, 1949.

1.11. V. V. Golubyov, ~~Lektsii~~ Lectures on airfoil theory, the State Technical Press, Moscow, 1949.

1.12. L. I. Sedov, ~~Ploskiyes the task~~ Two-dimensional problems of hydrodynamics the

aerodynamicists, the State Technical Press, Moscow, 1950.

1.13. A. K. Martynov, ~~Eksperimental'naya~~ Experimental aerodynamics, Oborongiz, Moscow, 1950.

1.14. S. P. Strelkov, ~~Vvedeniye in~~ Introduction to the theory of oscillations, the State Technical Press, Moscow, 1951.

1.15. Ye. A. Krasil'syuchyuikov, ~~Krylo~~ A wing in compressible flow, the State Technical Press, Moscow, 1952.

1.16. L. I. Sedov, ~~Metody~~ Methods and dimensionality in mechanics, the State Technical Press, Moscow, 1954.

1.17. U. F. Hilton, ~~the aerodynamicist~~ Aerodynamics of high speeds, trans. with Engl., IL, Moscow, 1955.

1.18. Ye. Karafoli, ~~the aerodynamicist~~ Aerodynamics of the wing of aircraft, trans. from Rumanian. , the publishing house of the AS USSR, Moscow, 1956.

1.19. R. L. Visplinghoff, Kh. Ashley, R. L. Khalfmen, ~~Aerouprugost'~~ Aeroelasticity, trans. from Engl., IL, Moscow, 1958.

1.20. Ya. Ts. Fyn, ~~Vvedeniyes in~~ Introduction to the theory of aeroelasticity, trans. from Engl., Fizmatgiz, Moscow, 1959.

1.21. Aerodynamics of aircraft components at high speeds. Collection of articles edited by A. F. Donoven and G. R. Lawrence, trans. from Engl., IL, Moscow, 1959.

Page 748.

1.22. G. G. Chernyy, ~~Techeniya~~ Flow of a gas at high supersonic speed, Fizmatgiz, Moscow, 1959.

1.23. A. Ferri, ~~aerodynamicist~~ Aerodynamics of supersonic flows, the State Technical Press, Moscow, 1953.

1.24. N. Z. Pinus, S. M. Shmeter, ~~Atmosfernaya~~ Atmospheric turbulence, which affects flight of aircraft, Gidrometeoizdat, Moscow, 1962.

1.25. General theory of high-speed aerodynamics, trans. with Engl., Voenizdat, Moscow, 1962.

1.26. J. U. Mayls, ~~Potentsial'naya the~~ The potential theory of the unsteady supersonic flows, trans. with Engl., Fizmatgiz, Moscow, 1963.

1.27. Yu. P. Dobrolenskiy, V. I. Ivanov, G. S. Pospelov, ~~Avtomatik~~ Automatic equipment of guided missiles, Oborongiz, Moscow, 1963.

1.28. N. Ye. Kochin, I. A. Kibel', N. V. Rose, ~~Teoreticheskaya~~ Theoretical hydromechanics, hr. I, Fizmatgiz, Moscow, 1963.

1.29. S. M. Belotserkovskiy, ~~Tonkaya~~ A thin lifting surface in the subsonic flow of gas, "Nauka", Moscow, 1965.

1.30. I. V., Ostoslavskiy, I. V. Strazheva, the dynamics of flight, stability the controllability of flight vehicles, "machine-building", Moscow, 1965.

1.31. G. S. Byushgens, R. V. Studnev, ~~Dinamik~~ The dynamics of flight, the stability and the controllability of flight vehicles, "machine-building", Moscow, 1965.

1.32. A. S. Vol'mir, ~~Ustoychivost'~~ Stability of the systems being deformed, "science", Moscow, 1967.

1.33. G. A. Gurzhiyenko, ~~Metod the~~ The method of bent models and his application/use to research on the curvilinear flight of airships, the transactions of TsAGI, iss. 182, 1934.

1.34. M. V. Keldysh, M. A. Lavrent'yev, to the theory of oscillating wing. Technical notes of TsAGI, iss. 45, 1935.

1.35. L. I. Sedov, to the theory of the unsteady motions of wing in liquid, the transactions of TsAGI, iss. 229, 1935.

1.36. L. I. Sedov, ~~Teoriya~~ The Theory of unsteady gliding and the motions of wing with trailing vortexes, the transactions of TsAGI, iss. 252, 1936.

1.37. M. V. Keldysh, to the airfoil theory of the final spread/scope, which varies in airflow, report AS USSR 21 (1938), No 5.

1.38. F. I. Frankl', ~~Osnovy~~ Principles of gas dynamics, the transactions of TsAGI, iss. 364, 1938.

1.39. A. L. Reich, Theory and the procedure of experimental determination rotary derivatives, the transactions of TsAGI, Issue 469, 1939.

1.40. L. I. Sedov, about unsteady motion within the liquid of body of revolution, the transactions of TsAGI, iss. 515, 1940.

1.41. A. A. Dorodnitsyn, ~~Obobshcheniye~~ Generalization of lift-line theory to the case of wing with bent axle and the axis, not perpendicular to flow, PMM

VIII (1944), iss. 1.

1.42. L. A. Simonov, S. A. Khristianovich, ~~Vliyaniyes~~ Influence on the induced velocities of wing and screw/propeller, PMM VIII (1944), iss. 2.

1.43. M. I. Gurevich, about the lift of sweptback wing in supersonic flow, PMM X (1946), iss. 4.

1.44. M. I. Gurevich, to the question concerning the fine/thin delta wing, which moves at supersonic speed, PMM XI (1947), iss. 3.

1.45. V. V. Golubyov, to the airfoil theory of small lengthening, Proceedings of the AS USSR, OTN [OTH - Department of Technical Sciences] (1947), No 3.

Page 749.

1.46. M. D. Khaskind, ~~Kolebaniya~~ Oscillations of wing in the subsonic flow of gas, PMM XI (1947), iss. 1.

1.47. I. S. Riemann, R. L. Kreps, the apparent additional mass of the bodies of various forms, the transactions of TsAGI, iss. 635, 1947.

1.48. N. Ye. Kochin, ~~Teoriya~~ Theory of the final spread/scope of circular

planform. Collected works, Vol. II, the publishing house of the AS USSR, Moscow, 1949.

1.49. Kh. Sh. Tzyan, about the two-dimensional unsteady motion of slender body in compressible liquid, trans. with the Engl. collection of articles "gas dynamic loudspeaker", IL, Moscow, 1950.

1.50. T. Karman, Zakony similarity for a transonic flow, a trans. with the Engl. collection of articles "gas dynamic loudspeaker", IL, Moscow, 1950.

1.51. K. K. Fedyaevskiy, S. M. Belotserkovskiy, ~~Aerodinamicheskiye~~ The aerodynamic ~~the~~ forces, which act on above-ground structures with squalls, Proceedings of the AS USSR, OTN (1954), No 6.

1.52. S. M. Belotserkovskiy, ~~Prostranstvennoye~~ Spatial the unsteady motion of lifting surface, PMM XIX (1955), iss. 4.

1.53. S. M. Belotserkovskiy, horseshoe vortex during unsteady motion, PMM XIX (1955), iss. 2.

1.54. M. N. Kogan, ~~Nekotoryye the~~ Certain integral properties of supersonic flows, the transactions of TsAGI, iss. 687, 1955.

1.55. S. M. Belotserkovskiy, ~~Predstavleniyes~~ Representation of unsteady aerodynamic torque/moments and forces with the aid of the coefficients of rotary derivatives, Proceedings of the AS USSR, OTN (1956), No 7.

1.56. P. I. Chushkin, ~~Chalchulation~~ Calculation of circulation distribution according to rectangular low-aspect-ratio wings. Collection "theoretical works on aerodynamics", Oborongiz, Moscow, 1957.

1.57. G. A. Kolesnikov, Metod ~~the~~ of calculation of the circulation distribution of low-aspect-ratio wings. Collection "theoretical works on aerodynamics", Oborongiz, Moscow, 1957.

1.58. V. V. Struminskiy, N. K. Lebed', Method ~~the~~ of calculation of circulation distribution according to the spread/scope of sweptback wing. Collection "theoretical works on aerodynamics", Oborongiz, Moscow, 1957.

1.59. N. F. Vorobyev, the unsteady motion of finite-span wing in supersonic flow in the case of an abrupt change in the speed, Proceedings of the AS USSR, MIM 1959, No 7.

1.60. S. M. Belotserkovskiy, ~~Issledovaniya~~ Studies in the theoretical determination of the coefficients of rotary derivatives. First All-Union congress/descent on theoretical and applied mechanics.

Abstracts of reports, the publishing house of the AS USSR, Moscow, 1960.

1.61. N. N. Polyakhov, ~~Teoriya the~~ The theory of unsteady motions of lifting surface, the publishing house of Leningrad university, 1960.

1.62. B. I. Ul'yanov, ~~Nekotoryes~~ Certain generalization and consequences of reciprocity theorem for unsteady motions, Proceedings of the AS USSR, MIM (1961), No 1.

1.63. M. K. Fursov, on the calculation of the ccefficients wing rotary derivative at supersonic speeds, Proceedings of the AS USSR, MIM (1961), No 2.

1.64. S. M. Belotserkovskiy, A. S. Ginevskiy, Ya. Ye. Polonskiy, ~~Aerodinamicheskiyes the~~ The aerodynamic forces, which act on airfoil cascade with unsteady flow; Industrial aerodynamics, iss. 20, Oborongiz, Moscow, 1961.

Page 750.

1.65. A. I. Golubinskiy, On the flow of being moved shock wave about the driving plate, engineering journal I (1961), iss. 2.

1.66. Yu. P. Dobrolenskiy, ~~Turbulentnost'~~ Turbulence as perturbation source for automatic control systems of aircraft, Proceedings of the AS USSR, power engineer automation (1961), No 5.

1.67. S. M. Belotserkovskiy, A. S. Ginevskiy, Ya. Ye. Polonskiy, ~~Gidrodinamicheskaya~~ The hydrodynamic the cascade theory. Power and moment aerodynamic characteristics of airfoil cascade, industrial aerodynamics, iss. 22, Oborongiz, Moscow, 1962.

1.68. A. I. Golubinskiy, the lift and the torque/moment of fine/thin airfoil/profile during arbitrary unsteady flow, engineering journal III (1963), iss. 3.

1.69. S. M. Belotserkovskiy, B. K. Skripach, V. G. Tabachnikov, to the determination of the coefficients of rotary derivatives in wind tunnels, Proceedings of the AS USSR, MZM (1964), No 3.

1.70. K. K. Fedyaevskiy, the rotary derivatives of the fine/thin wing of maximally small lengthening arbitrary planform. Collection of articles in aerohydrodynamics, the transactions of TsAGI, iss. 940, 1964.

1.71. S. M. Belotserkovskiy, Metod the calculation of the coefficients rotary derivative and of the apparent additional masses

of the fine/thin wing of arbitrary planform. Collection of articles in aerohydrodynamics, the transactions of TsAGI, iss. 940, 1964.

1.72. S. M. Belotserkovskiy, N. A. Kudryavtseva, V. G. Tabachnikov, experimental check of some positions of unsteady theory for finite-span wings, Proceedings of the AS USSR, MIM (1964), No 4.

1.73. V. G. Tabachnikov, I. B. Fedorov, the experimental determination of the coefficients of rotary derivatives by the method of curvilinear models, Proceedings of the AS USSR, Mekhanika (1965), No 4.

1.74. S. M. Belotserkovskiy, Role of the work of N. Ye. Joukowski, "On bound vortices" in the development of wing theory, Publication of BNI TsAGI, Moscow, 1966.

1.75. S. M. Belotserkovskiy, ~~Osobennosti~~ Features of the flow-field analysis of the wings of complex planform at subsonic speeds, MZhG (1966), No 6.

1.76. S. M. Belotserkovskiy, Method of the calculation of the effect of gust on arbitrarily fine/thin wing, MZhG (1966), No 1.

1.77. S. M. Belotserkovskiy, B. I. Ulianov, V. S. Khomenko, ~~Nekotoryye~~ Certain the questions of the procedure of the measurement of instantaneous pressures, MZhG (1966), No 2.

1.78. I. S. Shcherbakov, ~~krylo~~ a wing of simple planform in the sharply limited gust, MZhG (1966), No 2.

1.79. G. A. Kolesnikov, Method of the calculation of the unsteady aerodynamic characteristics of the lifting surface, which moves at high subsonic speed, MZhG (1967), No 6.

1.80. S. M. Belotserkovskiy, R. I. Shtepnberg, Questions of ~~Voprosy~~ aerodynamics of the wings of complex planform. Third All-Union congress/descent on theoretical and applied mechanics. Abstracts of reports, the publishing house of the AS USSR, Moscow, 1968.

1.81. Ye. A. Krasilsyuchyuikov , velocity field, excited by the wing flutters, which are spread over surface, MZhG (1968), No 5.

1.82. A. I. Golubinskiy, On the power impulse and torque/moments, communicated to fine/thin wing during unsteady flow, MZhG (1968), No 6.

Page 751.

1.83. V. E. Baskin, to the linear theory of the unsteady motion of gas under the action of nonpotential external forces, MZhG (1969), No 4.

1.84. S. M. Belotserkovskiy, N. A. Kudryavtseva, B. N. Fedotov, Method of the calculation of the aerodynamic wing characteristics of complex planform with subsonic leading and trailing edges, MZhG (1969), No 2.

1.85. S. M. Belotserkovskiy, G. A. Kolesnikov, ~~Chalchulation~~ Calculation of the effect of gust on the wing of complex planform at subsonic speeds, MZhG (1969), No 5.

1.86. S. M. Belotserkovskiy, S. A. Popytalov, ~~Chalchulation~~ Calculation of the effect of gust on wing with subsonic leading and trailing edges, MZhG (1970), No 2.

1.87. S. M. Belotserkovskiy, about reciprocity theorem for a wing with arbitrary time dependences, MZhG (1970), No 5.

1.88. A. I. Golubinskiy, M. N. Kogan, ~~ob~~ the momentum/impulse/pulse of the unsteady pressure, which acts on body in liquid or gas, MZhG (1970), No 1.

1.89. V. E. of Baskin, to the theory of the unsteady curvilinear motion of lifting surface in gas, the scientific notes of TsAGI, Vol. 1, No 2, 1970.

1.90. T. Karman, M. Biot, ~~Matematicheskiye~~ Mathematical methods in engineering,

trans. from Engl., the State Technical Press, Moscow, 1946.

1.91. A. F. Timofeev, ~~Integrirovaniye~~ Integration of functions, the State Technical Press, Moscow, 1948.

1.92. E. Grey, G. B. Met'yuz, Bessel functions and their application/appendix to physics and mechanics, publ. 2-e, trans. from the 2nd Eng, publ., IL, Moscow, 1953.

1.93. V. V. Smirnov, ~~Kurs~~ Course in advanced calculus, Vol. II, the State Technical Press, 1950.

1.94. I. M. Ryzhik, I. S. Gradstein, ~~Tablitsy~~ Tables of integrals, sums, series and products, "science", Moscow, 1968.

2. Literature in foreign languages.

2.1. Birnbaum W., Die tragende Wirbelfläche als Hilfsmittel zur Behandlung des ebenen Problems der Tragflügeltheorie, ZAMM 3 (1923), № 4.

2.2. Wagner H., Dynamischer Auftrieb von Tragflügeln, ZAMM 5, (1924).

2.3. Ackeret J., Gasodynamik, Handbuch der Physik, 7, 1927.

2.4. Ackeret J., Luftkräfte auf Flügel, die mit grosserer als Schallgeschwindigkeit bewegt werden, Z. f. Flugt. u. Motorl. (1928), № 16.

2.5. Theodorsen T., General theory of aerodynamic instability and the mechanism of flutter, NACA Report № 496, 1935.

2.6. Possio C., *L'azione aerodinamica sul profilo oscillante in un fluido compressibile a velocita iposonora*, L'Aerotecnica, XVIII, fasc. 4, апрель 1938.

2.7. Cicala P., Methoden zur Messungen der Luftkräfte auf schwingenden Flügeln. В сборнике «Gesammelte Vorträge der Hauptversammlung 1937 der Liliental-Gesellschaft für Luftfahrtforschung», 1938.

2.8. Prandtl L., Beitrag zur Theorie der tragenden Fläche, ZAMM 16 (1939), № 6.

2.9. Sears W. R., Kucthe A. M., The growth of the circulation of on airfoil flying through a gust, JAS VI (1939), № 9.

2.10. Sears W. R., A contribution to the airfoil theories for non-uniform motion. Proceeding of the Fifth International Congress for Applied Mechanics, London, 1939.

Page 752.

2.11. Dietze F., Die Luftkräfte der harmonisch schwingenden in sich verformbaren Platte (Ebenes Problem), Luftfahrtforschung 16 (1939), вып. 2.

2.12. Küssner H. G., Allgemeine Tragflächentheorie, Luftfahrtforschung, München XVII (1940), № 11—12.

2.13. Borbely S., Über die Luftkräfte, die auf einen harmonischschwingenden zweidimensionalen Flügel bei Überschallstromung wirken, ZAMM, 1943, № 4.

2.14. Busemann A., Infinitesimale Kegelige Überschallströmung, Schriften der Deut. Akad. der Luftfahrtforschung (1943), № 3.

2.15. Schade T., Krienes K., The oscillating circular airfoil on the basis of potential theory, NACA, Technical Memoranda № 1098, 1947.

2.16. Reissner E., Effect of finite span on the airload distributions for oscillating wings, I — Aerodynamic theory of oscillating wings of finite span, NACA Technical Notes № 1194, 1947.

2.17. Biot M. A., Loads on a supersonic wing striking a sharp-edged gust, Cornell Aeronautical Laboratory Report SA-247-S-7, 1948.

2.18. Ribner H. S., Malvestuto F. S., Stability derivatives of triangular wings at supersonic speeds, NACA Report № 908, 1948.

2.19. Word G., Supersonic flow past thin wings, Quarterly Applied Mathematics and Mechanics 11 (1949), № 3.

2.20. Timman R. and van de Vooren A. I., Theory of the oscillating wing with aerodynamically balanced control surface in two-dimensional subsonic compressible flow, Report F. 54, National Aeronautical Research Institute, Amsterdam, 1949.

2.21. Evvard J. C., Use of source destribution for evaluating theoretical aerodynamics of the finite wing at supersonic speeds, NACA Report 951, 1950.

2.22. Frank S., Malvestuto F., Theoretical lift and damping roll at supersonic speeds of thin sweptback tapered wings with stream wise tips, subsonic leading edges and supersonic trailing edges, NACA Report № 970, 1950.

2.23. Miles I. W., Transient loading of supersonic rectangular airfoils, JAS 17 (1950), № 10.

2.24. Dörr I., Beitrag zu einer Wirbeltheorie des kompressiblen Mediums, Ingenieur Archiv XVIII (1950), № 6.

2.25. Reissner E., On the application of Mathieu functions in the theory of subsonic compressible flow past oscillating airfoils, NACA Technical Notes № 2363, 1951.

2.26. Lomax H., Heaslet M. A., Fuller F. B., Sluder L., Two- and three-dimensional unsteady lift problems in high-speed flight, NACA Report № 1077, 1952.

2.27. Jones W. R., The calculation of aerodynamic derivative coefficients for wings of any plan form in non-uniform motion, ARC Report and Memoranda № 2470, 1952.

2.28. Garner H. C., Milthopp's subsonic liftingsurface theory of wings in slow pitching oscillations, ARC Report and Memoranda № 2885, 1952.

2.29. Mazelsky B., Numerical determination of indicing lift of a two-dimensional sinking airfoil at subsonic Mach numbers from oscillatory coefficients with numerical calculations for a Mach number of 0,7, NACA Technical Notes № 2613, 1952.

2.30. Flax A. H., Reverse flow an variotional theorems for lifting surfaces in nonstationary compressible flow, JAS 20 (1953), № 2,

2.31. Falkner V. M., The solution of lifting-plane problems by vortex-lattice theory, ARC Report and Memoranda № 2591, 1953.

2.32. Van de Vooren A. I., Aerodynamic coefficients of an oscillating airfoil with control surface in two-dimensional subsonic flow, JAS 20 (1953), № 3.

2.33. Heaslet M. A., Spreiter I. R., Reciprocity relations in aerodynamica, NACA Report № 1119, 1953.

2.34. Timman R., Linearized theory of the oscillating airfoil in compressible subsonic flow, JAS 21 (1954), № 4.

2.35. Timman R., van de Vooren A. I. and Greidanus J. H., Aerodynamic coefficients of an oscillating airfoil in two-dimensional subconic flow, JAS 21 (1954), № 7.

2.36. Lomax H., Lift developed on unrestrained rectangular wings envering gusts at subsonic and supersonic speeds, NACA Report № 1162, 1954.

2.37. Press H. and Houbolt I., Some applications of generalized harmonic analysis to gust loads on airplanes, JAS 22 (1955), № 1.

2.38. Lüssher F., Methode zur Bestimmung von Dämpfungsgrössen in Transonic und Überschallkanälen, Z. f. ang. Math. und Phys. VI (1955).

2.39. Watkins C. E., Rynyan H. L. and Woolston D. S., On the kernel function of the integral equation relating the lift and downwash distributions of oscillating finite wings in subsonic flow, NACA Report № 1234, 1955.

2.40. Russner F. R., Kritische Bemerkunsen zur dreidimensionalen Tragflächen Theorie in Unterschallgebiet, Z. f. Flugwiss. 4 (1956), № 1—2.

2.41. Scruton C., Woodgate L., Measurement of pitching-moment derivatives for aerofoils oscillating in two-dimensional supersonic flow, ARC Report and Memoranda № 3234, 1959.

2.42. Watkins C. E., Woolston D. S. and Cunningham H. I., A systematic procedure for determining aerodynamics forces on oscillating or steady finite wings at subsonic speeds, NASA Technical Report R-48, 1959.

2.43. Richardson I. R., A method for calculating the lifting forces on wings. (Unsteady subsonic and supersonic lifting-surface theory.) ARC Report and Memordanda № 3157, 1960.

2.44. Simpson R. W., An extension of Multhopp's lifting surface theory to include the effect of flaps, ailerons, etc., College of Aeronautical Cranfield, Rep. № 132, 1960.

2.45. Etkin B., Theory of the flight of airplanes in isotropic turbulence-review and extension, Advisory Group for Aeronautical Research and Development, Rep. № 372, 1961.

2.46. M. T. Landahl, Unsteady transonic flow, Pergamon Press, London, 1961.

2.47. Atmospheric turbulence and its relations to aircraft, Proceeding of a Symposium held at the Royal Aircraft Establishment Farnborough, on 16. IX. 1961, London, 1963.

2.48. Taylor J., Manual on aircraft loads, Pergamon Press. London, 1965.

2.49. Davies D. E., Calculation of unsteady generalized airforces on a wing oscillating harmonically in subsonic flow, ARC Report and Memoranda № 3409, 1965.

2.50. Andrew L. V. and Stenton T. E., Unsteady aerodynamic forces on a thin wing oscillating in transonic flow, AIAA Paper № 67-16, 1966.

2.51. Stark V. I. E., On the approximation of the normal velocity on oscillating wings, AIAA Journal 4 (1966), № 12,

2.52. Landahl M., On the pressure loading functions for oscillating wings with control surfaces. B сб. AIAA/ASME 8th Structures, Structural Dynamics and Materials Conference, Palm Springs, California, March 29—31, 1967.

2.53. Landahl M. T., Stark V. I. E., Numerical lifting-surface theory-problems and progress. AIAA Aerospace Sciences Meeting, New York. AIAA Paper № 68-72, 1968.

2.54. Tijdeman H. and Bergh H., Analysis of pressure distributions measured on a wing with oscillating control surface in two-dimensional high subsonic and transonic flow, Report National Luchtvaart laboratorium Technika Rabiport F-253, 1967.

List of the abbreviated designations in the literature.

TsAGI is a central aerohydrodynamic institute.

Izd-vo AN SSSR is the Publishing House of the Academy of Sciences of the USSR.

Oborongiz is the state publishing house of defense industry.

Gostexizdat is the state publishing house of technical-theoretical literature.

IL are publishing house of foreign literature.

Fizmatgiz is publishing house of physical and mathematical literature.

Voenizdat is military publishing house of the ministry of the defense of the USSR.

Gidrometeoizdat is publishing house of hydrographic and weather service.

PMM - applied mathematics mechanic.

OTN - Proceedings of the Academy of Sciences of the USSR, department of physical sciences.

MIM - Izvestiya the Academy of Sciences of the USSR, mechanic machine-building.

BNI - the bureaus scientifically of the information of TsAGI.

MZhG - the mechanic of liquid and gas.

ZAMM — Zeitschrift für angewandte Mathematik und Mechanik.
NACA — National Advisory Commitee for Aeronautics.
JAS — Journal of Aeronautical Sciences.
ARC — Aeronautical Research Council.
AIAA — American Institute of Aeronautics and Astronautics.

Page 755.

The principal notations.

I. Geometric parameters.

l - the wingspan,

b - root wing chord,

b_x - end wing chord,

b_a - the mean aerodynamic chord of wing (MAC),

b^* - the chord of wing section, is parallel to root chord, x, y, z - moving coordinates in the connected with wing coordinate system,

$\underbrace{\bar{x}=\frac{x}{b},\ \eta=\frac{y}{b},\ \zeta=\frac{z}{b}}$ are dimensionless coordinates with the significant dimension of b,

$\underbrace{\bar{x}=\frac{x}{b},\ \bar{y}=\frac{y}{b},\ \bar{z}=\frac{2z}{l}}$ - the dimensionless coordinates, when for z is undertaked as significant dimension the semirange of wing,

S - wing area,

$\lambda = \eta^2/S$ - wing aspect ratio,

$\eta = \frac{b}{b_к}$ -contraction wing,

$\bar{\eta} = \frac{b_к}{b}$ -reverse/inverse wing taper,

χ_0 - sweep angle on leading edge,

χ_1 are a sweep angle on trailing edge,

c - wing thickness,

$\bar{c} = c/b$ - wing chord ratio,

$x_т$ - distance from the origin of coordinates 0 to the wing leading edge,

$\bar{x}_т = \frac{x_т}{b}$ - centering of wing.

II. Kinematic parameters.

$U_0 = iU_{0x} + jU_{0y} + kU_{0z}$ the vector of the absolute velocity movable began,

$\Omega = i\Omega_x + j\Omega_y + k\Omega_z$ - the vector of the absolute angular velocity of wing,

(W_x, W_y, W_z) - the projection of the absolute disturbed velocity,

$(\Omega_x, \Omega_y, \Omega_z)$ - the projection of absolute angular velocity,

$\left(w_x = \frac{W_x}{U_0},\ w_y = \frac{W_y}{U_0},\ w_z = \frac{W_z}{U_0}\right)$ - the projection of the dimensionless (agitated) speed of the medium,

(W^*, W_0) - the vectors of movable and relative speed,

a - the speed of sound,

t - time,

$\tau = U_0 t/b$ - dimensionless time.

Page 756.

$\left(M = \frac{U_0}{a_\infty}\right)$ is a Mach number of undisturbed flow,

T - the oscillatory period,

$p = 2\pi/T$ - angular frequency,

$p^* = pb/U_0$ - Strouhal number,

$\omega = \frac{M^2}{k^2} p^*$ - reduced frequency, $k^2 = 1 - M^2$ with $M < 1$, $k^2 = M^2 - 1$ at $M > 1$,

q_i - the dimensionless kinematic parameter, which characterizes the motion of wing, his strain or gust,

$q_1 = \alpha$ - the angle of attack of wing (angle between the root chord and the projection of speed U_0 on the plane of the symmetry of wing Oxy),

$q_2 = \omega_x = \frac{\Omega_x b}{U_0}$ are a dimensionless rate of roll with the characteristic linear dimension of b,

$q_2 = \omega_{x1} = \frac{\Omega_x l}{2U_0}$ - dimensionless rate of roll with the characteristic linear dimension $l/2$,

$q_3 = \omega_z = \frac{\Omega_z b}{U_0}$ are a dimensionless rate of pitch with the characteristic linear dimension of b,

$q_3 = \omega_{za} = \frac{\Omega_z b_a}{U_0}$ dimensionless rate of pitch with characteristic linear dimension b_a,

$q_4 = \delta$ are the parameter of strain during harmonic oscillations,

$q_5 = \Delta$ - the parameter of harmonic gust,

$\dot{q}_1 = \dot{\alpha} = d\alpha/dt\ b/U_0$ - dimensionless derivative of angle of attack in terms of time,

$\dot{q}_2 = \dot{\omega}_x = \frac{d\Omega_x}{dt}\frac{b^2}{U_0^2}$ are dimensionless derivative of angular velocity Ω_x in terms of time with the characteristic linear dimension of b,

$\dot{q}_2 = \dot{\omega}_{x1} = \frac{d\Omega_x}{dt}\frac{l^2}{4U_0^2}$ - dimensionless derivative of angular velocity Ω_x on time with the characteristic linear dimension $b/2$,

$\dot{q}_3 = \dot{\omega}_z = \frac{d\Omega_z}{dt}\frac{b^2}{U_0^2}$ are dimensionless derivative of angular velocity Ω_z in terms of time with the characteristic linear dimension of b,

$\dot{q}_3 = \dot{\omega}_{za} = \frac{d\Omega_z}{dt}\frac{b_a^2}{U_0^2}$ - dimensionless derivative of angular velocity Ω_z in terms of time with characteristic linear dimension b_a,

$\dot{q}_4 = \dot{\delta} = d\delta/dt\ b/U_0$ are dimensionless derivative of the parameter of strain in terms of time,

$\dot{q}_s = \dot{\Delta} = d\Delta/dt\ b/U_0$ - dimensionless derivative of the parameter of gust in terms of time,

q_l^* are amplitude values of the kinematic parameter at harmonic time dependences or its characteristic value during aperiodic motions.

Page 757.

ϕ (x, y, z, t) is potential of the disturbed speeds of wing with the assigned number M,

$\varphi^{q_l}(\xi, \eta, \zeta), \varphi^{\dot{q}_l}(\xi, \eta, \zeta)$ - the aerodynamic derivatives of velocity potential with harmonic time dependences,

$\gamma_{z+}(x, z, t) = U_0 \cdot (\xi, \zeta, t)$ are intensity of the connected vorticity layer,

$$\gamma_z = \sum_{l=1}^{5} \left(\gamma_z^{q_l} q_l + \gamma_z^{\dot{q}_l} \dot{q}_l\right).$$

$\gamma_z^{q_l}(\xi, \zeta), \gamma_z^{\dot{q}_l}(\xi, \zeta)$ - the aerodynamic derivative intensities of the connected vorticity layer with harmonic time dependences,

$\Gamma_{+\mu kk-1} = U_0 b \Gamma_{\mu kk-1}$ are circulation of bound vortex,

$$\Gamma_{\mu kk-1} = \sum_{l=1}^{5} \left(\Gamma_{\mu kk-1}^{q_l} q_l + \Gamma_{\mu kk-1}^{\dot{q}_l} \dot{q}_l\right).$$

$\Gamma^{q_i}_{\mu k k-1}$, $\Gamma^{\dot{q}_i}_{\mu k k-1}$ - aerodynamic derivative circulations of bound vortex on μ-th ~~μ-m~~ the cord between sections k and k - 1 with the i form of motion,

$\Gamma_\Sigma(\xi) = \sum_{\mu=1}^{n} \Gamma_\mu(\xi)$, are the total circulation of bound vortexes.

III. Dynamic characteristics.

$\rho_\infty U_0^2/2$ is velocity head of undisturbed flow,

ρ_∞ - the mass density of the undisturbed medium,

$\bar{p} = \dfrac{p_H - p_B}{\dfrac{\rho_\infty U_0^2}{2}} = \sum_{i=1}^{5} \left(p^{q_i} q_i + p^{\dot{q}_i} \dot{q}_i\right)$ - the dimensionless coefficient of aerodynamic loading,

Y - lift,

$c_y = \dfrac{2Y}{\rho_\infty U_0^2 S} = \sum \left(c_y^{q_i} q_i + c_y^{\dot{q}_i} \dot{q}_i\right)$ - lift coefficient,

M_z - pitching moment (pitch),

$m_z = \dfrac{2M_z}{\rho_\infty U_0^2 Sb} = \sum \left(m_z^{q_i} q_i + m_z^{\dot{q}_i} \dot{q}_i\right)$ - the coefficient of pitching moment,

$m_{za} = \frac{2M_z}{\rho_\infty U_0^2 S b_a}$ - the coefficient of pitching moment with significant dimension b_a.

M_x are the moment of roll,

$m_x = \frac{2M_x}{\rho_\infty U_0^2 S b} = \sum \left(m_x^{q_i} q_i + m_x^{\dot{q}_i} \dot{q}_i\right)$ - coefficient of rolling moment

$m_{xl} = \frac{2M_x}{\rho_\infty U_0^2 S l}$ - the rolling-moment coefficient with the significant dimension of l,

$\bar{x}_F = \frac{x_F}{b}$ are a dimensionless coordinate of mean aerodynamic center of wing relative to leading edge/nose MAC.

Page 758.

$\underbrace{c_y' = \frac{2\,dY}{\rho_\infty U_0^2 b'\,dz} = \sum \left(c_y'^{q_i} q_i + c_y'^{\dot{q}_i} \dot{q}_i\right)}$ - the lift coefficient of wing section,

$\underbrace{m_z' = \frac{2\,dM_z}{\rho_\infty U_0^2 b'^2\,dz} = \sum \left(m_z'^{q_i} q_i + m_z'^{\dot{q}_i} \dot{q}_i\right)}$ - the coefficient of the pitching moment of wing section,

c^{q_i}, $c^{\dot{q}_i}$ - the coefficients of the aerodynamic derivatives ($c = c_y, m_x, m_z$; $i = 1, 2, 3, 4, 5$), is introduced with harmonic time dependences,

$\left[\frac{c_y}{\alpha^\circ}\right]$ - the transient function of the lift coefficient during a stepped variation in the angle of attack α,

$\left[\frac{m_z}{\alpha^\circ}\right]$ - the transient function of the coefficient of pitching moment during a stepped variation in the angle of attack α,

$\left[\frac{c_y}{\omega_z^\circ}\right]$ - the transient function of the lift coefficient during a stepped variation in the angular velocity ω_z,

$\left[\frac{m_z}{\omega_z^\circ}\right]$ - the transient function of the coefficient of the longitudinal torque/moment during a stepped variation in the angular velocity ω_z,

$\left[\frac{m_x}{\omega_x^\circ}\right]$ - the transient function of the coefficient of the bank of torque/moment during a stepped variation in the angular velocity ω_x,

$\left[\frac{c_y}{w_{y\Delta}^\circ}\right]$ - the transient function of the lift coefficient with the gradual descent of wing into step gust (Δ-problem),

$\left[\frac{m_z}{w_{y\Delta}^\circ}\right]$ - the transient function of the coefficient of pitching moment upon the gradual entrance of wing into step gust (Δ-problem),

$\alpha^\circ, \omega_z^\circ, \omega_x^\circ, w_{y\Delta}^\circ$ - the value of the jump of the angle of attack α, of angular velocities ω_z and ω_x and of the component of the vertical velocity $w_{y\Delta}$ during their stepped variation in time,

$c_{y\alpha} = \left(\frac{c_y}{\alpha^\circ}\right)$ are the normalized transient function of the lift coefficient during an arbitrary change in the angle of attack α,

$m_{z\alpha}=\left(\frac{m_z}{\dot{\alpha}}\right)$ - the normalized transient function of the coefficient of pitching moment during an arbitrary change in the angle of attack α,

$c_{y\omega_z}=\left(\frac{c_y}{\dot{\omega}_z}\right)$ are the normalized transient function of the lift coefficient during an arbitrary change in the angular velocity ω_z.

Page 759.

$m_{z\omega_z}=\left(\frac{m_z}{\dot{\omega}_z}\right)$- the normalized transient function of the coefficient of pitching moment during an arbitrary change in the angular velocity ω_z.

$m_{x\omega_x}=\left(\frac{m_x}{\dot{\omega}_x}\right)$are the normalized transient function of the rolling-moment coefficient during an arbitrary change in the angular velocity ω_x.

$c_{y\Delta}=\left(\frac{c_y}{\dot{w}_{y\Delta}}\right)$- the normalized transient function of the lift coefficient upon the gradual entrance into arbitrary gust (Δ- problem),

$m_{z\Delta}=\left(\frac{m_z}{\dot{w}_{y\Delta}}\right)$- the normalized transient function of the coefficient of pitching moment upon the gradual entrance into arbitrary gust (Δ-problem),

$x_{q_i}(\tau)=\left(\frac{m_z(\tau)}{\dot{q}_i}\right)\Big/\left(\frac{c_y(\tau)}{\dot{q}_i}\right)$ - the unsteady focus, which characterizes instantaneous

position on the wing of the point of the application/appendix of resultant to $\left(\frac{c_y(\tau)}{q_i^*}\right)$.

H_{c_y} are a transfer function of the lift coefficient under the influence of harmonic gust,

H_{m_z} is a transfer function of the coefficient of pitching moment under the influence of harmonic gust,

$k_{22}=\frac{\lambda_{22}}{\rho_\infty Sb}$, $k_{26}=\frac{\lambda_{26}}{\rho_\infty Sb^2}$, $k_{11}=\frac{\lambda_{11}}{\rho_\infty Sb^3}$, $k_{66}=\frac{\lambda_{66}}{\rho_\infty Sb^3}$ – the coefficients of apparent additional masses,

λ_{22}, λ_{26}, λ_{44}, λ_{66} are apparent additional masses,

$(k_{22})_a=\frac{\lambda_{22}}{\rho_\infty Sb_a}$, $(k_{26})_a=\frac{\lambda_{26}}{\rho_\infty Sb_a^2}$, $(k_{11})_a=\frac{\lambda_{11}}{\rho_\infty Sb_a l^2}$, $(k_{66})_a=\frac{\lambda_{66}}{\rho_\infty Sb_a^3}$ – the coefficients of apparent additional masses with significant dimensions b_a and l,

$k\lambda$, λ tg χ_0, η – the parameters of similarity $(k=\sqrt{|M^2-1|})$.

Page 760.

Index.

~~Indicators.~~

I. Basic concepts. General theoretical methods.

bio - savart law.

Eddy/vortex discrete unsteady in the incompressible medium.

-- in the compressed medium.

- stationary.

Chaplygina - Joukowski's hypothesis.

Duhamel integral for aerodynamic derivatives.

- for arbitrary time dependences.

Joukowski theorem.

- "in small" during noncirculating flow.

- "in small" during circulation flow.

koshi - Lagrange integral.

- the linearized expression.

Coefficients are aerodynamic.

- aerodynamic derivatives.

[redacted]--- of loads.

[redacted]--- of velocity potential.

- sections.

[redacted]--- of the total characteristics.

- pressure.

Coefficients of apparent additional masses.

Mach number.

Loads are aerodynamic.

Parameter geometric.

- kinematic.

- similarity.

Potential of the disturbed speeds.

Sweepback of wing.

Strouhal number.

Wing taper.

- reverse/inverse.

Theorem of momentum.

- reversibility.

-, its consequence for rigid wings.

-, for the deforming wings.

-, for wings with ccntrol surfaces.

Wing aspect ratios.

Equation of continuity.

- linearized.

Conditions are boundary.

- on vortex sheet.

Focus is stationary.

Foci are unsteady.

Page 761.

Formula for a velocity potential.

Functions of pressure.

- transmission.

- transient.

Fourier are integral.

Chord average is aerodynamic.

Center of pressure.

Centering.

Circulation of eddy/vortices.

II. Experimental studies.

Method is dynamometric.

- the bent models.

- instantaneous pressures.

- the determination of apparent additional masses.

- works.

- rotary machines.

Systematic investigations.

Methods are kinematic.

- for forced oscillations.

- for free oscillations.

Comparison of experimental data with the calculations in the incompressible medium.

---- for apparent additional masses.

---- at subsonic speeds.

---- at supersonic speeds.

Similarity conditions during experiment.

III. Precise or known solutions.

Incompressible medium (M = 0)

(1) Вид несущей поверхности и аэродинамической характеристики	(2) Формулы	(3) Таблицы (страницы)	(4) Рисунки
(5) *Крыло бесконечного удлинения* ($\lambda = \infty$)			
(6) Аэродинамические производные	(5.56), (6.91), (6.92), (13.21), (13.24), (13.32)—(13.35), (13.42)	13.1 (307), 13.2 (311)	13.2—13.4, 13.5
(7) Переходные функции	(13.43), (13.44)	13.3 (313), 13.4 (314)	13.6—13.7, 13.8—13.9
(8) Присоединенные массы	(13.36)		
(9) *Прямоугольное крыло весьма малого удлинения* ($\lambda \to 0$)			
(10) Аэродинамические производные	(5.56), (13.80), (13.82), (13.84), (13.86)		
(11) Переходные функции	(13.88), (13.89), (13.90)		
(12) *Крыло с рулевой поверхностью*	(13.46)—(13.48)		13.10—13.14

Key: (1). Form of lifting surface and aerodynamic characteristic. (2). Formulas. (3). Tables (page). (4). Figures. (5). Infinite-span wing ($\lambda = \infty$). (6). Aerodynamic derivatives. (7). Transient functions. (8). Apparent additional masses. (9). The rectangular wing of very small lengthening ($\lambda \longrightarrow 0$). (10). Aerodynamic derivatives. (11). Transient functions. (12). Wing with control surface.

Page 762.

Subsonic speeds (0 < M < 1)

(1) Вид несущей поверхности и аэродинамической характеристики	(2) Формулы	(3) Таблицы (страницы)	(4) Рисунки
(5) *Крыло бесконечного удлинения* ($\lambda = \infty$)			
(6) Аэродинамические производные	(5.56), (6.91), (6.94), (18.1)—(18.3) (18.8)—(18.11)	18.1 (429—430)	19.24—19.31
(7) Переходные функции	(4.30)—(4.34), (4.38), (4.39), (4.41), (4.44), (4.48)	18.2 (432), 18.3 (433), 18.4 (434)	19.1—19.4, 19.8—19.17, 19.20
(8) *Крылья произвольной формы в плане*	(4.30)—(4.34), (4.38)—(4.41), (4.46), (4.50)—(4.52), (5.56), (6.91), (6.94)		
(9) *Прямоугольные крылья*	(4.30)—(4.34), (4.38), (4.39), (4.41), (4.44), (4.48), (4.53), (4.56), (5.56), (6.91), (6.94), (18.9)—(18.11)	29.2 (737)	
(10) *Треугольные крылья*	(4.30)—(4.34), (4.38), (4.39), (4.41), (4.45), (4.49), (4.53), (4.57), (5.56), (6.91), (6.94)		
(11) *Крыло с рулевой поверхностью*	(7.94), (7.96), (7.97), (7.98), (18.4), (18.5)	29.1 (737)	

Key: (1). Form of lifting surface and aerodynamic characteristic. (2). Formulas. (3). Tables (page). (4). Figures. (5). Infinite-span wing ($\lambda = \infty$). (6). Aerodynamic derivatives. (7). Transient functions. (8). Wings of arbitrary planform. (9). Rectangular wings. (10). Delta wings. (11). Wing with control surface.

Supersonic speeds ($M > 1$)

(1) Вид несущей поверхности и аэродинамической характеристики	(2) Формулы	(3) Таблицы (страницы)	(4) Рисунки
(5) *Крыло бесконечного удлинения* ($\lambda = \infty$)			
(6) Аэродинамические производные	(6.91), (22.13), (22.16), (22.17), (22.25)—(22.27)	22.1 (518—520), 22.2 (526—527)	22.3—22.6, 22.8, 22.9
(7) Переходные функции	(6.94), (23.1)—(23.5), (4.30)—(4.34), (4.38), (4.39), (4.41), (4.44), (4.48)	23.1 (550—553)	23.2—23.9
(8) *Обратные треугольные крылья*	(6.91), (6.94), (22.30), (22.31)	22.3 (530—532)	
(9) *Треугольные крылья*			
(10) Аэродинамические производные	(6.91), (22.32), (22.33)	22.4 (533—535), (566)	22.10—22.14, 24.4—24.11
(11) Переходные функции	(6.94), (23.6)—(23.9), (4.30)—(4.34), (4.38), (4.39), (4.41), (4.45), (4.49), (4.53), (4.57), (5.56), (6.91), (6.94)		
(12) *Прямоугольные крылья*	(4.30)—(4.34), (4.38), (4.39), (4.41), (4.44), (4.48), (4.53), (4.56), (6.91), (6.94), (22.42)		
(13) *Крылья произвольной формы в плане*	(4.30)—(4.34), (4.38)—(4.41), (4.46), (4.50)—(4.52), (5.56), (6.91), (6.94)		

Key: (1). Form of lifting surface and aerodynamic characteristic. (2). Formulas. (3). Tables (page). (4). Figures. (5). Infinite-span

wing (λ = ∞). (6). Aerodynamic derivatives. (7). Transient functions. (8). Reverse/inverse delta wings. (9). Delta wings. (10). Aerodynamic derivatives. 811). Transient functions. (12). Rectangular wings. (13). Wings of arbitrary planform.

Page 763.

IV. Numerical methods of the flow-field analysis.

Incompressible medium (M=0)

Harmonic time dependences.

Small Strouhal numbers ($p^* \rightarrow 0$, including stationary characteristics).

Finite Strouhal numbers.

Arbitrary Strouhal numbers (with the aid of Duhamel integral).

Arbitrary time dependences.

Infinite-span wings.

Wings with constant chord on the spread/scope of ($\eta = 1$)

Wings of arbitrary planform.

Passage from stepped laws to arbitrary with the aid of Duhamel integral.

Noncirculating flow about the rigid and deforming wings of arbitrary planform.

Subsonic speeds ($0 < M < 1$)

Harmonic time dependences.

Small Strouhal numbers ($p^* \to 0$, including stationary characteristics).

Arbitrary Strouhal numbers (with the aid of Duhamel integral).

Arbitrary time dependences.

Wings with constant chord on spread/scope ($\eta = 1$)

Wings of arbitrary planform.

Supersonic speeds (M>1)

Harmonic time dependences.

Small Strouhal numbers ($p^* \rightarrow 0$, including stationary characteristics).

Finite Strouhal numbers (wings with supersonic edges.

Arbitrary Strouhal numbers (with the aid of Duhamel integral).

Arbitrary time dependences.

Flow-field analysis of the wings of arbitrary planform during stepped variation $q_i(\tau)$

Passage to any laws $q_i(\tau)$ with the aid of Duhamel integral.

Page 764.

V. Results of numerical calculations.

Aerodynamic derivatives (including stationary characteristics).

(1) Вид несущей поверхности	M=0		0<M<1		M>1	
	(2) Таблицы (страницы)	(3) Рисунки	(2) Таблицы (страницы)	(3) Рисунки	(2) Таблицы (страницы)	(3) Рисунки
(4) Крыло бесконечного удлинения ($\lambda = \infty$)	25.1 (592)	13.2—13.5		19.22—19.31	25.2 (592)	22.3—22.4, 22.8—22.9, 24.38—24.39
(5) Крылья произвольной формы в плане с прямыми кромками	27.2 (627—642)	27.2—27.61, 28.27—28.38	27.2 (627—642)	19.37, 27.2—27.61, 28.39—28.48		27.62—27.121, 28.39—28.48
(6) Прямоугольные крылья	27.2 (627)	14.26—14.33, 14.66, 14.75—14.76	27.2 (627)	19.34, 19.38, 28.7—28.16	27.3 (662)	24.35—24.36, 24.38—24.39, 24.47—24.48, 28.7—28.16, 28.62—28.68
(7) Треугольные крылья	27.2 (640)	14.58—14.61, 14.75, 28.78—28.85	27.2 (640)	19.33, 19.38, 19.35—19.36, 28.17—28.26 28.78—28.55	27.4 (663)	24.32, 24.40—24.41, 24.45—24.47, 28.17—28.26, 28.69—28.88
(8) Крыло сложной формы в плане						24.18—24.23, 24.51
(9) Деформирующиеся крылья и крылья с рулевой поверхностью		14.63—14.65, 28.52—28.59		19.14—19.15, 19.39, 28.52—28.59		

Key: (1). Shape of lifting surface. (2). Tables (page). (3). Figures. (4). Infinite-span wing. (5). Wings of arbitrary planform with direct/straight edges. (6). rectangular wings. (7). Delta wings. (8). Wing of complex planform. (9). Deforming wings and wings with control surface.

Page 765.

Apparent additional masses.

	(1) Таблицы (страницы)	(2) Рисунки
(3) Крылья произвольной формы в плане с прямыми кромками	27.1 (620—622)	14.52—14.57, 14.79—14.81

Key: (1). Tables (page). (2). Figures. (3). Wings of arbitrary planform with direct/straight edges.

Page 766.

Transient functions.

(1) Вид несущей поверхности	M = 0		0 < M < 1		M > 1	
	(2) Таблицы (страницы)	(3) Рисунки	(2) Таблицы (страницы)	(3) Рисунки	(2) Таблицы (страницы)	(3) Рисунки
(4) Крыло бесконечного удлинения ($\lambda = \infty$)		13.6—13.9		19.8—19.13, 19.16—19.17, 19.20		23.2—23.3, 23.6—23.9
(5) Крылья произвольной формы в плане с прямыми кромками		29.1—29.2		29.3—29.4		
(6) Прямоугольные крылья		14.47—14.48, 29.1—29.2, 29.5—29.8, 29.19—29.25		19.18, 29.3—29.4, 29.9—29.18, 29.19—29.25, 29.36		24.5—24.10, 29.19—29.25
(7) Треугольные крылья		14.49—14.50 29.1—29.2, 29.26—29.32, 29.34—29.35		19.19, 29.3—29.4, 29.26—29.32, 29.36—29.38		24.11, 29.13—29.14, 29.26—29.32, 29.37, 29.39
(8) Крылья сложной формы в плане		29.1—29.2		29.3—29.4		
(9) Деформирующиеся крылья и крылья с рулевой поверхностью		14.56—14.57		29.15—29.18		

Key: (1). Shape of carrier surface. (2). Tables (page). (3). Figures. (4). Infinite-span wing ($\lambda = \infty$). (5). Wings of arbitrary planform with direct/straight edges. (6). Rectangular wings. (7). Delta wings. (8). Wings of complex planform. (9). Deforming wings and wings with control surface.

Page 767.

VI. The approximation methods of the calculation of aerodynamic characteristics.

	(1) Формулы	(2) Страницы
(3) Гипотеза стационарности	(26.10)	601
(4) Гипотеза стационарности расширенная	(26.11)	601
(5) Гипотеза гармоничности	(26.1), (26.9)	598—601
(6) Гипотеза гармоничности при постепенном входе в порыв	(26.16)	603
(7) а) прямоугольное крыло	(26.17)	603, 605
(8) б) треугольное крыло	(26.18)	604, 605, 608
(9) Метод местных давлений	(26.25), (26.27), (26.29)	610
(10) Метод касательных клиньев	(26.31), (26.32), (26.33), (26.35)	611, 612
(7) а) прямоугольное крыло	(26.36)	612
(8) б) треугольное крыло	(26.37)	612
(11) Поршневая теория	(26.47), (26.50)—(26.54)	615, 616
(7) а) прямоугольное крыло	(26.55)	616
(8) б) треугольное крыло	(26.56)	616

Key: (1). Formulas. (2). Pages. (3). Stability hypothesis. (4). Stability hypothesis expanded. (5). Hypothesis of harmony. (6). Hypothesis of harmony upon the gradual entrance into gust. (7). rectangular wing. (8). delta wing. (9). Method of the local pressures. (10). Method of tangential wedges. (11). Piston theory.

REPORT DOCUMENTATION PAGE

READ INSTRUCTIONS BEFORE COMPLETING FORM

1. REPORT NUMBER: FTD-ID(RS)T-1543-77	2. GOVT ACCESSION NO.
3. RECIPIENT'S CATALOG NUMBER	
4. TITLE (and Subtitle): A WING IN AN UNSTEADY GAS FLOW	5. TYPE OF REPORT & PERIOD COVERED: Translation
6. PERFORMING ORG. REPORT NUMBER	
7. AUTHOR(s): S. M. Belotserkovskiy, B. K. Skripach, and V. G. Tabachnikov	8. CONTRACT OR GRANT NUMBER(s)
9. PERFORMING ORGANIZATION NAME AND ADDRESS: Foreign Technology Division, Air Force Systems Command, U. S. Air Force	10. PROGRAM ELEMENT, PROJECT, TASK AREA & WORK UNIT NUMBERS
11. CONTROLLING OFFICE NAME AND ADDRESS	12. REPORT DATE: 1971
	13. NUMBER OF PAGES: 1378
14. MONITORING AGENCY NAME & ADDRESS (if different from Controlling Office)	15. SECURITY CLASS. (of this report): UNCLASSIFIED
	15a. DECLASSIFICATION/DOWNGRADING SCHEDULE

16. DISTRIBUTION STATEMENT (of this Report)

Approved for public release; distribution unlimited.

17. DISTRIBUTION STATEMENT (of the abstract entered in Block 20, if different from Report)

18. SUPPLEMENTARY NOTES

19. KEY WORDS (Continue on reverse side if necessary and identify by block number)

20. ABSTRACT (Continue on reverse side if necessary and identify by block number)

20

ACCESSION for
NTIS White Section X
DDC Buff Section ☐
UNANNOUNCED ☐
JUSTIFICATION
BY
DISTRIBUTION/AVAILABILITY CODES
Dist. AVAIL. and/or SPECIAL
A

DISTRIBUTION LIST

DISTRIBUTION DIRECT TO RECIPIENT

ORGANIZATION		MICROFICHE
A205	DMATC	1
A210	DMAAC	2
B344	DIA/RDS-3C	8
C043	USAMIIA	1
C509	BALLISTIC RES LABS	1
C510	AIR MOBILITY R&D LAB/FIO	1
C513	PICATINNY ARSENAL	1
C535	AVIATION SYS COMD	1
C557	USAIIC	1
C591	FSTC	5
C619	MIA REDSTONE	1
D008	NISC	1
H300	USAICE (USAREUR)	1
P005	ERDA	1
P055	CIA/CRS/ADD/SD	1
NAVORDSTA (50L)		1
NASA/KSI		1
AFIT/LD		1

ORGANIZATION		MICROFICHE
E053	AF/INAKA	1
E017	AF/ RDXTR-W	1
E404	AEDC	1
E408	AFWL	1
E410	ADTC	1
E413	ESD	2
	FTD	
	CCN	1
	ETID	1
	NIA/PHS	1
	NICD	5